Proxy Evidence of Relative Sea Level Change

Indicators and Implications

Raglan (Whaingaroa) Harbour

New Zealand

A thesis

Submitted in fulfilment

of the requirements for the degree

of

Master of Philosophy in Earth Science

at

The University of Waikato

by

MICHAEL JAMES CARTER

THE UNIVERSITY OF
WAIKATO
Te Whare Wānanga o Waikato

2024

ABSTRACT

Geological observations and macrofossil dating of 4 raised marine terraces reveal active tectonic displacement in the Raglan Harbour, New Zealand (NZ). The 120 km-long harbour shoreline displays multiple examples of block-faulting, stratigraphic displacement, and fresh stress release fracture zones within rock sea-cliffs. Tide-zone rock platforms are indicative of a long-term uplift trend within a major portion of the harbour. Vertical land movement (VLM) rates are found to vary at different locations, signifying active fault displacement. Six proxies establish VLM magnitude and timing constraints applicable to the last 7 decades. One further proxy establishes maximum relative sea level (RSL) throughout the last 23.5 Ka at a specific location in the harbour.

Seventeen ^{14}C dated macrofossils from 4 raised marine terraces identified 2 groups of ages: pMC ~ 1 to 6.5 Ca yr BP and ~ 6.5 Ka yr BP respectively. Tide dissolution notches in rocks identifiable in historical photographs are compared with modern equivalents at 2 locations. These depict no apparent change in the upper dissolution notch boundary elevations since 1910. Characterisation and U-Th dating of a speleothem located ~ 0.4 m above the modern high tide level signifies that RSL is near its ~ 23.5 Ka maximum at this location. Historic aerial imagery identifies a marine terrace that uplifted by $\leq$ 0.4 m within the period 1979 to 1997. A fault demarcates this feature from a second terrace with stratigraphic evidence of a markedly different VLM history, indicating that the fault is active. Raised trace fossil castings exposed in the foreshore's mid-tide zone further substantiates evidence of relatively recent uplift at this location.

ACKNOWLEDGEMENTS

This work is intentionally a broad-brush to identify and characterise multiple proxies of historical RSL change in Raglan Harbour. My prime objective was to identify a range of proxies, each to be backed up with credible evidence that they are dependable indicators warranting further study and validation.

The work involved many field trips in a canoe. The harbour yielded far more evidence than I could have hope for. This research addresses a selection of proxies from many identified examples which are beyond the scope of this 1-year MPhil program.

With its high reliance on costly fossil dating, this research could not have proceeded without the financial support provided by the New Zealand Geotechnical Society and a University of Waikato research fund administered by Willem de Lange. I am particularly appreciative for the vote of confidence that I could get this over the line. I hope that the result can be seen as a worthy investment.

My thanks to Ben Roche and other University of Waikato technical support staff who helped with surveying and field equipment, and to Fiona Petchey with radiocarbon dating advice. I am also grateful for the access to the Patikirau property provided by owner Guido Locher.

My appreciation and thanks to my supervisory team of Kim de Graaf, and Willem de Lange. Also, to Bruce Hayward who willingly provided invaluable advice and guidance on a range of topics throughout the year.

Thorough fieldwork in a shallow tidal harbour is particularly challenging. This is probably why so little focused work has been done on the harbour. My special thanks to Raglan geology enthusiast Kevin Ansley, who not only provided all the seacraft logistics and most of the paddle-power, but also continually challenged me with his novel ideas and independent observations. Many were unprecedented and applicable. Without his contribution, this thesis would be considerably thinner.

TABLE OF CONTENTS

LIST OF FIGURES

Figures Chapter One

Figures Chapter Two

Figures Chapter Three

Figures Chapter Four

Figures Chapter Five

Figures Chapter Six

Figures Chapter Seven

Figures Chapter Eight

Figures Chapter Nine

LIST OF TABLES

GLOSSARY

Term	Acronym	Definition
Eustatic sea level	ESL	Mean global sea level as measured from the centre of Earth
Local mean sea level	LMSL	Mean elevation of the sea with respect to a land benchmark e.g. a tide gauge
Relative sea level	RSL	Sea level in relation to any one land-based entity the elevation of which is subject to change
Effective high tide	EHTL	Sea level as defined by the maximum elevation of a physical environmental imprint (trace) of the influence of high tides at any one location
Strandline		The maximum elevation of debris deposited by effective high tides at any one location
Age calibrated years BP	cal. yr BP	Calibrated ^{14}C age
Age percentage modern carbon	pMC	Raw uncalibrated ^{14}C age

CHAPTER ONE

INTRODUCTION

1.1: Introduction

Throughout the 21st century, many local governments in New Zealand (NZ) have added marine flooding and erosion hazard-zone overlays to their district plans. The Waikato District Council defines these as being 'Sensitivity Zones' with overlay boundaries established on a projected eustatic sea level (ESL) rise of ~ I m by 2120 (Waikato District Council, 2022). This value was established through the adoption of the most extreme projection within official NZ guidelines (NIWA, 2023; Bell, et al., 2017). A ESL rise of 1 m by 2120 is reliant on a representative concentration pathway (RCP) of 8.5. $W.m^{-2}$ i.e. RCP 8.5 additional radiative forcing. RCP 8.5 requires an unabated escalation in CO_2 emissions throughout the next century. Being the worst possible scenario, this prospect can be considered as unlikely or very unlikely. The NZ legislations RMA (1991) and NZCPS (2010) stipulate that local government planners should base decisions involving ESL change on the most likely projections.

This adoption of the most extreme official ESL rise projection available reflects a high degree of uncertainty over future relative sea level (RSL) influencing dynamics e. g. vertical land movement (VLM) which influences the actual sea level along beachfronts. Data is scant. The Raglan tide gauge record is as-yet not fit for purpose (refer to Section 2.4.). The closest continuous global positioning (cGPS) station measuring land surface displacement is ~ 15 km from the central Raglan Harbour. These 2 locations are separated by a major fault complex orientated approximately parallel to the Hakarimata Range, which has been subject to significant differential VLM in the past (Kamp et al., 2004). Based on varying evidence within published literature, ESL rise in Raglan Harbour throughout the next century could be anywhere between 0.25 m and 2.0 m (refer to Chapter 2).

Beachfront stakeholders, the insurance industry, and governmental regulatory bodies are therefore confronted with a high degree of uncertainty over the rate and impact of RSL change in the harbour within the near to long-term future.

Raglan Harbour has ~130 km of harbour foreshore. The Raglan catchment population grew by 21% (~700 persons) between 2013 and 2018 (New Zealand Ministry of Education, 2022). Twelve km of the beachfront is comprised of high-value urban properties, along with public amenities and infrastructure. A high proportion of these properties have retaining structures at their foreshore boundaries, signifying their existing susceptibility to marine erosion.

Dependable RSL change projections require both continuous tide gauge and VLM measurements over an adequate time-period. In the case of Raglan, this is likely to require another 20 years of accurate measurement (Wang, 2023)**.** Given this lack of data and the intermittent nature of VLM, records of past SL change, seismic activity, and tectonic dynamics are essential components for the formulation of dependable projections into the future.

Published literature interpretations of historical average VLM of the western Waikato coastline throughout the Pleistocene range from + 0.3 mm/year to + 0.7 mm/year (**r**efer to Chapter 2). In contrast, a study by NZ SeaRise (2024), based on satellite altimetry over an 8-year time-period, interprets VLM around the Raglan Harbour foreshore as being currently subject to an average subsidence of $\leq$ 2.59 mm/year (refer to Section 2.3).

The Raglan Harbour foreshore displays evidence of apparent uplift at multiple locations. This is largely in the form of raised marine terraces with apparent uplift magnitudes of 0.2 m - 1 m. Historical photographs spanning 110 years further support this observation by displaying no evidence of appreciable RSL change throughout this time-period at their locations. The differential nature of the RSL elevation traces along the foreshore indicates that faults in the harbour probably remain active.

1.2: Research Objective

Quantitative metrics on RS**L** change in Raglan Harbour consist entirely of inadequate tide gauge records (refer to Section 2.4). Two further decades of continuous data is likely required before meaningful analysis with an uncertainty of < 2 mm/year can be extracted (Wang, 2023). Regulatory authorities have addressed the consequential uncertainty by applying the most extreme (and considered unlikely) projections available within official NZ guidelines.

The objective of this study is to identify and characterise measurable proxies that provide a foundation on which meaningful metrics on RSL change along the foreshore can be established. It also endeavours to identify and describe unrecorded geological faults and their behaviour.

This research was instigated in support of a hypothesis that RSL at specific locations in the harbour has been $\leq$ 0.75 m above the modern level within the last 3 centuries**,** and that variations within the historic RSL at different locations is due to differential uplift. Moreover, that strain dynamics are currently active and likely to continue in an intermittent manner in the future.

The research objective was the compilation and characterisation of multiple proxies relating to the hypothesis. This involved:

- A comparison of historical photographs with modern imagery displaying the foreshore and tide erosion traces
- Observations and descriptions of indicative foreshore morphologies and relating entities, including tide-zone rock platforms, eroded rocks, raised terraces and shellbeds
- Collection and dating of macrofossils and speleothems
- The location and quantification of microfossils

Given the apparent differential nature of the VLM, focused characterisation and morphological description of multiple key sections was considered essential. A prime requirement was to accumulate enough fossil ages to establish statistically credible constraints on raised terrace evolution. During early reconnaissance it became apparent that along with multiple examples of terrace shellbeds there were copious deposits of anthropic debris. A means of differentiating this material from legitimate residual fossils was required. The presence or absence of microfossils was adopted as an important proxy on modes of deposition.

Given that the focus was on apparently young terraces of $\leq$ 1 m above the apparent mean high tide level, accurate vertical displacement measurements were considered crucial. An appropriate SL datum from which to measure elevations needed to be defined.

From accumulated evidence VLM strain models can be generated, aimed around resolving key questions:

- What is the nature and origin of the VLM driving forces?
- Are these strain events co-seismic, inter-seismic, of both of these?
- How is this evolution expressed in the geological structure?
- How and where is this activity likely to continue?

1.3: Methods

1.3.1: Methods Introduction

Given that the objective of this research was to identify and characterise any potential proxies relating to VLM and/or RSL change, a diverse range of methods was required. These included a comparison of historical photographs with modern satellite imagery, field observations, mapping and graphical descriptions, appropriate study site selection, and sample selection on which laboratory analysis could be based.

Field-based methods involved:

- Geological reconnaissance and mapping
- Compiling and summarising relevant stratigraphy, geological structure, and basic sedimentology
- Specific study section selection
- Elevation surveying
- Sediment core sampling
- Focused terraces, shellbeds, and fossils characterisation
- Macrofossil selection and dating
- Establishing microfossil locations and concentrations
- Speleothem selection and dating

1.3.2: Terrace Locations and Mapping

Initial reconnaissance involved observations of the entire harbour foreshore. This located multiple raised macrofossil shellbeds and terraces. Associated with these are near-vertical shoreline erosion scarps that usually include shellbeds. The shellbed upper boundaries are typically 0.3 m to 1 m elevation above the modern strandline which is the effective high tide (EHT) level. The second round of fieldwork further substantiated the authenticity of raised shellbeds, from which 3 sections were selected for focused study. These section selections were primarily based on the presence, nature, and elevation of raised macro-shellbeds.

1.3.3: Specific Study Section Selection

From > 20 identified raised shellbeds, 3 sites were selected for focused study. To ensure that the fossils were residual, these were checked for the presence and concentrations of articulated (intact) cockles (*Austrovenus stutchburyi*) and foraminifera (forams) within the host sediments. Concentrations of forams within intact cockle infill were measured to further substantiate the residual origin of the fossils.

1.3.4: Review of Relevant Geological Stratigraphy and Structure

An understanding of the likely structural evolution at the study sections required a focused study of the surrounding geology. The published literature on this geology is regional and rudimentary. This study established stratigraphic relationships along the NW foreshore of the harbour where evidence of relatively recent VLM is most apparent. From these observations site-specific geological deformation models could be generated.

1.3.5: Elevation Surveying

The relative elevations of shellbeds were a high-priority selection criterion. This was established using Leica GNSS equipment and Empire digital level methods. Given that relative vertical displacement at the study sections were mostly $\leq$ 1 m, a dependable measuring datum on the modern foreshore was required. The modern EHT level is identifiable around much of the foreshore through the presence of strand (wrack) lines. These contain high concentrations of freshly mobilised shell material and other flotsam. As this elevation is relatively constant around the sheltered estuaries in the harbour, the uppermost surface of the modern strandlines was adopted as an indicator elevation datum at less critical observation sections. This metric was corelated with the GNSS measurements, established at key sections. Strandlines are particularly useful as they can be compared with apparent paleo strandlines at higher elevations at any one site.

A means of differentiating between raised shellbeds originating as paleo-strandlines and raised residual shellbeds that had not been reworked during uplift had to be established. The proportion of intact articulated bivalves and their packing was the adopted criteria to establish this differentiation.

The lower measurement datum for establishing uplift of a paleo-strandline was the top of the modern strandline, whereas for uplifted residual (undisturbed) shellbeds it is the living equivalent in the tide-zone.

1.3.6: Sediment Core Sampling

The modern tide-zone and its associated raised terraces were core sampled to 0.9 m depth at 9 locations at 1 study section (Patikirau Bay). This site was selected due to it having 2 raised terraces of contrasting characteristics, demarcated by an apparent fault. Continuous cores of 250 mm length were extracted, using a manually operated soil core extraction device. Representative examples within the cores were photographed. (refer to Sections 8.3.2; 8.3.5).

1.3.7: Stratigraphic Cross-sections

From information derived from the surface features, core sampling, elevation surveying, and stratigraphic extrapolation, 3 stratigraphic cross-sections were created for 1 site (Patikirau Bay).

1.3.8: Sedimentary Beds, Shellbeds, and Fossils Description

Key sedimentary beds and shellbeds are described from a stratigraphical and basic sedimentological perspective. This included observations on the stratigraphy, bed locations, dimensions, and elevations. The concentrations and physical condition of macrofossils and microfossils were recorded. These observations were supported by relevant photographs. Shellbed host sediment samples were a mix of 3 samples, each being of ~150 cm^3, extracted randomly from sediments surrounding and including the macrofossils.

1.3.9: Macrofossil Selection and Dating

The Raglan Harbour terraces contain copious quantities of residual and disturbed macro and microfossils. 5 criteria were applied to the selection of macrofossil dating material.

The:

- Elevation of the host bed above the foreshore datum
- Sample position within the shellbed
- Sample physical state (ideally intact) and state of weathering
- Sample species
- Identification and concentrations of microfossils within the intact dating sample infill and surrounding host sediments

Based on the mean elevation of all identified terraces, it was decided that dating material needed to be hosted by beds that had been subject to an apparent $\geq$ 0.25 m vertical displacement. Most dating samples were selected from the upper region of the raised shellbeds.

Generally, macrofossils sent for dating were in a relatively fresh state. To further ensure that the samples were not anthropic relocated debris, most dating samples were intact (articulated) bivalves. Due to their abundance and dating dependability, cockles (*Austrovenus stutchburyi*) were selected as dating material.

The cockle valves were separated. One, or part of 1 valve was assigned for dating at the University of Waikato radiocarbon dating laboratory. The remaining shell material was packaged and filed as reference material. Sediments extracted from the intact macrofossils were retained for microfossil analysis.

1.3.10: Radiocarbon Age Interpretations

While both Percentage Modern Carbon (pMC) and ^{14}C calibrated ages are reported, this study adopts the precautions outlined in Reimer et al. (2004) where calibrated ages of 'post bomb' (1950) samples are considered potentially unreliable.

This is demonstrated in a laboratory chart where the 95% probability range for a sample (Pst_1_1) includes a negative value. Therefore, the pMC values are adopted as an approximate maximum age. The calibrated ages are reported as a guideline only and are not relied upon.

1.3.11: Microfossil Identification and Concentrations

The objective behind the identification of microfossils (foraminifera) and their proportional densities was to establish that the study shellbeds, host sediments, and dating materials were not derived from anthropic relocated debris. This process involved washing and sieving of bulk sediment samples to facilitate isolation of all grains retained between 212 µm and 355 µm sieves. From observations through a microscope, the approximate percentage proportion by number of foraminifera to the number of total grains was estimated and recorded (**Appendix C**). A percentage of 0.5 was adopted as a minimum metric. Microfossil species identification and their natural environment implications were not addressed. This field is outside of the scope of this MPhil thesis.

1.3.12: Speleothem Selection and Dating

Speleothems situated above the EHT level are unlikely to exist in a robust unaltered state if their elevation had been subject to extended tidal immersion within their lifetime (Antonioli et al., 2021). Consequently, they are a potential proxy of maximum relative sea levels within their lifetime.

This research located 3 flowstone speleothems, at elevations proximal to the modern mean high tide level (refer to Section 6.2). Two specimens located < 1 m above the modern mean high tide level was directly exposed to the open foreshore. The 3rd example was located within a ~ 1 m wide crevice at > 0.45 m above the modern mean high tide level and ~ 8 m from the open foreshore. While being subject to normal tide oscillations this location is sheltered from the spray and wave-splash effecting the former examples.

The 2 flowstones exposed to the open foreshore are in a highly advanced state of weathering. This state is likely due to regular surface saturation in sea water.

In comparison, the crevice flowstone is hard and crystalline throughout its structure, with no evidence of surface degradation. Consequently, it was selected as a maximum tide level proxy.

One dating sample was knapped from the crystalline flowstone. This sample contained 21 visible strata, 2 of which were selected and dated at the University of Melbourne U-Th dating laboratory. Given that the objective of the speleothem study was to establish an approximate mean age, the dating strata were selected in the laboratory on the basis of their physical properties.

1.3.13: Patikirau Bay Uplift Modelling

From the above-described data a model of the evolution of 2 contrasting raised terraces at Patikirau Bay was generated. These are demarcated by a newly identified fault. The model depicts differential displacement of the terraces along the fault, demonstrating that it probably remains active. It also depicts how future displacement along this fault is likely to occur.

1.4: Field Study Area and Sample locations

The Raglan Harbour is situated on the NW coast of the North Island (NI), New Zealand (NZ) (Figure 1.4.1). It covers an area of ~ 33 km^2, the majority of which becomes exposed at low tide. It is comprised of multiple tidal estuaries resulting in a foreshore extent of ~ 130 km. After foreshore reconnaissance, specific sections were selected for focused research (Figure 1.4.2).

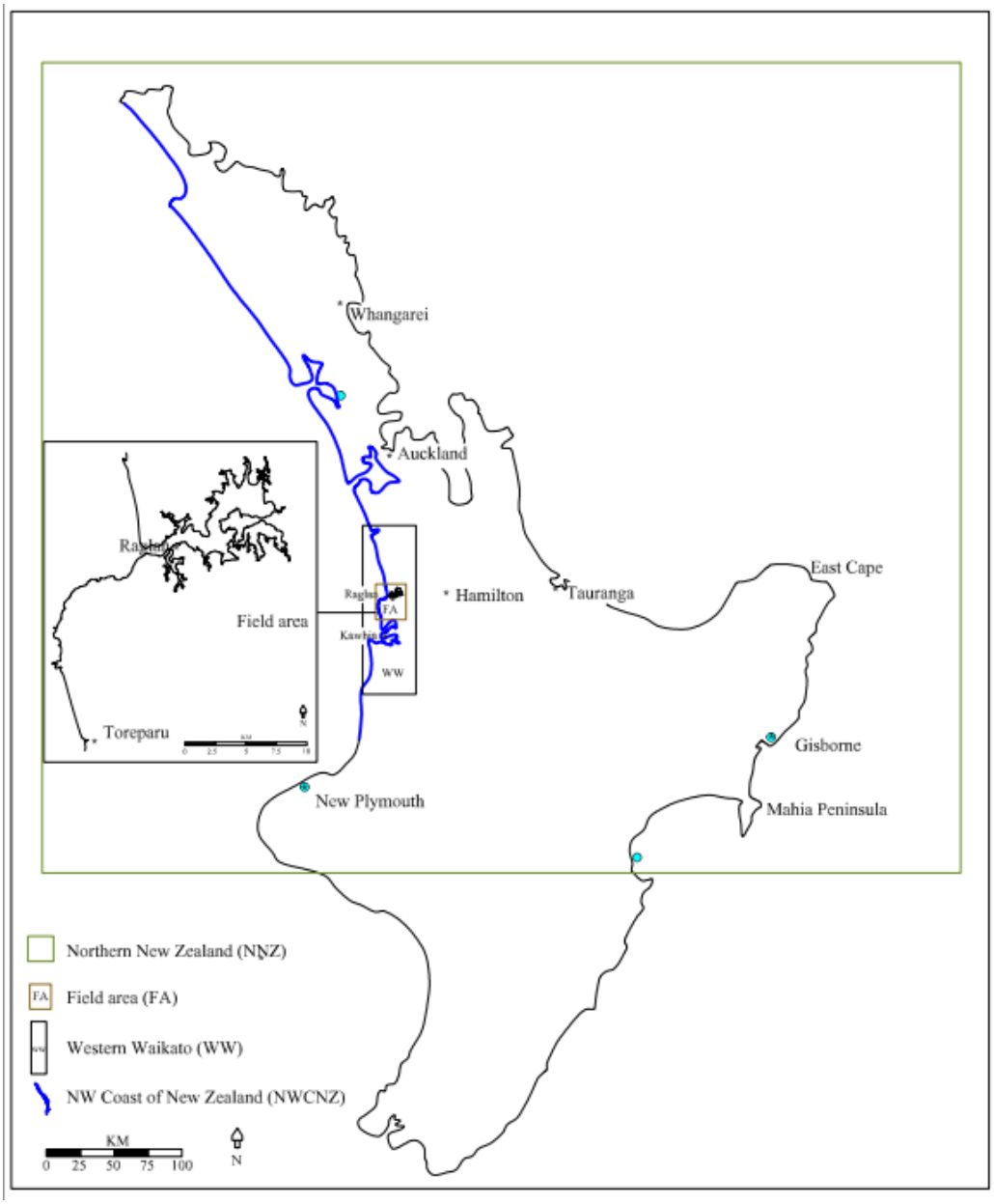

Figure 1.4.1: The North Island NW coast and Raglan Harbour locations.

Figure 1.4.2: Specific locations discussed in this study with focused study sections labelled in yellow.

1.5: Thesis Layout and Chapter Description

This thesis is a systematic description of field and laboratory procedures along with conclusions compiled within 9 chapters and 3 appendices.

Chapter One defines the research objectives, methods, geographical study area and the thesis structure.

Chapter Two is a review of past research relevant to this study. This includes research on raised marine terraces and shellbeds, VLM, SL change**,** geology, sedimentary and erosion processes, seismic history, and speleothems.

Chapter Three describes the regional and local geology. Localised geology and observed structural features relating to tectonic deformation at key sections are mapped. Included are several unpublished faults. The foreshore and terrace morphology relating to specific study sections are described.

Chapter Four discusses sedimentation and erosion processes. This includes a general characterisation and distribution of sediment bodies throughout the harbour. Included are areal images of erosion-prone foreshores, with comparisons using historical photographs. It argues that the nature of many of the modern tidal platforms are symptomatic of active uplift and that due to uplift, shoreline erosion does not necessarily result in shoreline retreat.

Chapter Five reviews seismic and tectonic history within the Raglan region. Through selective analysis of the seismograph record, possible relationships between concentrations of seismic events, published faults, and hydrothermal springs are identified. A potential source of the stress driving apparent differential VLM is identified.

Chapter Six describes the location, nature and age of a speleothem flowstone selected as a proxy of maximum RSL within a specific timeframe.

Chapter Seven compares tide dissolution notch development in rocks at 2 locations over a 110-year timeframe, comparing historic and 2022-23 photographs.

Chapter Eight describes the characteristics of 6 specific shellbeds located within 4 raised terraces. Macro and micro fossil distribution and concentrations are discussed in relation to potential deposition dynamics. Included are sediment core samples and cross-sections relating to 2 key terraces, along with uplift evolution modelling.

Chapter Nine briefly describes overall conclusions based on specific chapter summaries, along with recommendations on proposed future research pathways.

CHAPTER TWO

LITERATURE REVIEW

2.1: Literature Review Introduction

Prior to the 21st century the prime emphasis behind research on New Zealand's (NZ) raised marine terraces was an attempt to correlate these with eustatic glacial/interglacial-driven sea level (SL) curves. Particular attention was given to SL associated with the most elevated marine terraces, often 10's of meters above the present mean SL. The early researchers hypothesised over whether these large oscillations in SL were due to ESL change or mass vertical land movement (VLM) (Hutton, 1867; Henderson, 1926). Jobberns (1928) and King (1930) introduced the concept that RSL may vary due to differential VLM.

While attempts were being made to match the NZ terraces with other global examples and ESL curves, Gage (1953) questioned the validity of these correlations. Nevertheless, throughout the mid-20th century the research emphasis was on matching elevated marine terraces with the globally adopted Monastirian, Tyrrhenian, Milazzian, and Sicilian sequences of the Mediterranean (e.g. Brothers, 1954) and the Huon Peninsula, Papua New Guinea sequences (e.g. Chappell, 1975).

This era of terrace correlation through describable physical properties, such as paleo beach surfaces and identifiable tephra beds, resulted in credible models on RSL change in specific NZ regions over millennial timeframes (e.g. Chappell, 1970; 1975).

Along with the development of geochronological methodologies in the mid-20th century (e.g. ^{14}C radioisotope, luminescence dating, amino acid racemisation) more accurate correlations between terraces at different locations around NZ continued to develop (e.g. Kear and Waterhouse, 1961; Chappell, 1970, 1975; Ota et al. 1992).

However, Clement et al. (2016) find that RSL data in NZ is fragmented and sparse. This conclusion may be due to the differing research programs' objectives which are constrained by geographical and chronological scale.

With the start of the 21st century came the increased focus on SL change hazards. This was magnified by officially adopted models predicting RSL rise acceleration within the following century (NIWA, 2020). These predictions, should they eventuate, could be catastrophic for many NZ foreshore locations. According to this literature review 21st century SL change models were largely formulated via desktop interpretations of pre-existing information, rather than original research that could add to the knowledge.

Throughout its history, research has progressively shifted from global/national perspectives through to regional and localised scales, where the common impetus is on RSL change and impact within km-scale shoreline sections. This change in focus also relates to the time-periods over which change is established or predicted. Whereas early researchers were commonly focused on SL change involving tens of metres over tens of thousands of years, given the current governmental and industry focus on hazard projections, demand within the 21st century is more likely to focus on cm-scale SL change over single century timeframes.

It is within this cm-scale that the commercial impetus that drives much of modern research lies, as it directly impacts the value of beachfront properties and amenities. The research emphasis has shifted somewhat to predictions and impact of SL change in relation to small communities and/or individual properties on which local Government hazard boundaries have been overlaid in district plans.

However, the preceding large-scale work remains an indispensable record of how the regional and eustatic background influences interpretations from which we can make meaningful predictions. These preceding large-scale research programs can be considered important and applicable to century-scale projections.

The sparse NZ RSL data that Clement et al. (2016) refers to begins with limited and/or missing tide gauge data and/or the lack of sufficient dating materials from which rates of VLM could be measured. Metrics are particularly sparse in coastal locations outside of the NZ main centres, where direct measurement of land deformation is now being recorded by real-time communicative global positioning systems (cGPS) (LINZ, 2024).

On 20/01/2024 an internet accessible VLM tool created by NZ SeaRise (2022) reported subsidence of 0.68 to 3.8 mm/year at various locations around the Raglan Harbour foreshore (Section 2.3, page 22). This was based on Geodetic (InSAR) observations and cGPS VLM data. It cautions against adoption of these metrics on more granular scales than their 2 km datapoint separations. It acknowledges the integral uncertainty within the topic by including a disclaimer over its data applicability. Likewise, a guide for Local Governments in NZ on the impact of rising SL coastal hazards includes a disclaimer absolving the publication from any legal obligations regarding any action taken as a result of reading, or reliance placed on the publication (Bell, et al., 2017). These disclaimers underscore the uncertainties in determining SL rise and the need for further validated research, from which applicable metrics can be adopted with confidence.

This literature review traces the progression of publications relating to RSL change in NZ, with a particular emphasis on research directly addressing or incorporating VLM relating to the central west coast of the North Island (NI). While the majority of NZ's coastline has not been directly studied in relation to RSL this review will demonstrate that the combination of past studies can form a foundation on which future research can progress. While peripheral topics such as marine flooding projections, sedimentation and erosion rates are included in this review it is not designed to be exhaustive in these respects.

2.2: Marine Terrace Characterisation

Elevated terraces along northern NZ coastlines were being described in geological reports as far back as the mid-19th century (Dieffenbach, 1843; Hochstetter, 1867). These were often identified through their 'staircase' morphology. In general, terrace geology was described as comprised of noncohesive sands, silts and muds, of a marine or coastal eolian origin. ESL change was believed to be the main control over their origin i.e. that these were paleo-beaches exposed through marine regression.

By the early 20th century some researchers were questioning the assumption that NZ was a stable, rigid landmass and that terrace elevations were entirely the result of SL regression. Jobberns (1928) and King (1932) hypothesised that the landscape was subject to differential VLM.

Site-specific studies of terraces along the NW coast of NZ are mostly confined to the mid to late 20th century (Figure 2.1). The early studies attempted to categorise and correlate individual terraces with international geochronological benchmark type-sections, based on glacial/interglacial-driven ESL curves. These interpretations were not without controversy**.** Gage (1951) cautioned that the possibilities of correlations of terraces within New Zealand were limited and that overseas correlation was problematic**.**

Brothers (1954) correlated multiple terraces in the Kaipara region with the Pleistocene chronology of Europe, in particular the Mediterranean sequences (Monastirian, Tyrrhenian, Milazzian, Sicilian) with little consideration of the potential influence of VLM. On the Kaipara coast, terraces vary in elevation from 2 m to > 100 m (Table 2.1). Brothers (1954) hypothesises that the terraces were a result of steady marine regression beginning in the late Pliocene. This regression was terminated by the Flandrian transgression, which in turn was terminated by a post-Flandrian regression-transgression cycle of ~ 1 m RSL change. Brothers (1954) also infers that ESL oscillations occurred within a general regression.

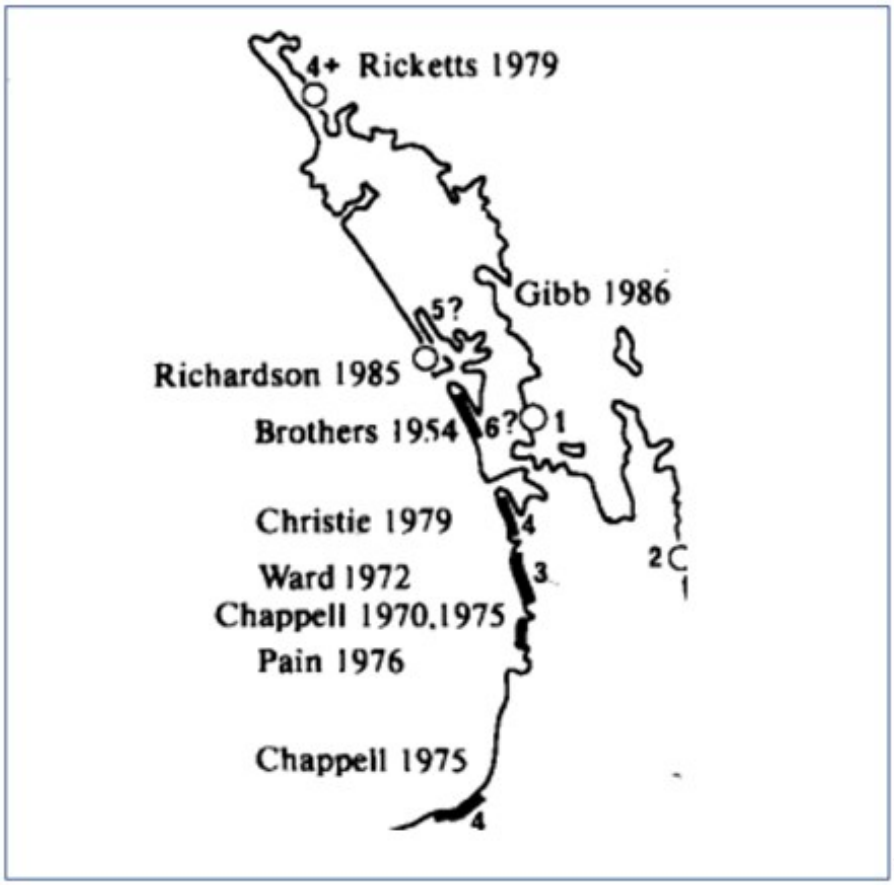

Figure 2.1: Twentieth century marine terrace studies along the northwest coast of New Zealand. After Pillans (1990, Fig 1).

Table 2.1: A corelation of glaciations with the Kaipara terraces. After Brothers (1954, Page 690)

Glaciations	*High Sea-levels*	*Average Height*	*Kaipara*
	Sicilian	100 metres	350 ft. (107 m.)
Early Glaciation:			
Antepenultimate Interglacial:	Milazzian	60 metres	220 ft. (67 m.)
Antepenultimate Glaciation:			
Penultimate Interglacial:	Tyrrhenian	32 metres	110 ft. (31 m.)
Penultimate Glaciation:			
Last Interglacial:	Main Monastirian	18 metres	50 ft. (16 m.)
	Late Monastirian	7.5 metres	20 ft. (6 m.)
Last Glaciation:			
	—— Flandrian transgression ——		
Postglacial:			

The attempted correlation of the NZ terraces with common global standards based on the globally accepted Mediterranean and Huon Peninsula datums was to dominate terrace research up until the publication of mean isotope stages (MIS) in the late 1970's, depicting global ice volume curves. Subsequently, throughout the late 20th century multiple authors began to correlate NZ terraces with the global datums (e.g. Berryman, 1993; Pillans, 1990a, 1994; Ota et al., 1996; Suggate, 1992).

In a reconstruction of stratigraphic nomenclature in the Whangaparoa area, Chapman-Smith & Grant-Mackie (1971) link terraces of ~ 30 m and 63 m above average mean SL with Milazzian and Tyrrhenian SL's. They propose that a variation in elevation of these terraces in relation to the historic ESL curves is evidence of VLM in the Bay of Plenty.

Many of the stratigraphic correlations along the NW Coast of NZ's North Island (NI) involved the Pleistocene Kaihu Group, which dominates the terraces' geology in this region. The Kaihu Group consists of poorly cemented sand, silt, and scarce lignite with some gravel overlying more consolidated rocks of late Pliocene age (Mildenhall et al., 1992). An attempt was made to identify marker beds within the Kaihu Group that could be recognised in other locations throughout the NI (e.g., Pillans, 1990a, 1994).

However, Gage (1953) expresses concern over the validity of the correlation of terrace elevations with ESL curves.

Wellman (1962), during a reconnaissance of the central NI coastlines, describes shellbeds in the Raglan Harbour as having an approximate elevation 0.65 m higher than their living tide-zone habitat. Based on this evidence, along with the elevation of rafted Taupo pumice deposited on dunes along the Raglan-Kawhia open coast the author concludes that "sea level could not have varied [sic] by more than 0.7 m since the last glacial age**".** Presumably by 'varied' he meant: 'not greater than'.

Chappell (1970) describes 6 Quaternary terraces along the NW coast of the NI. Paleo shore platforms are identified through the presence of sub-aqueous sediments, tephra beds, and wave-swept surfaces. Chapell (1970) finds that these terrace sequences correlate accurately with the Brothers (1954) interpretations. While VLM is not addressed in this work it is addressed in a later publication (Chappel, 1974).

Ward (1971) matches stranded shorelines in Gippsland, South Carolina, Morocco, Lebanon, and NW NZ, with those in Mangaia, Cook Islands. Mangaia is considered tectonically stable. Through comparing elevations of NZ terrace strandlines with matched Mangaia terraces he concludes that the NI central west coast was subject to an average VLM of 0.7 mm/year (uplift) throughout the Pleistocene.

Pain (1976), within his study of 3 Quaternary sand dune terraces in the Aotea-Kawhia region, draws upon the theory that marine regression resulted in an accelerated sand supply and correlates this with sand member volumes. Through adopting a VLM of 0.25 mm/year (uplift), established by Chappell (1975) he calculates terrace ages varying from 62 - 83 ka. Without an accurate benchmark and certainty over the corelation of specific terraces on the global scale, these variations could not be considered as absolute. By default, the earliest work by Brothers (1954) was often used as an appropriate datum, in the belief that the Kaipara region was essentially tectonically stable throughout the Holocene (Chappell 1970).

Chappell (1975) locates and describes multiple terraces along the NW coast of NZ, from Nth Taranaki to the Kaipara Heads. Notably, none of these examples are located on harbour foreshores (Figure 2.2).

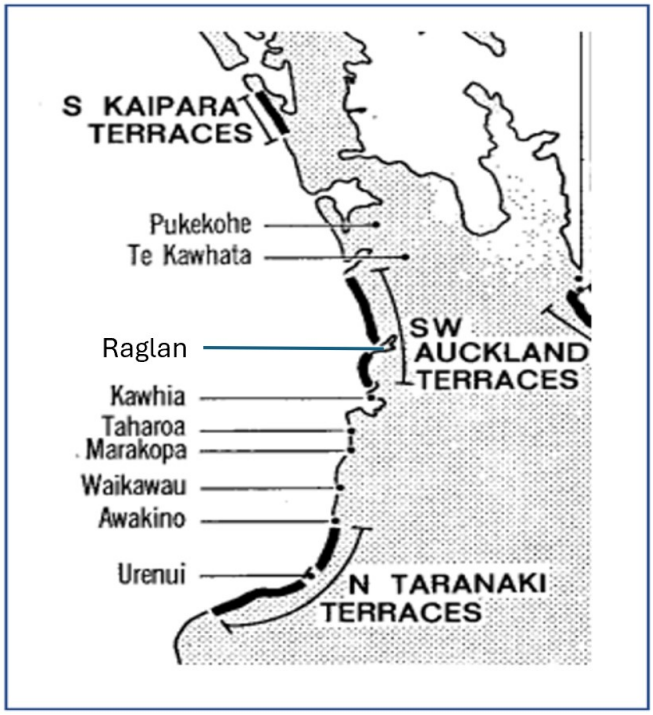

Figure 2.2: Northwest coast of New Zealand marine terrace locations. Adapted from Chappell (1975, Figure 1).

Chappell (1975) directly addresses warping and uplift rates. He proposes relationships between the younger terraces and MIS Upper-Quaternary ESL's**.** This work relies heavily on tephra marker beds within the Hamilton and Kauroa Ash formations, and paleo wave-swept platforms, as a NZ terrace correlation method. Based on these correlations, reconstructions of VLM and marine terrace age models for northern NZ are proposed (Figure 2.3). These appear to be credible in comparison with more recently acquired age metrics (e.g. Hayward et al., 1999b; Litchfield et al., 2022; Ota, et al., 1988; Pillans, 1990; Ryan, 2020). However, given the age-range and degrees of weathering in the older volcanic ash beds accurate identification of distinct maker beds is problematic (Briggs et al., 1989).

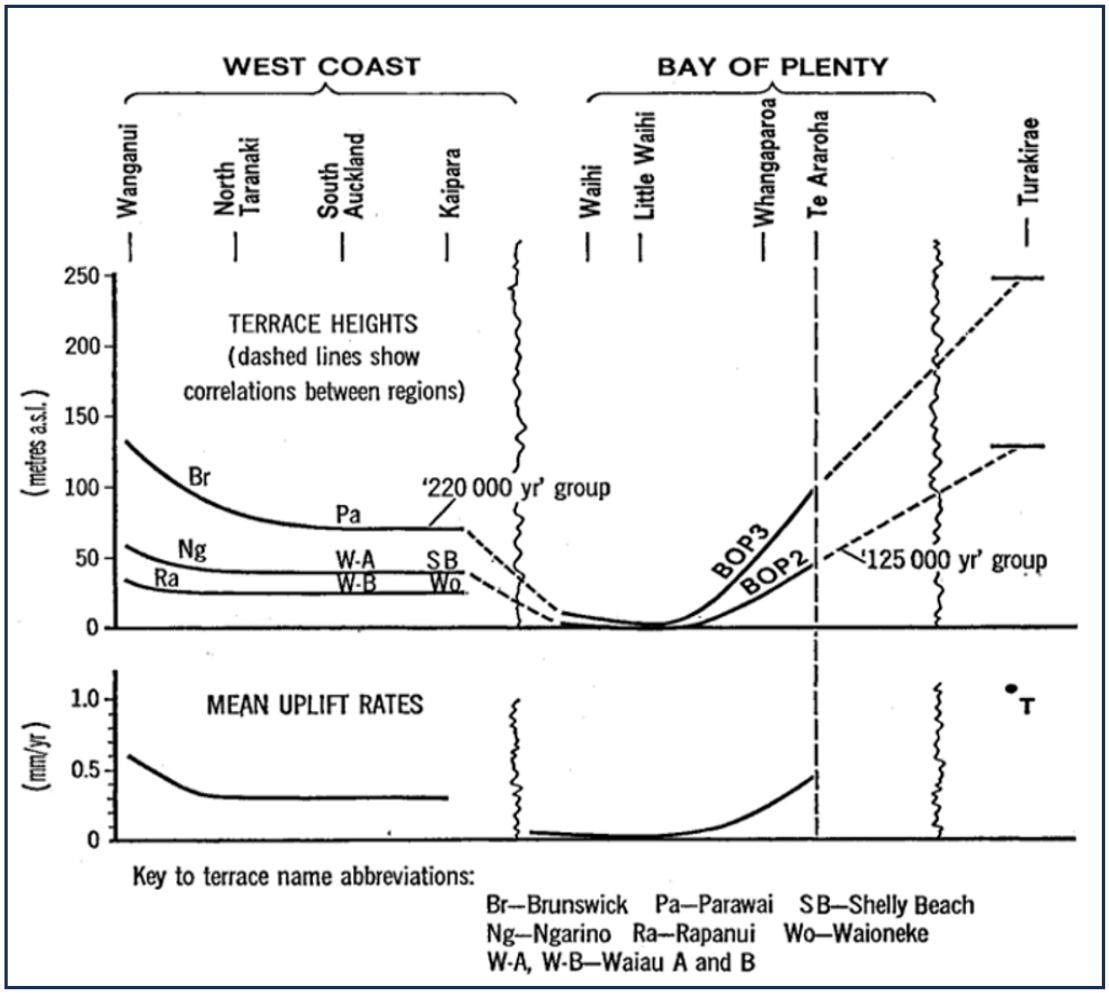

Figure 2.3: Age and rates of marine terrace uplift in northern NZ. Adapted from Chappell (1975, Figure 8).

Barter (1976) describes a sequence of terraces on the Awhitu Peninsula (25 km SW of Auckland) ranging in elevation from 8 m to 70 m. Through adopting Chappell's (1975) calculated mean uplift rate for this region of 0.3 mm/year, Barter (1976) dates and matches the age-event of these terraces with constructs in former studies**.** Sediments are found to be devoid of calcareous shell material (a common observation). While radiocarbon dating became available in the mid 1960's the absence of macrofossils within many studied terraces is a notable feature in the literature.

Pillans (1990) comments that while various authors proposed NZ terrace correlations with MIS's and the New Guinea sea-level record (e.g. Berryman, 1985; Chappell, 1975; Ward, 1988b) that only 2 of these studies' conclusions were based on dated material. He reports that only a few of the available dating methods (e.g. fission-track, amino-acid racemisation, uranium series) had been used for dating marine terraces up until 1990 with little suitable radiocarbon dating material discovered and that the radiocarbon dating methodology was unreliable (e.g. Gibb, 1986**).** However, based on research leading up to the late 20th century Pillans (1990) provides a credible summary of mean Pleistocene VLM in northern NZ (Figure 2.4).

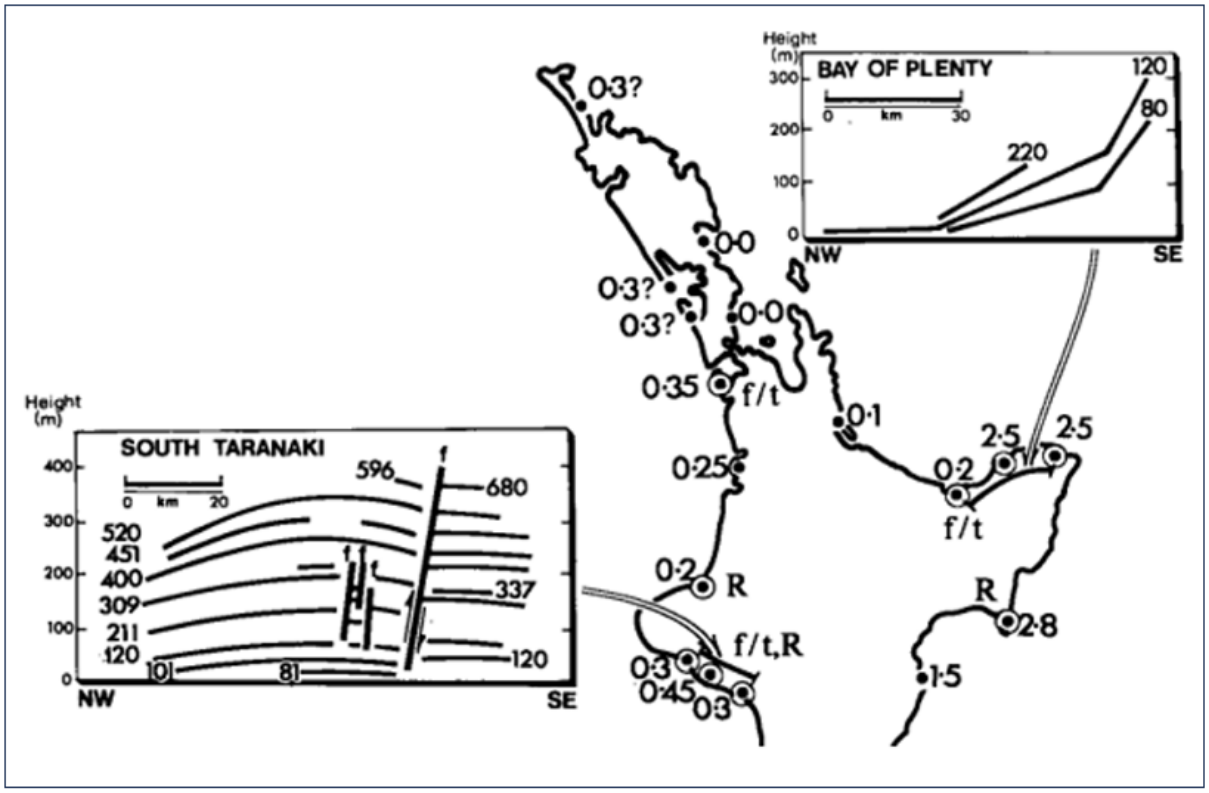

Figure 2.4: Average rates of uplift (mm/year) based on height of inferred 120,000 year old (stage 5e) terrace. Insets show detailed terrace deformation in three areas after Yoshikawa et al. (1980), Pillians (1983) and Ward (1988a). Sites are where identification of 5e terrace is supported by numerical ages and indicated (f/t, fission-track; R, racemisation; U/Th, 234U/230Th dating methods) except for NW Nelson where only 1 older terrace is dated by U/Th and palaeomagnetism (Williams, 1982). After Pillans (1990, Figure 9).

Radiocarbon dating of shell material and foraminifera chronology become more common in the late 20th century, after the impact of coastal flooding became a topical issue. This resulted in a focus on the younger low-lying terraces and salt marshes in which datable organic material has survived (e.g. Hayward et al., 2012; Ota et al. 2010). Moreover, dating of inorganic materials had become increasingly common by this time (e.g. Alloway et al., 2004; Chappell, 1975; Litchfield, 2008; Lowe et al., 2001; Milne, 1973; Pillans, 1990; Shane et al., 1996a).

The uncertainty over VLM direction and rates continued into the 21st century. Clement et al. (2016) report that studies addressing discrete aspects of paleo SL indicators often lacked the support of indicative geological contexts. However, these principles continued to be adopted in isolated studies in the early 21st century e.g. Claessens et al. (2009) provide evidence of an acceleration of uplift to a maximum of 0.42 mm/year throughout the last 50 ka through tephrochronological correlation of 13 fluvial and marine terraces in the Waitakere Ranges (West Auckland).

Due to its proximity to the tectonically active Hikurangi Trench, the NE coast of NZ has attracted more research attention than the more passive latitudinal equivalent on the west coast. Kear and Waterhouse (1971) conclude that a series of raised beaches at Waihi Beach correlate accurately with those at Kaipara - deemed by them to be tectonically stable throughout the late Pleistocene. Selby et al. (1971), through identification of tephras of known ages mantling the Waihi Beach terraces, proposed an adjustment to the Kear & Waterhouse (1971) interpretations. He proposes a more reliable datum from which to measure relative elevations.

Through radiocarbon dating of multiple shell, wood, and peat samples from terraces at 9 locations on the East Cape, Ota et. al. (1992) estimate that uplift rates at various terrace locations range from 1.5 - 4 m/ka years. However, the East Cape is within a very different tectonic setting to the NW coast of NZ (Nicol et al., 2007).

Through utilising palaeontological and amino acid dating methods Berryman (1993) correlates multiple terraces on the Mahia Peninsula with datums at the Huon Peninsula, Papua New Guinea, from which an average annual uplift of the youngest of 6 terraces to be in the region of 1 - 3 mm/year throughout the last ~ 40 ka is estimated.

The common perception that the Northland-Auckland region was tectonically stable attracted proxy ESL change indicator research in this region, an example being foraminiferal studies within harbour salt marshes by Hayward et al. (1999b).

Throughout the 21st century the weight of literature shifts towards summaries of prior research. Clement et al. (2016) summarise 164 unpublished reports, papers, and theses relevant to marine terraces in NZ. These include 216 radiocarbon-dated paleo sea-level indicators (Table 2.2). These authors argue that the commonly adopted marine terrace characterisation model proposed by Gibb (1986) is not fit for purpose due to potential radiocarbon dating inaccuracies. Based on a desktop study Clement et al. (2016) conclude Coromandel Peninsular on the NI east coast is subject to a long-term uplift rate of $\leq$ 0.3 mm/year. Auckland and Northland coastlines are concluded to be stable. This interpretation contrasts with the Claessens et al. (2009) study that reports long-term average uplift rates of $\leq$ 0.3 mm/year near Auckland**).** A further reconstruction by Ryan et al. (2020) is compiled from data within the World Atlas of Last Interglacial Shorelines (WALIS) in which Kawhia is deemed to be stable. Ryan et al. (2020) find that published indicators generally lack adequate description and age constraints, and that future work requires better stratigraphic descriptions, along with improved geochronological methods.

Table 2.2: Tectonic deformation (uplift) rates for the northern North Island. After Clement et al. (2016, Table 4)

	Area / Site	Region	Analysis of tectonic regime	Range of suggested tectonic deformation rates	Adopted tectonic deformation rate and error	Principal sources
A	Northland / Auckland	Northern North Island	Stable	-	-	Clement (2011); Beavan and Litchfield (2012); and many references therein
B	Coromandel Peninsula	Northern North Island	Long-term uplift	0.25-0.30 mm yr^{-1}	0.275 ± 0.025 mm yr^{-1}	Pillans (1986); Abrahamson (1987); Clement (2011); Beavan and Litchfield (2012)
C	Miranda / Kaiaua	Northern North Island	Stable	-	-	Schofield (1960); Woodroffe et al. (1983); Clement (2011)

King et al. (2020) discuss the temporal range and applicability of various VLM proxy analyses methods. They argue that the national cGPS VLM network data was of insufficient duration from which accurate VLM conclusions could be established, and that high-resolution studies of salt marsh foraminifera remained an important proxy when combined with the full range of methodologies (Figure 2.5).

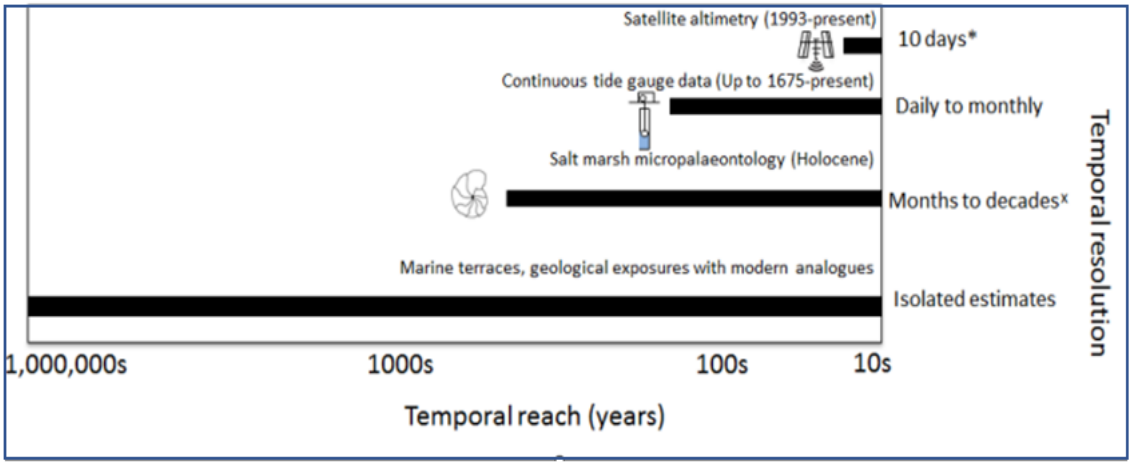

Figure 2.5: Temporal reach of methodologies relating to marine terrace characterisation (King et al., 2020, Figure 2).

Ryan et al. (2020) summarise the relevance of the current state of knowledge in NZ in relation to the latest interglacial period. 77 RSL indicators from 120 studies are analysed in this work. A notable feature of this summary is the wide range in terrace elevations (0 to 6 m) reflecting differing tectonic settings and differential VLM throughout NZ. The comparatively confined age range suggests that the dating of terraces by different researchers using different methods has become reasonably consistent (Table 2.3).

Table 2.3: Age and elevation of RSL-indicating terraces generated during the latest interglacial (MIS 5 and MIS 5e). Adapted from Ryan (2020, Table 3)

RSL Indicator Primary Reference	Last Interglacial		
	Height (m)	Age (ka)	Reference(s)
MIS 5			
Te Punga 1962; Fleming, 1972	-	120-80	-
Mildenhall, 1995	-	125-70	Pillans, 1991
MIS 5e			
Chappell, 1970; 1975	5 ± 3	120	Chappell, 1974; Bloom et al., 1974
Pillans, 1983; 1990b	5	120	Chappell & Veeh, 1978
Palmer, 1988	-	c. 120	Pillans, 1985
Berryman, 1993	6 ± 5	124 ± 5	Chappell & Shackleton, 1986
Kim and Sutherland, 2004	3 ± 2	120	Lambeck & Chappell, 2001
Litchfield and Lian, 2004	-	128-113	Chappell et al., 1996
Cooper and Kostro, 2006	5 ± 2	c. 125	Veeh & Chappell, 1970; Harmon et al., 1983; Chappell et al., 1996; Stirling et al., 1996
Wilson et al 2007	0 ± 5	125 ± 5	Pillans et al., 1998
Oakley et al, 2017; 2018	5 ± 2	124.5 ± 5.5	Lambeck & Chappell, 2001; Siddall et al., 2007

2.3: Tectonics and Vertical Land Movement Literature

Given its tectonic setting and significant earthquake history, NZ has attracted considerable tectonics research throughout the last century. Figure 2.6 identifies locations of seismic event epicentres at ≤ 35 km depth. This displays a lineal relationship between concentrations in the Huntly region and ~ 20 km offshore of Raglan (https://otago.maps.arcgis.com/ (2021). Chapter 5 of this thesis discusses these relationships and their association with active tectonics.

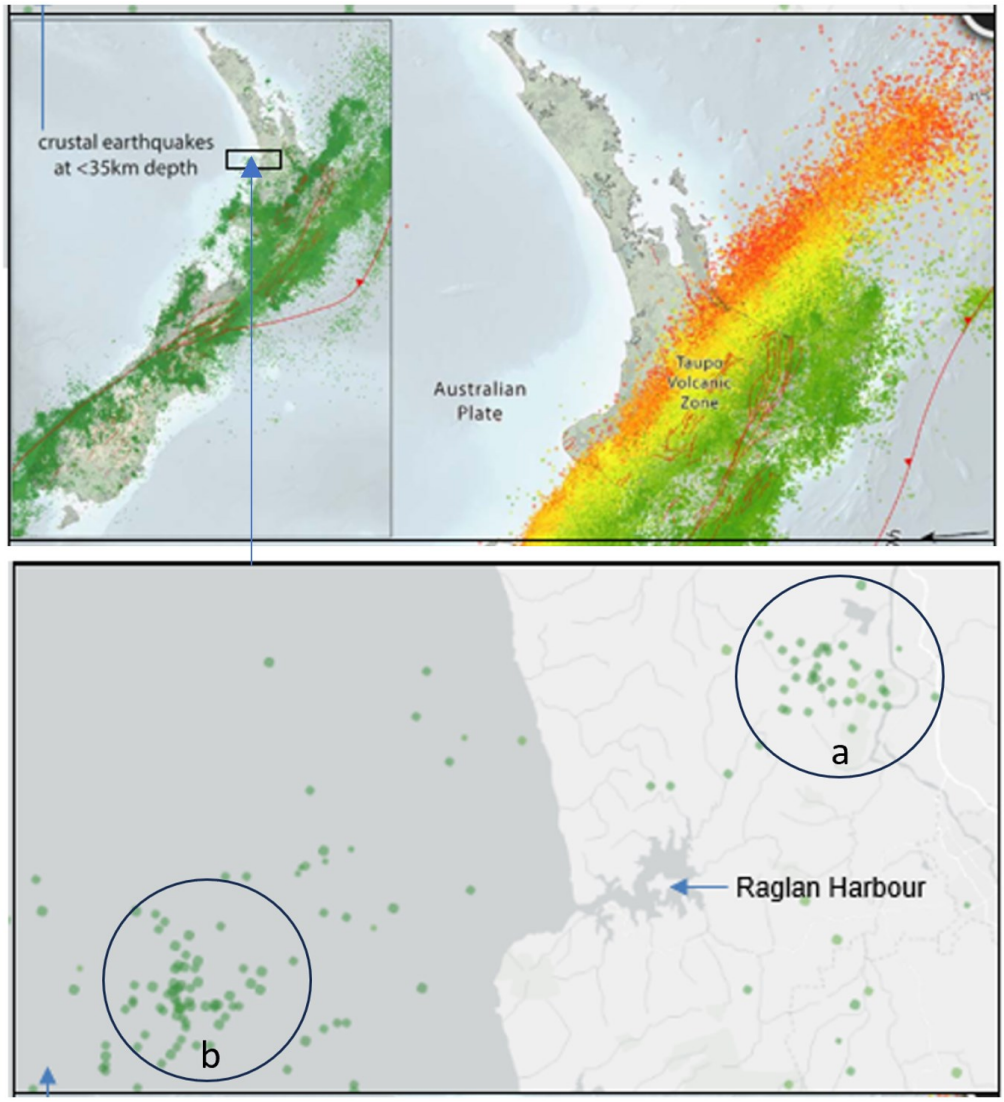

Figure 2.6: Earthquake depths and crustal earthquakes at <35 km depth in the Raglan region. Concentration in Huntly (a) and ~ 20 km offshore (b) are circled. Extracted from a generation by https://otago.maps.arcgis.com/ (2021). Data source: GeoNet (2020).

Researchers have utilised a wide range of proxies to establish past deformation in the NZ landscape. While Sections 2.1 and 2.2 demonstrate that constraints on large-scale VLM in NZ are becoming established, localised VLM and lateral displacement data remains sparse. Tectonic strain at a regional scale effecting the Raglan region involves the Taranaki Basin, located directly offshore from Raglan. This complex transitioned from a thrust zone to an extensional graben during the Cretaceous–Palaeocene (*c.* 80 – 55 Ma) (Strogen et al., 2017).

Nicol et al. (2007) create a model that outlines a significant change in tectonic strain rates and orientation throughout central NZ since the mid-late Miocene. They infer a cessation of compressional stress transitioning into modern-day extension (Figure 2.7). The uplifted Hakarimata range which forms the eastern boundary of the Raglan region is now considered to be tectonically stable (Kamp et al., 2014).

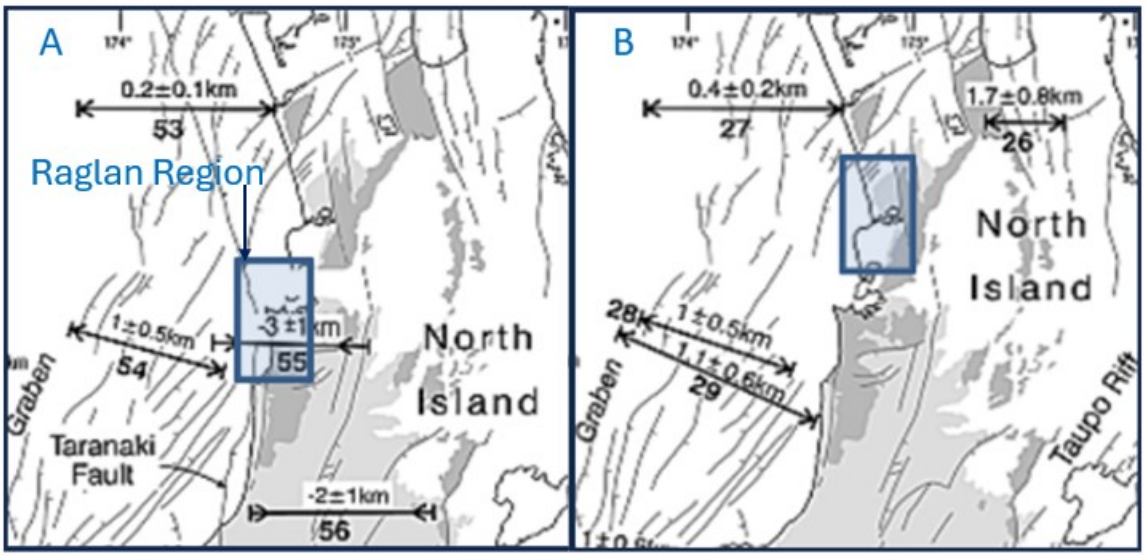

Figure 2.7: Estimated total pre and post tectonic transition strain values in the northern NI west coast region. Total tectonic compression of < 1 +/- 0.5 Km (A) changed to extension of < 1.7 +/- 0.8 km (B) in the inland Waikato during the Cretaceous–Palaeocene (c. 80 – 55 Ma). After Nicol (2007).

The sedimentary basin offshore from Raglan is referred to as the Taranaki Graben (McBeath 1977). Nicol et al. (2007) conclude that the Taranaki Graben is now subject to extension at an average rate of ≤ 1 mm/year. Accordingly, the area within the graben is likely to be subjected to subsidence. However, it is unclear from the Nicol et al. (2007) interpretation as to whether the onshore Raglan region is subject to this subsidence.

Litchfield et al. (2014) and GNS (2023) designate the Raglan region as part of the extensional western North Island fault zone which has relatively few recognised active faults. They recognise one active fault offshore that terminates at the coast south of Kawhia (Figure 2.8). It is deemed to have normal fault slip-rate of ≤ 1.5 mm/year. Aside from this, active faults influencing the western Waikato are not recognised.

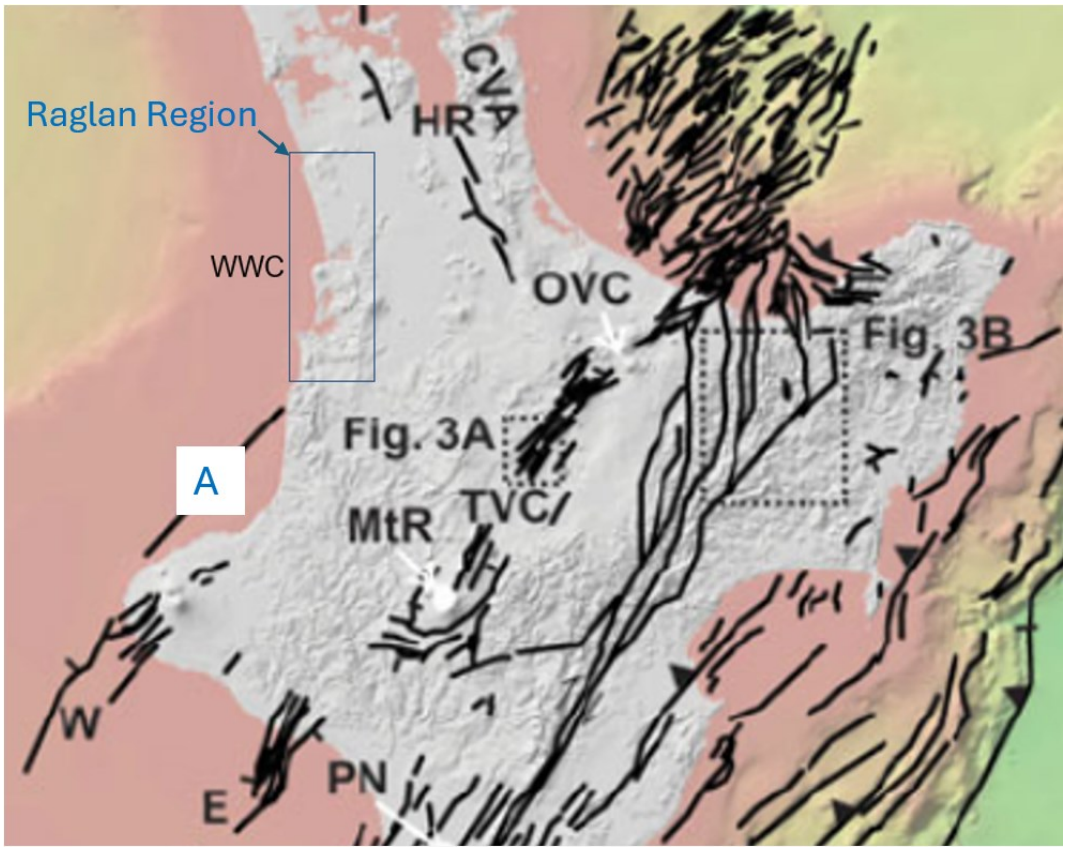

Figure 2.8: The absence of recognised active faults influencing the Raglan region within the NZ Active Fault Database (GNS 2023), with the closest being near Kawhai (A). Adapted from Litchfield et al., (2014, Figure 3).

By 2020, VLM measurement and data acquisition increased by a significant degree. Tide gauges at NZ's main centres were supplemented with continuous global positioning systems (cGPS). These apparatuses began to be installed in the 1990's, resulting in the current 39 cGPS stations throughout NZ. However, the majority of these are clustered in areas of interest relating to earthquake and volcanic eruption hazard prediction (GNS/GeoNet, 2023).

From cGPS station data covering the last decade Beavan and Litchfield (2012) estimate 0 – 1 mm/year uplift at the nearest cGPS station (HAMT) to Raglan Harbour (Figure 2.9).

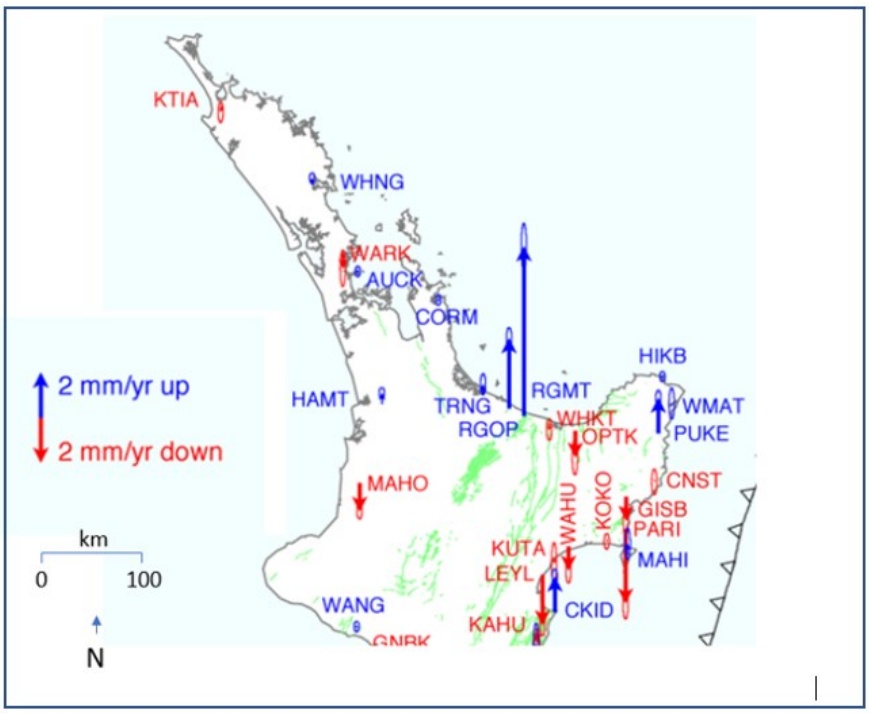

Figure 2.9: Projected VLM based on cGPS data. Adapted from Beavan and Litchfield (2012, Figure 6).

Given the lack of VLM and SL data for Raglan Harbour the Auckland record represents a possible alternative from which to derive approximate metrics. To estimate absolute SL change in Auckland, Hannah et al. (2010) adopt a tectonic-driven VLM of - 0.1 mm/year (subsidence) and a Glacial Isostatic Adjustment (GIA) of 0.3 mm/year (uplift**)** (Table 2.4). In comparison**,** Denys et al. (2020) calculate the Auckland VLM to be of the rate − 0.56 ± 0.17 mm/year (subsidence) based on nearly 20 years of cGPS data.

Table 2.4: Sea level change, GIA and tectonic displacement at New Zealand's 5 main centres (Hannah et al., 2010, Table 2)

Port	Relative sea level change (linear trend) ***a***	GIA Correction ***b***	GIA corrected sea level trend ***a + b***	Local Tectonic Motion from cCPS data ***c***	Absolute sea level trend ***a + c***
Auckland	+1.50 (0.09)	+0.30	1.80	-0.1	+1.4
Taranaki	+1.24 (0.32)	+0.33	1.57		
Wellington	+2.00 (0.17)	+0.30	2.30	-1.4	+0.6
Lyttelton	+1.90 (0.10)	+0.29	2.19	-0.2	+1.7
Dunedin	+1.28 (0.09)	+0.25	1.53	-0.2	+1.1
Mean	***1.6 mm/yr***		***1.9 mm/yr***		***1.4 mm/yr***

Hayward (2023) summarises the age and elevation of five marine terraces at two beaches in the Waitemata (Auckland) Harbour. These range in height from 0.15 to 4.3 m above the mean sea level (MSL) with ages varying from ^{14}C 3709 to 4835 cal. yr BP. From this data he concludes that significant subsidence has not occurred at these locations over the long-term (Table 2.5).

Table 2.5: Ages of and elevations of 5 marine terraces at Bucklands Beach (BB) and Eastern Beach (EB), Waitemata Harbour, Auckland (Hayward, 2023, Page 3)

Sample no	Year dated	Lab. no.	Dated material	Elevation wrt MSL	Radiocarbon age (yr BP)	Calibrated age age (yr BP)
BBi	2012	Wk33780	*Tuecetona* in situ	+0.15 m	4835±29	5152±210
BB1	2020	Wk50689	*Austrovenus*	+3.3 m	3720±43	3715±210
BB2	2021	NZA73444	*Paphies, Tawera*	+3.15 m	4822±28	5137±204
BB3	2021	NZA73453	*Austrovenus*	+3.6 m	3709±27	3699±192
EB1	2021	NZA73455	*Austrovenus*	+4.3 m	4440±28	4667±193

By 2017 sufficient data had accumulated to provide meaningful comparisons of cGPS with deformation rates established through conventional proxy methodologies. Houlie & Stern (2017) investigated potential statistical anomalies between stations clustered in specific geographical regions. cGPS stations with adequate data are found to be within a < 1 mm correlation with other proximal cGPS stations. This variation was considered statistically insignificant, indicating that there was general agreement between the stations.

The two cGPS stations most proximal to Raglan Harbour display contrasting VLM data (GeoNet, 2023). The Mahoenui (MAHO) station displays a trend of ~ - 20 mm since 2004 whereas Whatawhata (HMT) displays no significant change over this time-period (Figure 2.10). This variation is indicative of differential VLM between these two stations. It should also be noted that both stations display steps of ~ + 15 mm between the years 2018 – 2020. This is indicative of active tectonic behaviour and the potential for discrete dynamic VLM events within longer timeframes.

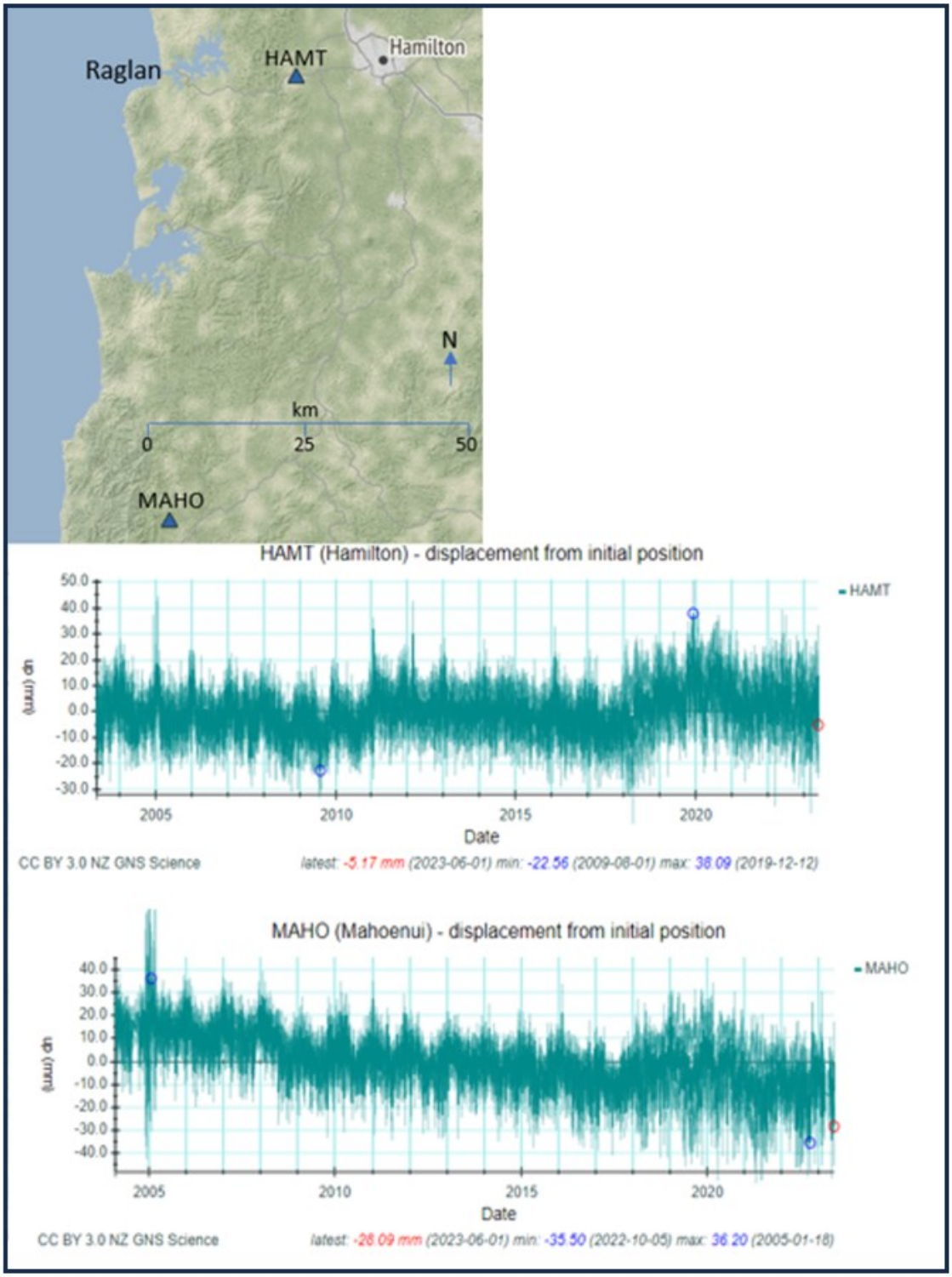

Figure 2.10: Vertical land surface displacement records of the Whatawhata (HAMT) and Mahoenui (MAHO) cGPS stations in the western Waikato. Retrieved from GeoNet. 2023.June.22.

By combining Radar (InSAR) observations from Envisat with interseismic campaign and continuous GNSS velocities throughout the period 2003 – 2011 Hamling et al. (2021) build a high-resolution velocity field of New Zealand, depicting VLM along the entire NZ coastline. The authors conclude that much of the west coast of the North Island is relatively stable with a slight subsidence of 1mm/year in the vicinity of Auckland. A cross-section from Hawkes Bay to Te Akau (Figure 2.11) generated by Hamling et al. (2021) includes the upper Raglan Harbour. This indicates that VLM for this locality has undergone around 1 to 2 mm/year (subsidence) throughout this time-period.

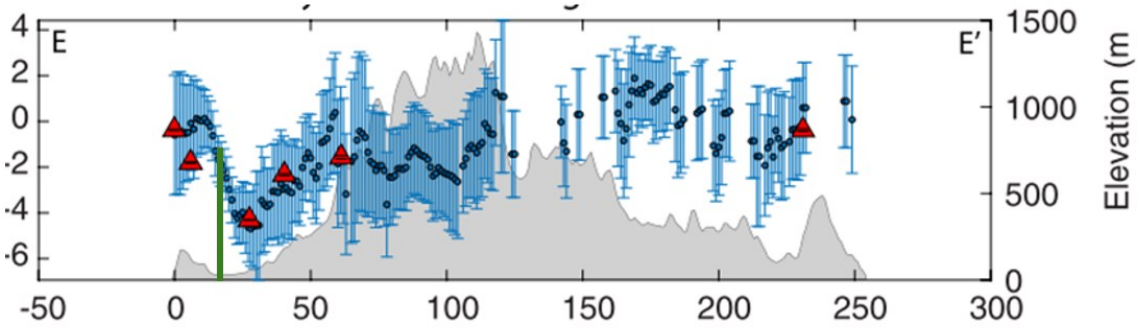

Figure 2.11: VLM cross section from Te Akau (E) to Hawkes Bay (E'). Blue dots and associated error bars are from the InSAR derived vertical velocities and the red dots are from GNSS located within 10 km of the profile. Topography is shown in grey with Raglan Harbour identified by the green vertical line. Adapted from Hamling et al. (2021, Figure 2).

Through using the same technology as Hamling (2021), the NZ SeaRise (2014), reported subsidence of 0.68 to 3.8 mm/year at 2 km interval locations around the Raglan Harbour foreshore. Most point data are within the range of 2 to 3.5 mm/year subsidence (Figure 2.12). This analysis was based on satellite altimetry (InSAR) records, calibrated to the NZ GeoNet cGPS network. It does not recommend adoption of this data for studies of scales within the 2 km spacings.

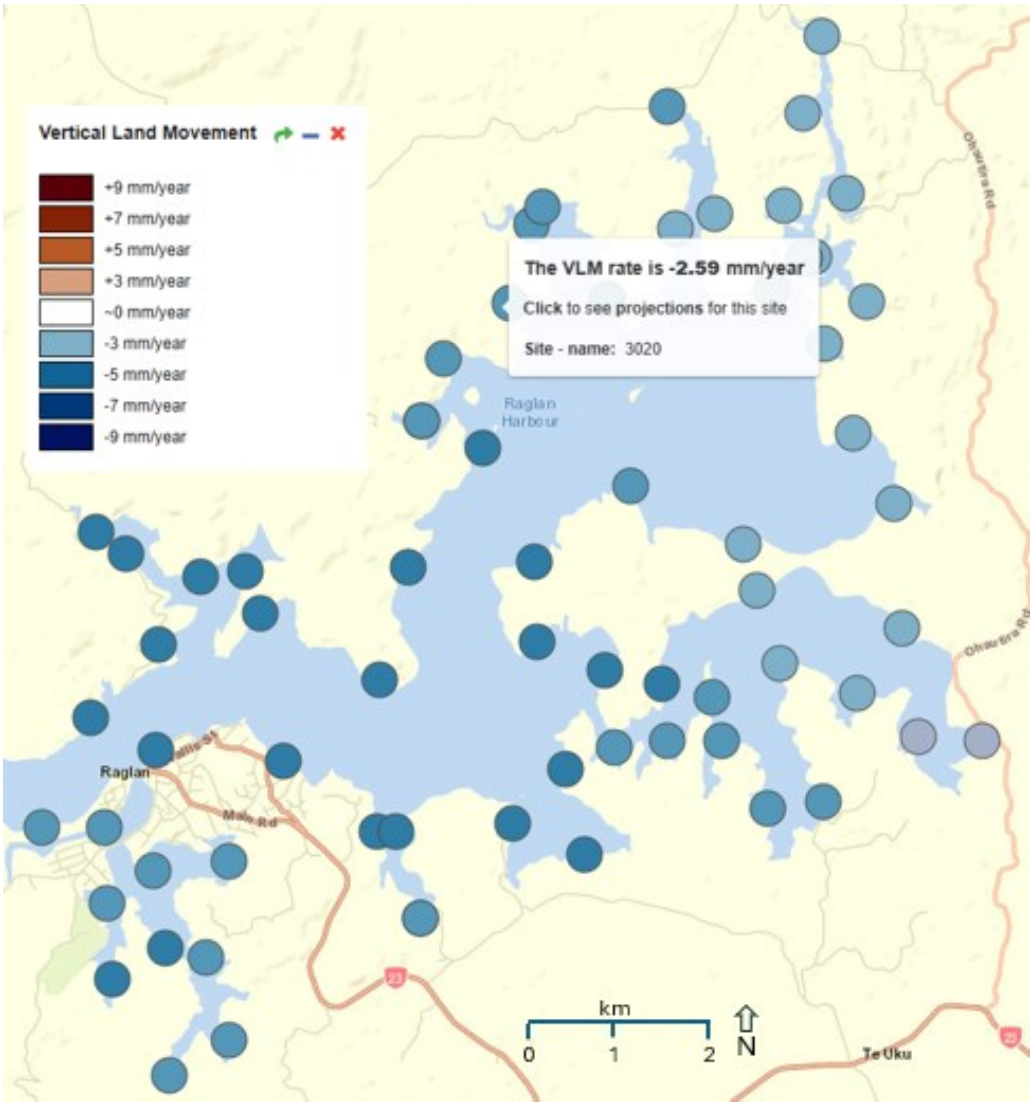

Figure 2.12: VLM point data in Raglan Harbour. Extracted as a portion of the NZ SeaRise online map.2024.Feb.12.

2.4: The Tide Gauge Record

In the absence of sufficient tide gauge data for Raglan Harbour the more complete Kawhia Harbour record is commonly used by researchers and authorities. The Kawhia Wharf gauge provides a near-complete record since 2008, in which there is no obvious RSL change trend (Figure 2.13a) The Raglan tide gauge record is incomplete (Waikato Regional Council, 2023). Gauges are located at 2 locations: Manu Bay boat ramp and Raglan Wharf. Both have been replaced within the recorded period of 2008 to present**.** The 2-year absence in data from 2010 and 2012 at Raglan Wharf was the result of a fire that destroyed the gauge. Given this missing data, and relatively short time-period over which data has been collected, the Raglan tide gauges can only be considered suitable for recent comparisons. (Figure 2.13)

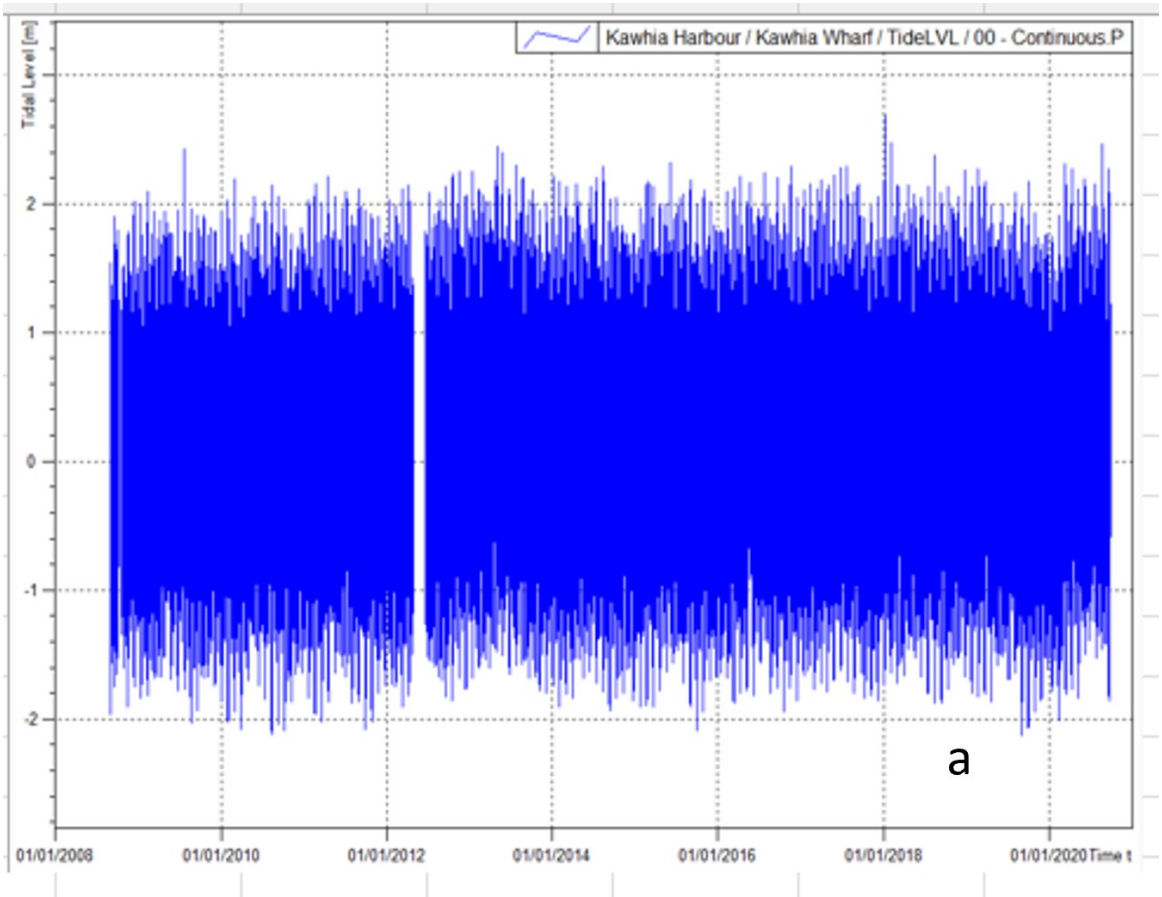

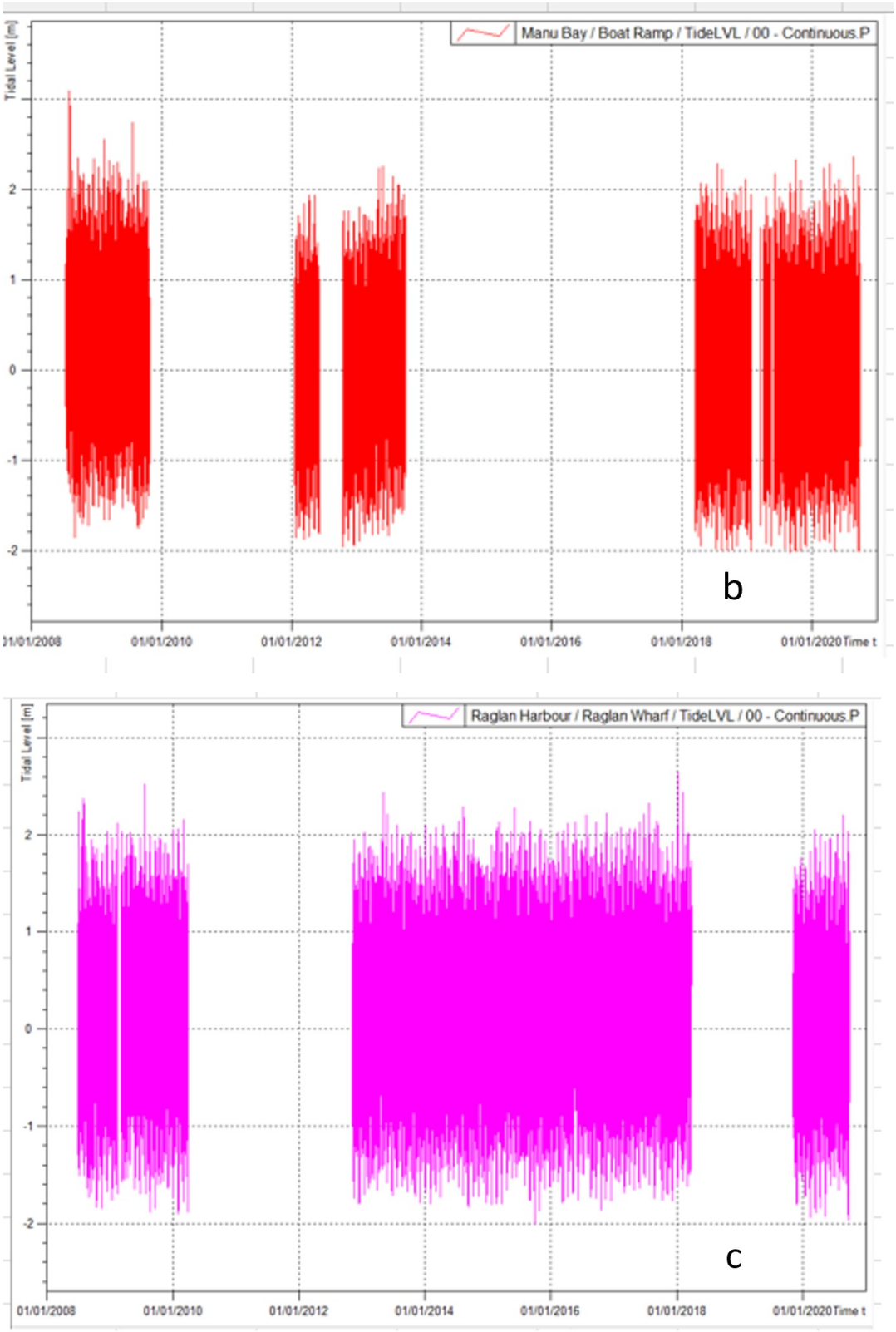

Figure 2.13: Tide gauge data at 3 western Waikato coast locations. Kawhia Wharf (a), Manu Bay (b), Raglan Wharf (c). Retrieved from Waikato Regional Council. 2023.Oct.10.

Tide gauges located within a 150 km distance from the research field area include those in Auckland and New Plymouth. Denys et al. (2020) provides a comparison between their own conclusions in regards to SL rise with that of Hannah (1990; 2004) where the RSL values range from + 1.3 to 2.18 mm/year (Table 2.6). In a re-analysis of tide gauge records and VLM at 5 NI locations the New Zealand Ministry for the Environment (2017) has similar values to Denys et al. (2020) for Auckland (1.6 mm/year vs 1.57 mm/year) (Figure 2.14).

Table 2.6: RSL trends for the 5 main centres in New Zealand. After Denys et al., (2020)

	Hannah (1990) (mm/year)	Hannah (2004) (mm/year)	This paper (mm/year)
Auckland	1.34 ± 0.11	1.30 ± 0.09	1.57 ± 0.15
New Plymouth			1.46 ± 0.54
Wellington	1.73 ± 0.27	1.78 ± 0.21	2.18 ± 0.17
Lyttelton	2.26 ± 0.14	2.08 ± 0.11	1.91 ± 0.13
Dunedin	1.36 ± 0.15	0.94 ± 0.12	1.35 ± 0.15

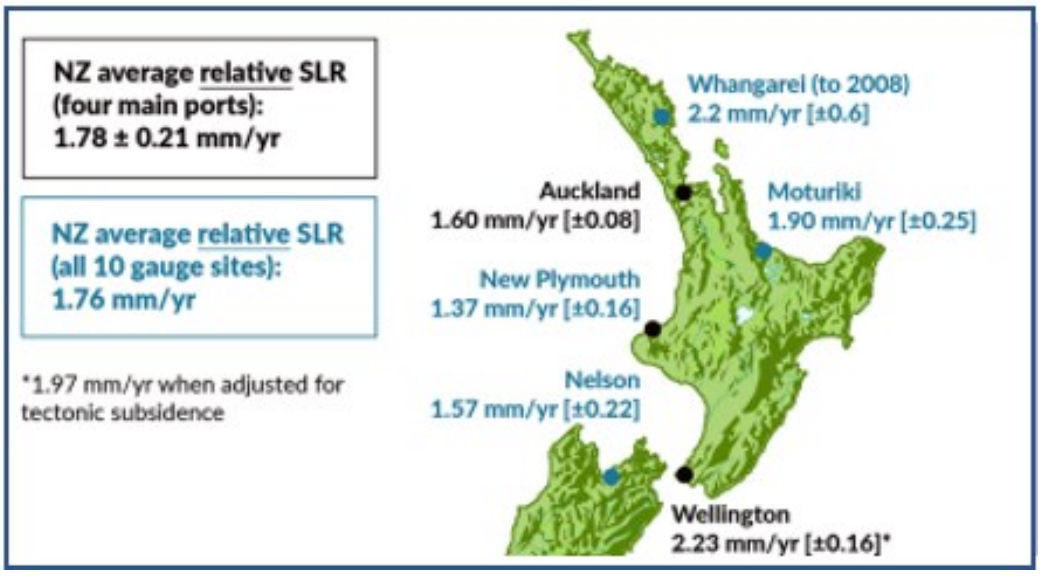

Figure 2.14: Average RSL rise at 6 tide gauge sites in northern New Zealand (extracted from NZ Ministry for the Environment (2017. Figure 2).

2.5: Geological Literature

In a study of sedimentation in the Raglan Harbour, Sherwood & Nelson (1979) define the geomorphology and structure of harbour as that of a drowned river valley (ria) formed within a structurally depressed fault-block, with a maximum depth of 18 m. Erosion throughout the last ≤ 85 ka has modified a stratigraphy dominated by Late Eocene to Early Miocene Te Kuiti Group calcareous mudstones and limestones, overlying Jurassic basement siltstone and sandstone. These rocks are commonly exposed as high-angle embankments or vertical cliffs of ≤ 40 m height around the foreshore (Waterhouse & White, 1994). Considerable tectonic faulting and deformation, combined with multiple lava flows from Okete and Karioi volcanic eruptions, result in a complex stratigraphic architecture (Briggs, 1983). Quaternary eolian sand and weathered tephra mantle much of the landscape (Barter, 1976; Carter, 2021).

Beginning with Hochstetter (1864) and Hutton (1867) a succession of studies of the Raglan Harbour geology have been published. Hochstetter (1864) describes the soils derived from the calcareous mudstone and the limestone outcrops. Hutton (1867) assigned the names 'Whaingaroa Clay' and 'Kawhia Limestone' to the dominant rocks in the harbour. Hutton (1867) appeared to be more interested in the productive potential of soils derived from these rocks than their specific geology.

The structural and stratigraphic complexity of the Te Kuiti Group rocks in Raglan harbour attracted multiple further studies (e.g. Kear & Schofield, 1959; Nelson, 1978a; Waterhouse & White, 1994). Based on lithostratigraphic and chronostratigraphic analysis, Tripathi et al. (2008) proposed an update of the nomenclature and stratigraphy of the Te Kuiti Group rocks exposed in the harbour (Figure 2.15).

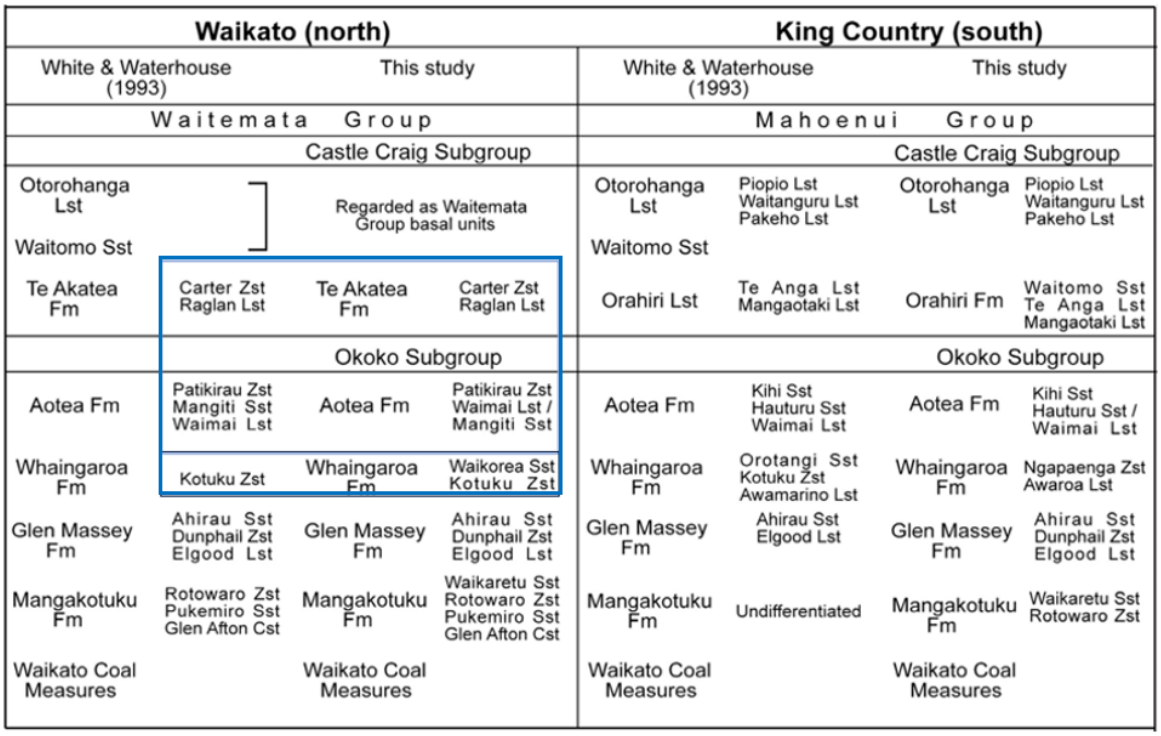

Waikato (north)				King Country (south)			
White & Waterhouse (1993)	This study			White & Waterhouse (1993)	This study		
Waitemata Group				Mahoenui Group			
Castle Craig Subgroup				Castle Craig Subgroup			
Otorohanga Lst	Regarded as Waitemata Group basal units			Otorohanga Lst	Piopio Lst Waitanguru Lst Pakeho Lst	Otorohanga Lst	Piopio Lst Waitanguru Lst Pakeho Lst
Waitomo Sst				Waitomo Sst			
Te Akatea Fm	Carter Zst Raglan Lst	Te Akatea Fm	Carter Zst Raglan Lst	Orahiri Lst	Te Anga Lst Mangaotaki Lst	Orahiri Fm	Waitomo Sst Te Anga Lst Mangaotaki Lst
Okoko Subgroup				Okoko Subgroup			
Aotea Fm	Patikirau Zst Mangiti Sst Waimai Lst	Aotea Fm	Patikirau Zst Waimai Lst / Mangiti Sst	Aotea Fm	Kihi Sst Hauturu Sst Waimai Lst	Aotea Fm	Kihi Sst Hauturu Sst / Waimai Lst
Whaingaroa Fm	Kotuku Zst	Whaingaroa Fm	Waikorea Sst Kotuku Zst	Whaingaroa Fm	Orotangi Sst Kotuku Zst Awamarino Lst	Whaingaroa Fm	Ngapaenga Zst Awaroa Lst
Glen Massey Fm	Ahirau Sst Dunphail Zst Elgood Lst	Glen Massey Fm	Ahirau Sst Dunphail Zst Elgood Lst	Glen Massey Fm	Ahirau Sst Elgood Lst	Glen Massey Fm	Ahirau Sst Dunphail Zst Elgood Lst
Mangakotuku Fm	Rotowaro Zst Pukemiro Sst Glen Afton Cst	Mangakotuku Fm	Waikaretu Sst Rotowaro Zst Pukemiro Sst Glen Afton Cst	Mangakotuku Fm	Undifferentiated	Mangakotuku Fm	Waikaretu Sst Rotowaro Zst
Waikato Coal Measures		Waikato Coal Measures		Waikato Coal Measures		Waikato Coal Measures	

Figure 2.15: Proposed update of the lithostratigraphy of the Te Kuiti Group. After Tripathi et al. (2009, Figure 5). Raglan Harbour rocks are within the blue rectangles.

Carter (2022) records several unmapped faults and raises questions regarding some of the Waterhouse & White (1994) and Tripathi et al. (2008) lithostratigraphic interpretations. These include the absence of a Whaingaroa Siltstone lithotype that overlies Raglan Limestone at specific locations. The published lithological interpretations do not match that of the Carter Siltstone lithotype classification assigned to it by Tripathi et al. (2009) and Waterhouse & White (1994). Carter (2022) recommends further research on this topic.

2.6: Sedimentation and Foreshore Evolution

Various studies underline the highly variable sedimentation dynamics throughout the harbour. Sherwood & Nelson (1979) describe Raglan Harbour as a sediment trap that transports and re-deposits a range of gravels, muddy sands, sandy muds and muds, comprised of quartz, feldspar, and clay minerals. They conclude that sediment transport and deposition is primarily under the control of cyclically variable multidirectional tidal flows of ≤ 500-1500 mm/s, and a complex bottom topography. The source of sediments is a combination of inland colluvium/alluvium transported by water courses into the harbour and directly eroded foreshore rocks. Sherwood & Nelson (1979) note a high occurrence of tidal wave-swept rock platforms of ≤ 100 m width, covered with a thin veneer of sediments. They conclude that the platform profiles were formed by erosion throughout the last 5 Ka (Figure 2.16).

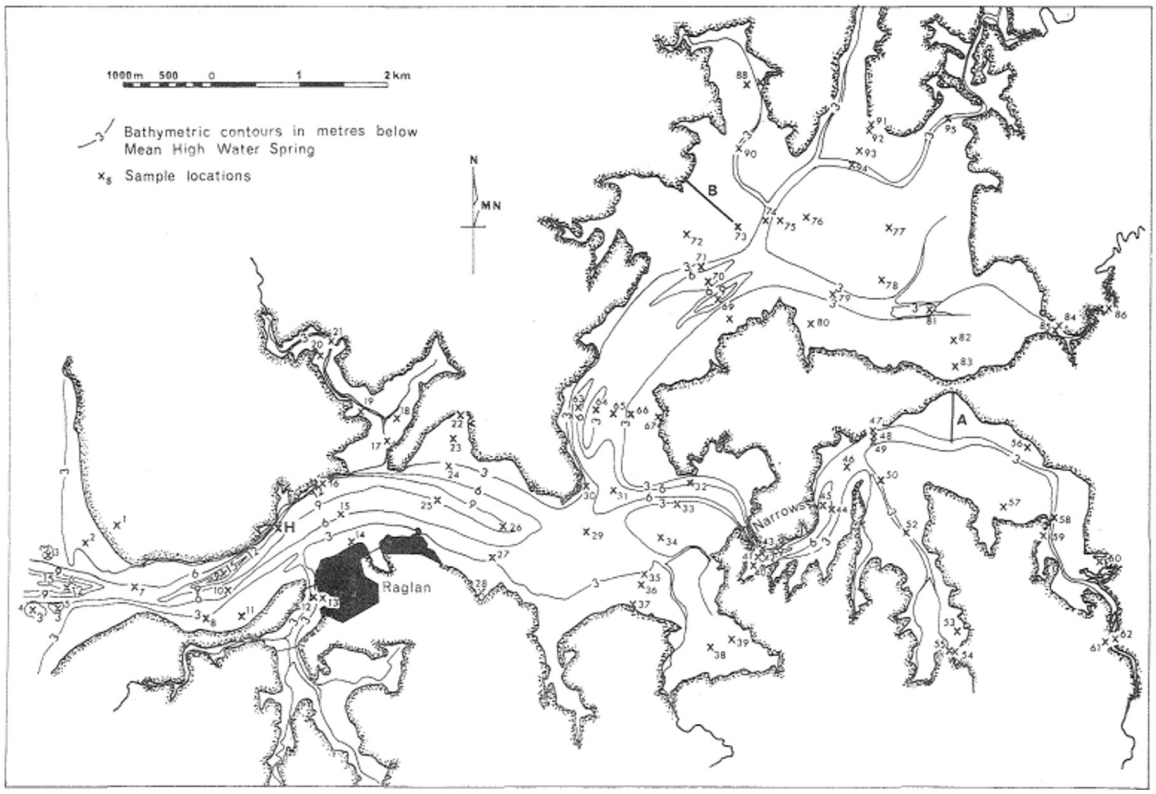

Figure 2.16: Generalised bathymetry of Raglan harbour (Sherwood & Nelson, 1979, Fig 4). **Large image**

With the objective of establishing baseline sediment accumulation rates (SAR) and the influence of changes in catchment land-cover, Swales et al. (2005) analysed the location, age and stratigraphic position of exotic pine pollen within 5 cores of sediment of up to 4 m depth. The age of pollen and sediments were established through ^{137}Cs, ^{210}Pb, and ^{14}C dating. The test sites were located within the two major upper harbour estuary branches fed by the Waitetuna and Waingaro rivers. Swales et al (2005) conclude that the SAR within the Waitetuna has increased ~ 3-fold, to a rate of 1.1 mm/year since 1890, from an average of 0.35 mm/year over the prior 6.5 – 8 ka. In contrast, the Waingaro estuary had insufficient pollen to establish robust constraints, the conclusion being that sedimentation due to human development in this estuary has not increased significantly.

Through sampling of suspended solids during and after a storm event within the Waitetuna estuary, McKergow et al. (2010) conclude that fine sediment load and flux are subjected to rapid escalation during extreme marine and/or rain-storm events. This is followed by tidal flushing and a return to pre-storm conditions within a relatively short time-period (4 tide cycles). They find that the dominant suspended grain-size is silt, 25 % of which is retained within the estuary. Half of the total mobilised sediment was identified as being of a sub-catchment origin i.e. imported via rivers and streams. By comparison, a geotechnical assessment of the Raglan bar (harbour mouth) conducted by Stark, et al. (2010) finds that sandbars that flank the Raglan bar surf-zone are highly mobile and can migrate laterally by as much as 220 m/year.

Stephenson et al. (2019) establish constraints on down-wear and back-wear erosion rates at terraces uplifted during the 2016 Kaikoura earthquake at Kaikoura (Cesca et al., 2017) The overall mean annual rate of down-wear (lowering) for all profiles was 2.3 mm/year post-uplift, compared to pre-uplift rates of 1.1 mm/year. Erosion rates are found to be comparatively rapid within the first years after uplift. The geomorphological evolution of seismically active foreshores subjected to increased subaerial exposure after uplift (e.g. the Kaikoura in 2016) is discussed in Horton et al. (2022). They conclude that accelerated rates of denudation due to enhanced post-uplift subaerial drying are likely.

2.7: Summary of Past Research

Aside from work by Ward (1971), Chappell, (1970 & 1975) and Pain (1976) (refer to Section 2.2) little attention has been paid to marine terraces along the western Waikato coast or harbours. The most relevant work was located proximal to Auckland, or on the more tectonically active east coast of the NI. Both are > 100 km from the Raglan study area. Given the complexity of NZ's tectonic architecture these studies are probably only partially relevant to VLM dynamics in Raglan Harbour.

Records of VLM involving low-lying terraces throughout NZ are comparatively sparse. Prior to the concern during the late 20th century over hazards imposed by projected SL rise, marine terrace research focused primarily on elevated terraces largely devoid of accurate dating material. Within the available literature, estimates of VLM along the western Waikato vary from a millennial-scale average of 0.7 mm/year uplift (e.g. Ward, 1971) to > 2.0 mm/year subsidence based on 8 years of inSAR data interpretations (NZ SeaRise, 2022). The dominant conclusion from the literature is that the location is stable. The 20-year record from the nearest cGPS station displays no significant change. Likewise, the Raglan and Kawhia tide gauge records for 2008 to 2021 display no apparent RSL change that matching the NZ SeaRise (2022) inSAR interpretations of significant RSL fall.

The weight of literature on NZ SL change suggests that in the absence of VLM, the RSL change in the Raglan Harbour is likely to be within the range 1.3 – 1.6 mm/year (de Lange, 2019; Denys et al., 2020; Hannah, 1990, 2004).

CHAPTER THREE

BASIC GEOLOGY AND GEOMORPHOLOGY

3.1: Geology and Geomorphology Introduction

The Raglan region is a portion of a coastal strip of similar geology extending from Mokau in the south to Port Waikato in the north. Its eastern extent is demarcated by elevated ranges and major fault-lines trending ~ north – south within uplifted Late Permian to Early Cretaceous basement (Kamp et al., 2014). This uplift is largely due to compressional forces imposed during the Kaikoura Orogeny beginning ~ 25 Ma BP.

The stratigraphy is largely comprised of a greywacke basement (the Murihiku Supergroup), overlain with Eocene to Early Miocene calcareous rocks (the Te Kuiti Group), and quaternary and volcanic materials (Waterhouse & White, 1994). Volcanic cones and lava flows of Pliocene-Pleistocene volcanics are common (Briggs et al., 1989). Due to differential erosion considerable missing time exists within major stratigraphic boundaries comprised of complex erosion surfaces (Figure 3.1).

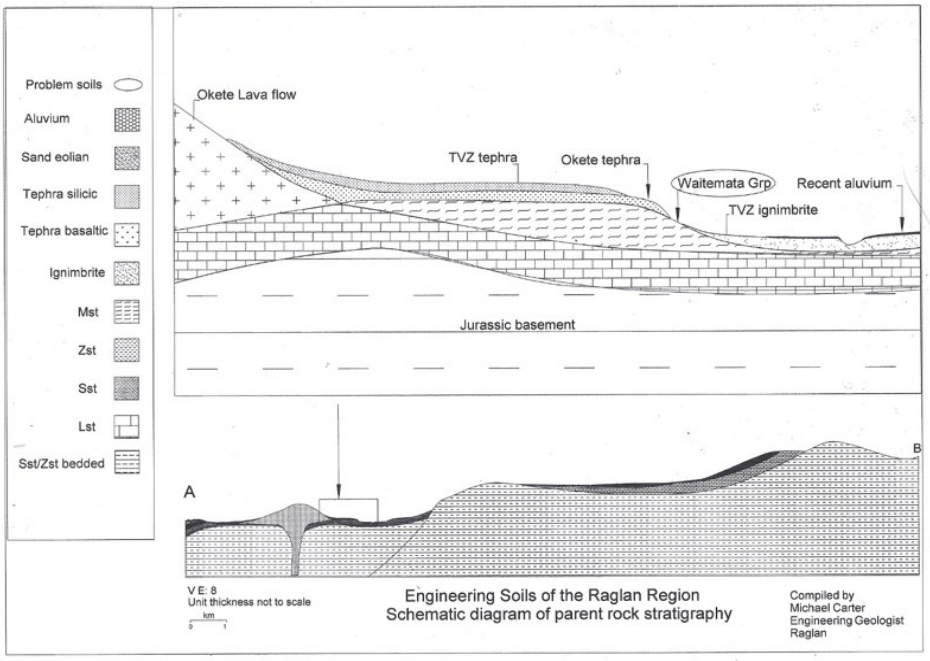

Figure 3.1: Simplified schematic west – east cross-section with stratigraphic relationships in the inland Raglan region. Adapted from Carter (2018). **Large image**

Te Kuiti Group sub-bituminous coal measures overlie the basement at isolated locations throughout the western Waikato region. These are commonly at or near the modern land surface. The minimum burial depth for coalification of similar grades of coal in the West Coast, South Island, New Zealand was 1.8 km (Suggate & Boyd, 2012). This indicates that the Te Kuiti Group has been uplifted by at least this extent. This degree of uplift has resulted in considerable disruption of the original stratigraphy. The modern expression of this complex deformed stratigraphy is a highly variable geomorphology of gentle to very steep contour. Level land is confined to narrow floodplains around streambeds. Erosion has exposed most of these rock groups at various locations on the Raglan Harbour shoreline. Rainfall of 1400 – 1600 mm/year has resulted in a network of incised drainage valleys that discharge into harbours or the open coastline.

Around 2 Ma BP basaltic-andesitic volcanism developed in the Raglan region, resulting in a prominent calcalkalic basaltic-andesitic cone (Karioi) and multiple alkalic-basaltic monogenic vents within the Okete Volcanic Formation (OVF) (Briggs, 1983; Briggs et al., 1989). Whereas the Karioi Volcanic Formation (KVF) lava is confined to an area proximal to its cone, the OVF is extensive throughout the Raglan region in the form of multiple cones and associated tephra, thin lava flows, scoria cones and occasional tuff rings.

Lava flows and isolated dikes are exposed at multiple locations around the Raglan Harbour shoreline and the open coastline. Aside from distal tephra these 2 formations' igneous rocks cover ~ 55 km^2 of the landscape (Briggs, 1983). Weathered silicic tephra from the Taupo Volcanic Field (TVZ) and/or basaltic tephra beds (Kauroa Ash) are present on most of the gentle-sloping topography throughout the entire Raglan region. On steeper slopes these relatively soft materials have been stripped off by erosion, exposing the older rocks.

In conjunction with these multiple events the Last Glacial Maximum (LGM) resulted in the cold arid period throughout 20 to 26 ka yrs BP (Marske & Boyer, 2022). These conditions led to enhanced physical weathering resulting in the Kaihu Group of eolian and colluvium pumiceous sands and silts that mantle the eroded Te Kuiti Group surfaces (Barter, 1976) (Figure 3.2). The silicic pumice provenance is most likely the Taupo Volcanic Zone (TVZ).

Figure 3.2: Cohesionless Kaihu Group pumiceous silty sand overlying a Whaingaroa Siltstone lithotype erosion surface. Waitetuna Estuary, Raglan Harbour.

Around the harbour outlets the Kaihu Group is expressed as mobile eolian titanomagnetite dunes, classified as the Nukumiti Sands Member by Pain (1976). These dunes are constantly being supplied by along-shore currents running north from the Taranaki Volcanic Zone (Brathwaite et al., 2021).

A dominant rock-type in the harbour is a bluish-grey calcareous mudstone: the Whaingaroa Siltstone lithotype. Based on the age constraints established through existing floral and faunal data within the NZ Fossil Record Electronic Database, and 26 strontium-dated macro fossil data points, Kamp et al. (2014) divide the Whaingaroa Siltstone lithotype into 2 members: the Kotuku Siltstone (29 – 30 Ma yr BP) and Patikirau Siltstone (27 – 28 Ma yr BP), so assigning them an age difference of ~ 1 Ma years. (Figure 3.3).

A Carter (2022) study, and field work during this thesis research, established that a third major rock body of the Whaingaroa Siltstone lithotype overlies the Raglan Limestone at Horongarara Point. Waterhouse & White (1994) assign the classification of Carter Siltstone to this stratigraphic position, the recorded lithology of which does not match that in the Raglan Harbour. However, they may be lateral equivalents, representing facies change.

Assuming that the Kotuku Siltstone is a legitimate rock member, there are 3 members of the distinctive Whaingaroa Siltstone lithotype in the harbour. These cannot be differentiated through their lithology in the field. Consequently, when the stratigraphic position is unclear this study often refers to them as being the 'Whaingaroa Siltstone lithotype' or 'Whaingaroa Siltstone'.

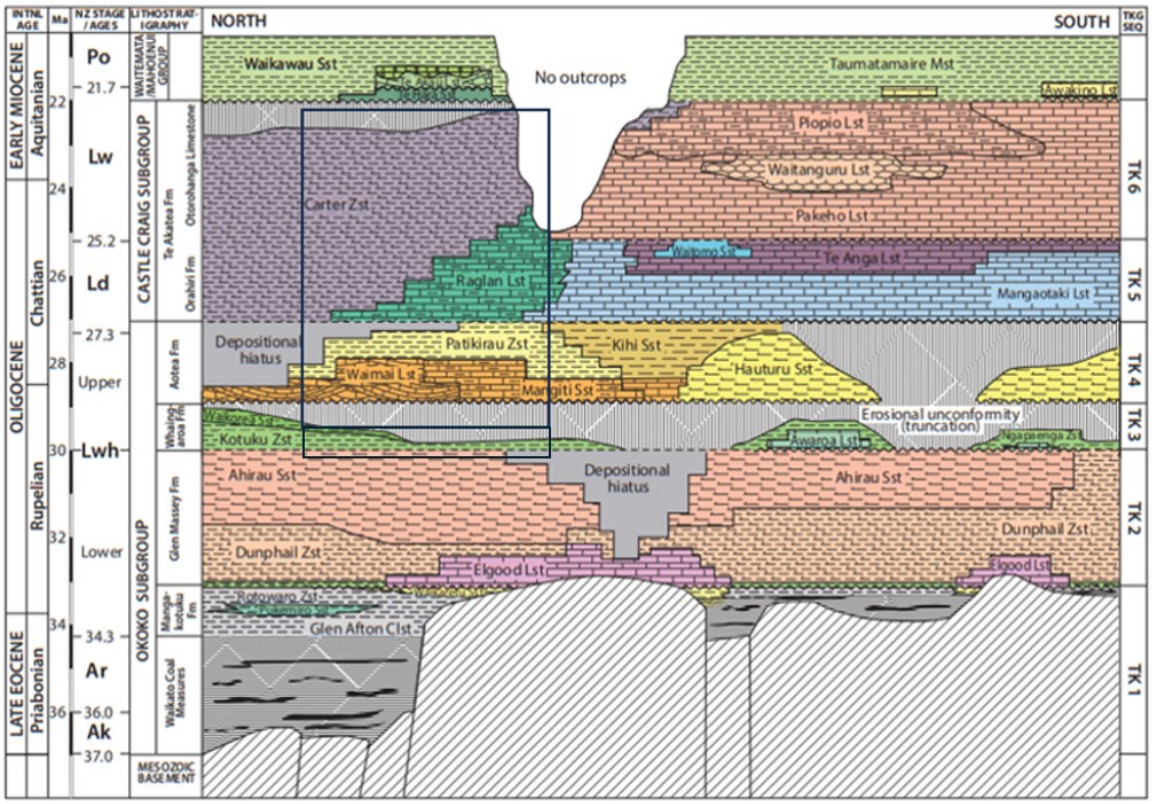

Figure 3.3: Chronostratigraphy of the Te Kuiti Group with the Raglan Harbour rocks shown within the rectangles. Adapted from Kamp et al. (2014, Figure 2). **Large image**

3.2: Geological Structure

The harbour shoreline provides a window into the structural relationships of the various rock members. While a minimum number of faults are recorded in the published literature, this study identified many more within the foreshore embankments (Figure 3.4).

Figure 3.4: Raglan Harbour. Published and prominent faults identified during this study. Image extracted from Google Earth 2024.Jan.12.

Generally, the structural orientation of the Te Kuiti Group rocks is one of gently dipping, semi-disturbed stratigraphic architecture, delineated by confined fault-zones involving significant deformation and offsets. The faults are expressed through fractured bedding and/or abrupt change in lithology or dip-strike orientation along horizontal planes. Vertically displaced blocks and tectonic stress-release fracture zones are visible at multiple locations. These blocks are usually < 30 m in width (Figures 3.5; 3.6). A predominance of block faulting within normal fault surfaces signifies a general trend of extension.

Figure 3.5: A block-fault scarp in Raglan Limestone (a), fault-zone toppled rocks (b) and Whaingaroa Siltstone (c) with a paleo slope-failure surface (d). Vertical offset: is ~ 30 m. Horongarara Point, Raglan Harbour.

Figure 3.6: Stress-release fracture-zone rockfall in Whaingaroa Siltstone lithotype. Hawea Bay, Raglan Harbour.

Faults within the pumiceous Kaihu Group is evidence that fault strain displacement occurred within the age of these deposits. The most likely source of reasonably fresh pumice clasts within the Kaihu Group is the Oruanui eruptions of ~ 26.5 ka BP (Wilson, 2001). This event mantled the Raglan landscape with silicic tephra beds of ≤ 1 m thickness. Therefore, fault displacement as shown in Figure 3.7 probably occurred within this timeframe.

Figure 3.7: Fault planes (a) in Whaingaroa Siltstone (b). Shearing ≤ 26.5 ka Kaihu Group pumiceous sand (c; d). Vertical displacement is > 1 m. Horongarara Peninsula, Raglan Harbour.

3.3: The Prominent Foreshore Geology

Sea cliffs and beaches provide visible expressions of the lithologies discussed in Sections 3.1 and 3.2. This study did not identify any exposures of basement greywacke or coal in the harbour. Proximal to the harbour entrance, energetic tide-flows and a constant open-ocean sand supply has resulted in cyclical deposition and erosion of unconsolidated sandbars, sandy channels, and beaches. The central and upper harbour consists primarily of tidal estuaries. These are supplied with fresh water and terrestrial sediments via 2 major water courses (the Waitetuna & Waingnaro rivers), and multiple minor freshwater streams. The heads of these estuaries are usually comprised of low-lying brackish swamps and/or mangroves within deep muddy silt and silty clay.

The terrestrial drainage valleys are incised into an elevated landscape. Based on aerial imagery observations sea cliffs of 6 - 40 m height and of 60 ^{o} - 80^{o} slope-angle constitute ~ 25 % of the foreshore. Most of these cliffs are comprised of Te Kuiti Group limestone and siltstones, with some exposure of the Te Kuiti Group member Mangiti Siltstone at discrete locations. The Late Pliocene Kaihu Group pumiceous silty sands are also exposed in cliffs at various locations. Due to their relatively high resistance to erosion, Okete formation basaltic lava flows and the Raglan Limestone extend into the tide-zone at multiple locations.

The main contributor to erosional sediment supply in the harbour is the Whaingaroa Siltstone lithotype (Kotuku Siltstone and Patikirau Siltstone). While this rock-type is moderately hard and stable in its residual position, it fritters rapidly into cohesionless silt and smectite clay on exposure to the surface elements and/or as dislodged clasts (Nelson & Hume, 1987) (Figure 3.8).

Figure 3.8: The effects of surface expose and confinement-release on the Whaingaroa Siltstone.

The Whaingaroa Siltstone lithotype has a major influence over shore platforms and beach morphologies in the harbour. It forms many extensive tidal wave-swept platforms with little or no overlying unconsolidated sediments (Figure 3.9). Tidal inundation dissolves the clay component within the platform rock surfaces, leaving a hard wave-swept surface (Figure 3.10).

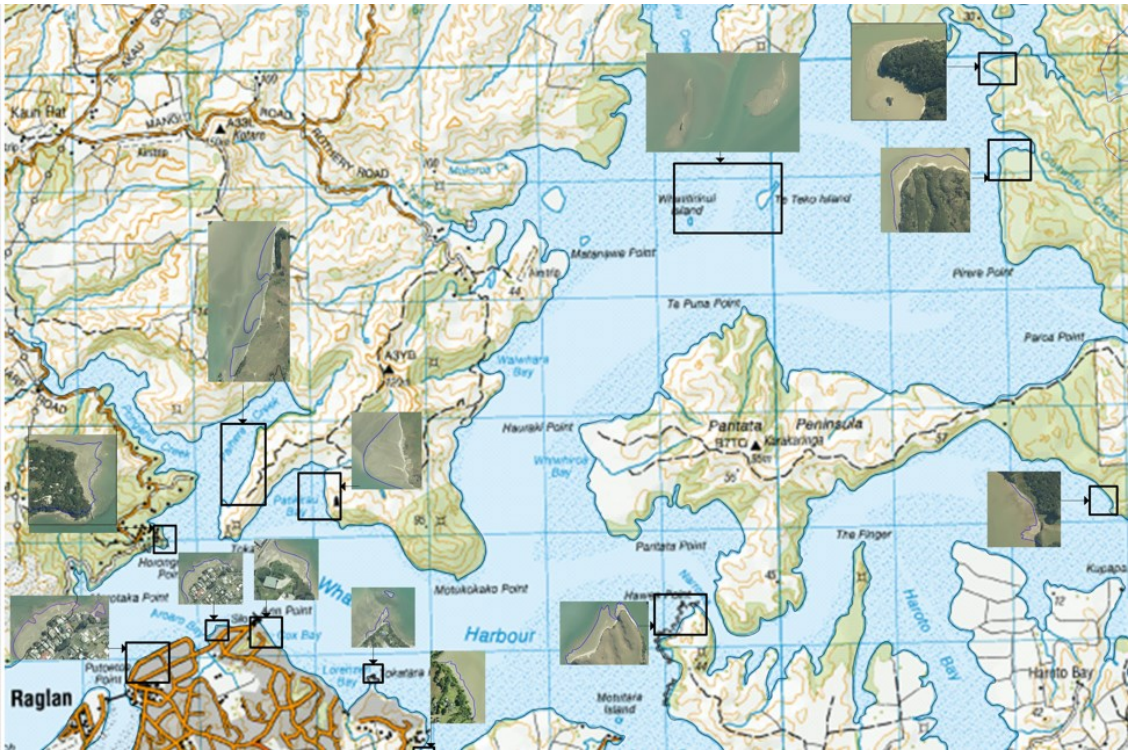

Figure 3.9: The extent and locations of a selection of the tide-zone Whaingaroa Siltstone lithotype rock platforms in Raglan Harbour**.** Adapted from Google Earth 2013.Oct.22); Topo50 map, (2003), Land Information, New Zealand (2023)**.** **Large image**

Figure 3.10: A hard rock wave-swept Patikirau Siltstone platform at low tide. Patikirau Bay, Raglan Harbour.

3.4: Basic Geology and Geomorphology Summary

The Raglan Harbour is a ria (drowned river-valley). Its foreshore is comprised of 4 groups of rocks, spanning 30 Ma. The groups' contact surfaces are commonly unconformities representing ≤ 10 Ma of missing deposition. The lithologies include calcareous and non-calcareous sedimentary rocks. Early Pleistocene basaltic volcanic lava flows and intrusions protrude into foreshore platforms at multiple locations. Tephra from these events and more distal silicic eruptions are intermixed with Quaternary colluvium and alluvium of up to 20 m in thickness.

Uplift of ≤ 2 km throughout 20 Ma has resulted in interconnected faults, many of which have not been recorded in published literature. These are often associated with localised block-fault displacement, indicative of general extension. Stress-release fracture zones at some locations are fresh in appearance.

Terrestrial water drainage systems driven by relatively high rainfall have sculptured this geological complex into a rolling landscape terminating by sea cliffs, beaches, and tidal estuaries.

Multiple geological units are exposed at various locations around the harbour foreshore. Stronger rocks form many shallow wave-swept platforms in the tidal zone, which constitutes ~ 70% of the total harbour area.

CHAPTER FOUR

SEDIMENTATION AND FORESHORE EROSION

4.1: Sediment Characteristics

Raglan Harbour is a drowned river valley system with a maximum depth of 18 m and a total area of ~ 33 km^2. 70% of the total area consists of tidal platforms of up to 700 m width, dissected by channels up to 5 m deep (Sherwood & Nelson, 1979).

Sediment grain-size within the harbour is highly variable, ranging from fine clays to gravels, mixed in varying proportions according to the tide-controlled waterflow energy and harbour bathymetry. Overall, the mean sediment grain size is inversely proportional to the proximity with the high-energy harbour head, where sand dominates.

Channel banks are commonly comprised of very soft silty mud of > 1 m depth. Channel beds accumulate sorted sands and gravels**.** The upper harbour tidal estuaries are relatively shallow. With the exception of the Waingaro branch, the tidal flats are dominated by sandy/silty mud. The Waingaro branch shore platforms primarily consist of rock platforms with occasional thin (< 0.2 m) sediment coverage (East, 2005).

Sediment provenances include the eroding harbour foreshore and inland terrestrial materials transported into the harbour by multiple streams and 2 rivers. Rounded gravels of diameter $\leq$ 50 mm are sparsely distributed throughout the harbour foreshore and open coastline. These materials most likely originate from eroded conglomerate within Jurassic basement that forms the Hakarimata Range (Graham & Korsch, 1990). The gravels are particularly concentrated in channel floors. They are also exposed at elevations of $\leq$ 4 m above mean SL within paleo fluvial channels exposed in foreshore embankments.

4.2: Foreshore Characteristics

Tide-zone characteristics range within the extremes of hard rock platforms through to gravels, sand, and soft silty mud. Most rock sea-cliffs have associated tidal wave-swept platforms with minimal overlying sediments (Figure 4.1).

Figure 4.1: The hard rock foreshore platform extending > 200 m out to low tide level. Patikirau Bay. Raglan Harbour.

These rock platforms constitute all or most of the tidal foreshore at multiple locations. This study identified 12 rock platforms exceeding 80 m in width. Given that this observation was derived from aerial images taken at mid-tide the total area of rock platforms is likely to exceed this finding by a considerable margin. Bedding planes within these rocks show as a tiger-skin pattern within aerial images, from which dip and strike orientations can be established. The strike and dip orientations are highly variable, signifying the stratigraphic architecture complexity (Figure 4.2).

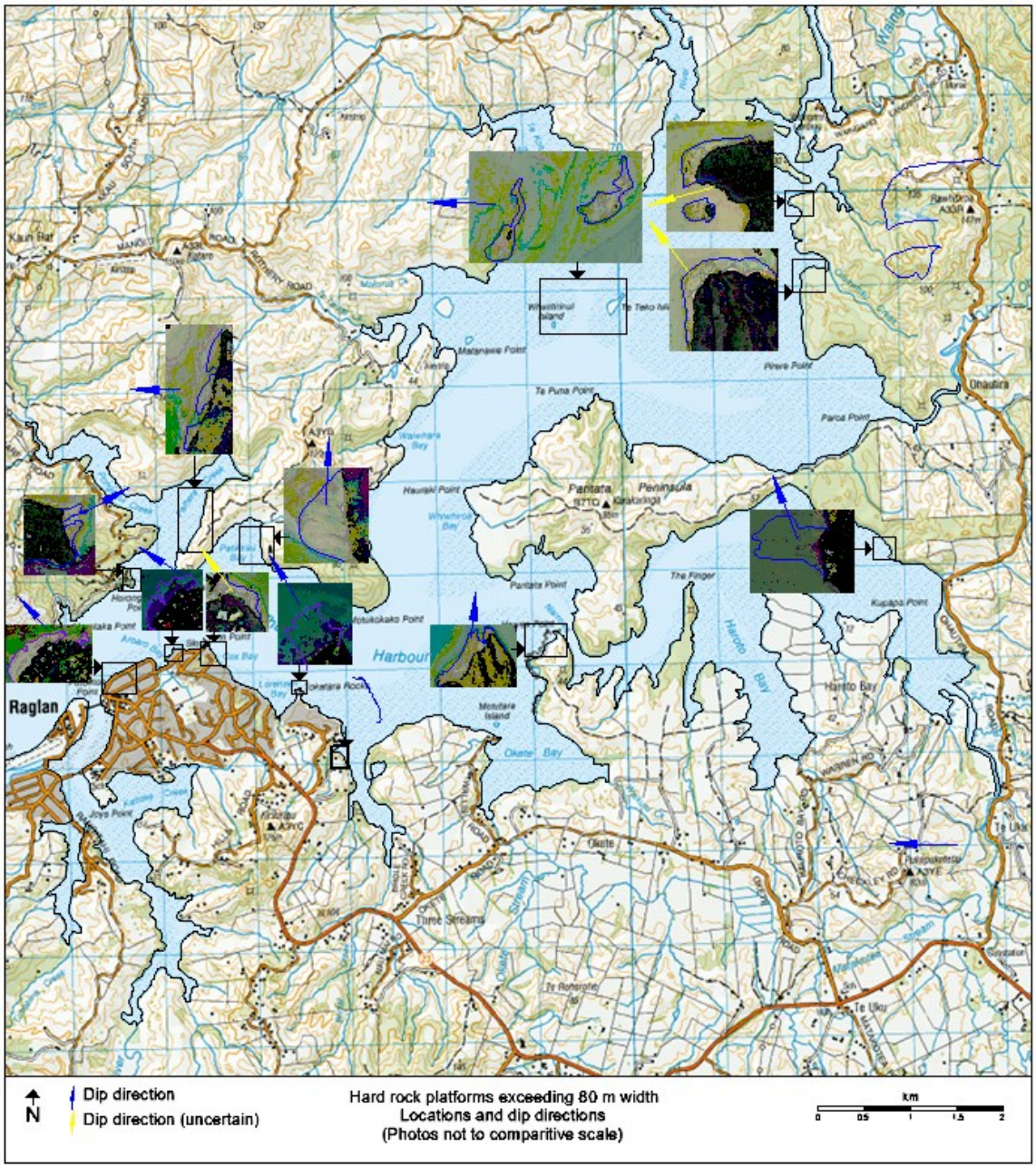

Figure 4.2: Location, extent and dip directions of tidal rock platforms exceeding 80 m width. Sources: Google Earth (2023) and Land Information New Zealand (2023). **large image**

Sherwood & Nelson (1979) describe the rock platforms as commonly being 100 m in width and suggest that surface characteristics of these platforms is primarily a result of wetting and drying during tide cycles. This process, along with the dominating elevations of the platforms, signifies that rates of surface erosion are in a state of approximate equilibrium with SL.

The Whaingaroa Siltstone lithotype is particularly susceptible to fragmentation when exposed to cyclical wetting-drying of its surface. The derivatives of this process are fine silt and expansive smectite clay (Nelson & Hume, 1987).

Should there have been significant RSL rise over the last several centuries the elevation of these rock platforms relative to SL would likely be lower than their modern state – reflecting a historical lower RSL. Sediments can be expected to have accumulated on these rock surfaces as RSL increased. This sedimentation would especially occur in the lower-energy upper harbour estuaries. This is the case in the Waitetuna branch, where relatively thick, muddy sediments dominate the tide-zone.

East (2005) makes specific note of the absence of sediments overlying rock platforms in the Waingaro branch, which constitutes ~ 33% of the total harbour area. The author concludes that within the Waingaro branch there has been insignificant sediment accumulation rates (SAR) within the past several centuries. In contrast, the Waitetuna branch has been accumulating sediments at rates that have accelerated by > 1 order of magnitude throughout the last century. The explanation for the variation in this SAR is that the Waingaro branch is subject to higher energy wave action due to exposure to the prevailing SW wind and that tidal platforms in the Waingaro branch have been swept of sediment. The prospect that the Waingaro branch may have been subject to uplift was not considered by East (2005).

4.3: Foreshore Accretion and Erosion

Sediment accumulation rates are highly variable throughout the harbour. Sediment accretion of well-sorted sand is occurring at various locations in the high-energy lower harbour. A consolidated sandspit (Te Kopua) developed as an airfield and recreational reserve during World War II has been subjected to moderate accretionary extension with insignificant erosion at isolated locations (Figure 4.3). This extension is likely to be a continuation of the historical evolution of this paleo sandspit.

Accretion is particularly evident in fresh eolian dunes at the northern side of the harbour inlet where unconsolidated dunes continually migrate inland from the surf zone (Figure 4.4).

Figure 4.3: Accretion of sand and vegetation since 1944 on Te Kopua Peninsula, Raglan, showing sand accretion in a NE direction and insignificant erosion (2023 boundary in blue). Images from Retrolens and Google Earth (2023). **Large image**

Figure 4.4: Mobile eolian titanomagnetite-rich sand (a) migrating inland on the northern heads of Raglan Harbour inlet (b). Image from Google Earth 2023.Sept.21.

Within the harbour, lateral erosion (back wear) of terraces and sea-cliffs is far more prevalent than accretion deposits, which are primarily limited to sand spits and mudflats visible at low tide. Sea-cliffs are commonly > 50 m in height with slope angles of $40^0 – 80^0$ (Carter, 2021). Based on vegetation cover of cliff faces rates of shoreline retreat are highly variable. This back-wear is primarily due to wave action, surficial fritter, and extreme rain events: commonly resulting in shallow translational slide failure. Field observations and aerial imagery indicate that most faces revegetate rapidly after failure.

While minor cliff toe undercutting is visible at some locations, observations and historical aerial images indicate that this is insignificant at locations where the tide-zone is comprised of hard wave-swept rock platforms.

The intertidal platform characteristics are consistent with the impact of uplift-driven RSL fall at locations where back wear is being offset by uplift of a sloping cliff face. A comparison of aerial images of a section of 30 m-high sea-cliffs at Hawea Point indicates that the maximum average rate of back wear since 1944 was ~ 3.5 mm/year. A large portion of the cliff faces has re-vegetated within this time-period (Figure 4.5).

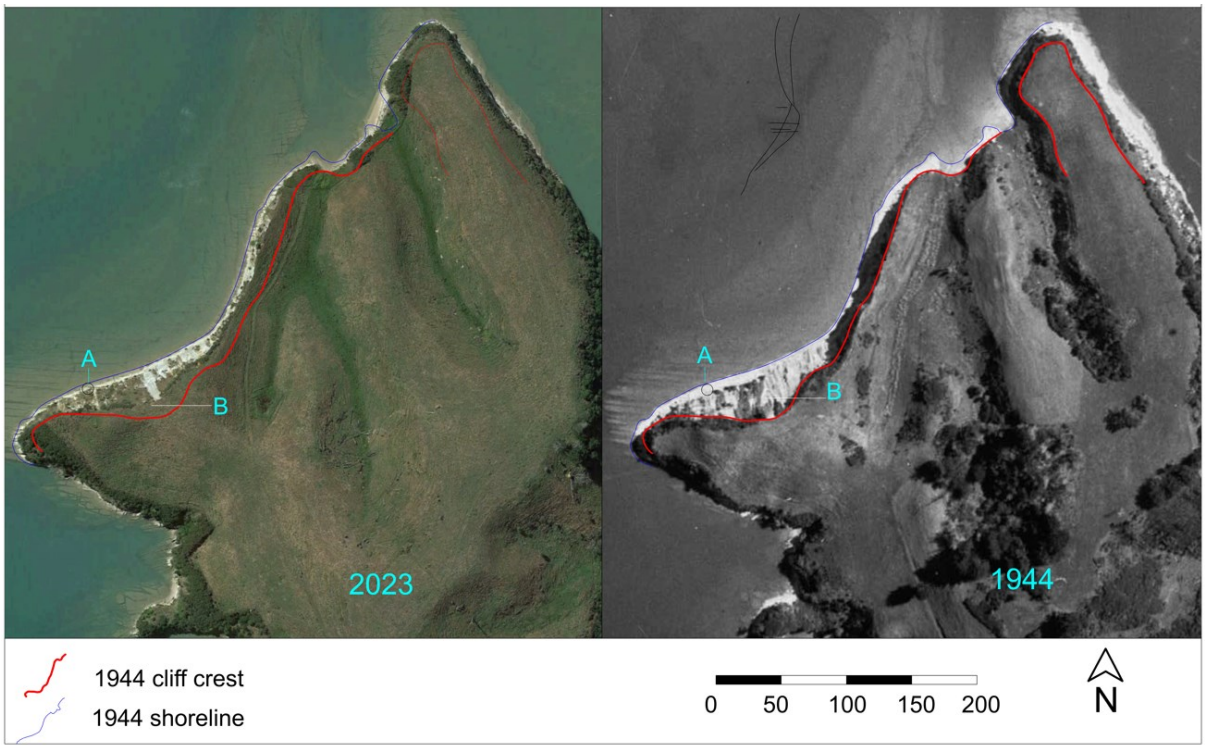

Figure 4.5: Maximum toe retreat (a) and re-vegetation (b) of the 30 m-high sea-cliff at Hawea Bay, Raglan Harbour. Images by Google Earth 2023.Oct.07; Retrolens (2023). **Large image**.

Vegetation on sea-cliffs is of varying degrees of maturity, indicative of the slope failure history. Surfaces range from bare rock that has failed within the very recent past, through to native trees of > 50 years in age (Figures 4.6; 4.7). Based on this historical footprint, cyclical shallow translational slide failure is considered the process most responsible for the modern cliff morphology. Within the harbour, deep-seated rotational or wedge failure of sea- cliffs is rare. This study's reconnaissance of 120 km of foreshore identified only 1 significant deep-seated rotational failure of a rock sea-cliff. This was near an obvious fault. The most significant wedge failure observed was < 2 m in depth (thickness).

Figure 4.6: Short-rotation translational failure surfaces on Whaingaroa Siltstone. Hawea Point, Raglan Harbour.

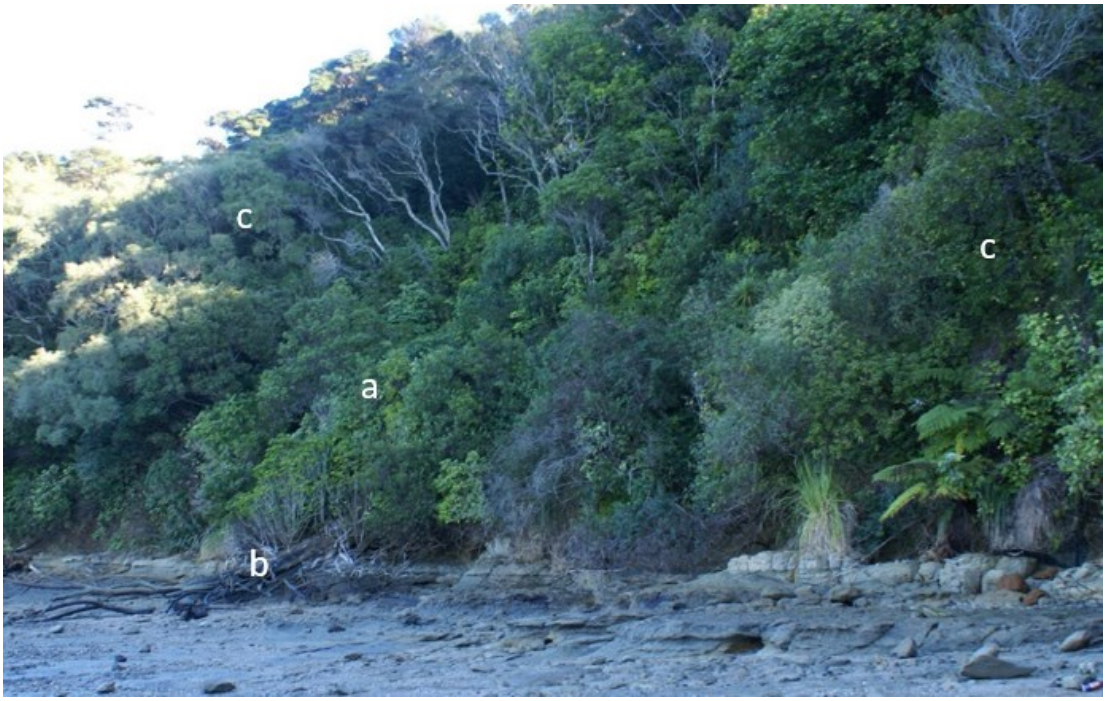

Figure 4.7: Long-rotation cyclical translational failure footprint in Whaingaroa Siltstone. Regenerating slide surface (a) including a mature puriri log remnant (b) within ~70-year-old manuka (c). Horongarara Point, Raglan Harbour.

Rock materials displayed in Figures 4.6 and 4.7 are dominated by medium-hard calcareous siltstone that weathers and weakens rapidly near its surface. Other sea-cliff rocks in the harbour include bedded sandstone. The Mangiti Sandstone can display apparent paleo tide notches due to differential weathering of near-horizontal beds. These need further substantiation before being interpreted as being tide dissolution notches (Figure 4.8). Many low-lying marine terraces have fresh near-vertical erosion scarps of < 2 m height that are affected to varying degrees by tide dynamics (Figure 4.9).

Figure 4.8: Modern and apparent paleo tide dissolution notches in Mangiti Sandstone. Motukokako Peninsula. Raglan Harbour

Figure 4.9: A rapidly eroding beach scarp within an elevated marine terrace comprised of a rafted pumice bed overlying terrestrial clay. Te Mata Creek Estuary, Raglan Harbour.

4.4 Extreme Tide Event Accretion

The selection of focused study sites was based on the presence of datable materials within raised marine terraces. These often share a common stratigraphy with their modern tidal-zone equivalent. These include elevated strandlines comprised of a mix of flora and fauna (wrack) washed up by wave action at high tide and storm events. These features commonly consist of 2 contrasting types representing prevailing and extreme storm events. Prevailing conditions result in a strip of fresh material debris. The extreme event beds are grassed over and contain driftwood. The elevation difference between the two is commonly 0.2 – 0.5 m. The state of the driftwood indicates that the grassed terraces are not a product of RSL change, but rather a result of periodic storm surges. Genuine raised terraces representing relative SL fall are somewhat higher in elevation than their modern equivalents (Figure 4.10).

Figure 4.10: The 3 styles of sedimentary strandline beds. Te Kotuku Inlet, Raglan Harbour.

.

4.5: Sedimentation and Foreshore Erosion Summary

Raglan Harbour is a sediment accumulation and generation regime, being flushed bidirectionally by tides and periodic terrestrial flooding. It is a dynamic erosion, deposition and transport system, involving sediments ranging from soft clays through to hard gravels.

Sediment grain size distribution is directly proportional to water-flow velocity, wave agitation and the extent of intertidal zones. Extensive soft mudflats dominate many estuaries, while mobile sands and gravel are prominent at the high-energy harbour outlet.

Active erosion and shoreline retreat in the form of beach erosion scarps are apparent at numerous locations. Conversely, historical aerial imagery shows accretion and extension of sand spits located near the harbour entrance.

While in many locations intertidal shallow wave-swept rock platforms are largely devoid of sediments, in other locations platforms are comprised of deep noncohesive sands, silts and clays. This variation is likely to be due to differential VLM.

At many beaches heaped marine shells and other wrack materials (strandlines) mark the modern EHT level. Grassed-over strandlines at higher elevations are common, reflecting historic extreme storm events. At some locations more elevated terraces comprised of marine sediments and undisturbed shellbeds are suggestive of uplift.

CHAPTER FIVE

THE SEISMIC RECORD

5.1: Seismic History Introduction

Relative sea level (RSL) change is directly linked to vertical land movement (VLM), which has a co-relationship with seismic activity, along with other possible processes. Given the inherent difficulty of earthquake prediction, the recorded history of earthquakes is of primary importance.

As a result of the number of catastrophic earthquakes throughout its recorded history there has been multiple focused studies and modelling of seismic activity for NZ throughout the last century. This has been approached from both scientific and economic perspectives (e.g. Bradley, 2008; Stirling et al., 2012). All central and local governments in NZ require seismic risk to be integrated into structural designs and this is mandatory within geotechnical assessments relating to building consent applications. (e.g. New Zealand Geotechnical Society, 2021). Earthquake risk has also influenced the compilation of engineering standards for national infrastructure development, such as roading, bridges, railways, and dams (e.g. NZ Transport Agency, 2022).

The National Seismic Hazard Model (2012) commonly adopted by design engineers, designates the Raglan region is as being within the lowest seismic risk region in NZ (Figure 5.1). This ranking is likely to be due to the limited seismograph record, plus the absence of recorded destructive earthquakes and recognise active faults in the region. The closest faults recognised as being active are located near Ngaruawahia and offshore from Kawhia: 30 Km and 25 km distance from Raglan respectively.

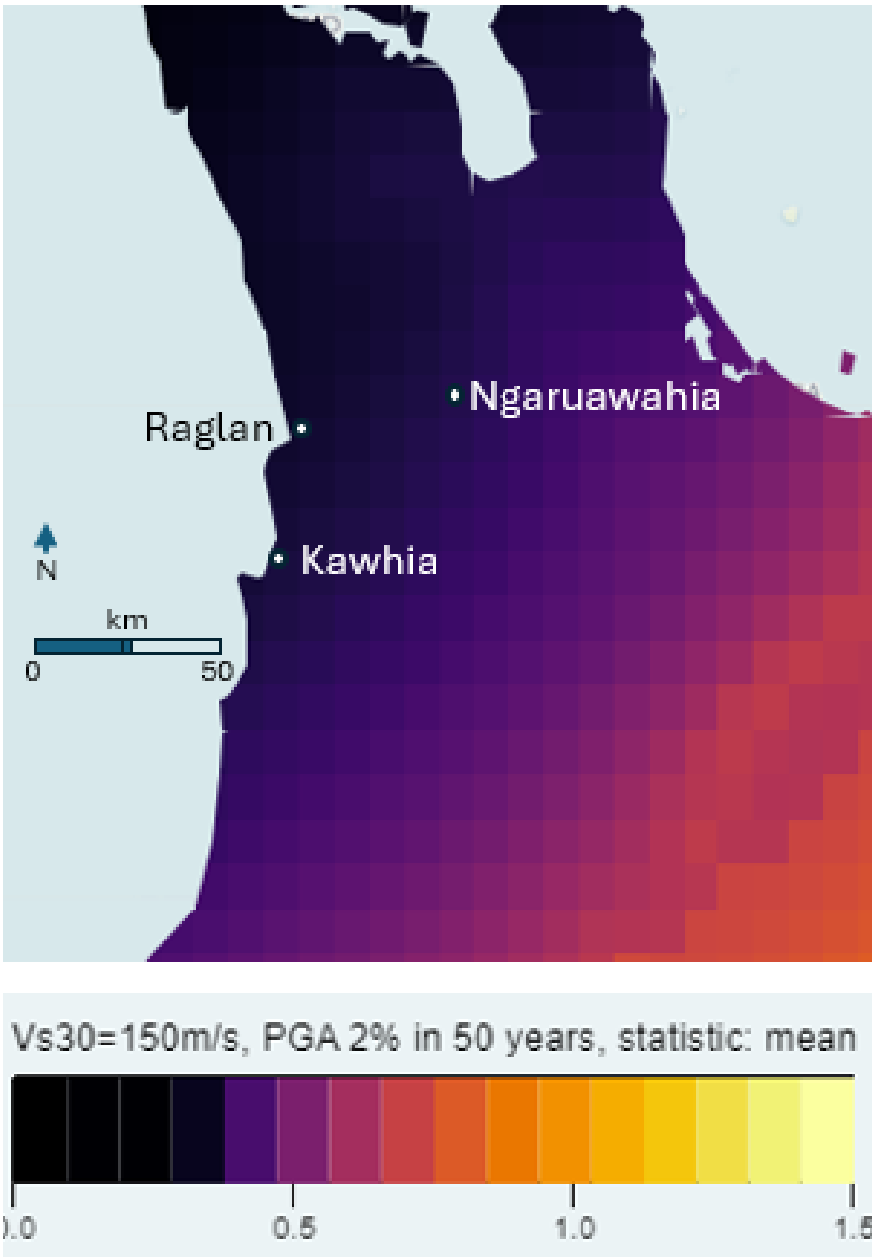

Figure 5.1: The relative seismic risk for Raglan and surrounds. Adapted from Stirling (2012)

5.2: Media and Personal Communication Earthquake Reports

Newspapers covering the Raglan region periodically reported seismic shaking from the mid-19th century onwards. One instance was after the severe 1863 Hawkes Bay earthquake. An event widely reported in Raglan and the inland Waikato occurred on 24th June 1891. The newspapers' reports identify the epicentre as being near Raglan and Kawhia. Shaking was reported in Auckland and the inland Waikato (Waikato Times, 1891). This earthquake corresponds with an event recorded in the GeoNet earthquake search tool (GeoNet, 2024). Three further 19th to mid-20th century earthquakes are recorded (Figure 5.1). As the first seismographs in NZ were installed in 1900 (Petersen, et al. 2022) these earlier records are reliant on archive resources.

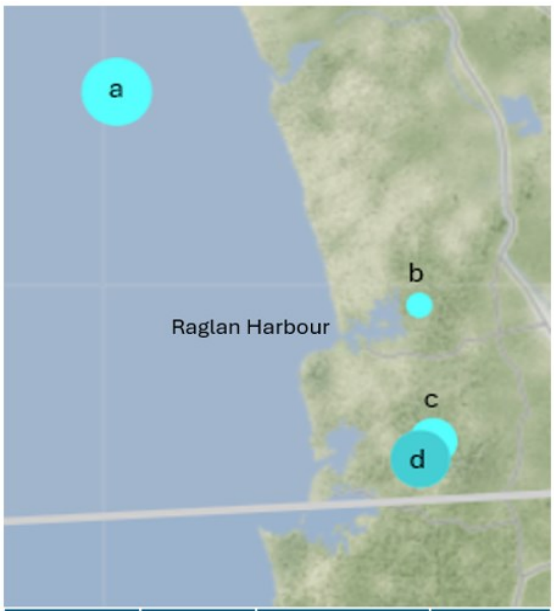

Avent	Year	Magnitude	Depth (km)
a	1891	6.2	12
b	1949	2.2	12
c	1944	4.9	12
d	1840	5.5	25

Figure 5.2: Recorded earthquakes in the Raglan region throughout the period 1800 – 1950. Retrieved from GeoNet Quake Search tool. Retrieved from Geonet 2024.Feb.03.8am GeoNet: Quake Search

Most of these early reports originate from citizens relaying their experience to newspapers. Others are word-of-mouth reports from local citizens. For example, an earthquake in the 1930's was of sufficient severity to topple 2 brick chimneys in Te Mata, 15 km SW from Raglan (D. C. Newton, social media post, June 22, 2023). Within 24 hours of the Kaikoura earthquake the collapse of a road bridge buttress in the Otonga Valley was reported by local earthmover, R. Poolton (Pers. Comm. November 15, 2016).

Eiby (1968), through researching newspapers, books, manuscripts, and transcripts held within archives, catalogued NZ earthquakes dating back to 1460. Reports from Kawhia involving 6 different events occurring within the years 1840 – 1841. These are all earthquakes 'felt' rather than reports of damage.

5.3: The Seismograph Record

Raglan and Kawhia lie near the eastern boundary of the Taranaki Sedimentary Basin. Extensive hydrocarbon exploration seismic surveys and over 400 wells make it the most studied marine subsurface in NZ. Consequently, the geological structure is relatively well defined.

The Taranaki Basin has a history of back-arc volcanism and thrust faulting that evolved into a rift-system originating in the north of the basin. This migrated south throughout the Neogene, reaching its full development in the early Pleistocene (Giba, et al., 2010). The authors conclude that the northern Taranaki Basin is now tectonically stable, which should result in the absence of significant seismic activity offshore from Raglan.

The seismograph record in NZ extends back to 1900. While the pre-1900 record is relatively sparse due to absence of seismograph data, the post-1900 record of shallow, low-intensity earthquakes is substantial (GeoNet: Quake Search).

Some seismic events have relevance to Raglan Harbour. These include the timings, and densities within specific epicentre locations. Within the period 15th November – 15th December 1995, 32 seismic shocks occurred ~ 30 km offshore from Raglan (Figure 5.3.A). This timing could relate to an apparent uplift in the harbour between 1979 and 1997. Evidence of this uplift is discussed in Section 8.3 of this thesis. The nature and timing of this swarm is more suggestive of localised volcanic or hydrothermal activity, rather than fault stress-release. Figure 5.3.B displays multiple aligned faulting and igneous rock bodies in the northern Taranaki Rift Basin. These are considered now redundant (Giba et al., 2010). Should they be currently active, the recent seismic record should corelate in a linier fashion with these faults to some degree. This does not appear to be the case in the northern sector (Figure 5.4.A). A more likely association is between the offshore centre of activity and 2 further seismic activity concentrations east of Raglan. These locations (Waingaro and Te Aroha) are in the vicinity of hydrothermal systems (Figure 5.4.B).

The alignment of these 3 locations is conforms with the axis of the 3 harbours (Raglan, Aotea and Kawhia) and offshore faults displayed in Figure 5.3.B. It is also the orientation of a fault discussed in Section 8.3 of this thesis, where evidence is presented indicating that this fault is active.

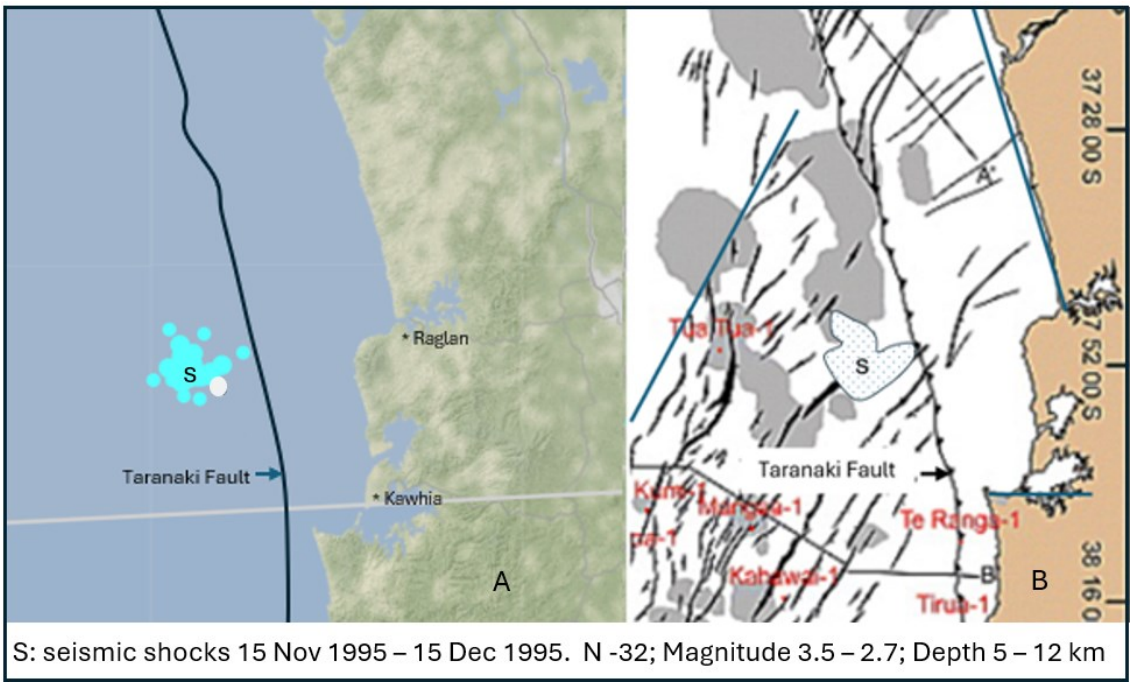

Figure 5.3. A swarm of 32 seismic shocks (S) over the period 15th Nov 1995 and 15th Dec 1995 (A). The location of S in relation to faults and buried igneous rock, in grey (B).Extracted and adapted from GeoNet: Quake Search., 2024.Feb.05; Giba et al. (2010).

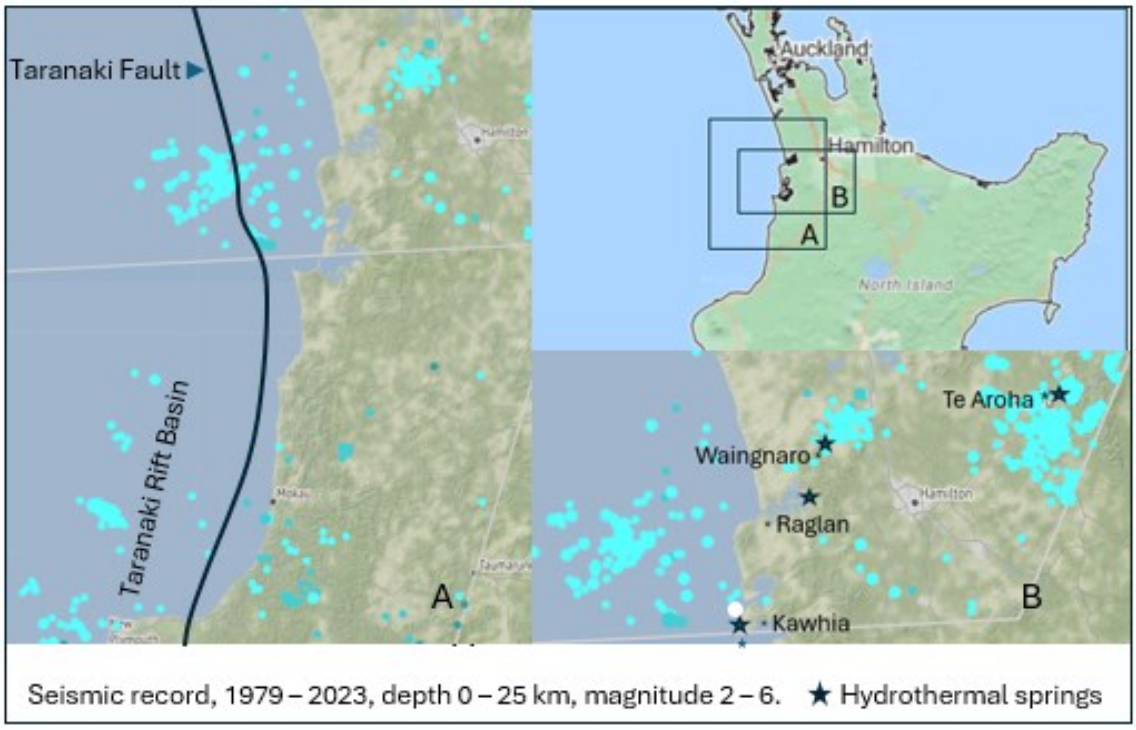

Figure 5.4: Earthquake distribution 1979 -2023 within the northern Taranaki Basin (A) and the western Waikato (B). Extracted and adapted from GeoNet: Quake Search. 2024.Feb.07.

5.4: Seismic Record Summary

Raglan Harbour and its surrounding landscape have been created through deformation and fracture in a tectonic back-arc setting. The open coastline runs approximately perpendicular to multiple faults created by extensional strain in the adjacent offshore Kawhia Syncline portion of the Taranaki Basin.

Periodic reports of earthquakes and minor damage in the Raglan region are documented within archives and the seismograph record. However, epicentres of these events were mostly at distal locations. While the Raglan region has been largely regarded as being technically passive, the seismograph record demonstrates that considerable low-level activity has occurred on a regular basis. These events were largely of magnitudes of < 4 MW.

While these seismic events could be expected to be associated with faults, the spatial patterns of these events as recorded by seismographs are more suggestive of localised volcanic activity and/or geothermal systems than stress-release along faults within the offshore Taranaki basin. Most epicentres are clustered into concentrations rather than being in linear alignment which would be expected for a major fault.

Two discrete clusters of seismic events of similar depths and magnitudes are proximal to hydrothermal springs located at Waingaro and Te Aroha. A cluster of a similar nature is located ~ 20 km offshore from Raglan. These 3 centres align with the orientation of many faults mapped directly offshore from Raglan.

This seismic event alignment is indicative of a linked subsurface system that warrants further study. While seismic epicentres are largely absent from Raglan Harbour, its axis orientation conforms with offshore faulting and seismic epicentre alignment. Consequently, if differential VLM is occurring in the western Waikato it is likely to involve Raglan Harbour.

CHAPTER SIX

SPELEOTHEM PROXIES

6.1: Speleothem Proxies Introduction

Constructing reliable constraints on historical VLM is reliant on a record of eustatic sea level (ESL) change over a defined timeframe. For example, Chapter 8 characterises and dates multiple raised shellbeds at 5 locations. Six bivalve samples from 2 sites were ^{14}C dated at ~ 6 Ka (Appendix B). Their elevations above their modern tide-zone equivalent habitats ranged from 0.3 m to 0.9 m. It is possible that their position is the result of a ESL high and/or VLM, throughout the last 6 Ka. Establishing the maximum possible RSL height and matching this with recognised ESL highs is therefore important. Without this constraint VLM cannot be established from field evidence.

Two proxies relating to maximum RSL over specific timeframes identified during this study are marine dissolution notches in limestone outcrops and the position, condition, and age of a flowstone (speleothem). Flowstones are formed by flowing films of water that move along cave floors or down positive-sloping walls, building up layers of minerals such as calcium carbonate and to some degree aragonite, and other impurities imposing colour variations. Their normal growth is halted or altered in subaquatic settings. Variations in environmental conditions are often reflected in their strata composition and growth rates.

A significant amount of research has been conducted using evidence of periodic aqueous immersion of speleothems as indicators of paleoclimate and SL change. In the Mediterranean Sea more than 300 submerged speleothems sampled in 32 caves have been analysed (Antonioli, et al., 2021). These authors compile a comprehensive review of the results obtained from the studies of submerged speleothems since 1978.

The researchers conclude that when a rising sea level inundates a coastal cave, resulting in brackish water flooding, speleothems stop growing. Several events can occur:

- Marine biogenic overgrowth can cover the speleothem surface
- Boring bivalves can colonize the speleothem surface, creating large burrows
- Mineral deposits can precipitate on the speleothem surface
- A carbonate encrustation, termed 'phreatic overgrowth on a speleothem' (POS), can precipitate inorganically around the speleothem surfaces

The nature of a flowstone ('Horongarara Flowstone') located during this thesis reconnaissance does not match with any of the characteristics indicative of immersion as defined by Antonioli, et al., (2021). Literature research found no publications on the effects on speleothems subjected to occasional seawater drenching or immersion.

This MPhil thesis contends that seawater immersion of speleothems has significantly different effects to those listed for brackish water immersion and that the Horongarara Flowstone has not been subject to alteration that would occur should it have been immersed during high tides. This interpretation is justified through comparing the physical properties of the Horongarara Flowstone with nearby flowstones that are regularly drenched in sea water. From these comparisons and the established age of the Horongarara Flowstone, a maximum RSL constraint within the last 34.5 Ka is proposed. The implication of this is discussed in Section 6.2 below.

6.2: The Speleothem Locations and Properties

The Horongarara Flowstone is attached to one wall of a 1 m-wide rock crevice orientated near-perpendicular to a near-vertical limestone sea-cliff. Being 5 meters inland from the exposed shoreline the flowstone is protected from marine spray and splash. The crevice's width allows the tides to ebb and flow freely into the flowstone's location.

The rock host wall is notably smooth in comparison to the flaggy limestone surfaces along the exposed foreshore sea-cliff. The host rock's position and bedding are consistent with surrounding lithology, indicating that it has not being subject to independent toppling.

The flowstone's lowest extent is 0.4 m above an effective high tide level (EHTL), identifiable through a significant discolouration of the wall (Figure 6.1). The tide immersion zone is rich in attached biota (Figure 6.2).

The maximum dimensions of the flowstone are ~ 350 mm (height) x ~ 250 mm (width). The maximum thickness perpendicular to the depositional strata is ~ 150 mm. The surface of the flowstone is smooth and hard with minimal surface weathering or accretionary deposits. There is no evidence of any of the various aqueous immersion indicators listed in Antonioli, et al. (2021).

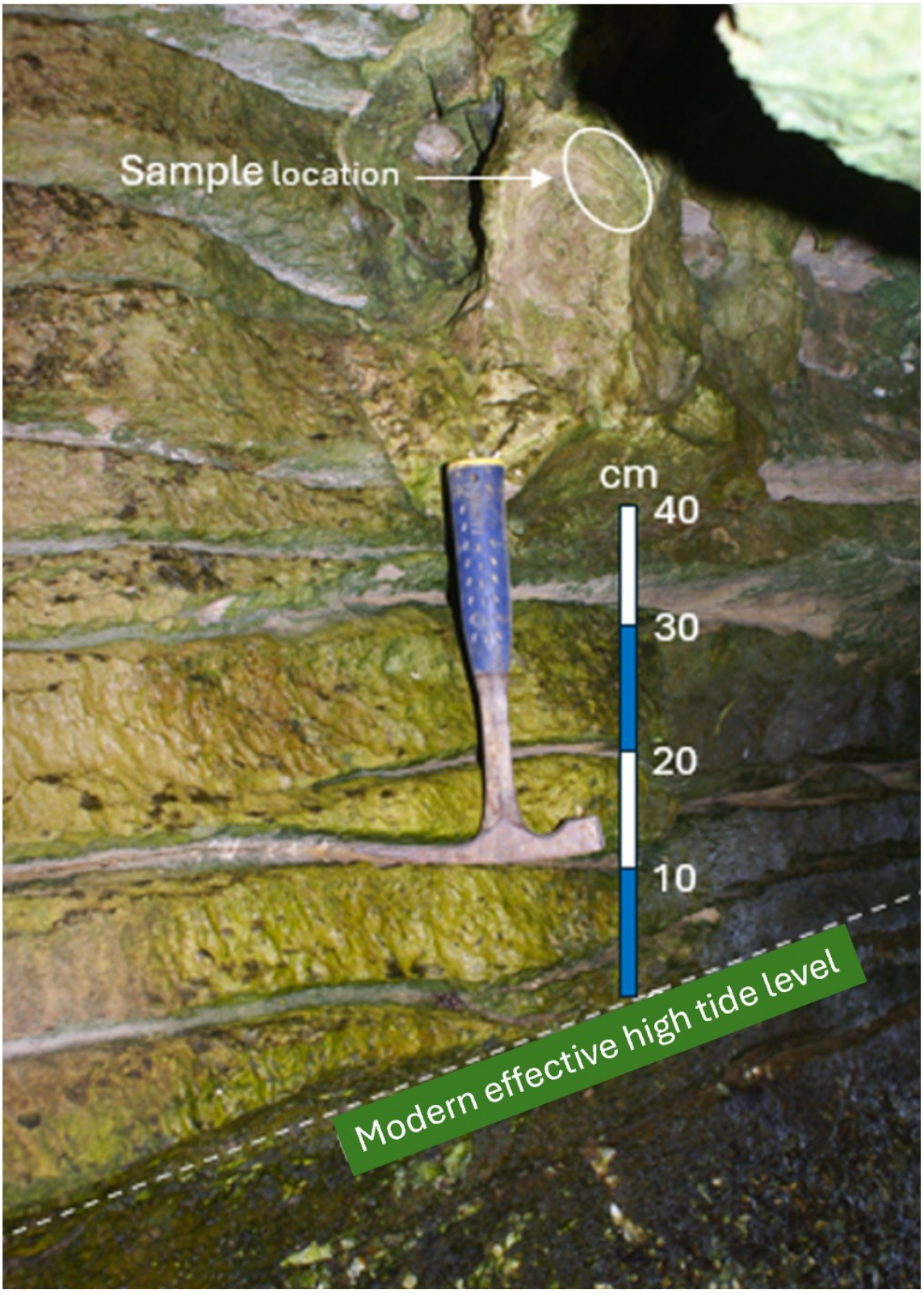

Figure 6.1: The Horongarara Flowstone attached to smooth Raglan Limestone displaying the modern effective high tide level.

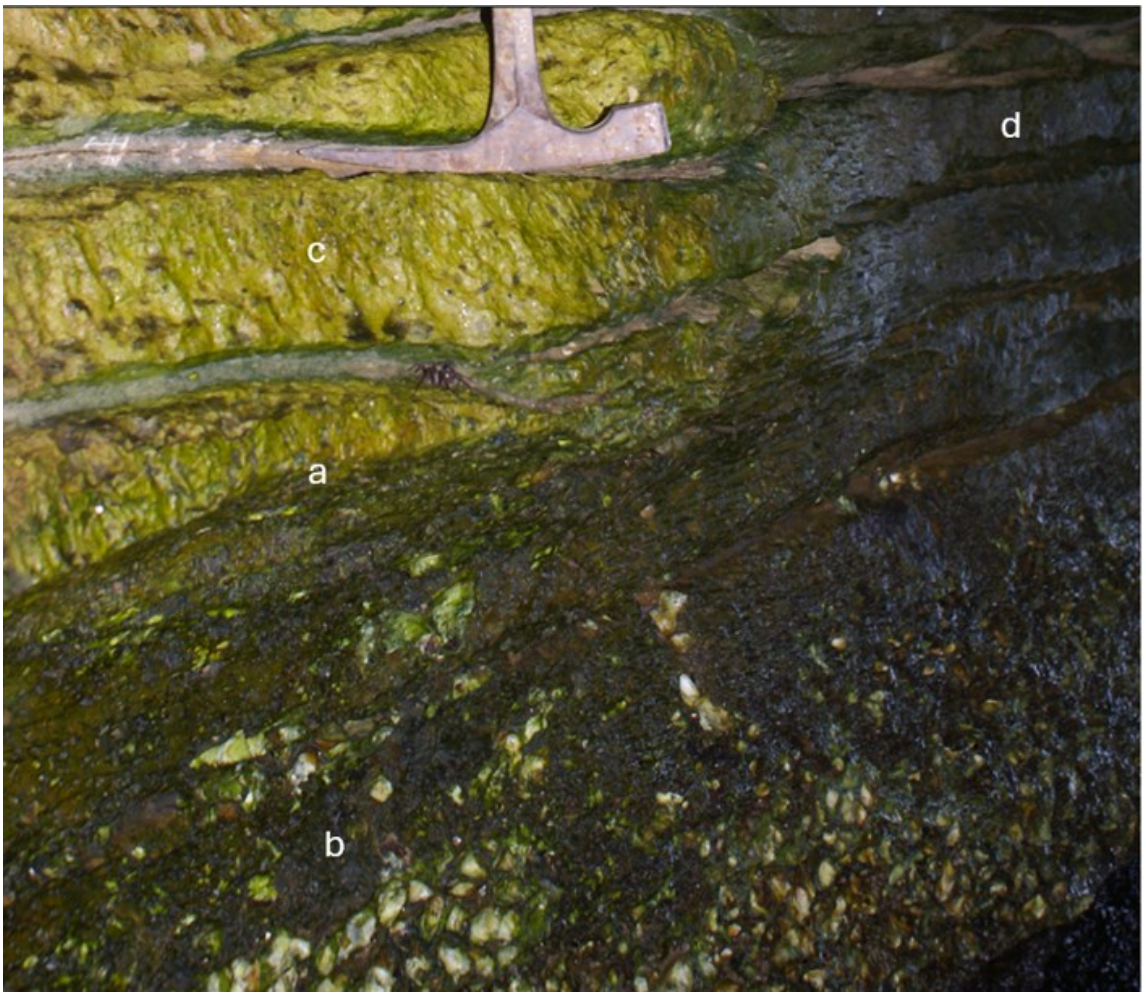

Figure 6.2: The modern effective high tide level (a) displaying a distinct colour change between a marine biota-rich immersion zone (b) and smooth Raglan Limestone (c). The black zone (d) is the result of ground water seepage through overlying soils.

All internal strata in the flowstone are hard and crystalline. The knapping of the dating sample required several heavy blows from a geological hammer. Varying depositional environments are displayed through colour variations of the layers (Figure 6.3). Two strata from a sample extracted from an elevation of 0.6 m above the modern EHTL were U-Th dated at ~ 23.4 Ka and ~ 23.5. Ka respectively (Figure 6.4) (Appendix B).

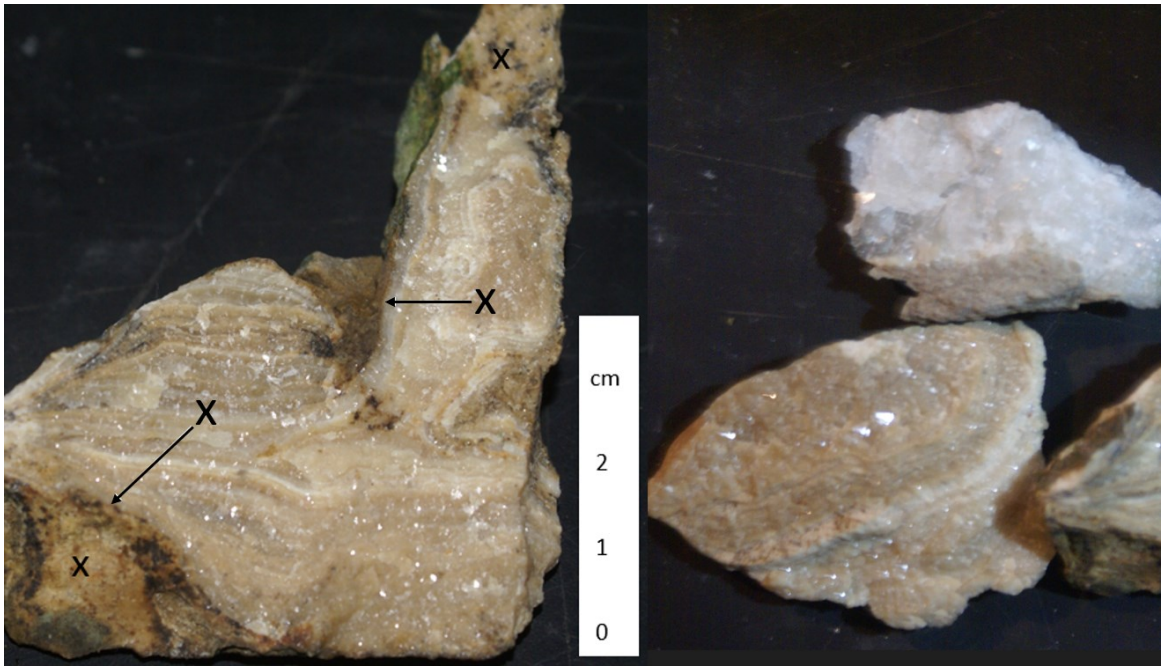

Figure 6.3: Hard knapped fragments of the Horongarara Flowstone with consistent crystalline strata and minimal alteration of the natural surface (x).

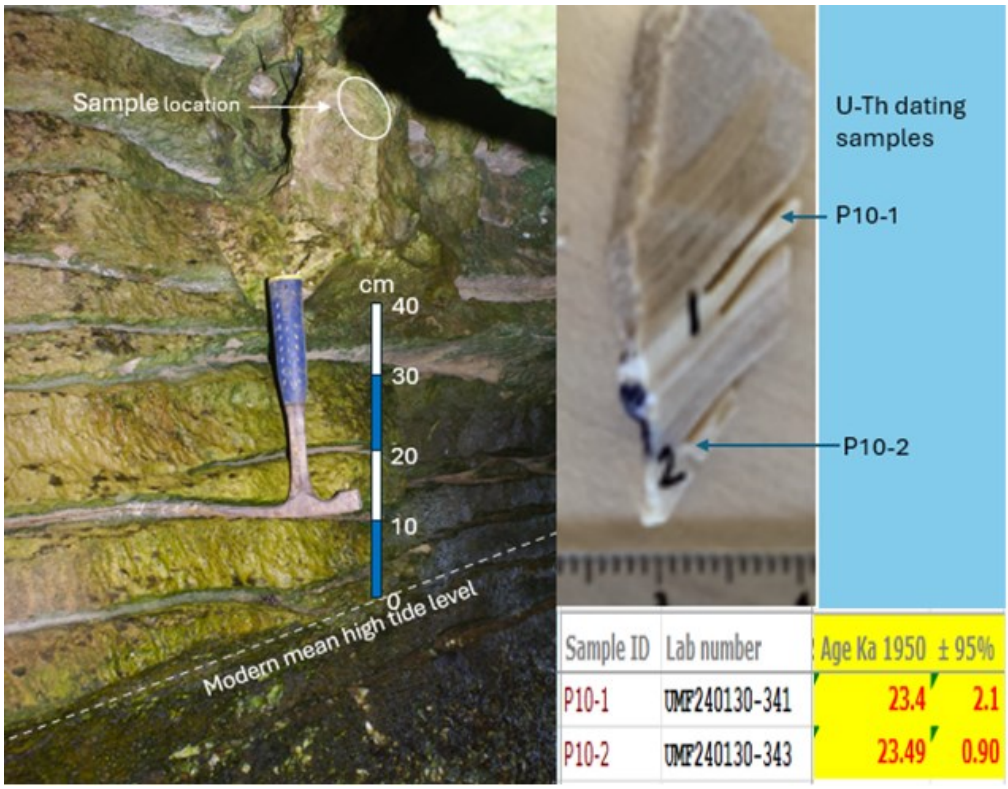

Figure 6.4: The Horongarara Flowstone precipitation record with ages of specific strata.

6.3: Speleothem Position, Condition, and Age

Six properties relating to the Horongarara Flowstone have been established, from which implications relating to RSL can be derived. The:

- Physical condition of the entire flowstone
- Physical condition of the host rock surface
- Physical condition of 2 further flowstones exposed to tidal emersion and wave-splash on the open shoreline
- Position of the modern EHTL
- Elevation of the Horongarara Flowstone above the modern EHTL
- Age of 2 strata from within the flowstone

The flowstone is comprised of hard crystalline strata with an external surface exhibiting no evidence of dissolution or deposition indicative of marine immersion. The host rock's surface above the EHTL is in a similar condition to the flowstone: smooth and hard. The modern EHTL is clearly identifiable through discolouration and the presence of marine flora and fauna. There is no evidence of a paleo high tide level in the form of notching or erosion between the modern EHTL and the flowstone.

In contrast, 2 flowstones situated on sea-cliffs 20 m distance away are exposed to open-marine spray and wave-splash. These have been degraded to the state that their remnants can be crushed between the fingers (Figure 6.5). Their age is undetermined.

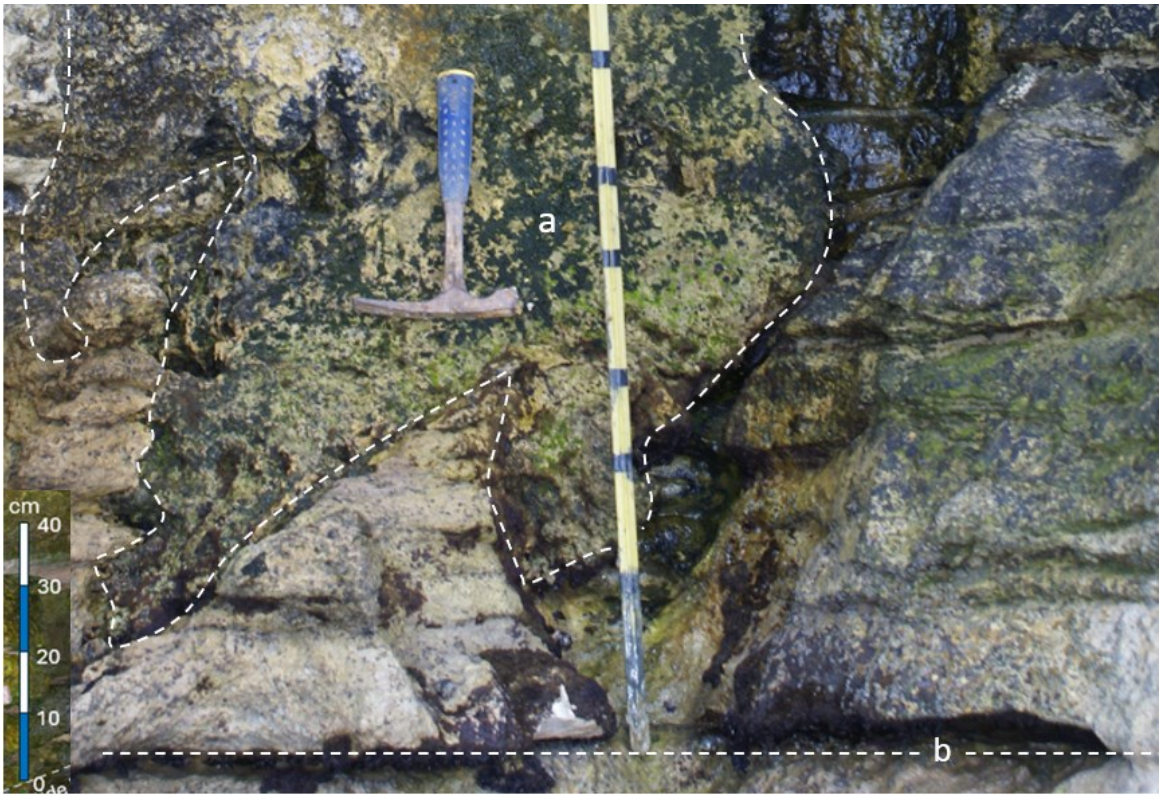

Figure 6.5: A highly degraded flowstone (a) directly above the modern effective high tide level notch (b) exposed to open-marine spray and wave-splash. The composition consists of a crust over powdered materials that can be penetrated by finger pressure.

6.4: Speleothem Properties Implications

Assuming that the Horongarara Flowstone's condition is indicative of it not having been impacted by sea water immersion or regular drenching, a reasonable conclusion is that the modern ESL at this location is near its maximum within the last ~ 23.5 Ka. Working with this supposition and that the current EHTL – Horongarara Flowstone separation is 0.4 m, there are 6 possible combinations of EHTL and VLM scenarios occurring throughout the last ~ 23.5 Ka:

- EHTL and VLM have remained static
- EHTL is now near its ~ 23.5 Ka maximum height while VLM remained static
- EHTL has been higher by > 0.4 m while VLM has been negative (subsidence)
- Both EHTL and VLM have been positive (rising)
- Both EHTL and VLM have been oscillating outside of a separation of 0.4 m
- The speleothem location was physically isolated from sea water immersion during the event of a historical relative sea level high

Once combined with dependable metrics on historical ESL change and/or VLM the Horongarara Flowstone becomes an important datum.

6.5: Speleothem Proxy Summary

Through alterations in composition and morphology, speleothems can contain a record of water immersion. While extensive research has been conducted on speleothems in caves subject to brackish water flooding, no studies relating to full marine environments were located during this thesis research.

Field reconnaissance during this study discovered several speleothem flowstones on limestone bluff surfaces exposed to the harbour foreshore. These were in an advanced state of degradation and not suitable as dating samples. In a crevice protected from open-marine spray and wave-splash, a flowstone in a robust condition was located at 0.4 m above the modern EHTL. Two flowstone strata were U-Th dated at 23.4 and 23.5 Ka yr BP respectively.

Through adopting the evidence that the dating flowstone had never been immersed in seawater it becomes an important positional datum for maximum RSL within a substantial timeframe at this location in the Raglan Harbour.

CHAPTER SEVEN

MARINE DISSOLUTION NOTCHES

7.1: Dissolution Notches Introduction

Through comparison of dissolution notches exhibited in historic photographs with modern equivalents this chapter proposes constraints on RSL change and VLM since 1910 at 2 locations in the Raglan Harbour.

Dissolution (tide) notches are observable physical zones imprinted on rock surfaces where grooves, indentations, or irregularities are displayed on the surface of rock due to physical erosion and/or rock cement dissolution due to marine immersion or regular drenching. A dissolution notch includes all those rock surfaces below a notches' uppermost extent. The uppermost extent of a dissolution notch is an obvious boundary between those rock surfaces displaying the effects of marine immersion or drenching and those where these effects are absent. These boundaries are relatively sharp and are clearly observable from a 10 m distance. Both modern and paleo notches are discussed in this chapter. The term 'effective high tide level' (EHTL) is here defined as the uppermost extent of a dissolution notch (the boundary).

The Raglan Harbour has extensive coastal sections comprised of rocks that display dissolution notches that are clearly observable below the EHTL. Rock surfaces above the EHTL often display traces of paleo-notches that may be representative of paleo SL highs. These may be definable only through the rocks' surface profiles i.e. evidence of surface alteration through immersion is absent.

The most durable dissolution notches are in limestone. However, due to variations in sedimentary bed lithologies, apparent notches above the modern EHTL may be entirely a result of varying erosion susceptibility. Limestone and sandstone beds can vary from being hard and crystalline through to softer calcareous sandstone, reflecting environmental change during deposition.

These beds are commonly orientated to a near-horizontal plane. Softer lithologies can weather in a manner that mimic paleo-notches. Therefore, care must be taken over paleo dissolution notch identification.

Other forms of subaerial rock-surface morphologies can reflect paleo sea levels. Near-vertical concave drainage channels formed by rainwater-induced dissolution are common in the more elevated sections of limestone. Paleo and modern sea levels result in a clearly distinguishable boundary where the rainwater channels terminate (Figure 7.1).

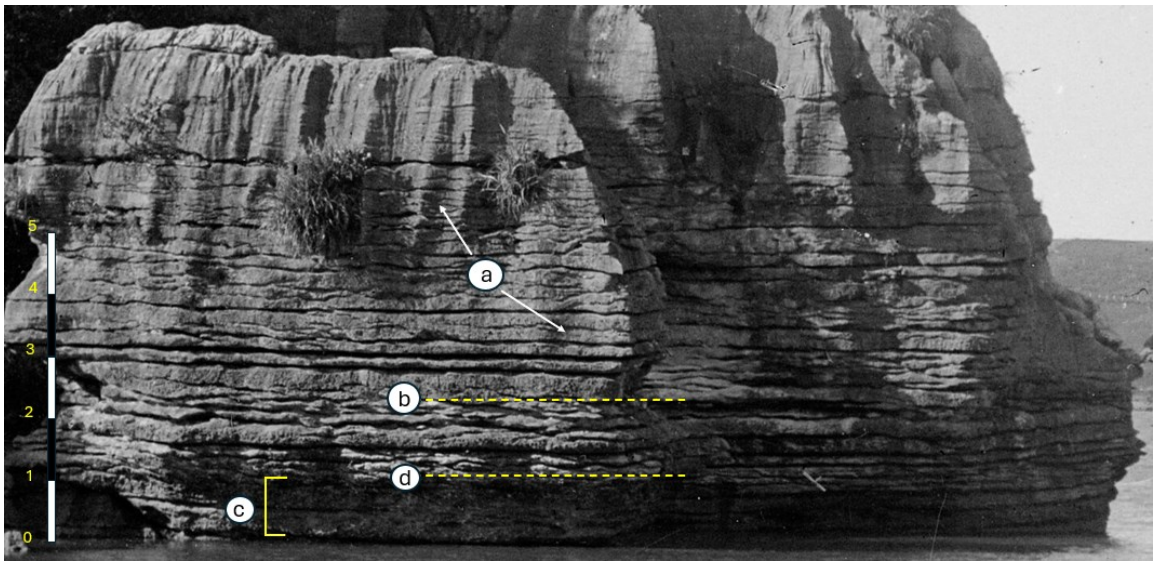

Figure 7.1: Rain erosion channels (a) terminating at a boundary (b). The modern tidal dissolution notch (c) underlies the modern effective high tide level (d). Raglan Limestone, Bird's Bay. **Large image**

7.2: The Wine Glass Rock

The Wine Glass Rock is an isolated pillar of limestone located in Bird's Bay, Raglan Harbour. Its stem of ~ 1.2 m diameter supports a bowl of ≤ 5 m diameter. Three historic photographs taken by Gilmore Bros in 1910 are held by the Alexander Turnbull Library (Figure 7.2).

Figure 7.2: The Wine Glass rock at half-tide. Photo by Gilmore Bros (1910).

Photographs taken in 2022 from perspectives best matching the historic photos are here used as a comparison to establish changes throughout the 112-year period (Figure 7.3). The uppermost extent of the dissolution notch is distinguishable through a sharp contrast in the rock surface properties. This boundary (the EHTL) is observable in both the historic and modern photographs. Rock surfaces within the dissolution notch are weak and flaky, whereas the supersurface subaerial rock surfaces are hard and smooth. There has been no appreciable change in the vertical position of the boundary between these contrasting surfaces since 1910. A distinguishable feature in the 2022 photograph is brown discolouration of the rock and surrounding tree branches to a maximum elevation of ~ 0.25 m below the notch boundary/EHTL. The extent of discolouration represents the EHTL.

Based on this evidence, the EHTL is no higher than that which formed the dissolution notch prio to 1910. Moreover, based on modern tide-related discolouration, it may be ≤ 0.25 m lower than in 1910.

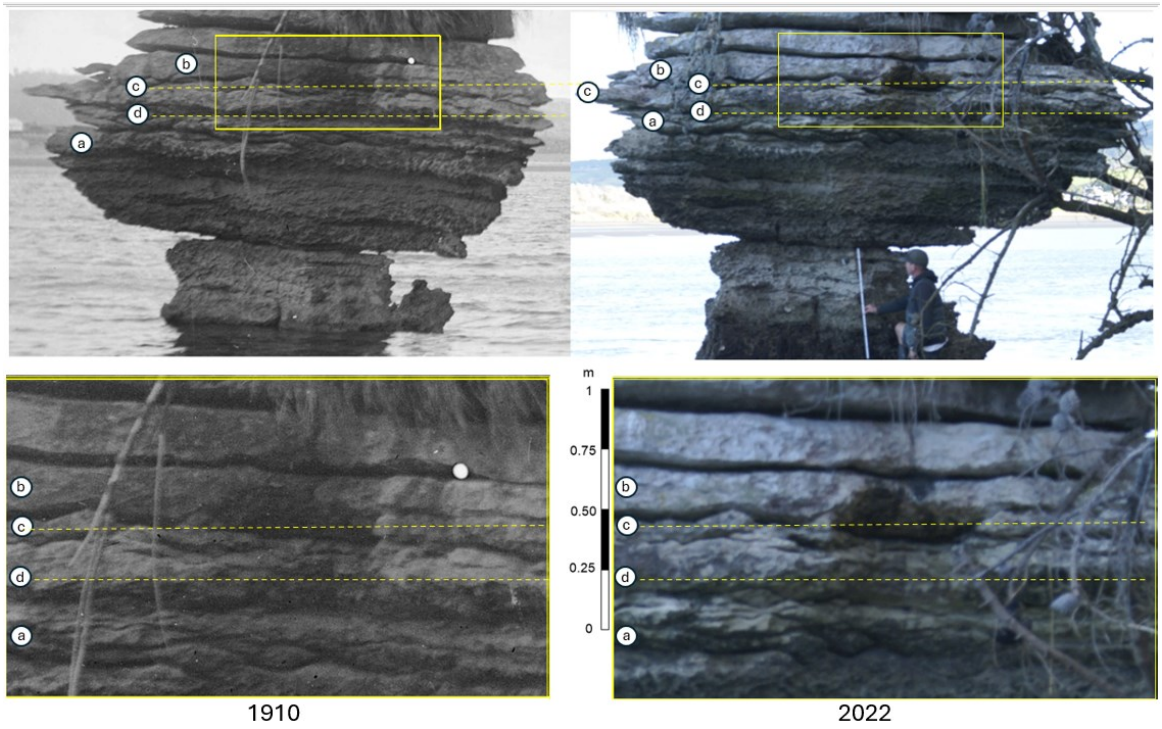

Figure 7.3: The flaky-surfaced marine immersion notch zone (a) and the supersurface rock (b) demarcated by the notch boundary/EHTL (c). Brown discolouration below boundary (d) is the modern EHTL, indicating that RSL may have dropped to level (d) since a maximum at level (c). Historic photo by Gilmore Brothers (1910). **Large image**

7.3: Pakawau Rock

Pakawau rock is also an isolated remnant of Raglan Limestone situated in the Ponganui Bay, Raglan Harbour. A historic photograph of this rock is labelled with the date 1/8/1910 (Figure 7.3**).** The rock sits in its residual position on a base of limestone located below mid-tide level.

Figure 7.4: Pakawau Rock at mid-tide in a residual position with bedding dip and strike conforming with the shoreline outcrops of Raglan Limestone. Photo by Gilmore Brothers (1910).

Pakawau Rock displays a modern dissolution notch subjected to tide immersion, underlying an apparent paleo dissolution notch. The apparent paleo EHTL is ~ 0.5 m above the modern EHTL. As is the case for the Wine Glass Rock, the modern tidal immersion notch is clearly distinguishable through its flaky surface. Limestones flags directly above this notch boundary/EHTL display smooth surfaces similar to that of the supersurface zone on the Wine Glass Rock. The 2023 photo shows living moss-like vegetation growing from ~ 0.25 m above the modern notch boundary to the top of the rock. If this vegetation will not grow below the EHTL it is another indicator that the modern EHTL is no higher than the EHTL that formed notch prior to 1910. (Figure 7.5).

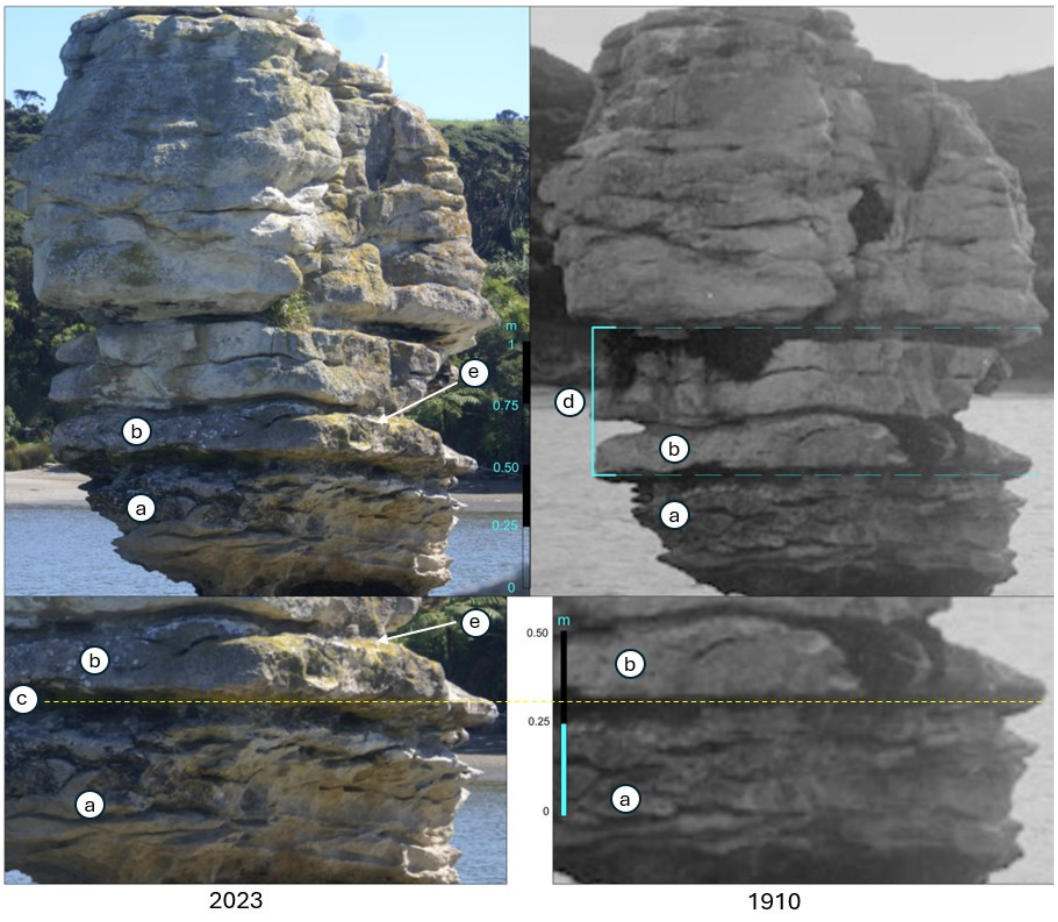

Figure 7.5: Pakawau Rock, Raglan Harbour. The modern dissolution notch (a) underlying smooth-surfaced limestone (b) forming a possible paleo-dissolution notch (d) demarcated by a sharp notch transition boundary/EHTL (c). Living moss-like vegetation (e) is evidence that the modern effective sea level does not impact the rock higher than the boundary (c). 1910 photo by Gilmour Brothers (1910). **Large image**

7.4: Dissolution Notch Implications

7.4.1: Implications Regarding Eustatic and Relative Sea Level Change

Photographs of rock surfaces dated 1910 of 2 rocks provide an opportunity to compare the extents and morphology of tide-induced dissolution notches over a 110-year timespan. The photographs demonstrate that the notch elevations on the rocks have not appreciably changed within a range of +/- 50 mm. When adopting a conservative ESL rise of average 1.2 mm/year and a VLM of zero, RSL rise since 1910 should have risen by 0.134 m. There is no evidence of this change.

The field evidence indicates that when adopting an assumption that the EHTL in 1910 was at the level of the notch boundary shown in the 1910 photographs, then:

- There has been no discernible change in VLM or ESL since 1910

  or
- VLM (uplift) has either equalled or exceeded ESL rise throughout the 112-year period

The only circumstances where ESL rise could have exceeded uplift in the last 112 years is when in 1910 it was lower than the notch boundary i.e. uplift had occurred prior to 1910.

7.4.2: Implications Regarding Vertical Land Movement

Throughout the period 2003 to 2011 NZ SeaRise measured VLM at multiple locations in Raglan harbour. This was achieved by combining spaceborne geodetic observations from interferometric Synthetic Aperture Radar (InSAR) and Global Navigation Satellite Systems (GNSS) (NZ SeaRise, 2023). VLM at locations within 300 m from Wine Glass Rock and Pakawau Rock were reported as being subject to subsidence of 3.8 mm/year and 3.31 mm/year respectively (Figure 7.6). When combined with the assumptions listed in Section 7.4.1 and in the absence of VLM, the sum of this subsidence and ESL rise of 1.2 mm/year should have resulted in a RSL rise of $\geq$ 500 mm since 1910. Neither rock display any evidence of effective/relative SL rise of this magnitude.

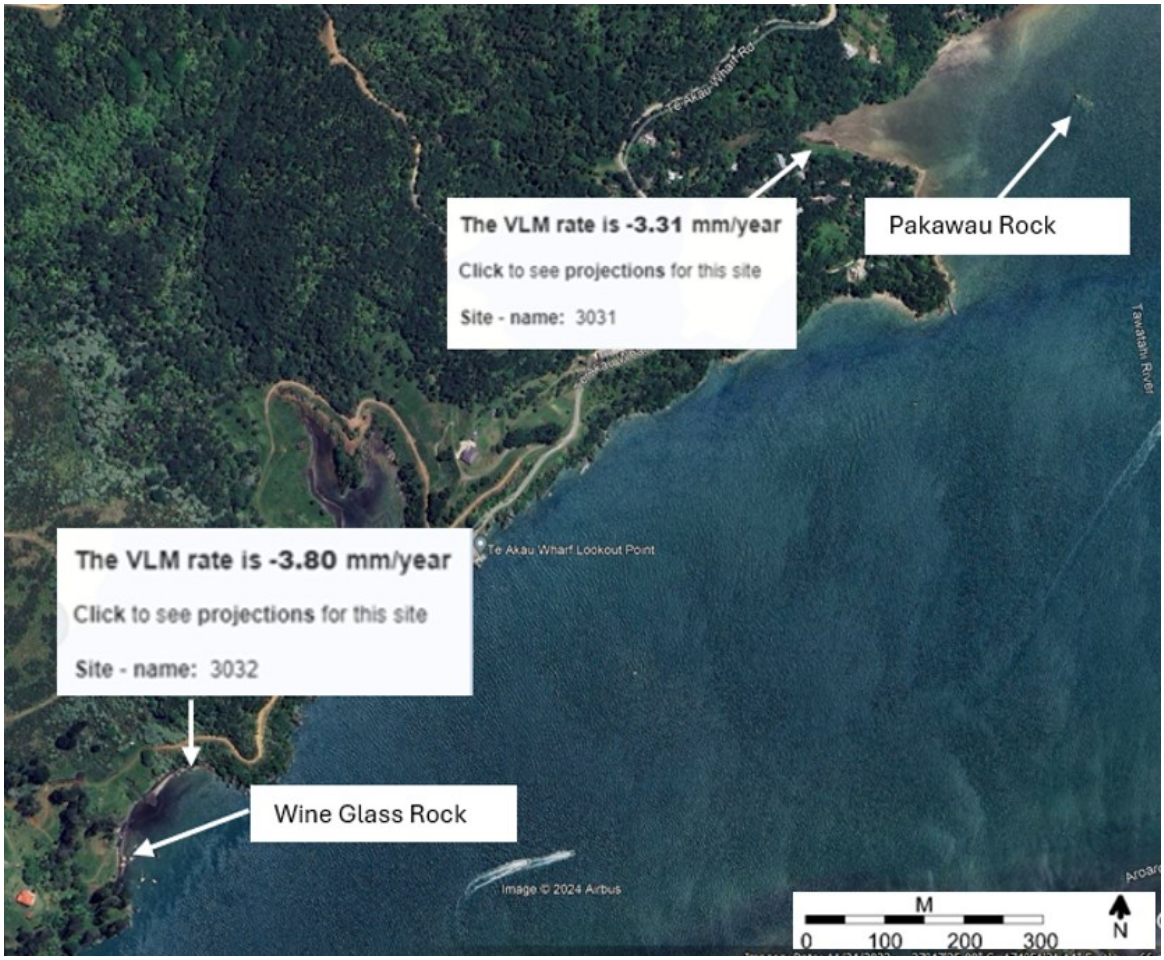

Figure 7.6: Magnitude of measured subsidence at locations proximal to Wine Glass Rock and Pakawau rock throughout the period 2003 to 2011. Extracted from NZ SeaRise 2023.Dec.08.

Assuming that there has been no appreciable change in the rocks' notch boundary positions since 1910, then 5 VLM and/or RSL change scenarios are possible:

1. An ESL rise of 1.2 mm/year was negated by uplift
2. No appreciable VLM or ESL change
3. Subsidence of 3.5 mm/year negated by periodic uplift events
4. RSL in 1910 was lower than the EHTL notch and that ESL has risen by 1.2 mm/year throughout the 110-year time period
5. A combination of all these dynamics

Scenario 1 allows for average ESL rise of 1.2 mm/year. Given the lack of evidence of an EHTL at higher elevations than the notches, it requires that the EHTL in 1910 was lower than the dissolution notches displayed in the 1910 photos. This also requires that the effective SL responsible for the 1910 notch erosion occurred sometime prior to 1910, to be followed by effective SL fall by no less than 135 mm. This fall could have been due to an uplift event prior to 1910. Scenario 2 requires the unlikely event that no ESL and VLM change occurred. The weight of evidence involves some degree of VLM (uplift).

.

7.5: Dissolution Notches Summary

Photographs of 2 rocks spanning 112 years display no evidence that the modern RSL/EHTL is higher than that which formed the notches prior to 1910.

Through adopting the assumption that ESL rise has been a conservative 1.2 mm/year average throughout the last century, an explanation for the apparent absence of such evidence in these rocks' morphology is that uplift has at a minimum matched ESL rise throughout this 110-year timeframe. These uplift events may have occurred prior to 1910.

An additional possibility is that VLM may involve incremental subsidence, periodically overridden by abrupt uplift events. However, uplift events of magnitudes sufficient to negate the subsidence rates as reported by NZ SeaRise (2023) are unlikely. From a field observation perspective, a more likely scenario is that VLM trend is upward, negating ESL rise prior to and throughout the last century.

CHAPTER EIGHT

SPECIFIC STUDY SITE DESCRIPTIONS

8.1: Site SB_1. Raglan Recreation Ground

8.1.1: Site SB_1. General Description and Geology

Site SB_1 is exposed within an excavated drain bank located within a paleo tidal estuary. Prior to the early 20th century when a causeway and floodgate were constructed. The mean high tide coverage included a significant area that is now a reclaimed recreational ground.

While the floodgate was designed to control tidal inflow, its operation has been intermittent due to poor maintenance. Currently, a proportion of tidal inflow reaches the study section via drains, where fresh water backs up on each high tide, forming a brackish mix at this study-site's shellbeds. While more reclamation has occurred since 1944 this has not influenced water dynamics of the drainage system.

Upstream from the study-site the drain's banks are comprised of fully saturated soils within swamp at some locations. The comparatively low pH of this fresh water has is the probable cause of extraordinary degradation of shell material within the lower sedimentary units.

The site is situated within 6 m from a major fault scarp within the late Eocene - early Miocene Te Kuiti Group limestone (Raglan Limestone) and an overlying calcareous siltstone (Whaingaroa Siltstone lithotype). Forming the NE shoreline of the paleo estuary, this scarp was identified during this study's desktop and field research. The SW extent of the estuary is comprised of the low-lying Quaternary Kaihu Group silts and sands overlying the siltstone (Figure 8.1.1).

The fault extends from the Raglan Harbour main channel to the head of the estuary where it is integral to an apparent fault network that transects Raglan township and its foreshore (Chapter 3).

Being situated within a fault zone, the study site displays evidence of being subject to considerable disruption during the fault development. Limestone fault breccia is common within the drain channel and on its banks (Figure 8.1.2).

Figure 8.1.1: Geology of the Raglan Recreation Ground and Surrounds. Background image: Google Earth 2023.Dec.19. **Large image**

8.1.2: Site SB_1. Quaternary Stratigraphy

Site SB_1 is comprised of 4 sedimentary beds (Figure 8.1.2)

- RG_4: Fossil-poor organic-rich drained swamp soils
- RG_3: Sandy silt hosting a condensed shellbed
- RG_ 2: Residual fossil-rich residual silty sand
- RG_1: Bioturbated fossil-poor silty sand

Figure 8.1.2: Drained organic-rich swamp soil (RG_4) overlying reworked fossil-rich sandy silt (RG_ 2) containing limestone fault breccia (B), overlying bioturbated fossil-poor silty sand (RG_1). Sparse pockets of RG_3 consisting of condensed fresh bivalves located in confined pockets near the mean high tide level (dashed line).

A record of bioturbation within bed RG_1 has been preserved in the form of castings located in the drain channel. These castings are comprised of indurated burrow infill that is more durable than the host bed sediments that have been removed through erosion. The castings contain macrofossil valves. It is likely that these valves were residual within a sandy bed that washed into burrows (Figure 8.1.3).

Figure 8.1.3: Bioturbation burrow casting with integral cockle shell originating from Bed RG_1.

8.1.3: Site SB_1. Macrofossil Shellbeds

Site SB_1 contains 2 shellbeds distinctly different in nature. The lower shellbed consists of chaotically dispersed shell material throughout bed RG_2 (Figure 8.1.2). The shell material is in an advanced state of weathering, being weak enough to fracture between 2 fingers. The percentage of intact bivalves is relatively low. One sample consisting of 1 cockle (*Austrovenus stutchburyi*) valve from near the top of bed RG_2 was Percentage Modern Carbon (pMC) dated at 637 yr BP **(**Appendix B).

Bed RG_3 is comprised of confined pockets of condensed fresh-appearing cockles (*Austrovenus stutchburyi*) with articulated (joined) examples at ≤ 50% concentrations by number. Its elevation is directly above the apparent mean high tide level, within 0.3 m from the drain bank crest. Five samples of intact cockles (*Austrovenus stutchburyi*) from bed RG_3 were pMC dated at 6423 – 6465 Ka yr BP (Table 8.1.1). This anomaly of 5 samples at ~ 6 ka age at a higher elevation than the 0.637 Ca yr sample is likely due to the mechanised drainage that has laid materials from the bottom of the drain onto the drain banks. The presence of the indurated trace fossil castings (Figure 8.1.3) at the bottom of the drain channel supports an interpretation that paleo marine beds of pMC ~ 6 Ka yr BP age are located at depths of ~ 1.5 m below the modern land surface at the study site. Further work is required in relation to this hypothesis. If this is validated it becomes an important constraint on VLM and/or RSL change at this location dating back to ~ 6 Ka yr BP.

Table 8.1.1: Raglan Recreation Ground dating sample locations and ages

Sample	Age pMC	Age calibrated* (95%)	Sample	Age pMC	Age calibrated* (95%)
Rag_1_SB	637	70 – 430 cal. BP	RG_2_a	6465	6560 – 6900 cal. BP
Rag_S2_1	6442	6690 – 7090 cal. BP	RG_2_b	6460	6560 – 6890 cal. BP
Rag_S2_2	6423	6670 – 7050 cal. BP	RG_2_c	6430	6520 – 6860 cal. BP

* See Section 1.3.10 and Appendix B for age interpretations

8.1.4: Site SB_1. Microfossils

All sedimentary beds were evaluated for foram concentrations. Most forams counted were within the fraction range 212 – 355 µm (sand). Proportions were established as the percentage of forams by number in relation to the total number of grains within this size range. A full summary of microfossil concentrations is reported in Appendix C.

The basal bed RG_1 is dominated by silty sand. Grains are subrounded, indicating a high-energy environment (Figure 8.1.4). It contains insignificant proportions of forams in the diameter range 212 – 355 µm. However, there are concentrations of ≤ 0.5 % forams exceeding 355 µm in minimum diameter, indicating that forams of ≤ 355 µm diameter may have been completely dissolved. Along with very weak macrofossil shell fragments, these forams are in an advanced state of chemical weathering (Figure 8.1.5). The state of weathering of the organic materials is consistent with daily immersion in brackish water, which is likely to have a lower pH than seawater.

Bed RG_2 contains > 95% of the *Austrovenus stutchburyi* macrofossils found at the Raglan Recreation Ground site (SB_1). The host sediments have concentrations of 5 – 10 % foraminifera by total number of grains in the 212 – 355 µm range (Figure 8.1.6).

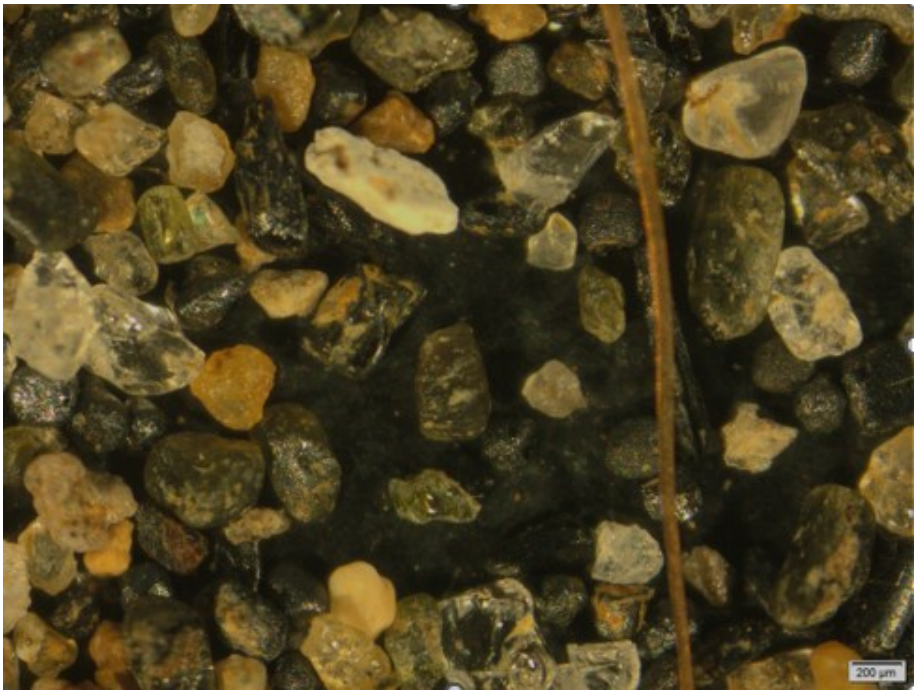

Figure 8.1.4: Bed RG_1. Subrounded mineral sand grains of 212 – 355 µm diameter devoid of microfossils. Raglan Recreation Ground.

Figure 8.1.5: Bed RG_1. Weathered foraminifera and bivalve shell fragments exceeding 355 µm minimum diameter. Raglan Recreation Gound.

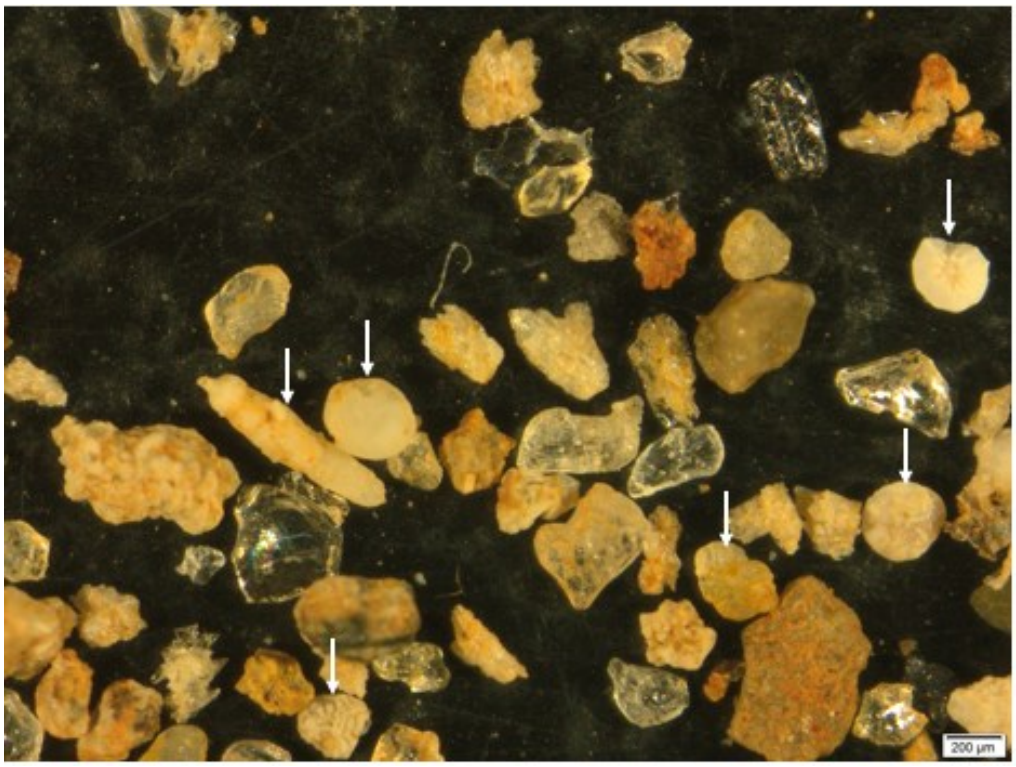

Figure 8.1.6: Bed RG_2. Foraminifera concentrations of 5% - 10 % of total grain numbers of 212 µm – 355 µm diameter. Raglan Recreation Gound.

Bed RG_3 is located at the mean high tide level and directly below topsoil. It is subject to regular saturation from both brackish water and fresh ground water. It has very low concentrations of forams within the host sediments. This is likely due to the relatively low pH of the water with which it is regularly saturated.

Shellbeds within RG_3 consist of very isolated pockets of fresh-appearing cockles (*Austrovenus stutchburyi)* 50 % of which are intact. The dating samples from bed RG_3 consisted of 1 valve from each of 5 intact cockles. These all contained well sorted fine sand sediment within which foram concentrations were established as being 15 – 20 % (Figure 8.1.7). These are notably less weathered than the host bed forams. The cockles (*Austrovenus stutchburyi)* from which this infill was extracted were ^{14}C dated within the range pMC 6.423 – 6.465 Ka yr BP.

Bed RG_4 is organic topsoil derived from drained swamp. The proportion of forams is insignificant.

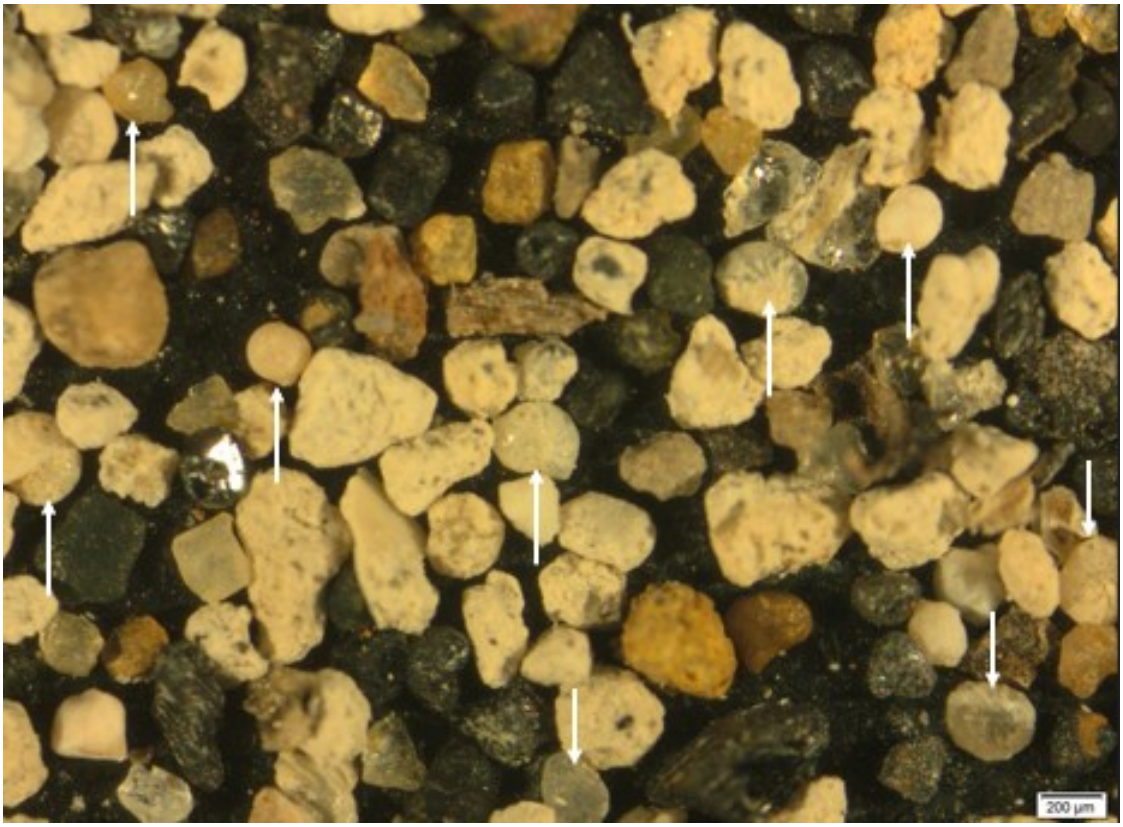

Figure 8.1.7: Foram concentration of 15% – 20 % within bed RG_3 intact bivalve infill. Raglan Recreation Gound.

8.1.5: Site SB_1. Relative Elevations and Relative Sea Level Change

A GNSS elevation survey of the shellbeds and the estuary provided data from 4 waypoints. These were located at the:

- Top of the shellbed RG_2
- Mean high tide mark on the floodgate buttress
- Extreme high tide mark on the floodgate buttress
- Top of the most inland living cockle bed within the tide-zone

The objective of this exercise was to establish the elevation difference between the top of shellbed RG_2 and the top of its equivalent modern living shellbed in the tide-zone. The elevation difference is 0.972 m (Figure 8.1.8). This indicates that combined uplift and/or SL change of this magnitude has occurred within the age of the dated fossil extracted from this bed: pMC 637 yr BP. (Appendix B).

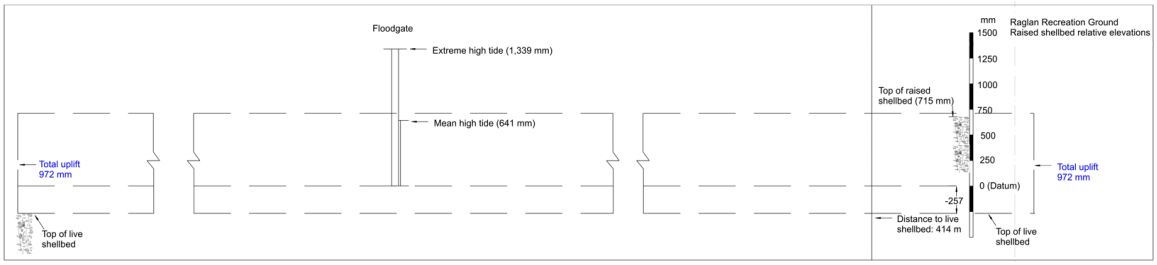

Figure 8.1.8: Site SB_1. Schematic cross-section between the raised shellbed RG_2 and its modern living equivalent in the tide-zone. **Large image**

The nature of the 4 identified stratigraphic units (Figure 8.1.2) reflects their residual and reworked environments. The basal bed RG_1 is a clayey/silty sand with sparse shell fragments and pebbles. It is notable through its high degree of bioturbation, scarce macrofossils and low occurrence of microfossils (Appendix C).

The setting in which the bioturbation burrowing occurred is unclear. It could be the original residual marine environment, or the more recent conditions of periodic brackish water saturation during an uplift phase. Relatively fresh burrows within the overlying bed RG_2 indicates that burrowing of this nature can occur in brackish environments.

Bed RG_2 is notable through the chaotic distribution of weak macrofossil valves and fragments (Figure 8.1.2). The age of a dating sample extracted from this bed is pMC 637 yr BP (Appendix B). This age and saturation in brackish water are the probable causes of the weak state of macrofossil material within bed RG_2.

The cockle *Austrovenus stutchburyi* (formerly known as *Chione stutchburyi*) is a shallow-burrowing suspension feeder of the family *Veneridae*. Individuals are rarely found deeper than 5 – 10 cm below the host sediment surface (Anderson et al., 2019). Shell material within bed RG_2 is distributed in a random, chaotic manner throughout a depth of 50 cm. This is probably a result of crushing and reworking by shellfish consuming biota.

Bed RG_2 is similar in nature to a bed at the study site SB_3 (Patikirau Bay) that probably uplifted relatively abruptly and may not have been subjected to significant reworking during uplift.

Bed RG_3 is comprised of discrete pockets of relatively fresh bivalves,~ 50 % of which are intact. These are embedded in a burrowed sandy silt (Figure 8.1.9). While only I shellbed of this kind was discovered, 6 isolated intact (articulated) cockles (*Austrovenus stutchburyi)* of a similar condition were found within a 10 m section of the drain channel-bed. Five samples were pMC dated at 6423 – 6465 yr BP. This age indicates that the original position of shellbed RG_3 is probably below bed RG_2, at the drain channel-bed level and that its elevated position Is due to re-deposition by drain excavation machinery.

Figure 8.1.9: A confined pocket of fresh bivalves within burrowed bed RG_3. Five samples from this bed were ^{14}C dated at ~ 6 Ka. Given their position above bed RG_2 dated at 637 yr BP this bed has probably been relocated by drain excavation machinery.

A combination of stratigraphic, sedimentological, palaeontological, and chronological properties indicates that Raglan Recreation Ground has been subject to uplift phases. The age, distribution, and concentrations of macro and micro fossils within bed RG_2 indicates that it has not been reworked and that it was subject to a relatively rapid uplift progression occurring since ~ 637 yr BP.

Bed RG_3 is a condensed shellbed that has probably been re-deposited by machinery from a position underlying RG_2. Infill within the dating sample bivalves contains 15 - 20 % forams. These are fresh in appearance and are representative of present-day species found in the Raglan Harbour foreshore. Most of these forams are not reworked Oligocene species but modern *Ammonia aoteana* - which will be the dominant intertidal forams in the modern harbour environment. (B. Hayward 2023, pers. comm., 28th Sept).

8.1.4: Site SB_1. Raglan Recreation Gound Summary

The Raglan Recreation Ground study site is comprised of 2 shellbeds exposed in the banks of excavated drains. Prior to the installation of tide floodgates in the early 20th century the site was near the banks of a tidal estuary. It is now daily exposed to brackish swamp water saturation. The site is within 10 m of an obvious major fault, identifiable through morphology and the presence of fault breccia. The estuary upslope from the floodgate is now mostly infilled by engineered back-fill and terrestrial sediments. Due to a recent policy of leaving the floodgate open, brackish water floods the shellbeds at high tides.

Fossil dating established that the shell beds are of significantly differing ages, one bed being of age ~ 6 Ka yr BP and the second of age ~ 6 Ca yr BP. The older samples were likely out-of-position, signifying probable anthropic disturbance. The hardness and position of common trace fossil casts found on the drain channel beds suggests that these may be of a similar age as the older fossils and that the original position of the fossils found in Bed RG_3 is below Bed RG_1 at and below the drain channel bottom elevation.

GNSS surveying established that the younger shellbed in Bed RG_2 is ~ 0.9 m above its living species' habitat in the harbour tide-zone. The combined data collected at this site identifies 3 tide-zone habitats that have been subject to significant RSL fall throughout the last ~ 6 Ca. Given the combined evidence of VLM presented throughout this chapter VLM (uplift) has likely been a significant contributor to the amount of RSL at the Raglan Recreation Ground site.

Given its location within the Raglan Township, and an abundance of datable fossils, the Raglan Recreation Ground site warrants further study. The apparent absence of fossils aged within the 0.6 – 6 Ka yr BP period also warrants further attention as it may represent a history of uplift and erosion, or a significant change in paleo-habitats.

8.2: Site SB_2. Motukokako Point

8.2.1: Site SB_2. General Description and Oligocene Stratigraphy

Motukokako Point is a peninsula with an average width of 600 m and a length of ~ 1 km. Sea cliffs of ≤ 60 m in height form most of its shoreline. A ridge of ≤ 85 m elevation forms its central axis, from which 3 dominant incised drainage valleys radiate. Vegetation is predominantly native forest. The shoreline exposes fault traces, and at one location a fault-associated basaltic dike (Figure 8.2.1).

Figure 8.2.1: Motukokako Point showing identified faults and raised shellbed locations. Image extracted from Retrolens 2023.Nov.29.

Three Oligocene Te Kuiti Group rock members are present, overlaid with a ≤ 15 m thick deposit of the Quaternary Kaihu Group pumiceous silty sand. The stratigraphic and structural relationships of these rocks is notably complex. While the various formations were deposited in a vertical sequence, due to faulting they are often now at similar elevations at various locations along the shoreline. This architecture is the result of considerable vertical displacement of rock bodies, delineated by 3 major faults that dissect the peninsula. Multiple small-scale faults and stress fractures are common within these rock bodies. At one location a discrete basaltic dike of ~ 0.3 m average width extends inland in a direction consistent with a fault network identified at Patikirau Bay, 1 km distance away (refer to Section 8.4).

Bare rock cliff faces of ≤ 70^{o} slope angle and marine erosion scarps of ≤ 1.5 m height are exposed along > 50% of the peninsula shoreline. The balance is mostly comprised of unstable colluvium and rockfall debris. Foreshore intertidal platform surfaces are mostly comprised of wave-swept rock or thin sandy sediment overlying rock. Rockfall blocks are common on the beaches.

The beaches are atypical for Raglan Harbour, due to these being relatively narrow and of high shoal slope angles. This is probably due to the proximity of the main harbour channel 20 – 40 m from the shoreline. The channel depth is 6 – 8 m. While some beach sections do have marine shell-rich beach deposits, many others are barren (Figure 8.2.2).

Figure 8.2.2: Slide-failure slope colluvium (a) overhanging an erosion scarp along a 7° shoaling beach (b) with a very thin sand veneer overlying bare rock (c), Motukokako Point, Raglan Harbour.

The Oligocene calcareous rocks present include Mangiti Sandstone; Patikirau Siltstone (Whaingaroa Siltstone lithotype); Raglan Limestone and (possibly) Carter Siltstone. While considerable work has been done to establish the stratigraphic relationship of the rocks on a regional scale (e.g. Trapathi et al., 2008) these models are not granular enough to correlate accurately with the focused observations made during this study. For example, the distinctive Whaingaroa Siltstone lithotype (Kotuku Siltstone and Patikirau Siltstone) can be found to both underlay and overlie the Raglan Limestone. Moreover, the relationship of the Mangiti Sandstone with these rocks remains unclear. It can be found to overlie the Whaingaroa Siltstone lithotype in some locations and to be a lateral equivalent at others, due to faulting (Figure 8.2.3). These anomalies can be due to structural displacement and/or depositional facies variation. Facies variation can result in rocks of the same age and stratigraphic position having differing properties within their horizontal extent.

This reflects differing depositional environments during deposition on the marine shelves on which calcareous rocks are formed. For example, it is conceivable that Mangiti Sandstone grades horizontally into the Whaingaroa Siltstone lithotype within relatively short distances (Figure 8.2.4).

Figure 8.2.3: Normal fault with igneous dike (X) in the three Oligocene base rocks on Motukokako Point. The original stratigraphic position from top down was: Raglan Limestone (A); massive Patikirau Siltstone (B); Mangiti Sandstone (C). Vertical displacement is > 30 m. Motukokako Point, Raglan Harbour.

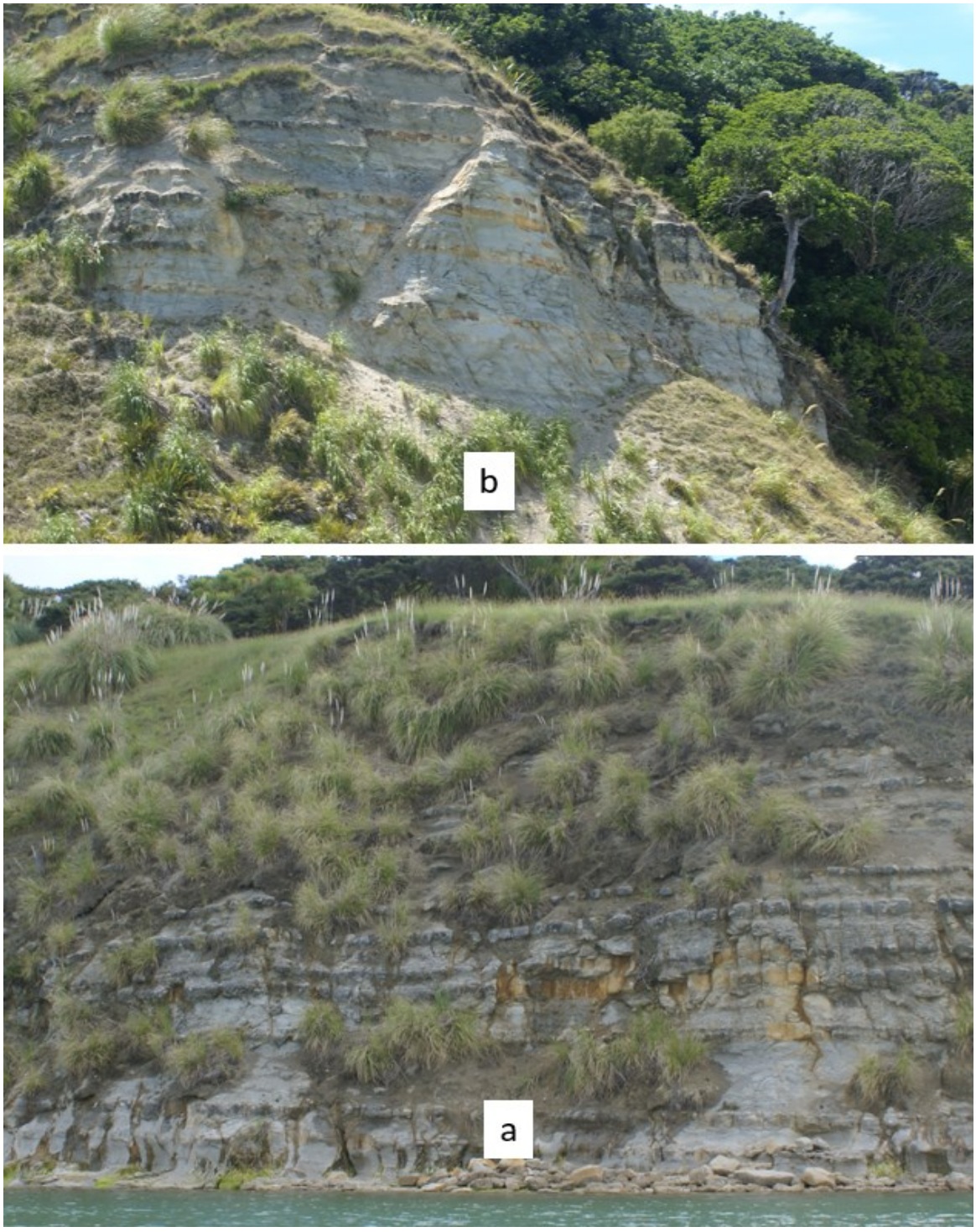

Figure 8.2.4: Examples of bedded Mangiti Sandstone (a) and massive Whaingaroa Siltstone (b) grading upwards into bedded sandy siltstone more typical of Mangiti Sandstone. Motukokako Point, Raglan Harbour.

8.2.2: Site SB_2. Quaternary Stratigraphy

Beginning in the Late Pleistocene copious quantities of tephra, colluvium, alluvium and eolian sand deposits (the Kaihu Group) began to mantle an erosion surface incised into the Te Kuiti Group and Alexandra Volcanic Field rocks (Barter, 1976; Richardson, 1985). This has resulted in $\leq$ 8 m of cohesionless bedded silty sand deposits which form much of the modern geomorphological surfaces and embankments in the Raglan coastal region. (Figure 8.2.5). Given its cohesionless nature, the Kaihu Group sediments are highly mobile and probably constitute a primary source of Raglan Harbour sediments.

Figure 8.2.5: Bedded Kaihu Group deposits overlying a sharp upper boundary of the massive Whaingaroa Siltstone lithotype. Okete Bay, Raglan Harbour.

While Motukokako Point would have been mantled in Kaihu Group soils at one time, these have since been eroded off most steeper slopes. Translation slide slope failure involving a mix of these quaternary soils and weathered Oligocene colluvium are evident at multiple locations along the shoreline (Figures 8.2.6; 8.2.7).

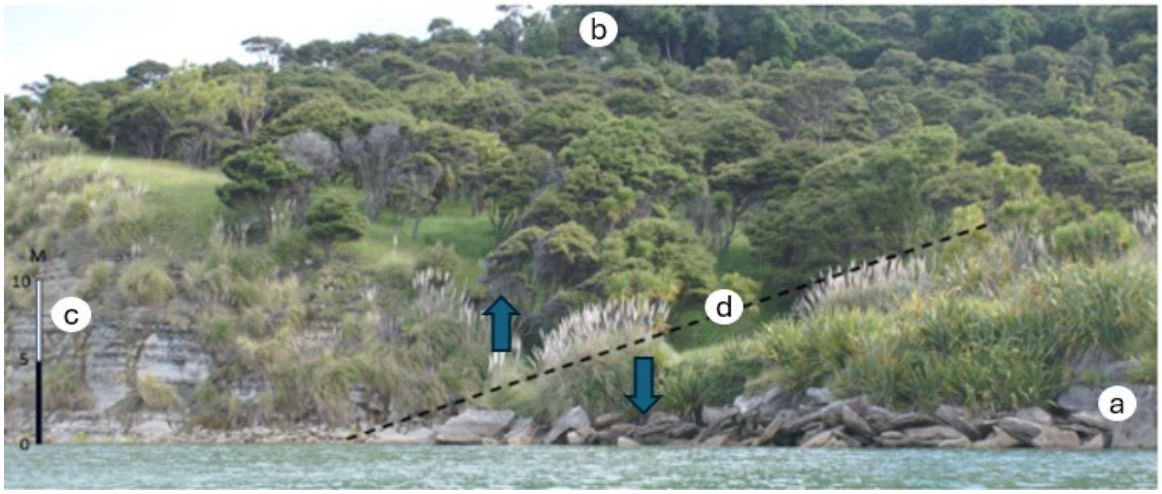

Figure 8.2.6: Landslide of Quaternary sand and toppled limestone (a) originating from a Raglan Limestone outcrop (b) within block faulted Mangiti Sandstone (c) with Fault scarp (d). The elevation of b is 65 m. Motukokako Point, Raglan Harbour.

Figure 8.2.7: Rotational slumping of Mangiti Sandstone (a) and translation slide failure of Quaternary sand (b) over a Whaingaroa Siltstone glide-plane (c) along a fault line (d). Motukokako Point, Raglan Harbour.

8.2.3: Site SB_2. Shellbeds

Raised shellbeds within beach erosion scarps were identified at 6 locations, of which 4 were selected for more focused analysis (refer to Figure 8.2.1). Shellbed elevations varied between 0.3 – 0.8 m above the modern strandlines which represent the modern effective high tide level (EHTL).

Two *Austrovenus stutchburyi* dating samples were extracted from a shellbed at location SB_2_1. This bed was chosen due to its condensed packing, the condition of its macrofossils, and a high incidence of intact bivalves (Figure 8.2.8). The samples were dated as pMC 103 and 104 yr BP. Calibrated ages are recorded in **Appendix B.**

Figure 8.2.8: Shellbed SB_2_1. Elevation above modern effective high tide level: 0.6 m. Refer Appendix B for age details

Shellbed host sediments vary in nature. Within the NE shoreline sector (sites SB_2_1; SB_2_2) these were of one distinct unit: brownish-grey silty clay (Figures 8.2.8; 8.2.9). The remaining shellbeds had a close association with highly disrupted terrestrial colluvium and Whaingaroa Siltstone which forms the intertidal wave-swept platforms (Figures 8.2.10; 8.2.11).

All of the Motukokako Point shellbed sites are influenced to varying degrees by unstable terrestrial materials inland from the beach erosion scarps in which they are embedded. Two of the shellbeds (SB_2_1; SB_2_2) appear to be of typical residual concentrations and configuration. The remainder are located within a mixture of soils and rocks which have been subjected to significant rearrangement. The environment in which this disturbance took place is unclear. It may have been within the range of fully marine to fully terrestrial, or the result of both in combination. The relatively high occurrence of intact (articulated) bivalves of edible size and microfossils (forams) in these shellbeds suggests that the deposition mechanisms were not anthropic (Appendix C).

Figure 8.2.9: Site SB_2_2. Reworked shell hash within brownish-grey silty clay at 0.6 m above the modern effective high tide level.

Figure 8.2.10: Site SB_2_2. Discrete condensed shellbed within a mix of brown terrestrial colluvium and reworked grey marine clayey silt at 0.3 m above the modern effective high tide level.

Figure 8.2.11: Site SB_2_3. Reworked shell hash within weak mobile colluvium overlying folded Whaingaroa Siltstone at 0.4 m above the modern effective high tide level.

8.2.4: Site SB_2. Microfossils

The presence of microfossils (forams) within host sediments and the infill of the intact bivalves is considered credible evidence that these fossils were not subject to anthropic deposition. The proportion of benthic forams by number of total grains of diameter 212 to 355 µm (sieve size) within the Site 2_1 host bed sediments and intact bivalve internal sediments were 1 – 2% (Figures 8.2.12; 8.2.13)

Figure 8.2.12: Location SB_2_1. Foraminifera at a concentration of 1 – 2% within clayey host sediments.

Figure 8.2.13: Location SB_2_1. Foraminifera at a concentration of 1 – 2% within the intact macrofossil infill sediments.

These concentrations are notably lower than those established for Patikirau Bay (Table 8.2.1) (Appendix C). These low concentrations are probably due to significantly differing foreshore characteristics at the sites, in particular foreshore widths and high shoal slope angles at Motukokako Point. The average width of the tidal platform at Patikirau Bay is > 300 m. At Motukokako Point it is often < 50 m. Consequently, the extent and thickness of sediments necessary to provide for marine fauna habitats is significantly less at Motukokako Point. Moreover, the relatively steep shoal slope angle of ~ 7° (from horizontal) at Motukokako Point provides a less stable surface on which sediments and benthic forams can accumulate.

Table 8.2.1: Microfossil concentrations at Motukokako Point, Raglan Harbour

Sample location	Sediment	%*	**Age of macrofossils** (pMC yr BP)
SB_2_1	Host bed	0.8	
SB_2_1 (a)	Infill	2	103
SB_2_1 (b)	Infill	2	104
SB_2_2	Host bed	9	
SB_2_2	Infill	0.01	
SB_2_3	Host bed	5	
SB_2_4	Host bed	10	

* Proportion of benthic forams by number of total grains of diameter 212 to 355 µm (sieve size)

8.4.5: Site SB_2. Historical Vertical Land Movement

A consistent feature of Motukokako Point is the instability of its sea cliffs, embankments and slopes. All identified shellbeds have been affected to varying degrees by mobile ground conditions within and around discrete blocks, demarcated by faults (Refer to Figures 8.2.3; 8.2.4).

The structural complexity within the peninsula reflects a dynamic stress-strain history dating back to the beginning of the Kaikoura Orogeny ~ 25 Ma. The magnitude of the Oligocene Te Kuiti Group rocks' uplift and associated erosion is established through the surface exposures of its basal unit, the Waikato Coal Measures, at Huntly, 20 km to the NE. The sub-bituminous Huntly Coal requires > 1.5 km of burial for maturation to occur (Suggate & Boyd, 2012). Therefore, significant stress-strain distortion and faulting would have occurred during uplift of this magnitude.

Fault-aligned igneous dikes within the sedimentary sequences indicate that rupturing and intrusion were active during the Alexandra Volcanic Zone activity, 1 – 2.75 Ma (Figure 8.2.13).

Figure 8.2.14: A branched basaltic dike (a) extending into a sea cliff face (b). SW shoreline, Motukokako Point, Raglan.

The age and position of raised shellbeds at the peninsula signify vertical displacement within the last 200 years**.** Similar evidence was identified ~ 1 km away at Patikirau Bay (Section 8.3). Logically, should stress-strain displacement have been active throughout recent centuries, the likelihood of this involving movement along existing faults is high.

An important proxy relating to VLM is the nature of tidal wave-swept rock platforms. Their significance is recognised in 2 prior studies from Sherwood & Nelson (1979) and Swales et al., (2005). Sherwood & Nelson (1979) comment that often only a thin veneer of sediment covers the modern shore platform which has been cut during the last 5 ka years.

These platforms are invariably comprised of the Whaingaroa Siltstone lithotype which also forms many of the sea cliffs in the harbour. Two of the 4 identified raised shellbeds on Motukokako Point overlie an erosion surface on Whaingaroa Siltstone, indicating that this surface represents paleo foreshore platforms that were subject to down-wear erosion during tectonic uplift.

Along the NE shoreline of the peninsula this surface is exposed as a sharp contact between the Whaingaroa Siltstone and overlying Kaihu Group pumiceous sand (Figure 8.2.13). This is duplicated directly across the channel on Paritata Peninsula. The Paritata example has a bed of mixed Oligocene siltstone and quaternary marine sand. It contains credible (> 0.5%) concentrations of Oligocene microfossils (Figure 8.2.14).

In places these erosion surfaces are 1 – 1.5 m above the modern mean high tide level. The sharpness and regularity of these surfaces is indicative of these being paleo wave-swept platforms, similar to modern equivalents in the tide-zone. The modern erosion scarps are most probably cross-sections of paleo tidal platforms that existed prior to subsequent uplift, along with alterations during uplift.

Figure 8.2.15: A sharp contact dipping at ~ 3° between Whaingaroa Siltstone and overlying Quaternary Kaihu Group sand at Motukokako Point, Raglan Harbour.

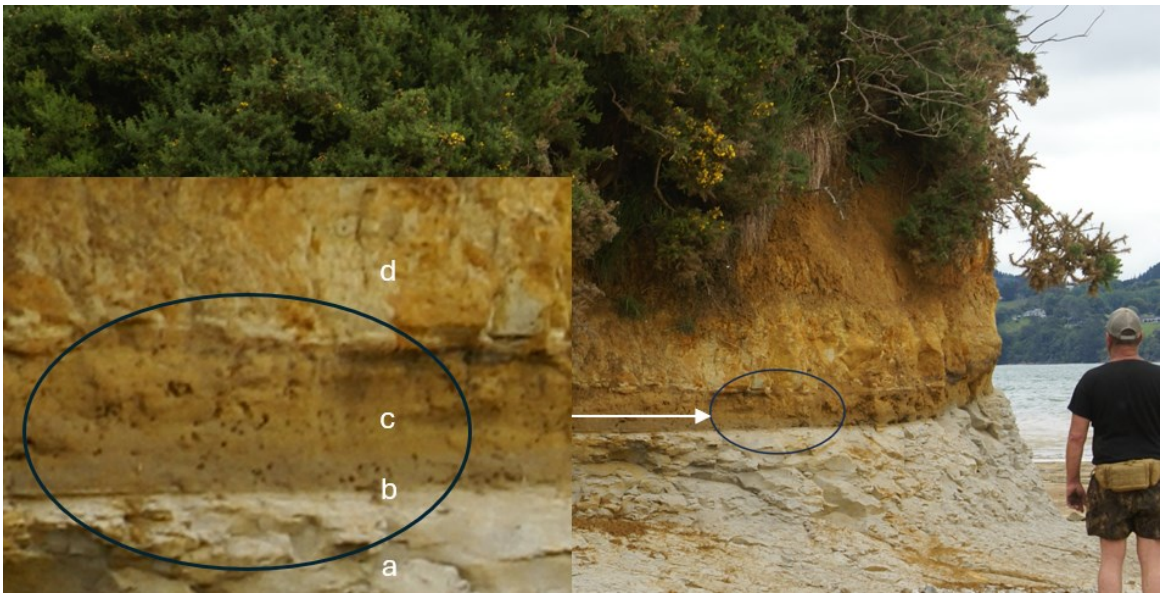

Figure 8.2.16: A sharp contact (b) between Whaingaroa Siltstone (a) and reworked marine sand and Whaingaroa siltstone (c) overlain by Quaternary Kaihu Group terrestrial sand at Paritata Peninsula, Raglan Harbour.

The depositional environment of the overlying Kaihu Group at Paritata Peninsula is unclear and requires a focused investigation. Microscopic observation of a sample from Bed C directly overlying the Whaingaroa Siltstone revealed a notably high presence of charcoal and microfossil concentrations of $\leq$ 0.1%. An apparent paleosol forms the upper contact of this bed. A feasible interpretation is that this bed represents the transition from a marine to a terrestrial environment during uplift. While a focused study and dating of these beds could establish further VLM history constraints for Raglan Harbour, this work is beyond the scope of this study.

8.4.6: Motukokako Point Summary

Motukokako Point is representative of tectonic-driven displacement dating back > 15 Ma years. The long-term trend has been one of uplift. This study provides evidence that this trend is ongoing and has remained active within the last 2 centuries. Logically, stress release is likely to occur along pre-existing faults. Given the geological structure of the peninsula, differential displacement between existing fault-bound blocks is likely, rendering some faults as being currently active. The modern structure supports a hypothesis that extension is occurring at specific locations in the harbour and that associated VLM is differential.

The evidence for this interpretation includes relatively fresh stress-release fracture zones, elevated paleo-foreshores, and raised shell beds. The ^{14}C dating of raised fossils at < 2 Ca yrs BP indicates that a degree of uplift has occurred relatively recently and that land movement is probably still active. The upper contacts of down-cut paleo-foreshore rock platforms at elevations of > 1 m indicates that the uplift trend possibly dates to the late Holocene.

8.3: Site SB_3. Patikirau Bay

8.3.1: Patikirau Bay General Description and Oligocene Stratigraphy

The onshore expression of Patikirau Bay is a drainage basin terminating at 2 beach erosion scarps. These are demarcated by a drained swamp that discharges on to the foreshore. Quaternary alluvium and colluvium mantles ~ 30% of the 1 km^2 catchment. The basin is incised into the calcareous Patikirau Siltstone member of the Oligocene Te Kuiti Group. At low tide this is exposed as a shallow wave-swept rock platform extending > 200 m seaward from the southern extent of the erosion scarps (Figure 8.3.1). Its surface dips below overlying marine sediments midway along the bay. These tidal rock platforms constitute a significant proportion of the Raglan Harbour's foreshore, notable through their shallow depth and absence of overlying sediments (refer Chapter 4).

Figure 8.3.1: The Patikirau Siltstone shore platform at low tide.

Due to a dip of 1 – 3°, bedding is visible within the siltstone platform indicating the strike of the strata. This shows as a banded pattern in aerial images. Foreshore exposures of Raglan Limestone also provide an opportunity to measure the dip and strike in these base-rocks. The swamp defines the location where a distinct change in the dip and strike within the base-rocks occur. This involves a ~ 40° rotation of the strike orientation (Figure 8.3.2).

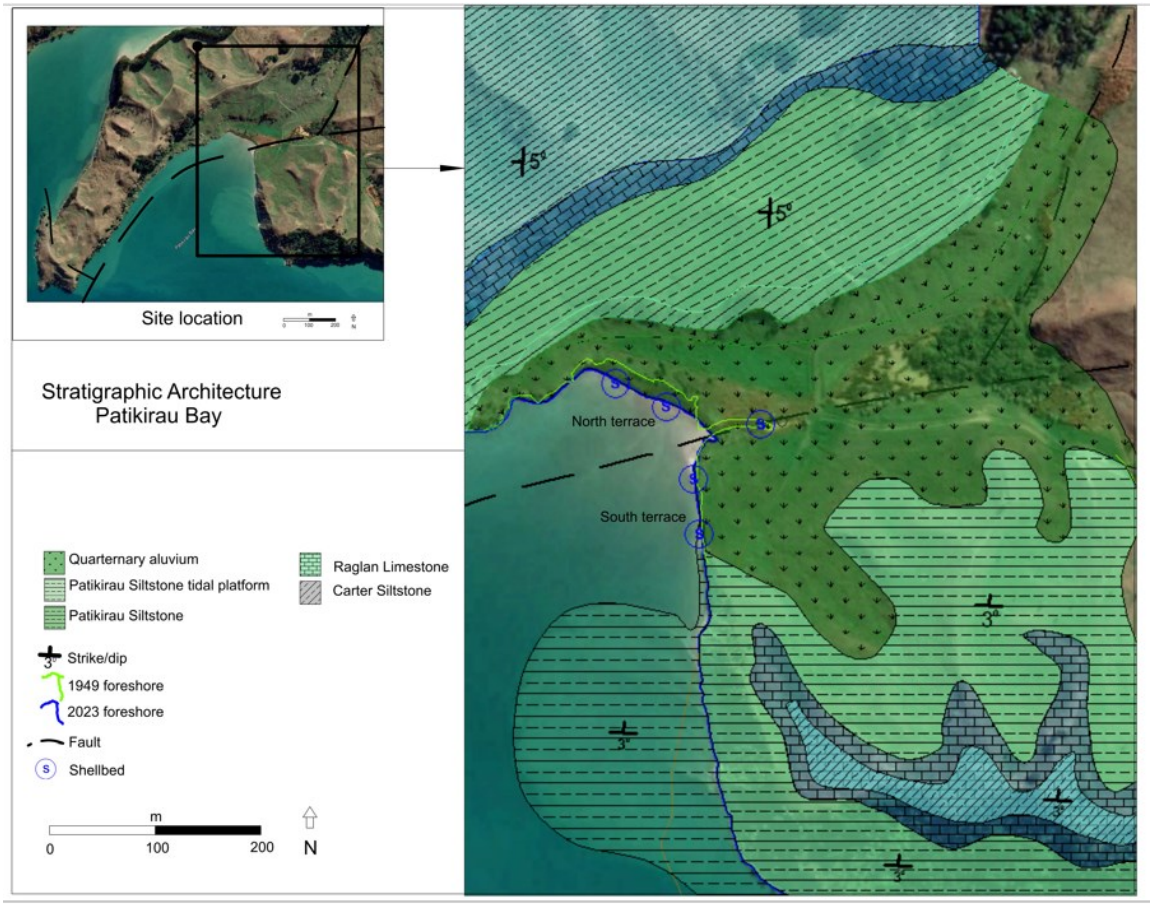

Figure 8.3.2: Lithostratigraphic architecture of Patikirau Bay. **Large image**

The Patikirau Siltstone is exposed as a sea cliff of 6 m - 40 m height along a 250 m long coastal section within the bay. While bedding is dipping at ~1° Nth (strike E – W) throughout most of the section its northern end has been subject to stress release fracture beyond which the dip abruptly increases to ~ 3 ° (Figure 8.3.3).

Figure 8.3.3: Fresh stress-release fracture in the Patikirau Siltstone where its dip increases by 2° while underlapping a raised marine terrace (a). **Large image**

The bay's foreshore is comprised of two distinct raised terraces exposed at beach erosion scarps. These are herein referred to as the *North Terrace* and the *South Terrace*. Each scarp is ~ 120 m in length and 0.3 – 0.8 m in height. The swamp's long axis approximates the location of a likely fault that demarcates these terraces into approximately equal lengths (Figure 8.3.4).

Figure 8.3.4: Patikirau Siltstone (A) dipping due north beneath the South Terrace (B) and the North Terrace (C), demarcated by a fault (D).

8.3.2: North Terrace Quaternary Stratigraphy

Field testing included core sampling to 0.9 m depth, at 9 locations. These included 3 onshore locations and 6 tide-zone locations placed along a linear line perpendicular to the terrace scarps (Figure 8.3.5). From this information cross-sections were generated.

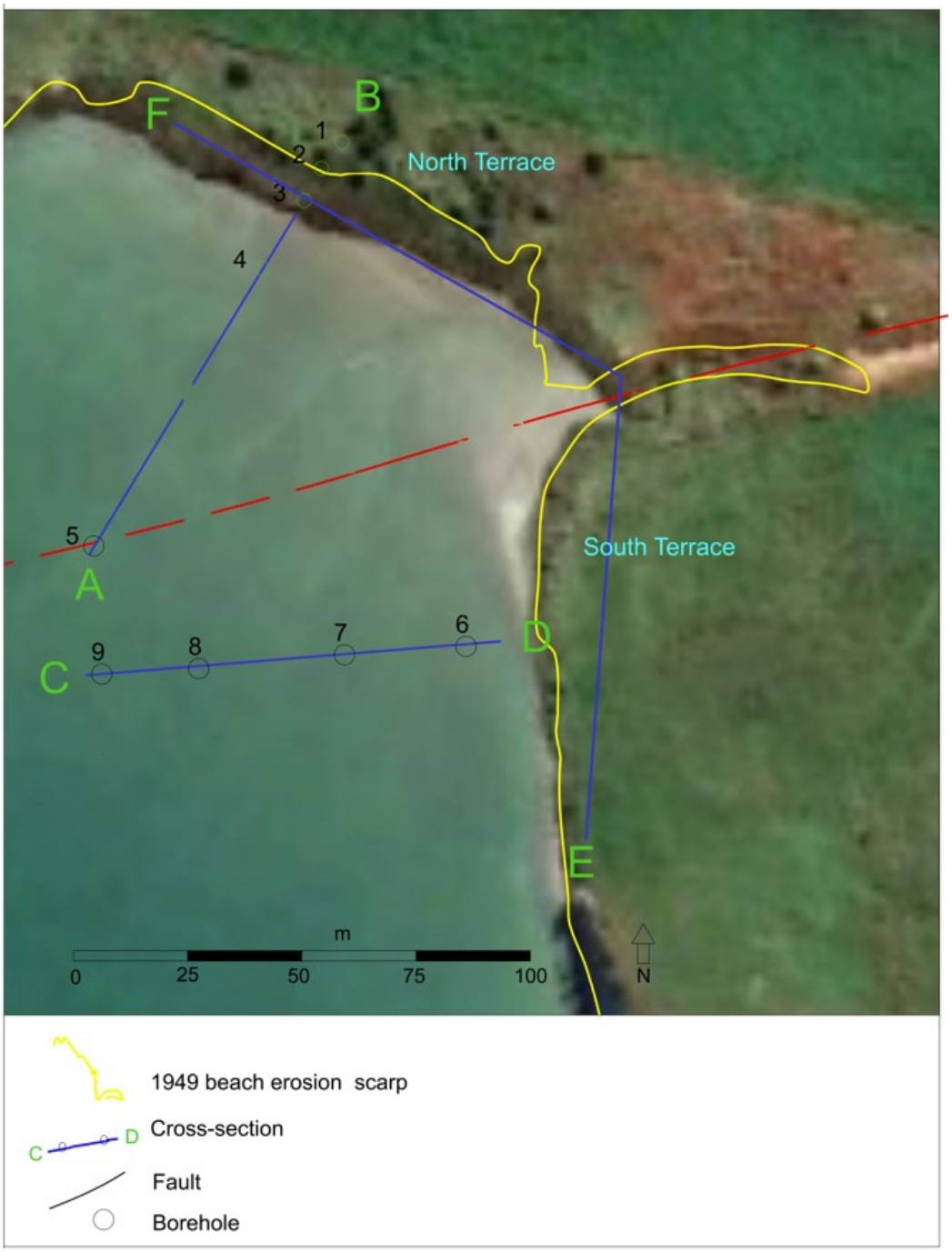

Figure 8.3.5: Patikirau Bay core sample locations. Image: Google Earth 2023.Nov.11.

Core sampling provided an understanding of the subsurface stratigraphy, beach evolution, and VLM history. The sampling allowed for relationships to be established between the nature of raised shellbeds and their living residual equivalents**.** From this information the degree of reworking (if any) and displacement of shellbeds during uplift could be established. The degree of reworking is likely to be indicative of VLM strain velocity. Through a comparison with core sample data the elevated shellbeds described in Section 8.3.3 demonstrate that reworking is unlikely in shellbeds that have been abruptly elevated through the strandline zone.

Relative elevations of key surfaces were established using RTK GNSS and inclinometer equipment. The North Terrace beach erosion scarp crest and an associated paleo-estuary have a height range of 0.4 - 0.6 m above the modern strandline. The implications of this are discussed in Section 8.3.9.

While the North Terrace has one subaerially exposed sedimentary bed, three other beds of differing characteristics were identified in the boreholes completed offshore. These beds can be divided into two groups based on the parent rocks' contrasting clastic components:

- Brown sandy/silty clay, originating as alluvium from the eroding terrestrial landscape.
- Blueish-grey clayey silt/sand, originating as calcareous siltstone situated along the harbour foreshore.

Each of these units may contain fossil-poor and/or fossil-rich beds as shown in the core samples (Figure 8.3.6).

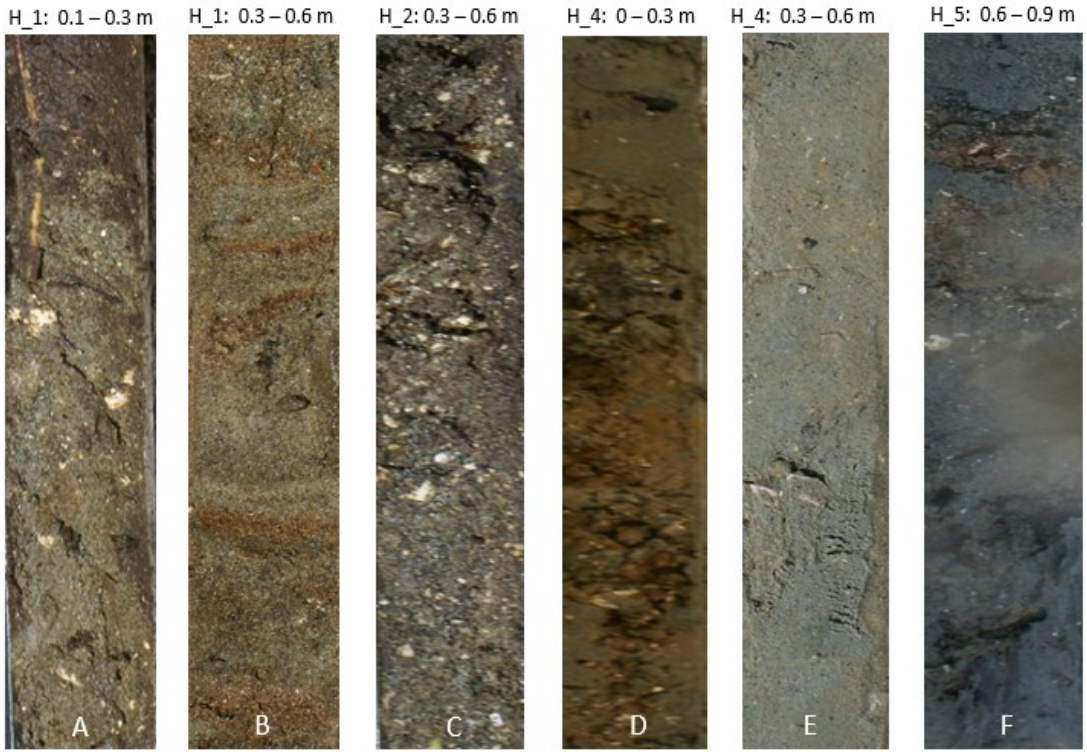

Figure 8.3.6: Representative portions of cores, north sector, Patikirau Bay. Holes 1; 2; 4; 5 (Figure 8.3.5). Ripple-bedded marine sediments (A; B) originating as terrestrial alluvium at depths 0.1 – 0.6 m within the raised marine terrace. Fossil-rich clayey silt (C) at 0.3 – 0.6 m depth within the raised terrace. Fossil-rich high tide-zone clayey silt at 0 – 0.3 m depth in the upper tide-zone (D). Progressively weathered, fossil poor Patikirau Siltstone (E; F) on the tidal platform at locations 50 m and 100 m offshore respectively.

The modern terrace consists of the existing beach erosion scarp and a relic beach scarp located ≤ 15 m inland from the former. The relic scarp crest elevation is ~ 0.1 m (average) higher than the modern terrace. Section 8.3.9 addresses the evolution of these two terraces.

The nature of the North Terrace onshore shellbed and its modern offshore equivalent does not differ significantly. This suggests that the onshore shellbeds at this site were not subject to reworking during uplift. Fractured bivalve shell materials at low-medium distribution and density dominate in both the onshore and offshore shellbeds. Individual shellbeds are typically of ≤ 0.3 m in vertical thickness. Given that that the dominant cockle bivalves are rarely found deeper than 0.05 – 0.1 m below the host sediment surface other mixing mechanisms may be involved (Anderson et al., 2019).

Contributors to submarine shell mixing are likely to include stingray that are very common in Patikirau Bay and other shallow estuaries in the harbour. These burrow into sediment and crush shellfish, resulting in common burrowing indentations and shell debris visible throughout the profile and sediment surfaces within the tide-zone.

A notable feature within borehole 4 is the presence of macrofossils at 0.9 m. Given that most of the evidence at this site indicates a history of uplift, fossils at this depth present an enigma. Ripple bedding is present in boreholes 1 and 4 where borehole 1 is onshore and borehole 4 is in the modern high tide zone. Both boreholes are located within 20 m of the paleo estuary shown in Figure 8.3.9. The ripple bedding is indicative of energetic fluvial/tidal deposition processes. This may explain the macrofossils at 0.9 m depth in borehole 4 i.e. they were deposited in a meandering paleo estuary drainage channel.

The raised North Terrace's subsurface is similar in sedimentary and biostratigraphic nature to a present-day equivalent at lower elevations within the tide-zone (Figure 8.3.7). The subsurface is comprised of a thin layer of modern biota-rich sandy mud in the tide-zone overlying 2 macrofossil-rich clayey silt beds of $\leq$ 0.5 m thickness. These extend from entire width of the raised North Terrace to the mid-tide zone where the base-rock Whaingaroa Silestone becomes exposed. The lower of these fossil-rich beds correlates with bed ST_2 described in Section 8.3.5.

The North Terrace surface is remarkably consistent throughout its vegetation, elevation, and morphology (Figure 8.3.8). It is largely absent within a 1979 aerial photograph, indicating that it was uplifted since this date (Figure 8.3.9).

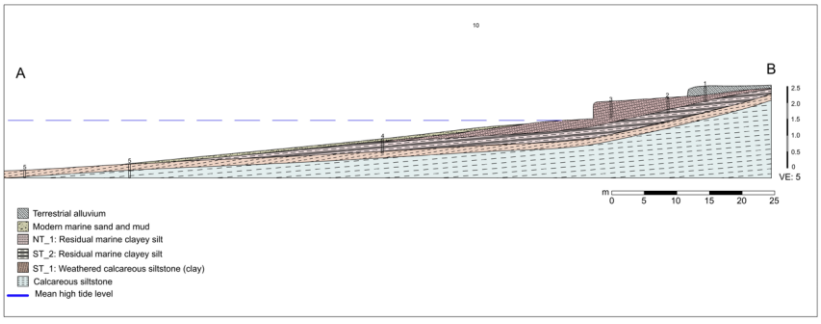

Figure 8.3.7: North Terrace cross-section. **Large image**

Figure 8.3.8: Consistent vegetation and morphology of the North Terrace, looking S.E.

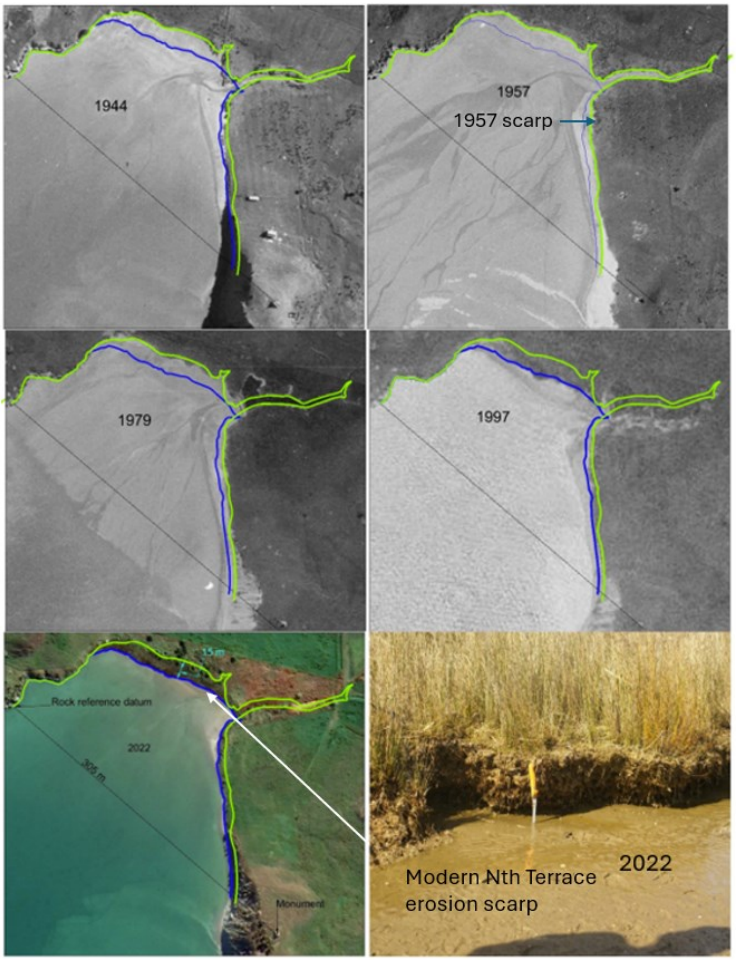

Figure 8.3.9: North Terrace erosion scarp migration, 1944 to 2022 with a comparison between 1957 (yellow) and 2022 (blue). Images after Retrolens (2022.Dec.05) (Google Earth 2022.Dec.05). **Large image**

The degree of reworking displayed within elevated terraces is a potential indicator of uplift rate and mixing dynamics. A relatively slow rate of uplift will result in a prolonged period of reworking as materials pass through the high-energy strandline zone. The absence of the typical strandline materials within the exposed North Terrace indicates that it has been uplifted relatively abruptly. Consequently, it is likely an onshore equivalent of undisturbed offshore shellbeds that have been subject to biota-mixing.

8.3.3: North Terrace Shellbeds

The Patikirau Bay study involved field observations, land surveying, core sampling, and extraction of suitable dating samples. The shellbed exposed in the North Terrace's modern erosion scarp is dominated by macrofossil fragments, distributed throughout the sediments in a chaotic manner (Figure 8.3.10). Condensed shellbeds, common at other locations around the harbour foreshore, are absent. The distribution of shell material of this nature extends throughout its length of the > 100 m. The shell material distribution is similar to that within core samples extracted from upper sedimentary beds within the tide-zone (Figures 8.3.5; 8.3.6).

Figure 8.3.10: Relatively sparse distribution of macrofossil shell fragments in the North Terrace beach erosion scarp.

A recently excavated drain exposes a shellbed located 40 m inland from the modern beach erosion scarp. Aerial photographs up to 1979 show that an estuary extended to this location at that time (Figure 8.3.9). The elevation survey substantiated that the paleo-estuary shellbed is at the same elevation as the modern North Terrace erosion scarp.

While both Percentage Modern Carbon (pMC) ages and calibrated ^{14}C ages are reported, the latter should be considered unreliable for the dating of fossils of less than 1 Ka yr BP (refer to Section 1.3.10). This inaccuracy is demonstrated in sample PST_1-1 where the 95% probability range includes a negative value of – 10 years BP (Table 8.3.2).

Two articulated cockle (*Austrovenus stutchburyi*) samples (SP_1a; Pat_1_B) were extracted from the paleo-estuary shellbed for dating (Table 8.3.1). A further 2 samples (PNT_1; PNT_2) were selected from the foreshore erosion scarp (Figure 8.3.11). The age of pMC 6332 yr BP for sample SP_1a constitutes a significant anomalous variation from the remainder of samples from the North Terrace. Sample Pat_1_B is from the same immediate location as SP_1a. Its age of pMC 110 yr BP correlates well with the balance of dates for the North Terrace, their range being pMC 108 – 110 yr BP. Consequently, the age of sample SP_1a (pMC 6332 yr BP) is considered an anomaly. Given the location of the shellbed in a recently excavated drain, it is possible that SP_1a was relocated during excavation. This is a similar scenario to 5 Raglan Recreation Ground samples dated at pMC ~ 6000 yr BP (Section 8.1.3) (**Appendix B**).

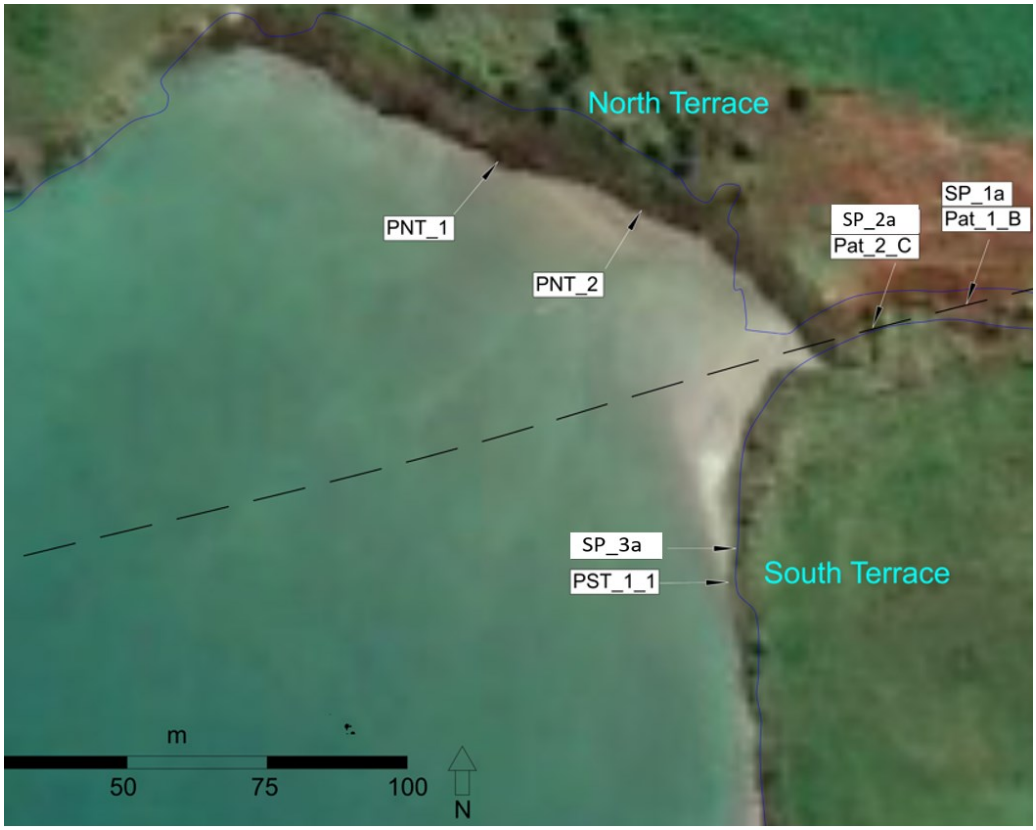

Figure 8.3.11: Dating sample locations, Patikirau Bay. Image from Google Earth 2003.Dec.20.

Table 8.3.1: Patikirau Bay North Terrace ***Austrovenus stutchburyi*** ^{14}C ages

Sample	Age pMC	Age calibrated (95%)	Sample	Age pMC	Age calibrated* (95%)
SP_1a	6332	6410 – 6740 cal. BP	PNT_1	109	1999 – 2003 cal. AD
Pat_1_B	110	1994 - 2001 cal. AD	PNT_2	108	2003 - 2005 cal. AD

*Refer to Section 1.3.10 and Appendix B for calibrated age interpretations

8.3.4: North Terrace Microfossils

All host-bed sediments and sediment infill within the intact cockles selected for dating were checked for the presence of microfossils. The presence of microfossils (largely benthic foraminifera) within these sediments is considered credible evidence that these fossils were not subject to anthropic deposition. From 2 representative locations on the North Terrace the proportion of benthic forams by number of total grains of diameter 212 to 355 µm (sieve size) averaged 5% within bivalve infill and 10% within host sediments (Figures 8.3.12; 8.3.13) (Appendix C).

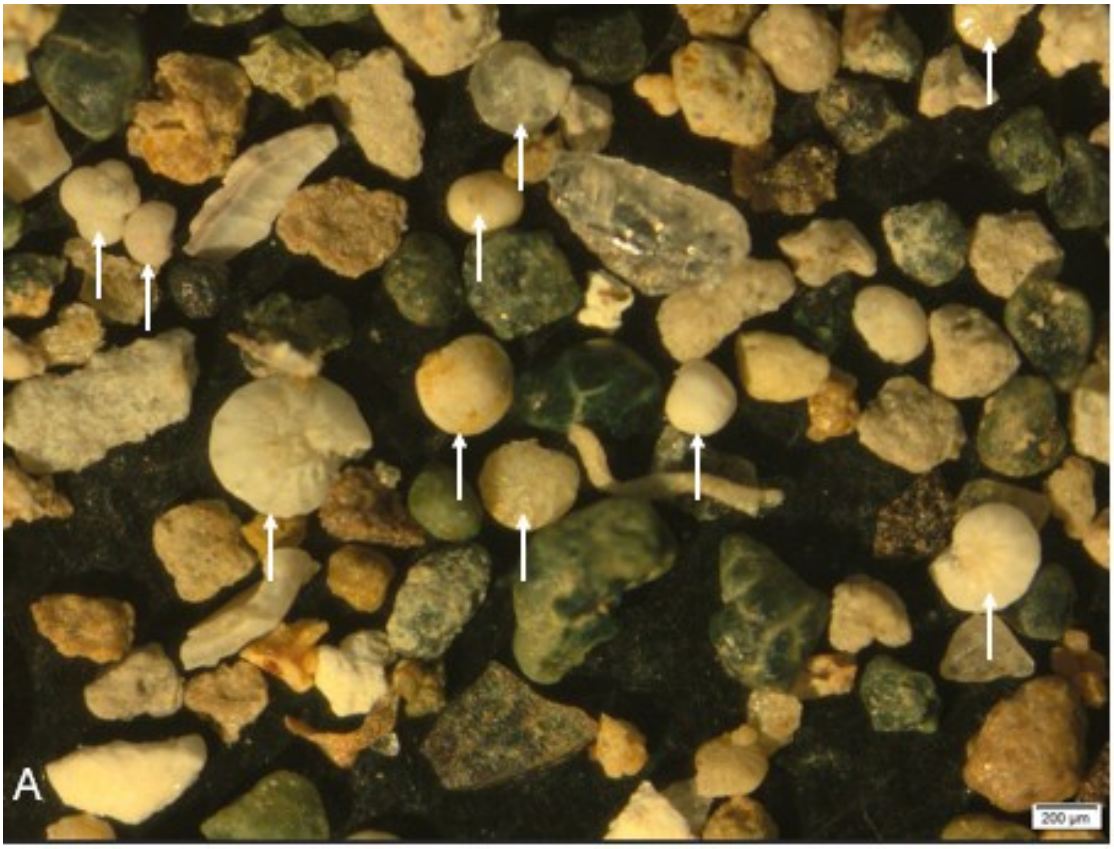

Figure 8.3.12: Natural proportion of benthic forams of diameter 212 to 355 µm within cockle infill of intact dated cockle, PNT_2. North Terrace, Patikirau Bay.

Figure 8.3.13.: Natural proportion of forams of diameter 212 to 355 µm within terrace host sediment. North Terrace, Patikirau Bay.

8.3.5: South Terrace Quaternary Stratigraphy

Due to its thickness above the underlying dipping Patikirau Siltstone base-rock the offshore stratigraphy of the South Terrace is relatively basic. Core sampling to ≤ 1 m depth was conducted at 4 locations out to 110 m from the shoreline. The core samples all displayed a similar pattern: a rapid transition from a relatively thin (< 0.1 m) marine biota habitat at the surface to barren clayey silt or silty clay. The underlying unit is the weathered surface of the Patikirau Siltstone that dips progressively to greater depths in a northerly direction. This results in the thick fossil-rich tide-zone marine beds at the North Terrace being absent in the South Terrace tide-zone (Figure 8.3.14).

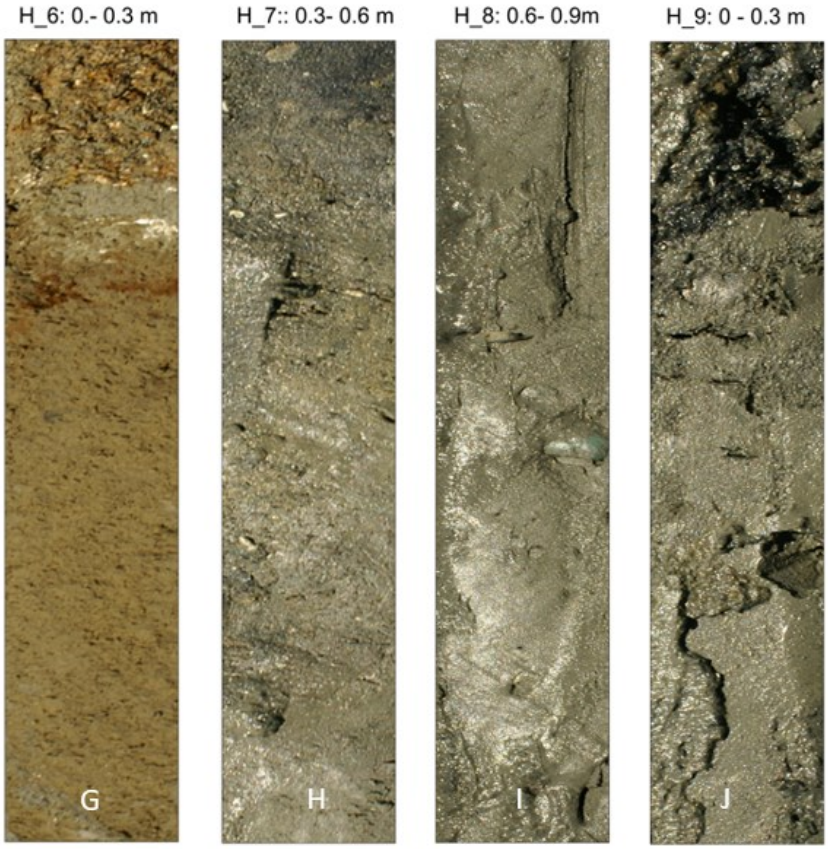

Figure 8.3.14: Representative portions of core samples evenly located at from 6 - 110 m offshore from the central South Terrace. Holes 6; 7; 8; 9 (Figure 8.3.5). A < 0.1 m-thick marine biota habitat zone overlying barren terrestrial silty clay (G). Barren weathered Patikirau Siltstone at depths 0.3 – 0.9 m (H; I). Dark-brown marine biota bed of < 0.1 m thickness overlying barren Patikirau Siltstone in the low tide zone (J).

However, the South Terrace onshore stratigraphy is considerably more complex than that of the North Terrace. Aside from organic topsoil of 0.05 – 0.1 m thickness, the South Terrace erosion scarp is comprised of 4 stratigraphic units (Figures 8.3.15; 8.3.16).

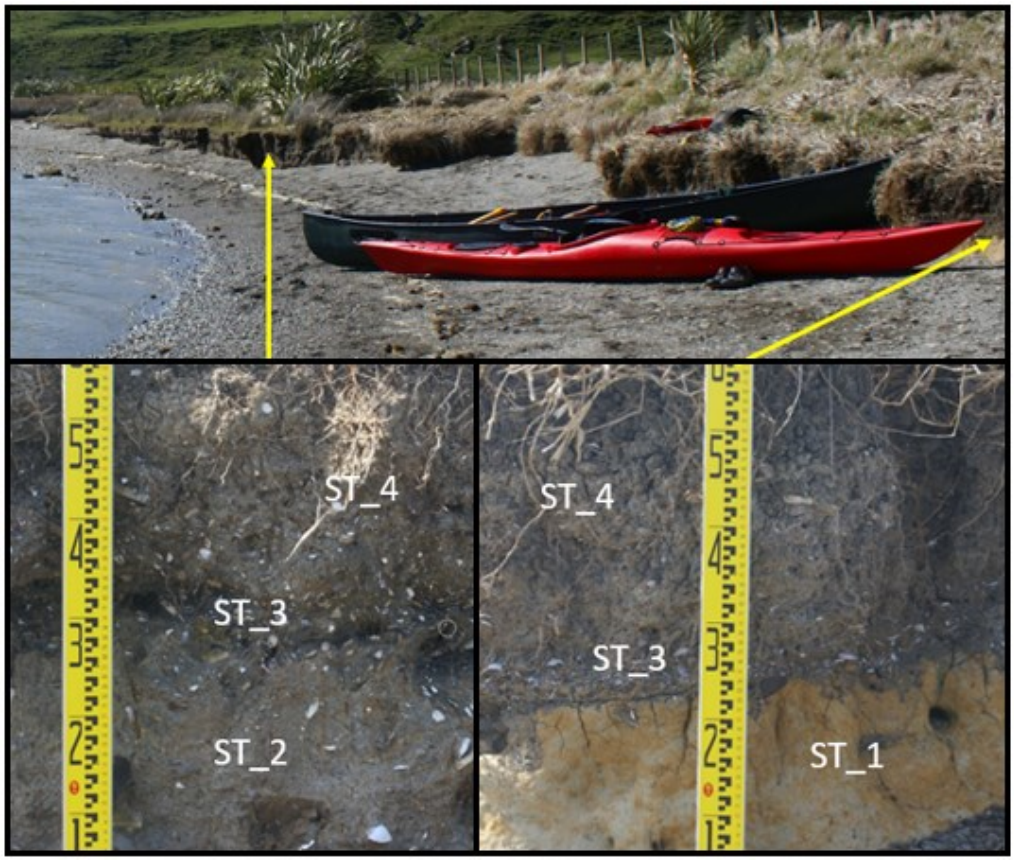

Figure 8.3.15: The South Terrace strata. Weathered terrestrial siltstone clay (ST_1) and residual fossil-rich marine bed (ST_2), underlying erosion boundary and infill (ST_3), underlying reworked strandline bed (ST_4).

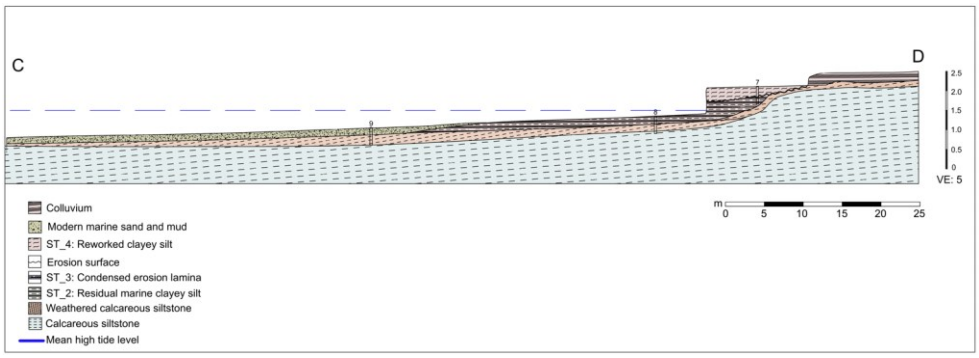

Figure 8.3.16: South Terrace cross-section. **Large image**

The nature of these beds is variable (from the top down):

- ST_4: Reworked fossil-rich marine clayey fine sand
- ST_3: Fossil-rich erosion-surface infill
- ST_2: Fossil-rich residual marine clayey silt/fine sand
- ST_1: Barren marine silty clay

The origin of the terrestrial clay unit ST_1 is most likely the weathered surface of the Oligocene Patikirau Siltstone that was drowned during a SL transgression. A dip of ~ 3^{o} north results in units ST_1 and ST_2 being lateral equivalents along the erosion scarp.

Unit ST_2 is similar in nature to beds identified within the North Terrace offshore drill cores (Figures 8.3.5; 8.3.6). It is rich in macro and micro fossils (Appendix C). There is no evidence of anthropic materials being present. This evidence is consistent with it being a residual marine bed that was uplifted rapidly after being subjected to surface erosion and deposition of overlying units. Section 8.3.9 discusses these evolutionary processes. A sample from the bottom of unit ST_2 was dated at pMC 469 yr older than samples from the overlying unit ST_4 (Section 8.3.6).

A continuous rill-eroded surface forms the upper contact of both these lower beds. This small-scale unconformity underlies the rill-infill shellbed, unit ST_3. The irregular erosion surface could be due to tidal wave-wash and infilling over a soft silty clay bed during slow-rate uplift. The Unit ST_3 profile is similar to the modern residual upper tide-zone surface, where small-scale drainage rills appear to form and infill in a cyclical manner.

Overlying unit ST_3 is a reworked shell-and-wrack bed, unit ST_4. The materials and mixing are consistent with ST_4 being an uplifted strandline where mixing of residual marine and terrestrial materials occurred during high tides. The lamina bedding and strandline materials within unit ST_4 are absent in the North Terrace, indicating that different depositional and uplift dynamics occurred at each terrace.

Plastic and an equine bone dated at pMC 86 yr BP were found directly above the rill-erosion surface. Along with these relatively modern materials, unit ST_4 contains intact articulated bivalves and benthic forams. These concentrations indicate mixing and deposition of residual and anthropic materials occurred during an uplift event and/or during extreme storm events.

8.3.6: South Terrace Shellbeds

Shellbeds are exposed throughout the entire 120 m length of the South Terrace beach erosion scarp. The scarp varies in thickness (height) from 0.4 - 0.8 m. This variation is due to irregular lateral erosion rates within a sloping surface and some variation in the strandline surface elevation. At the southern end of the scarp a stratified fossil host-bed (ST_4) overlies a highly irregular-surfaced fossil-poor clay bed, unit ST_1. ST_1 is likely to be the weathered surface of the Patikirau Siltstone (Figure 8.3.17).

Figure 8.3.17: Stratified Fossil-rich, cover-bed (ST_4) overlying the irregular surface of a fossil-poor clay bed (ST_1).

Unit ST_4 is relatively rich in macrofossil cockle fragments. These largely lie in a chaotic orientation indicative of re-working. Other materials include charcoal and organic shore-wrack materials. This mix is indicative of reworking of an uplifting residual marine sequence. The stratification may be due to cyclical storm surges that mixed natural strandline materials with anthropic debris**.** The presence of intact (articulated) bivalves of an edible size and microfossils within both the host sediments and intact bivalve infill indicates that the anthropic materials are only part of the mixture of materials forming the unit ST_4.

Aside from one cockle (*Austrovenus stutchburyi*) shell fragment from unit ST_2, all dating samples extracted at Patikirau Bay were from intact cockles containing internal forams at concentrations of > 5% by number of grains of similar size (Appendix C). Two macrofossil samples from each of two locations were selected for ^{14}C dating of the South Terrace (Figure 8.3.11). Ages ranged from pMC 105 - 579 yr BP (Table 8.3.2). The oldest sample (pMC 579 yr BP) was located at the base of the scarp exposure within sedimentary unit ST_2. The remaining 3 samples extracted from bed ST_4 were within an age range of pMC 103 – 110 yr BP (Appendix B). This range of ages correlate well with the elevation from which the samples were extracted and are indicative of uplift within the last two centuries.

An equine pastern bone located in the condensed shellbed (ST_3) overlying the erosion surface of bed ST_2 was dated at pMC 83 yr BP (Appendix B). Horses arrived in New Zealand in around 1815. Therefore, the deposition of unit ST_3 must have occurred within the last 208 years.

Table 8.3.2: Patikirau Bay South Terrace macrofossil (Austrovenus stutchburyi) ^{14}C ages

Sample	Age pMC	Age calibrated (95%)	Sample	Age pMC	Age calibrated* (95%) cal AD
SP_2_a	103	2012 – 2016 cal. AD	SP_3_a	110	1996 – 2002 cal. AD
Pat_2_C	105	2015 – 2017 cal. AD	PST_1_1	579	330 – (-10) cal. Yr BP

*See Section 1.3.10 and Appendix B for calibrated age interpretations

8.3.7: South Terrace Microfossils

Benthic forams were present in all sedimentary beds aside from the terrestrial clay unit, ST_1. Dating samples SP_2_a, SP_3_a, Pat_2_c, consisted of a valve taken from an intact cockle. PST_1_1 was a cockle (*Austrovenus stutchburyi*) valve fragment. All intact cockles (*Austrovenus stutchburyi*) had benthic forams within their internal sediments of proportions exceeding 2% by number of grains of 212 – 355 µm minimum diameter. The host beds had typically 0.5 – 1% concentrations. This presence of forams indicates that the modern wrack materials (plastic, equine bone, charcoal) found in units ST_3 and ST_4 were mixed with residual marine sediments. This mixing likely occurred at a high tide strandline during uplift and extreme storm events. The absence of foraminifera in the basal bed ST_1 validates the interpretation that this stratum is of a terrestrial origin (Figures 8.3.18 A, B, C, D).

Figure 8.3.18.a: Benthic foraminifera (circled) at a concentration of ~ 15% within unit ST_2 host sediments.

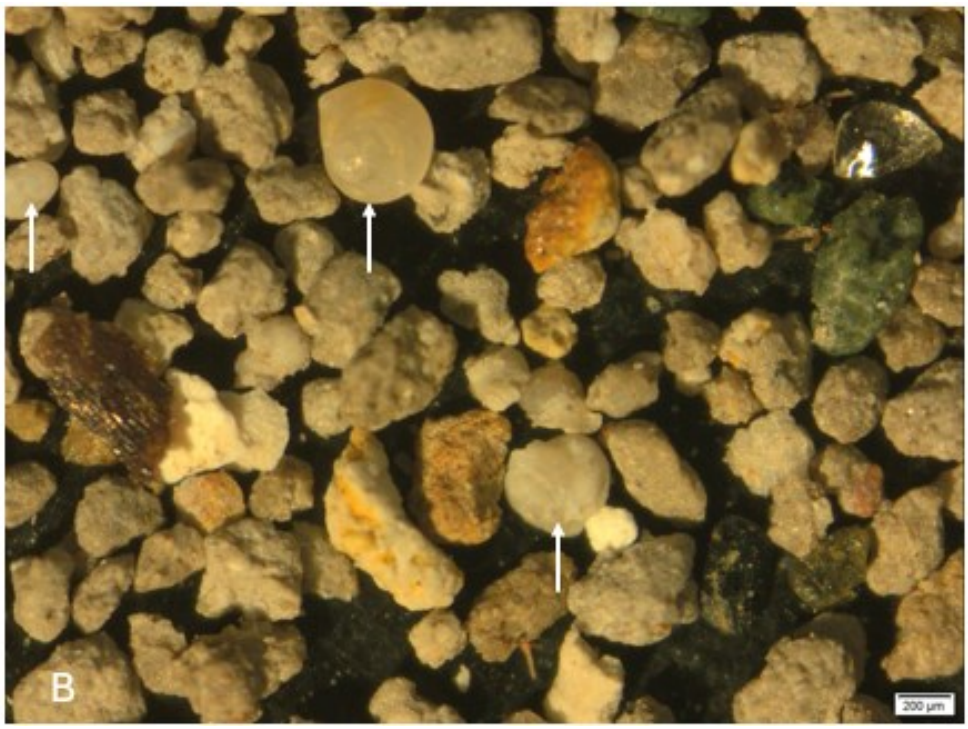

Figure 8.3.18.b: Typical benthic foraminifera concentration of 0.5 – 1% in host bed ST_ 3.

Figure 8.3.18.c: Typical benthic foraminifera concentration of 0.5 – 1% in host bed ST_ 4.

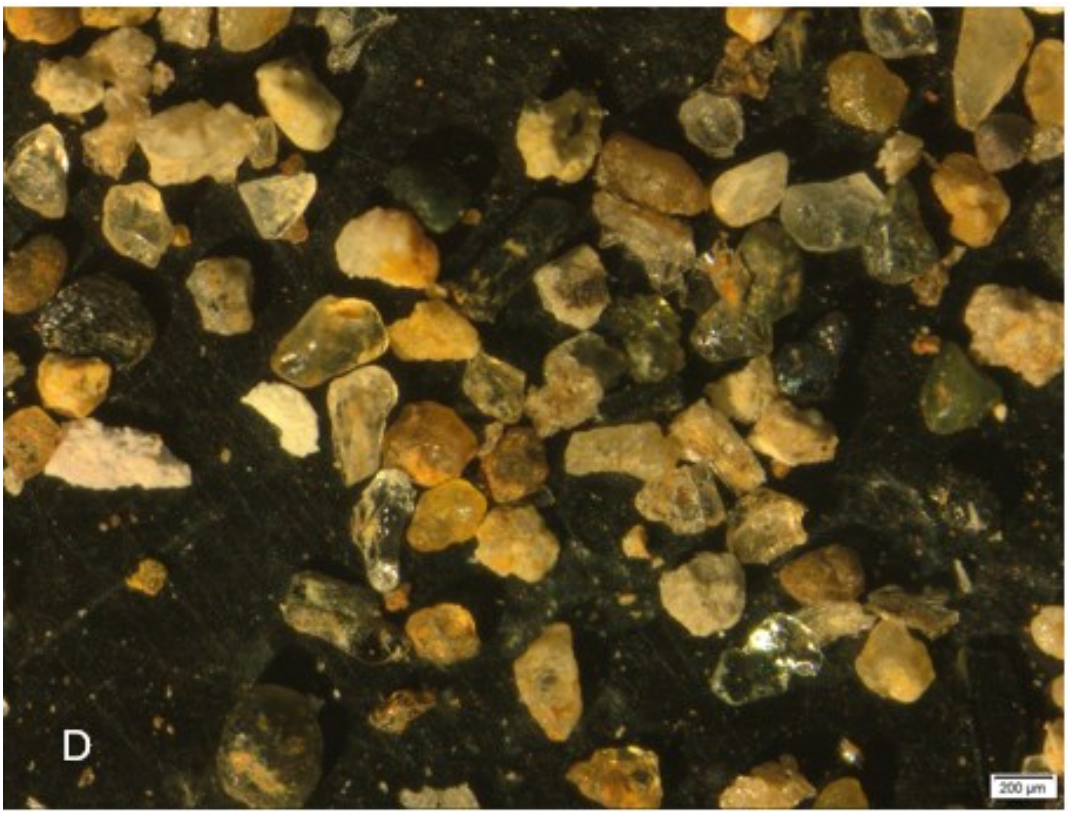

Figure 8.3.18.d: Angular clasts with no foraminifera, depicting the terrestrial origin of bed ST_ 1.

8.3.8: Other Relative Sea Level Change Proxies

Located ~ 300 m perpendicular from the North Terrace an elevated portion (~1000 m^2) of the mid-tide zone has been stripped of soft sediments leaving protruding trace fossil casts (Figure 8.3.19).

Figure 8.3.19: Trace fossil casts in the mid tide zone, Patikirau Bay, Raglan Harbour.

While the sediments surrounding the casts are very soft silty mud, the casts are comprised of hard indurated sand, with inclusions of marine shell fragments and complete *Pholadidae* macro-fossils (Figure 8.3.20). The habitat of NZ *Pholadidae* is located below the mid-tide level (B. W. Hayward 2023, pers. Comm., December 31).

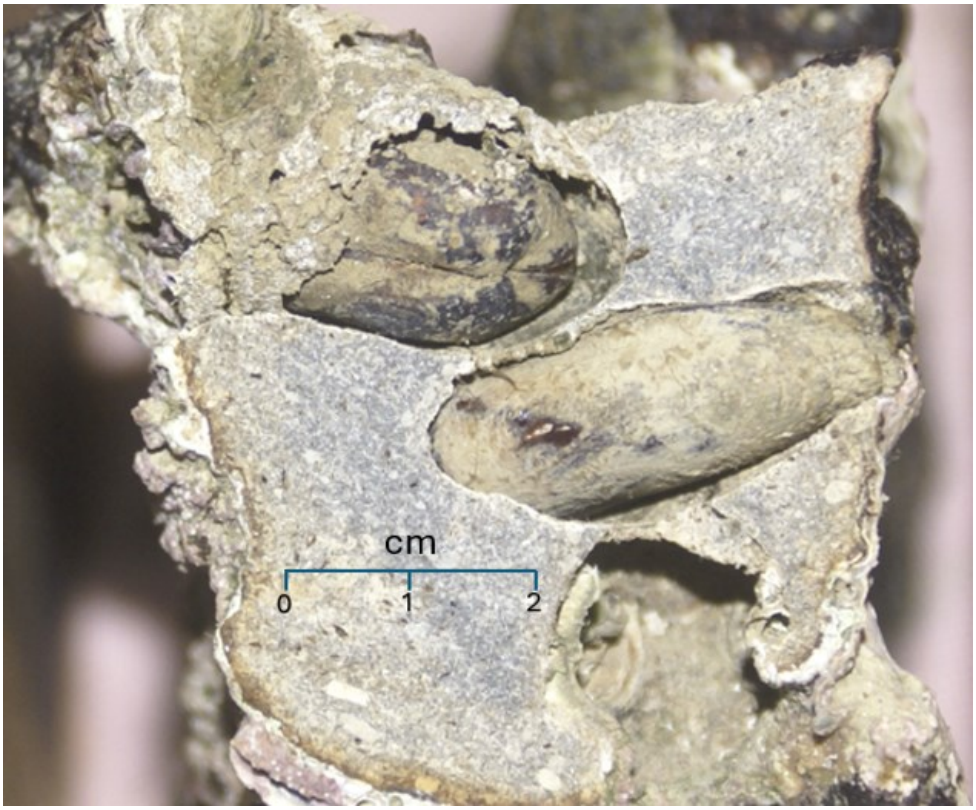

Figure 8.3.20: End view of a trace fossil cast exposing Pholadidae (razor clams).

The most likely process responsible for the differential erosion is one where uplift and associated RSL fall has resulted in the removal of soft sediments that surrounded the indurated casts during a rising RSL. When combined with other evidence of uplift in Patikirau Bay this evidence is symptomatic of both general and localised differential uplift. It is an isolated 'island' within extensive (> 5,000 m^2) mudflats of a similar nature. This feature of exposed trace fossil casts is the only one of its kind discovered during this study. This indicates that localised differential VLM has probably occurred in the bay. The net loss of soft sediments is consistent with the predominance of intertidal wave-swept surfaces in Patikirau Bay's southern sector and elsewhere in the Raglan Harbour.

8.3.9: Relative Stratigraphic Relationships and Differential Vertical Land Movement

A GNSS elevation survey of the North and South terraces provided data from 15 waypoints on the modern land surface. The elevation of key surfaces within the subsurface were further established through direct measurements and stratigraphic correlation. A resulting long-section demonstrates the contrasting stratigraphy of the 2 terraces (Figure 8.3.21).

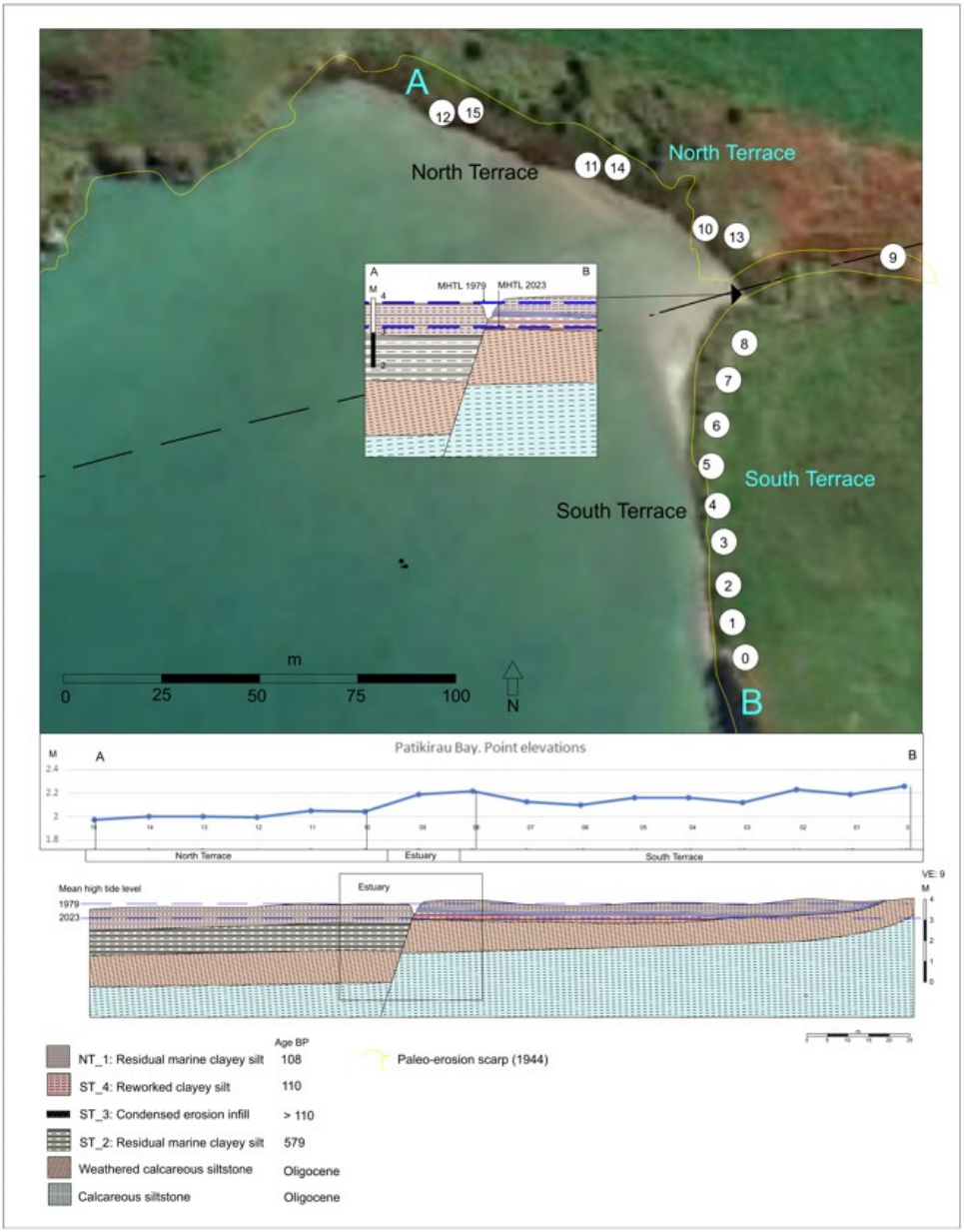

Figure 8.3.21: Patikirau Bay contrasting quaternary stratigraphy. **Large image**

The VLM strain history can be considered as being a sequence of phases. Based on the stratigraphy, chronostratigraphy and aerial images, 4 phases are identified. Each phase represents periods of change in VLM direction, velocity, and sedimentary processes (Figure 8.3.22).

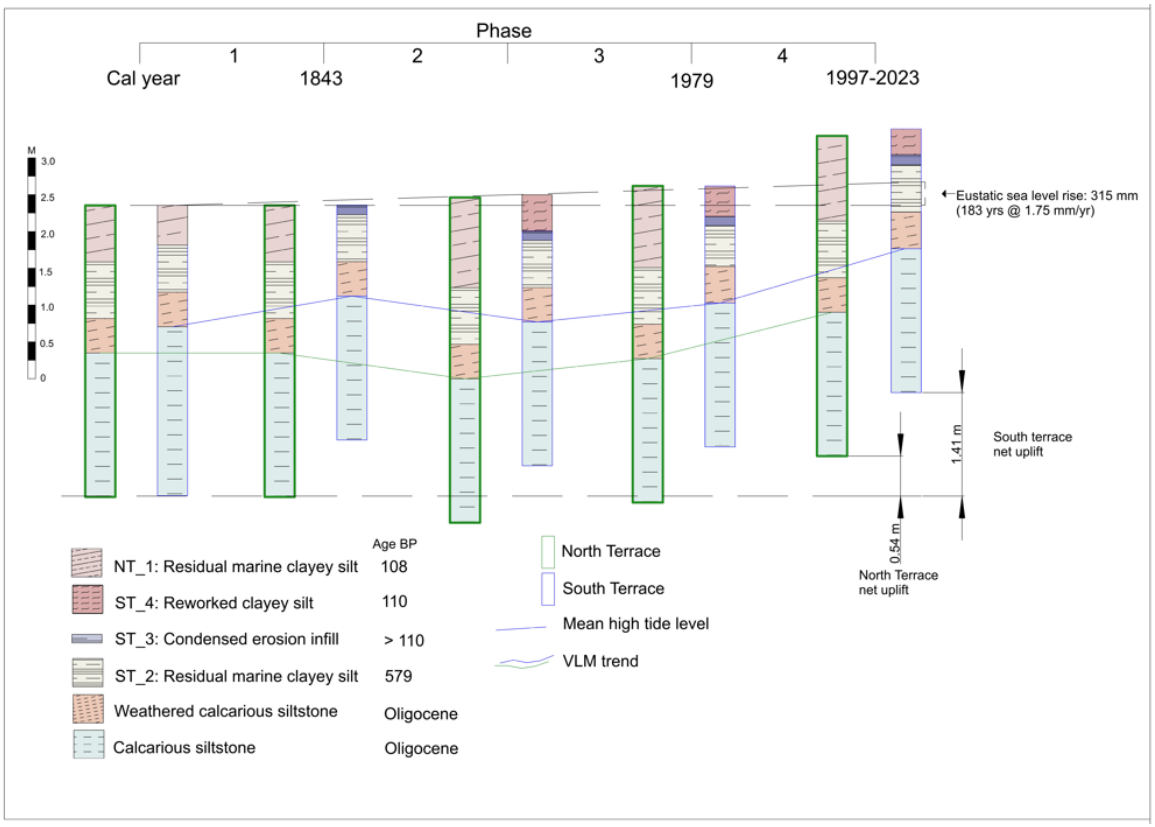

Figure 8.3.22: Patikirau Bay vertical land movement model. **Large image**

Prior to the onset of the sequence beginning before 1843, the entire upper tide-zone is assumed to have surface sediments similar in nature to the youngest modern residual bed (NT_1) as observed in the modern tide-zone profile. While the raised North Terrace is the most elevated extent of this bed, it is absent in the South Terrace. This signifies a different uplift and erosion history at the South Terrace.

Phase 1 involves uplift of the South Terrace, resulting in the erosion surface created before the year 1843 AD (Figure 8.3.23). This erosion surface forms the upper contact of the significantly older (> 400 years) bed ST_2.

The North Terrace displays no evidence of an erosion surface within its profile of ≤ 0.6 m depth. It was therefore subsiding or static during this phase.

Figure 8.3.23: The South Terrace reworked beds ST_4 and ST_3 infilling the erosion surface of the residual marine bed ST_2. The inverted chronology in the upper 2 beds reflects the high degree of reworking of these units. Dates: pMC cal. BP.

During Phase 2 subsidence of the South Terrace provided an opportunity for units ST_3 and ST_4 to accumulate. Both are comprised of reworked wrack, anthropic and shell material. The degree of reworking is signified by relatively young materials located directly over the erosion surface at their base. These include plastic and an equine bone ^{14}C dated at 86 years BP.

The units also contain significant concentrations of intact bivalves and benthic forams (Appendix C). The thickness of ST_3 and ST_4 within the modern beach erosion scarp indicates that the potential subsidence was > 0.3 m over a time-period of ≤ 136 years. It is assumed that the North Terrace is either static or subsiding during this phase, as its core logs display a steady accumulation of sediments.

Phase 3 represents the onset of uplift of both terraces prior to 1979. The 1979 aerial photograph shows the first appearance of the North Terrace and minor changes at the South Terrace (Figure 8.3.24). The North Terrace's exposed scarp and borehole cores show no evidence of reworking within its profile. This signifies that uplift was abrupt and of significant magnitude, as a slow migration through the high tide-zone would result in mixing with terrestrial materials seen in unit ST_4.

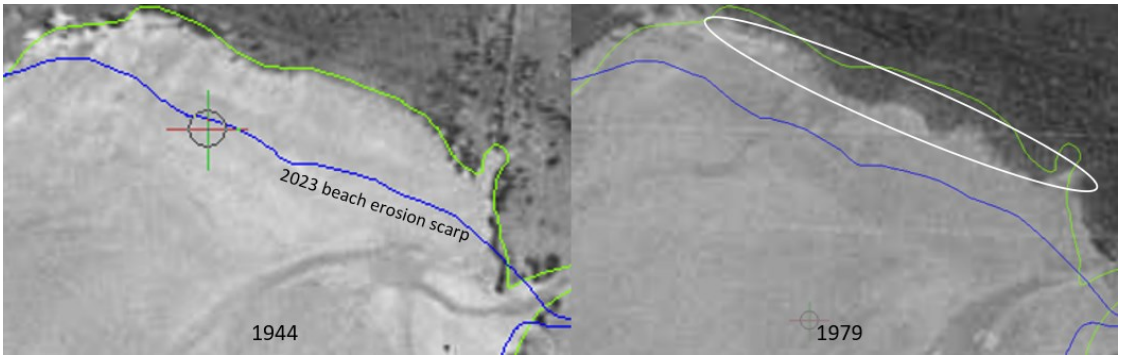

Figure 8.3.24: The onset of apparent uplift of the North Terrace prior to 1979 (circled in white).

Phase 4 involves the completion of the sequence up until 2023. It involves a continuation of rapid uplift totalling 0.3 – 0.7 m occurring within an 18-year time-period. Total uplift of the South Terrace during phases 3 and 4 was likely to have been > 0.1 m more than that of the North Terrace. Uplift during phase 4 probably involved a single seismic event or a rapid succession of events. The North Terrace beach scarp shows no evidence of disturbance associated with gradual uplift. It is equivalent in nature to residual marine beds, core sampled in the tide-zone.

8.3.10: Patikirau Bay Summary

The Patikirau Bay foreshore is comprised of 2 terraces of contrasting lithostratigraphic, chronostratigraphic, and paleontological properties. This evidence, along with historic aerial imagery, indicate that significant differential VLM occurred at the bay within the last 2 centuries and that the most recent uplift occurred since 1979.

The relative thinness of the tide-zone surficial sediments within the southern sector of Patikirau Bay indicates that VLM has occurred over prolonged time periods in a differential manner. Figure 8.3.1 shows a hard rock platform adjacent to the South Terrace is exposed to > 200 m in width at low tide. This rock surface is mostly devoid of sediments, signifying a long-term trend of uplift and wave-sweeping. A subsiding surface would most probably accumulate sediments, as is common at other locations in the harbour.

Core sample drilling in the North Terrace tide-zone intersected the weathered surface of this rock-type (Patikirau Zst.) at 0.6 - 0.9 m depths (Figure 8.3.5). Based on deep core drilling of this rock-type at other locations in the Raglan Harbour this weak weathered zone can be expected to be > 4 m thick (Carter, 2022).

The sea cliff exposure of this rock shows an abrupt change in dip, demarcated by a fractured stress-release zone proximal to the southern-most extent of the terraces. Along with an abrupt change in strike orientation at the swamp location this signifies active fault displacement has been occurring over a prolonged period and is likely to continue.

CHAPTER NINE

CONCLUSIONS AND FURTHER RESEARCH

9.1: Conclusions

This research identifies and describes multiple field-based proxies relating to RSL change and associated VLM in Raglan Harbour. These can be grouped into 6 categories (Table 9.1). The proxies fall within 1 of 5 categories based on the time-period (age) they represent (Table 9.2).

Table 9.1: Proxy categories and supporting evidence methodologies

Proxy	N	Supporting evidence
Raised marine terraces	4	Elevation surveys, sedimentology, stratigraphy, microfossil studies, historic aerial imagery
Raised shellbeds	6	Elevation surveys, sedimentology, microfossil studies, ^{14}C dating
Raised trace fossil castings	1	Field observations, physical properties
Tide notches	2	Historic aerial imagery
Speleothem	1	Elevation measurement, U-Th dating
Raised foreshore platforms	10	Stratigraphic and foreshore exposure observations, microfossil studies

Table 9.2: Proxy categories based on age

Proxy	Age (pMC)		Comment
Shell fossils	1 - 7 ca	6.5 Ka	The 6.5 Ka result requires further validation. It does not correlate well with the stratigraphy
Stratigraphy	?		Paleo-foreshore wave-cut rock platforms elevated ≤ 1.5 m above the modern effective high tide level
Tide notches	1910 – 2023		No applicable change since 1910
Speleothem	≤ 23.5 Ka BP		RSL is probably within 0.3 m of its 23.5 Ka maximum at 1 location
Trace fossil casts	?		Elevated by ≥ 0.3 m above their modern equivalents

At 4 locations in Raglan Harbour, the magnitude of VLM within specific time periods were established with a high degree of confidence. These metrics were determined through fossil dating and elevation surveying. The stratigraphy and sedimentology at 4 further sites exhibit uplift of similar magnitudes within undetermined timeframes.

Evidence of more substantial uplift over longer timeframes is displayed in the form of exposed trace fossil beds and stratigraphic contacts overlying raised wave-swept paleo tide-zone rock platforms. At one location a dated speleothem provides a maximum SL constraint at that location.

The results indicate that uplift magnitudes, velocities, and timing, have not been consistent throughout the harbour, signifying differential land movement and active faulting. At one location VLM variation is demarcated by a fault which links to an unpublished fault network that possibly extends across Raglan Harbour (Figure 9.1).

Displacement may be a result of incremental aseismic creep or abrupt coseismic events, or a combination of these dynamics. The prospect of periodic subsidence at any location in the harbour cannot be discounted.

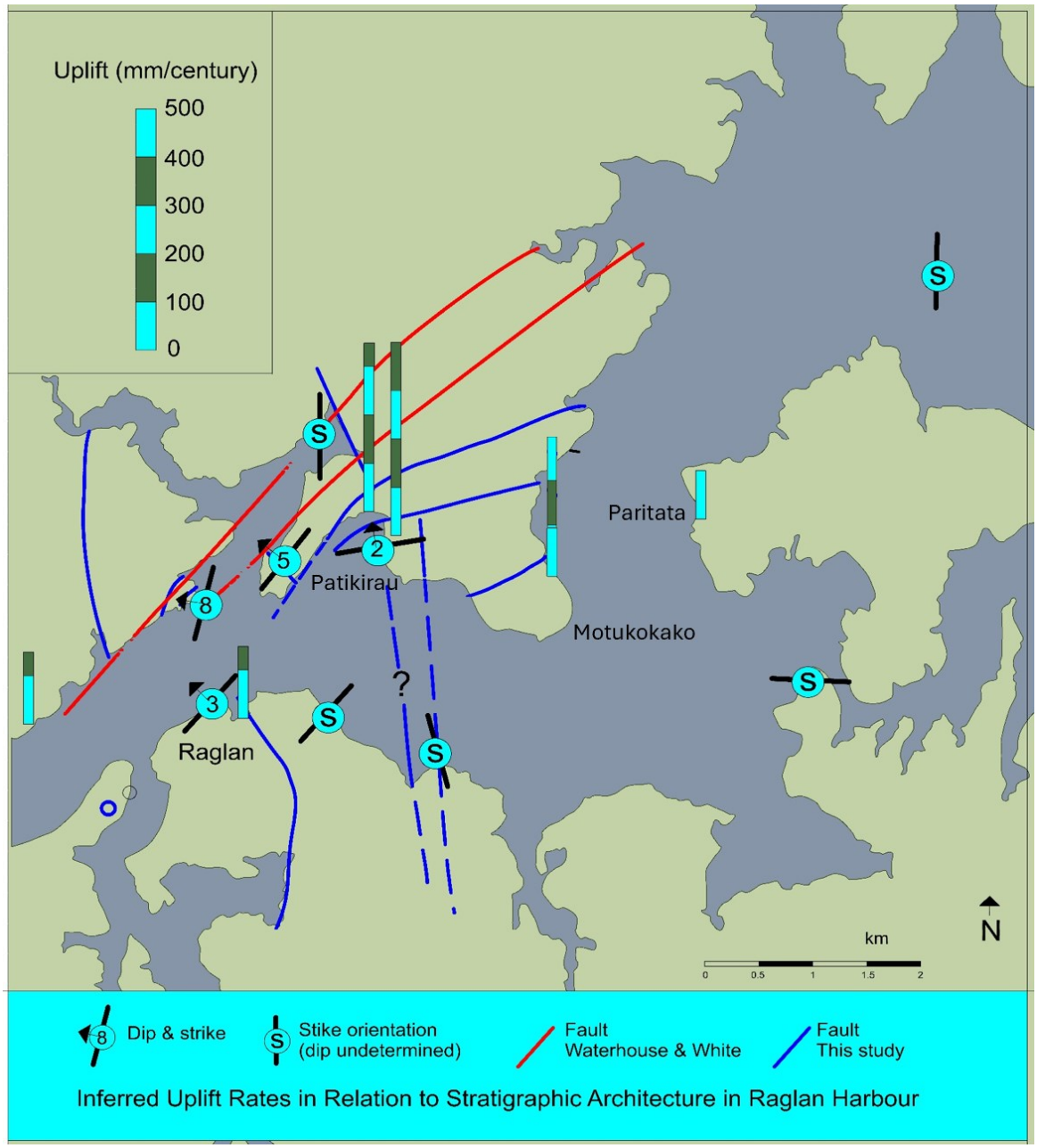

Figure 9.1: Variations in estimated uplift (mm/ca) in relation to geological structure. Central Raglan Harbour.

9.2: Further Research

The prime objective of this study was to identify and characterise credible proxies of historic RSL change in Raglan Harbour. Due to the breadth of the investigation none of these proxies have been exhaustively characterised. However, credible research pathways on tectonically driven RSL change in Raglan Harbour have been identified, through which more meaningful metrics may be substantiated in the future.

The field study-sections addressed in this research were selected from multiple similar examples identified during preliminary reconnaissance. The entire Waingaro branch of the harbour displays evidence of an apparent active uplift trend. This can be compared with the Waitetuna branch where such evidence is absent. These branches constitute ~ 70% of the total harbour area. The significance of this variation justifies further attention.

Over 20 raised terraces were located during reconnaissance, many of which contain macrofossils. Many other raised marine beds where shellbeds are absent contain microfossils. Foraminifera volumes at many locations are likely to be adequate for dating purposes. This dating and species characterisation of microfossils were not addressed during this research. Paleoenvironmental evolution and VLM relationships can be studied from a microfossil perspective.

The dated speleothem proxy was located within 2 hours of focused searching. The extensive exposures of limestone along the shoreline are highly likely to contain more flowstones suitable for focused studies. These are potentially a record of Holocene paleo-environments and maximum RSL.

A more intensive study of the identified tide dissolution notch sites could yield additional proxy evidence. For example, higher resolution copies of the original 1910 images are probably achievable. The clarity of the modern photos can also be improved.

Another potential datum is the seaweed level on the Wine Glass Rock which shows up clearly in a 1910 photo. An initial comparison of seaweed levels indicated no discernible change. This datum can relate to the actual effective SL in 1910, whereas the dissolution notches cannot. Due to time constraints this proxy was not included in the study. There a more 1910 photographs specifically of limestone rocks in Raglan Harbour that warrant attention.

The trace fossil casts which appear to be at out-of-place elevations in relation to their original habitat warrant further research. The dating and characterisation of the cast cements and internal macrofossils could yield valuable age constraints. A study of the low tide zone in their location may establish the elevation of the fossilised razor clam's living equivalents, and hence metrics on the relative uplift of the fossil castings.

The Raglan Harbour's geological stratigraphy and structure has had minimal attention on a local scale. Examples of tectonic stress-release zones and fault offsets are exposed at multiple locations along the 120 km-long shoreline. Comprehensive geological mapping and structural modelling is warranted, from which an enhanced understanding of historical land movement can be derived. Aerial images show traces of apparent faults crossing the harbour and through Raglan Township. These link up with a fault deemed to be probably active in this study. Geophysical surveying may better define these submarine features.

From a more regional perspective this study identifies multiple research paths relating to tectonic dynamics in the upper NI west coastal region. The nearby harbours Aotea and Kawhia are of a similar geology and orientation to Raglan Harbour. There is a high likelihood that they contain similar proxies.

REFERENCES

Alloway, B., Westgate, J., Pillans, B., Pearce, N., Newnham, R., Byrami, M., & Aarburg, S. (2004). Stratigraphy, age and correlation of middle Pleistocene silicic tephras in the Auckland region, New Zealand: a prolific distal record of Taupo Volcanic Zone volcanism. *New Zealand Journal of Geology and Geophysics, 47(3), 447-479.*

Anderson, T., Barrett, H., & Morrisey, D. (2019). Effects of sediment deposition on the New Zealand cockle, Austrovenus stutchburyi. *New Zealand journal of marine and freshwater research*, *53(3), 363-376.*

Antonioli, F., Furlani, S., Montagna, P., & Stocchi, P. (2021). The use of submerged speleothems for sea level studies in the mediterranean sea: a new perspective using glacial isostatic adjustment (GIA). *Geosciences, 11(2), 77.*

Barter, T. P. (1976). The Kaihu Group (Plio-Quaternary) of the Awhitu Peninsula, Southwest Auckland. Unpublished Ph.D. thesis, lodged in the Library, University of Auckland, Auckland.

Beavan, R.J. and Litchfield, N.J. (2012). Vertical land movement around the New Zealand coastline: implications for sea-level rise. *GNS Science Report, 2012/29.*

Bell, R., Lawrence, J., Allan, S., Blackett P., Stephens, S., Hannah, J., Shand, T., Thomson, P. Glavovic, B., Britton, R. Dickson, M., Quilter, P., Hudson, N., Davies K. (2017). Coastal Hazards and Climate Change. *Ministry for the Environment. New Zealand Government.*

Berryman, K. R. (1993). Distribution, age, and deformation of late Pleistocene marine terraces at Mahia Peninsula, Hikurangi Subduction Margin, New Zealand. *Tectonics, 12, 1365–1379.*

Bradley, B.A., Dhakal, R.P., Cubrinovski, M., MacRae, G.A., Lee, D.S. (2008). Seismic loss estimation for efficient decision making. Wairakei, New Zealand: *NZSEE Annual Technical Conference, 11-13 Apr 2008*. https://hdl.handle.net/10092/17651

Brathwaite, R. L., Christie, A. B., & Gazley, M. F. (2021). Stratigraphy, provenance and localisation of the titanomagnetite placer at Waikato North Head, South Auckland, New Zealand. *Mineralium Deposita*, *56*, 343-362.

Briggs, R. M. (1983). Distribution, form, and structural control of the Alexandra Volcanic group, North Island, New Zealand. *New Zealand journal of geology and geophysics*, *26*(1), 47-55.

Briggs, R. M., Itaya, T., Lowe, D. J., & Keane, A. J. (1989). Ages of the Pliocene—Pleistocene Alexandra and Ngatutura volcanics, western North Island, New Zealand, and some geological implications. *New Zealand journal of geology and geophysics*, *32*(4), 417-427.

Brothers, R. N. (1954). The relative Pleistocene chronology of the South Kaipara District, New Zealand, T. *Roy. Soc. N Z, 82, 677–694.*

Carter, M. J. (2018). Unpublished presentation to Engineering New Zealand Membership Application Panel.

Carter, M. J. (2022). Slope stability Assessment, Te Akau Sth. Raglan. 23 09 2022 Version 2. Unpublished geotechnical report. *Raglan Geotech.*

CEI. 2021. IPCC Report Relies on RCP 8.5 Despite Determining It a Low Likelihood Scenario - Competitive Enterprise Institute (cei.org).

Chapman-Smith, M., & Grant-Mackie, J. A. (1971). Geology of the Whangaparaoa area, eastern Bay of Plenty. *New Zealand journal of geology and geophysics, 14(1), 3-38.*

Chappell, J. (1970). Quaternary geology of the south-west Auckland coastal region. *Transactions of the Royal Society of New Zealand, 8 (10), 133-153.*

Chappell, J. (1975). Quaternary warping and uplift rates in the Bay of Plenty and west coast, North Island, New Zealand. New Zealand Journal of Geology and Geophysics. Volume 18, 1975 – Issue 1.

Claessens, L., Veldkamp, A., ten Broeke, E.M., Vloemans, H. A. (2009). Quaternary uplift record for the Auckland region, North Island, New Zealand, based on marine and fluvial terraces. *Global and Planetary change, 68, 383-394.*

Clement, A.J.H., Whitehouse, P.L., Sloss, C.R. (2016). An examination of spatial variability in the timing and magnitude of Holocene relative sea-level changes in the New Zealand archipelago. *Quaternary Science Reviews., 131 (Part A). pp. 73-101.*

de Lange, W. P. (2019). Auckland Sea level Changes: Past, present, & future. Presentation to the Otorohanga Rotary Club, Otorohanga. 9 July 2019.

Denys, P. H., Beaven, R. J., Hannah, J., Pearson, C. F., Palmer, N., Denham, M., Hreinsdottir, S. (2020). Sea Level Rise in New Zealand: The Effect of Vertical Land Motion on Century-Long Tide Gauge Records in a Tectonically Active Region. *Journal of Geophysical Research: Solid Earth*

East, H. (2005). Whaingaroa (Raglan) Harbour: Sedimentation and the Effects of Historical Catchment Landcover Changes.

Fisher, M. (2014). The Environmental Management of Whaingaroa/Raglan Harbour with a Focus on the Period Since 1970. Unpublished report for the Waitangi Tribunal.

G.A. Eiby (1968). A descriptive catalogue of New Zealand earthquakes, *New Zealand Journal of Geology and Geophysics, 11:1, 16-40*, DOI: 10.1080/00288306.1968.10423671.

Gage, M. (1953). The study of Quaternary strand-lines in New Zealand. Transactions of the Royal Society of New Zealand, 81 (1), 27-34.

GeoNet: Quake Search GNS (2023).

Giba, M., Nicol, A., & Walsh, J. J. (2010). Evolution of faulting and volcanism in a back-arc basin and its implications for subduction processes. *Tectonics*, *29*(4).

Gibb, J.G. (1986). A New Zealand regional Holocene eustatic sea-level curve and its application to determination of vertical tectonic movements. *Royal Society of New Zealand, Bulletin 24, 377-395.*

Gilmour Brothers (1910). Wineglass Rock, Raglan Harbour, Photograph taken by Gilmour Brothers. Price, William Archer, 1866-1948. Collection of post card negatives. Ref: 1/2-001085-G. Alexander Turnbull Library, Wellington, New Zealand. /records/23196506

GNS Science (2023). Active Faults Database of New Zealand. http://data.gns.cri.nz/af/

Graham, I. J., & Korsch, R. J. (1990). Age and provenance of granitoid clasts in Moeatoa conglomerate, Kawhia Syncline, New Zealand. *Journal of the Royal Society of New Zealand, 20(1), 25-39.*

Hamling, I.J., Write T. J., Hreinsdóttir, S., Wallace L. M. (2021). A Snapshot of New Zealand's Dynamic Deformation Field From Envisat InSAR and GNSS Observations Between 2003 and 2011. *Geophysical Research Letters 10.1029/2021GL096465.*

Hannah, J., Bell, R., Paulik, R. (2010). Sea Level Change in the Auckland Region. Prepared by Otago University for Auckland Regional Council. *Auckland Regional Council Technical Report 2010/65.*

Hayward B. and Morley M. (2014). Is the Coromandel Peninsula Rising? (2014). *Auckland Geoclub Journal. Geocene 11.*

Hayward, B. W., Grenfell, H. R., and Scott, D. B. (1999b). Tidal range of marsh foraminifera for determining former sea-level heights in New Zealand. *New Zealand Journal of Geology and Geophysics 42, 395–413. doi:10.1080/00288306.1999.9514853.*

Henderson, J., Grange, L. I., Ongley, M., Morgan, P. G., Macpherson, E. O., & Gibson, W. (1926). The Geology of the Huntly-Kawhia Subdivision, Pirongia and Hauraki Division (No. 28-31). *Department of Scientific and Industrial Research, Geological Survey Branch.*

Hochstetter, F. R. (1864). Geologie von Neu Seeland. Beitrage Zur Geologie der Provinzen Auckland und Nelson. *Reise der Novara Geologischer Theill (1): 274 p.*

Horton, S. L., Stephenson, W. J., & Dickson, M. E. (2022). Changes in shore platform wetting and drying cycles following the 2016 Kaikōura earthquake: implications for incipient marine terrace evolution. *Earth Surface Processes and Landforms, 47(12), 2972-2988*.

Houlié, N., & Stern, T. A. (2017). Vertical tectonics at an active continental margin. *Earth and Planetary Science Letters, 457, 292-301.*

Hunt, S., & Jones, H. F. (2019). Sediment grain size measurements are affected by site-specific sediment characteristics and analysis methods: implications for environmental monitoring. *New Zealand Journal of Marine and Freshwater Research, 53(2), 244-257.*

Hutton, F. W. (1867). Geological report on the Lower Waikato District. *New Zealand Geological Survey reports of geological exploration 1867 [2]: 1-8.*

Jevrejeva, S. , J.C. Moore, A. Grinsted, A.P. Matthews, G. Spada. 2014. "Trends and acceleration in global and regional sea levels since 1807". *Global and Planetary Change*. %vol 113, 10.1016/j.gloplacha.2013.12.004 https://www.psmsl.org/products/reconstructions/jevrejevaetal2014.php.

Jobberns, G. (1928). The raised beaches of the north east coast of the South Island of New Zealand. In *Transactions of the New Zealand Institute (Vol. 59, No. 3, pp. 508-570).*

Kamp, P. J. J., Tripathi, A. R. P., & Nelson, C. S. (2014). Paleogeography of Late Eocene to earliest Miocene Te Kuiti Group, central-western North Island, New Zealand. *New Zealand Journal of Geology and Geophysics*, *57*(2), 128-148.

Kamp, P.J.J., Vonk, A.J., Nelson, C.S., Hansen, R.J., Tripathi, A., Hood, S.D., Ngatai, M. & Hendy, A.J.W. (2004). Constraints on the evolution of Taranaki Fault from thermochronology and basin analysis: Implications for the Taranaki Fault play. In Proceedings of New Zealand Petroleum Conference 2004, 7 – 10 March, Crown Minerals, *Ministry of Economic Development, Wellington.*

Kea, D. and Waterhouse B. C. (1961). Quaternary surfaces and sediments at Waihi Beach. *New Zealand Journal of Geology and Geophysics*, 4:4, 434-445.

Kear, D. and Schofield, J.C. (1959). Te Kuiti Group. *New Zealand Journal of Geology and Geophysics 2 (4): 685-717.*

King, D.J., Newnham, R.M., Gehrels, W.R., Clark, K.J. (2020): Late Holocene sea-level changes and vertical land movements in New Zealand. *New Zealand Journal of Geology and Geophysics. Volume 64, 2021, issue 1. Pages 31 – 36*.

King, L.C. (1930). Raised beaches and other features of the south-east coast on the North Island of New Zealand. *Transactions of the New Zealand Institute, 61 (3-4), 498-523.*

LINZ (2024). NZ Government GNSS CORS. NZ Government GNSS CORS, LINZ Data Service. NZ Government GNSS CORS | LINZ Data Service

Litchfield, N. J. (2008). Using fluvial terraces to determine Holocene coastal erosion and Late Pleistocene uplift rates: an example from northwestern Hawke Bay, New Zealand. *Geomorphology, 99(1-4), 369-386.*

Litchfield, N. J., Van Dissen, R., Sutherland, R., Barnes, P. M., Cox, S. C., Norris, R., Beavan, R. J., Langridge, R., Villamor, P., Berryman, K., Stirling, M., Nicol, A., Nodder, S., Lamarche, G., Barrell, D. J. A., Pettinga, J. A., Little, T., Pondard, J.N., Mountjoy J., Clark, K. (2014). A model of active faulting in New Zealand. *New Zealand Journal of Geology and Geophysics,* 57:1, 32-56.

Lowe, D. J., Tippett, J. M., Kamp, P. J., Liddell, I. J., Briggs, R. M., & Horrocks, J. L. (2001). Ages on weathered Plio-Pleistocene tephra sequences, western north Island, New Zealand. *Les Dossiers de l'Archeo-Logis, 1, 45-60.*

Marske, K. A., & Boyer, S. L. (2022). Phylogeography reveals the complex impact of the Last Glacial Maximum on New Zealand's terrestrial biota. *Journal of the Royal Society of New Zealand, 54*(1),8–29. https://doi.org/10.1080/03036758.2022.2079682

McBeath, D. M. (1977). Gas-condensate fields of the Taranaki basin, New Zealand. New *Zealand journal of geology and geophysics, 20(1), 99-127.*

McKergow, L. A., Pritchard, M., Elliott, A. H., Duncan, M. J., & Senior, A. K. (2010). Storm fine sediment flux from catchment to estuary, Waitetuna-Raglan Harbour, New Zealand. *New Zealand Journal of Marine and Freshwater Research, 44(1), 53-76.*

Mildenhall, D. C. (1992). Palynology, Age, and Paleoenvironments of Carbonaceous Facies in the Kaihu Group:(late Pliocene-Pleistocene), Northern North Island (Vol. 46). *DSIR Geology & Geophysics.*

Milne, J. D. (1973). Upper Quaternary geology of the Rangitikei drainage basin. North Island, New Zealand [Ph. D. dissert.]: Wellington, New Zealand. Unpublished Thesis University of Victoria, Wellington.

National Institute of Water and Atmospheric Research (NIWA). (2023). Sea levels and sea-level rise. Sea levels and sea-level rise | NIWA

Nelson, C. S. & Hume, T. M. (1987). Paleoenvironmental controls on mineral assemblages in a shelf sequence: Te Kuiti Group, South Auckland, New Zealand. *New Zealand Journal of Geology and Geophysics, 30:4, 343-362'.*

Nelson, C.S. (1978a). Stratigraphy and Palaeontology of the Oligocene Te Kuiti Group, Waitomo County, South Auckland, New Zealand. *New Zealand Journal of Geology and Geophysics 21: 553-594.*

New Zealand Geotechnical Society. (2021). *Earthquake Geotechnical Engineering Practice Series. 1.*

New Zealand Ministry for the Environment (2017). Coastal hazards and climate change: Guidance for local government. *Ministry for the Environment, Wellington. 279 p + appendices*.

New Zealand Ministry of education (2022). Raglan Steady Growth. https://assets.education.govt.nz/public/ENP/Wai-Raglan.pdf

Nicol, A., Mazengarb, C., Chanier, F., Rait, G., Uruski,. C., Wallace,. L. (2006). Tectonic evolution of the active Hikurangi subduction margin, New Zealand, since the Oligocene. *Tectonics 26: TC4002, 24 pp.*

NIWA (2023). Sea levels and sea-level rise | NIWA

New Zealand Transport Agency (2022). Bridge Manual (SP/M/022). https://www.nzta.govt.nz/resources/bridge-manual/.

Ota, Y., Hull, A.G., NozoIso, N., Ikeda, T., Moriya, I., Yoshikawa, T. (1992). Holocene marine terraces on the northeast coast of North Island, New Zealand, and their tectonic significance, New Zealand. *Journal of Geology and Geophysics*, 35:3, 273-288.

Pain, C. F. (1976). Late quaternary dune sands and associated deposits near Aotea and Kawhia Harbours, north island, New Zealand. *New Zealand journal of geology and geophysics*, *19*(2), 153-77.

Petersen, T., Gledhill, K., Chadwick, M., Gale, N. H., & Ristau, J. (2011). The New Zealand national seismograph network. *Seismological research letters*, *82*(1), 9-20.

Pillans, B. (1983). Upper Quaternary marine terrace chronology and deformation, south Taranaki, New Zealand. *Geology 11.5 (1983): 292-297.*

Pillans, B. (1990): Pleistocene marine terraces in New Zealand: A review. *New Zealand Journal of Geology and Geophysics, 33 (2), 219-231.*

Retrolens.Historic.Imagery.Resource.2024,02,31.https://retrolens.co.nz/map/#/1760725.9790623598/5810325.590419863/1772812.5841599368/5818619.007988795/2193/9

Ryan, D. D., Clement, A. J., Jankowski, N. R., & Stocchi, P. (2020). The last interglacial sea-level record of New Zealand (Aotearoa). *Earth System Science Data Discussions, 2020, 1-43.*

Selby, M. J., Pullar, W. A., McCraw, J. D. (1971). The age of Quaternary surfaces at Waihi Beach. *Earth Science Journal 5: 106-113.*

Shane, P. A., Black, T. M., Alloway, B. V., & Westgate, J. A. (1996). Early to middle Pleistocene tephrochronology of North Island, New Zealand: implications for volcanism, tectonism, and paleoenvironments. *Geological Society of America Bulletin, 108(8), 915-925.*

Sherwood, A. M., & Nelson, C. S. (1979). Surficial sediments of Raglan harbour. *New Zealand Journal of Marine and Freshwater Research, 13(4), 475-496.*

Stark, N., Greer, D., Phillips, D. J., Borrero, J. C., Harrison, S., & Kopf, A. (2010, December). In-situ geotechnical investigation of sediment dynamics over "The Bar', Raglan, New Zealand. *In AGU Fall Meeting Abstracts (Vol. 2010, pp. OS43C-02).*

Stirling, M., McVerry, G., Gerstenberger, M., Litchfield, N., Van Dissen, R., Berryman, K., ... & Jacobs, K. (2012). National seismic hazard model for New Zealand: 2010 update. Bulletin of the Seismological Society of America, 102(4), 1514-1542. GNS. https://pubs.geoscienceworld.org/ssa/bssa/article-abstract/102/4/1514/349800/National-Seismic-Hazard-Model-for-New-Zealand-2010

Suggate, R. P., & Boyd, R. J. (2012). Greymouth Coalfield, New Zealand: vertical coal rank gradients, depths of burial and palaeotemperatures. *New Zealand Journal of Geology and Geophysics*, *55*(2), 111-126.

Swales, A.; Ovenden, R.; McGlone, M. S.; Hermanspahn, N.; Budd, R.; Okey, M. J.; Hawken, J. (2005). Whaingaroa (Raglan) Harbour: sedimentation rates and the effects of historical catchment landcover changes. *Environment Waikato Technical Report 2005/36.*

Tripathi, A.R.P., Kamp, P.J.J., Nelson, C.S. (2008). Te Kuiti Group (Late Eocene – Oligocene) lithostratigraphy east of Taranaki Basin in central-western North Island, New

Zealand. Ministry of Economic Development, New Zealand, unpublished Petroleum Report PR3900, 70 pp.

Waikato Regional Council (2023). Environmental Maps and Data. https://waikatoregion.govt.nz/environment/envirohub/environmental-maps-and-data/station/38477/WL?dt=Change+in+level

Waikato Times. Volume 36, issue 2957, Page 2. 1891,06, 27. https://paperspast.natlib.govt.nz/newspapers/WT18910627.2.36?fbclid=IwAR1CyhzRyRCbI50pVFG-G_eBZ14asJX4dBChxB2XhXHGX1DDRMjdo78i_p0

Wang, G. (2023). The 95 per cent confidence interval for the mean sea-level change rate derived from tide gauge data. *Geophysical Journal International*, *235*(2), 1420-1433.

Ward, C.M. (1998b). New Zealand Marine Terraces: Uplift Rates. *Science, 240 (4853), 803-804.*

Ward, W. T., Ross, P.J., Colquhoun, D. J. (1971). Interglacial high sea levels—an absolute chronology derived from shoreline elevations. *Palaeogeography, Palaeoclimatology, Palaeoecology 9.2 (1971): 77-99.*

Waterhouse, B. C., & White, P. J. (1994). Geology of the Raglan-Kawhia area. Lower Hutt: *Institute of Geological and Nuclear Sciences*.

Wellman, H. W. (1962). Holocene of the North Island of New Zealand a coastal reconnaissance. *Transactions of the Royal Society of N.Z. 88: 29-99.*

Appendices

A.0

Appendix A.1: Figure 2.16. Generalised bathymetry of Raglan harbour

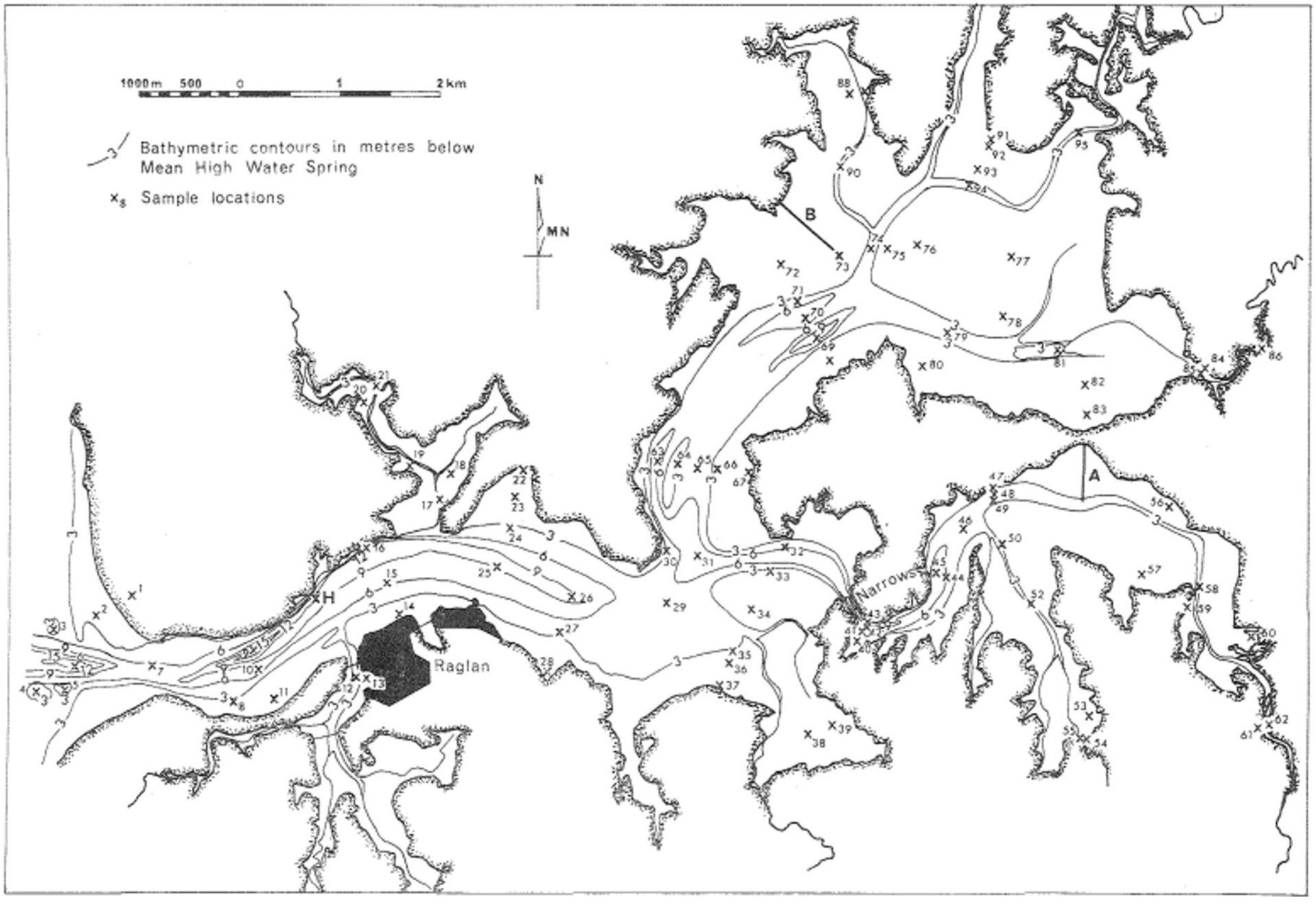

Appendix A.2: Figure 3.1. Schematic W – E cross-section Raglan region

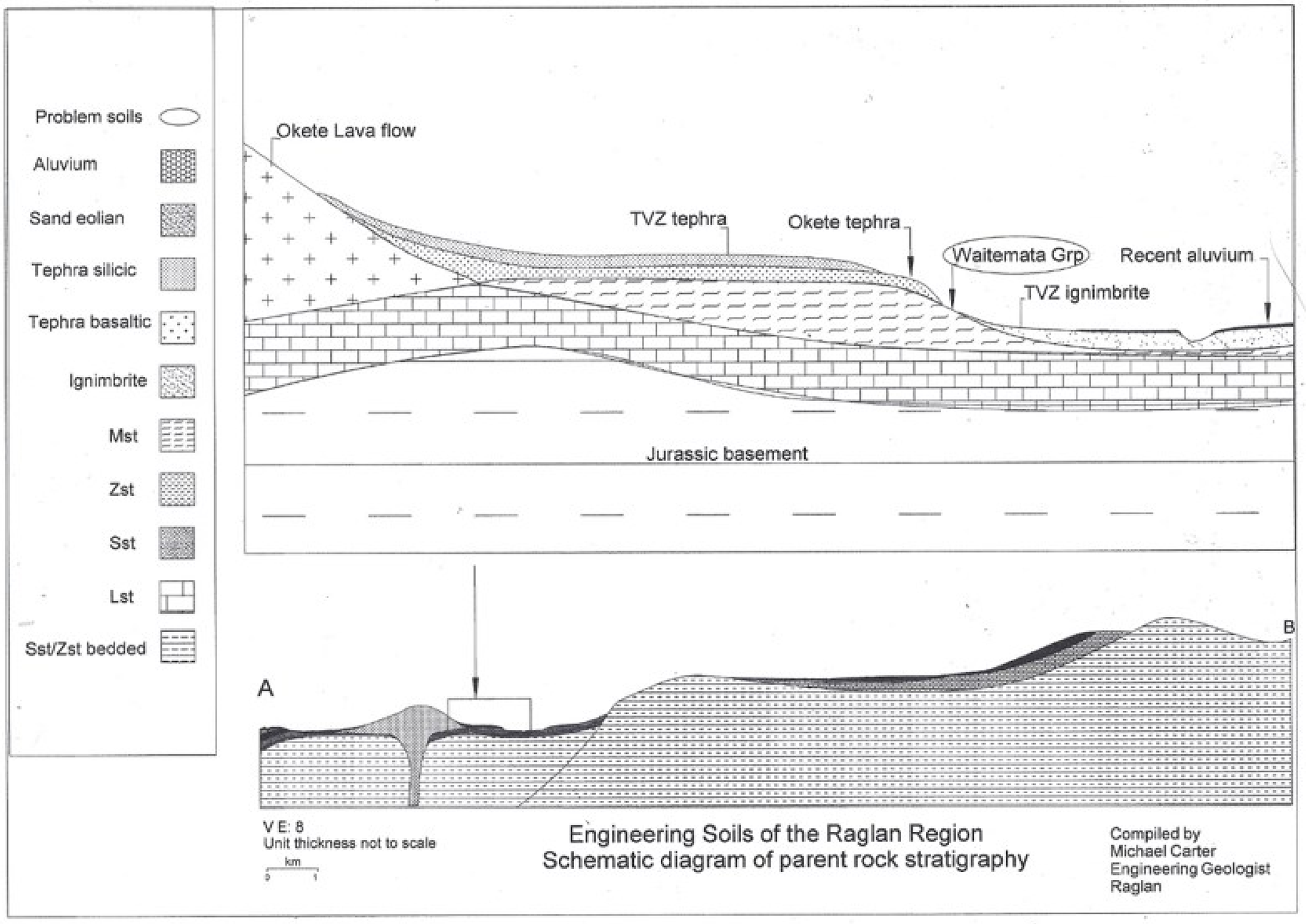

Appendix A.3: Figure 3.3. Chronostratigraphy of the Te Kuiti Group

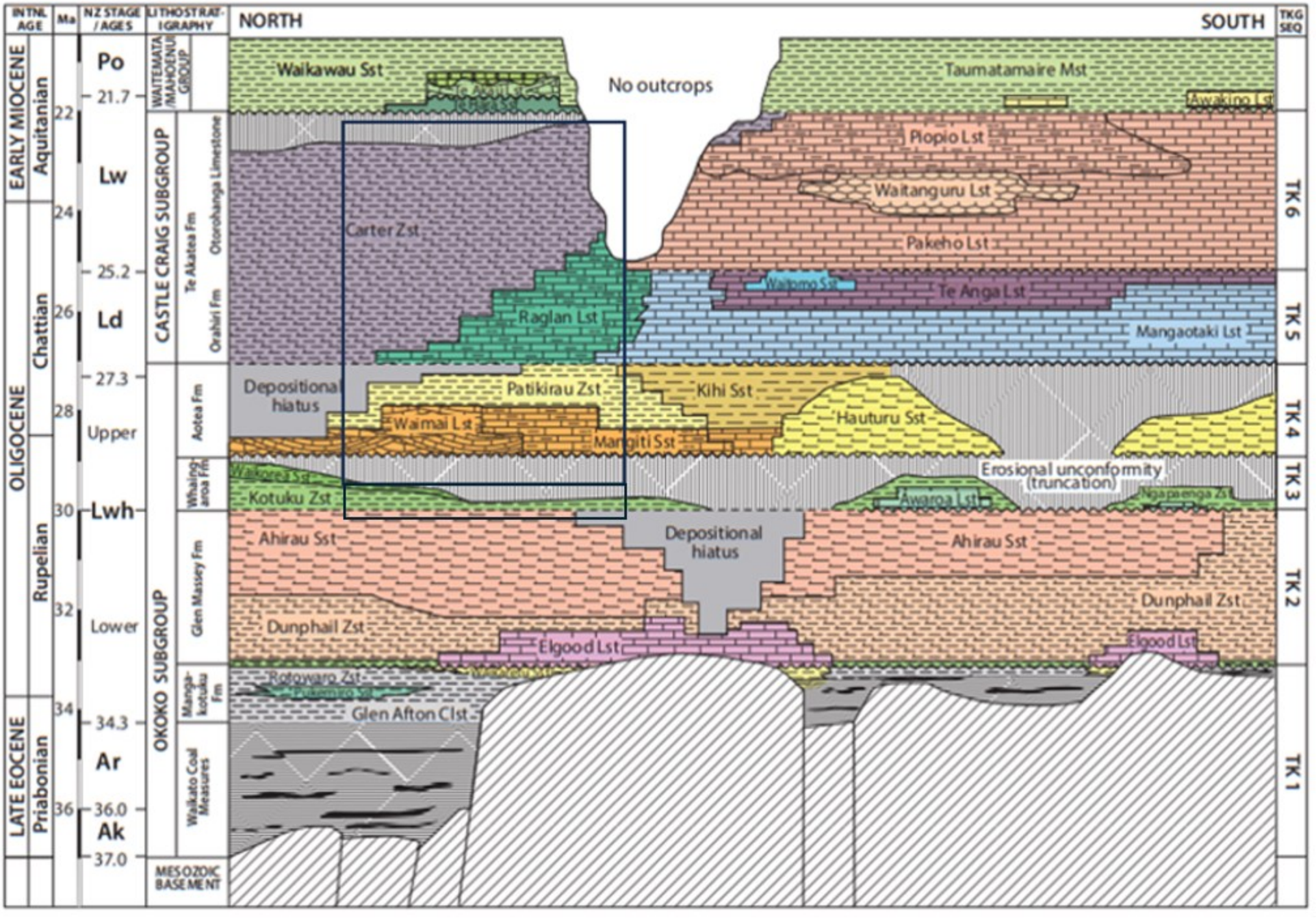

A.3

Appendix A.4: Figure 3.9. The extent and locations of wave-swept platforms

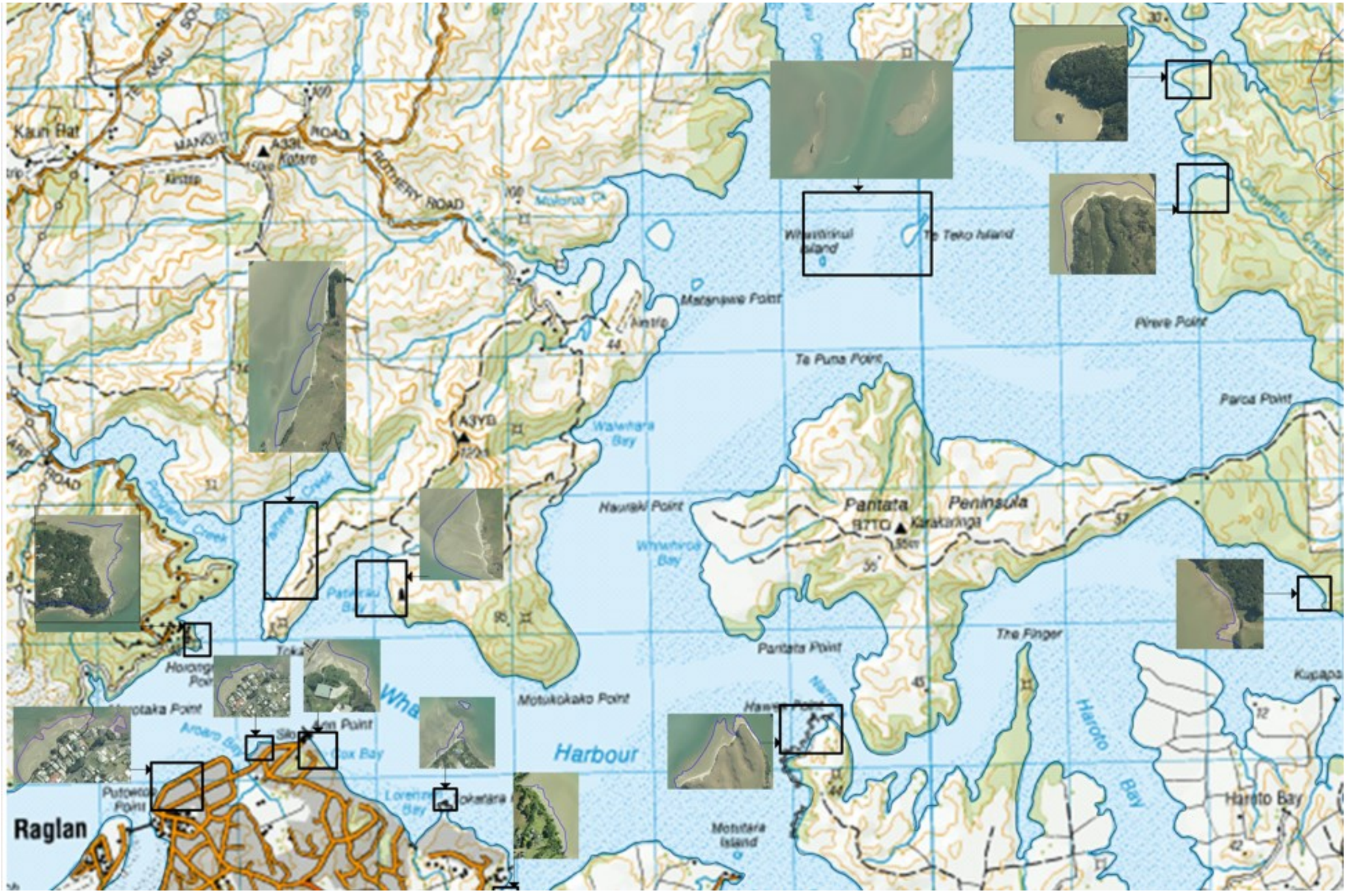

A.4

Appendix A.5: Figure 4.2. Dip directions of tidal wave-swept rock platforms

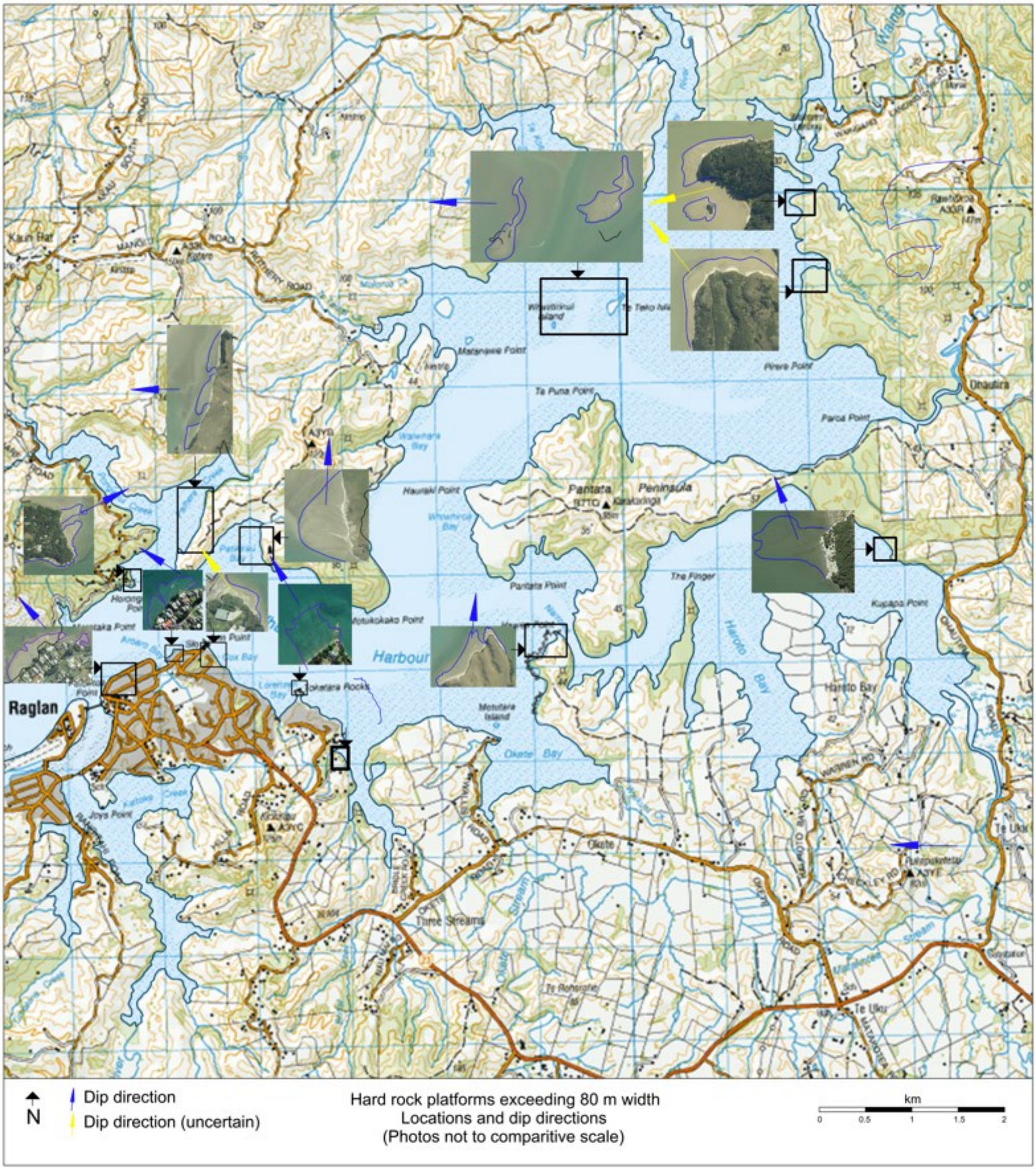

Appendix A.6: Figure 4.3. Accretion of sand and vegetation Te Kopua Peninsula

Appendix A.7: Figure 4.5. Maximum toe retreat and re-vegetation. Hawea Bay

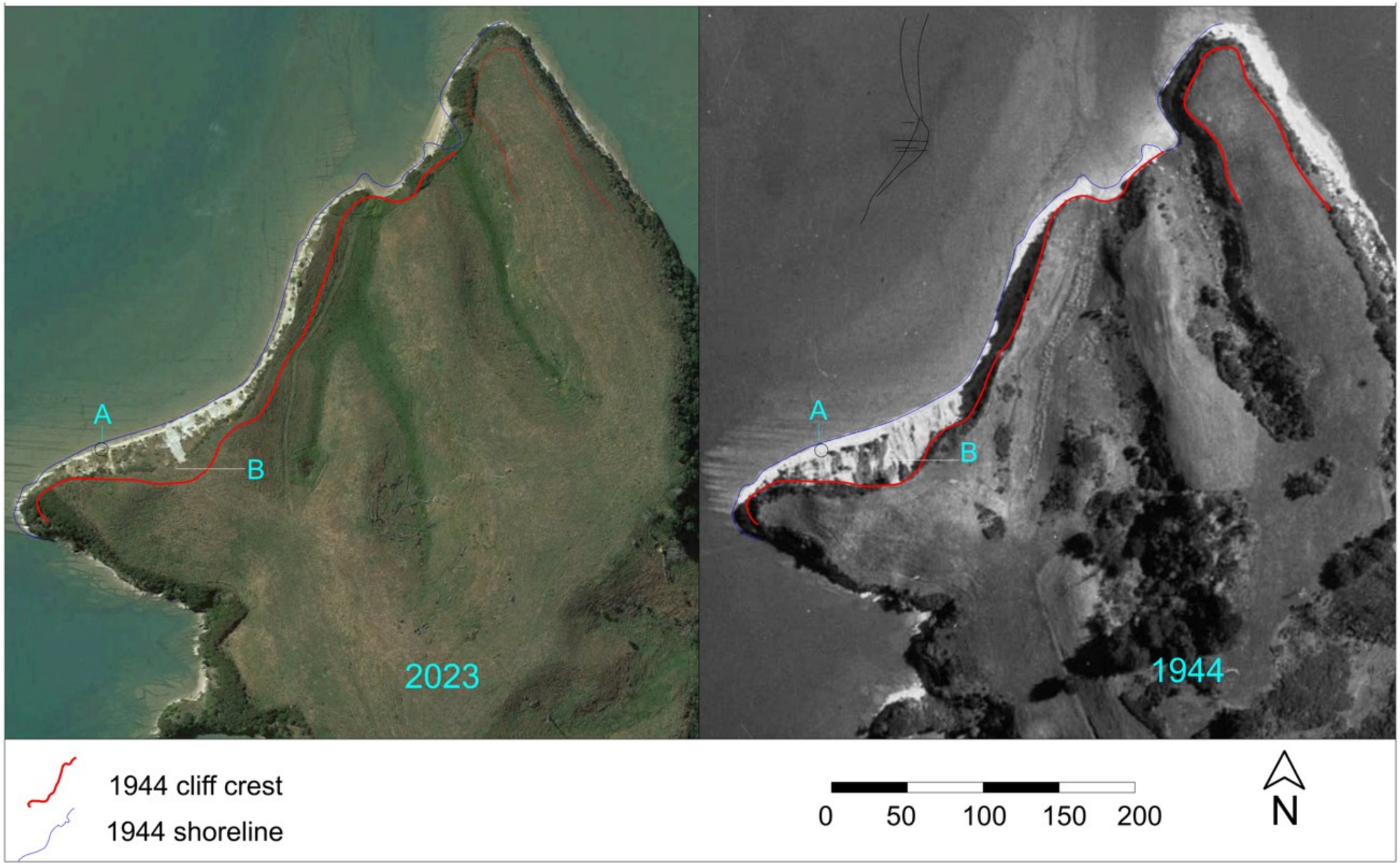

Appendix A.8: Figure 7.1. Rain erosion channels in Raglan Limestone

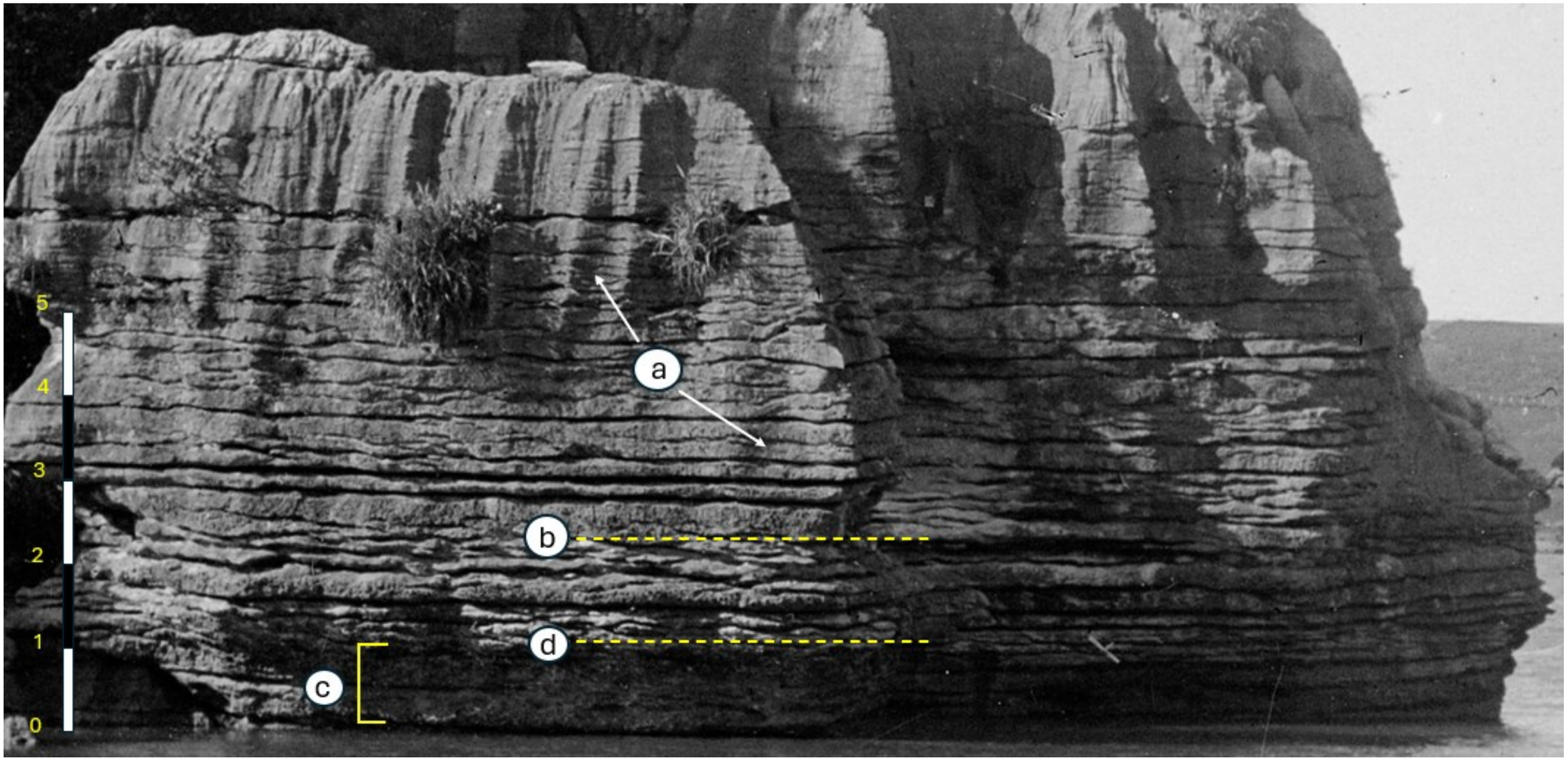

Appendix A.9: Figure 7.3. Dissolution notches in the Wine Glass Rock

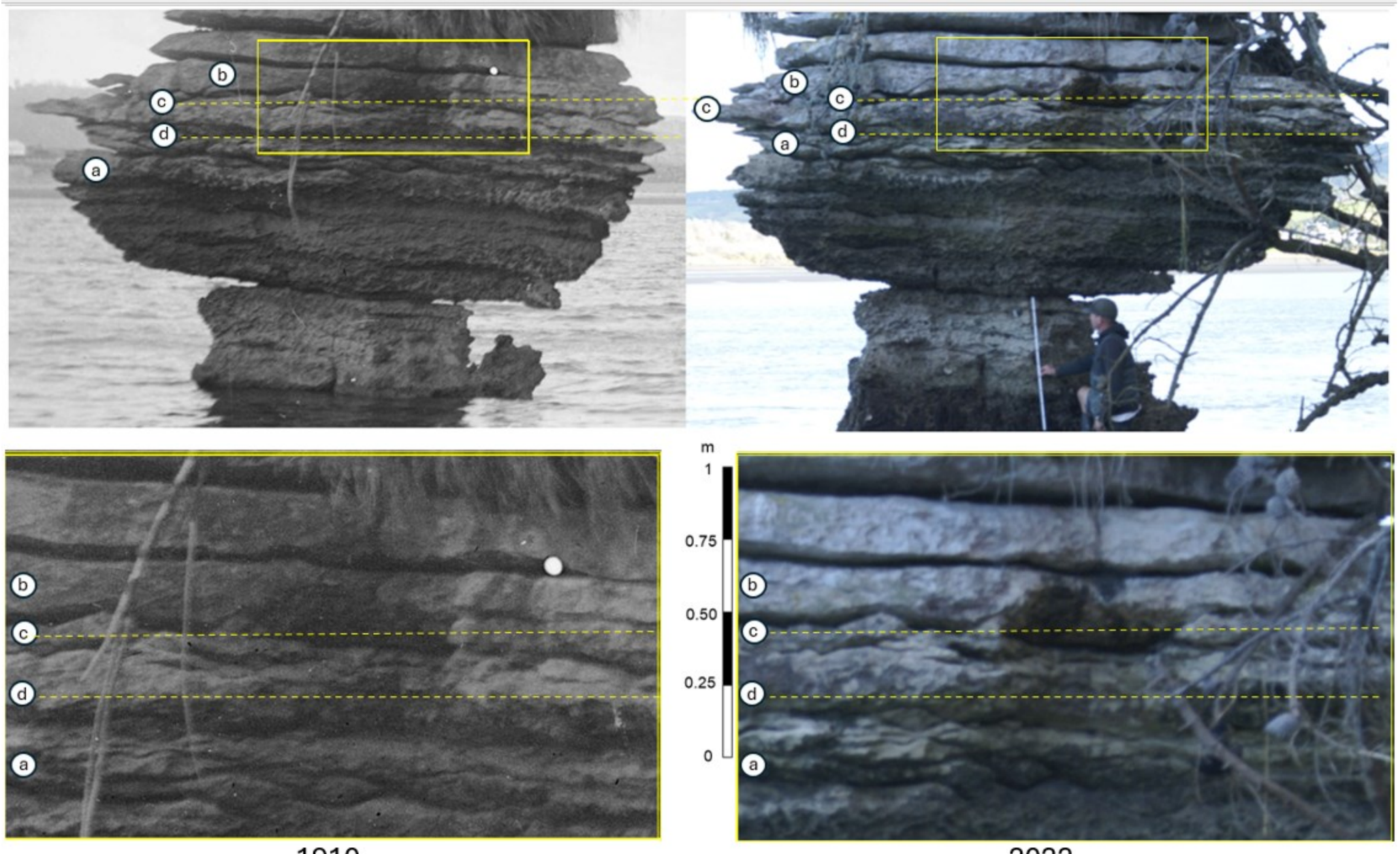

Appendix A.10: Figure 7.5. Dissolution notches in the Pakawau Rock

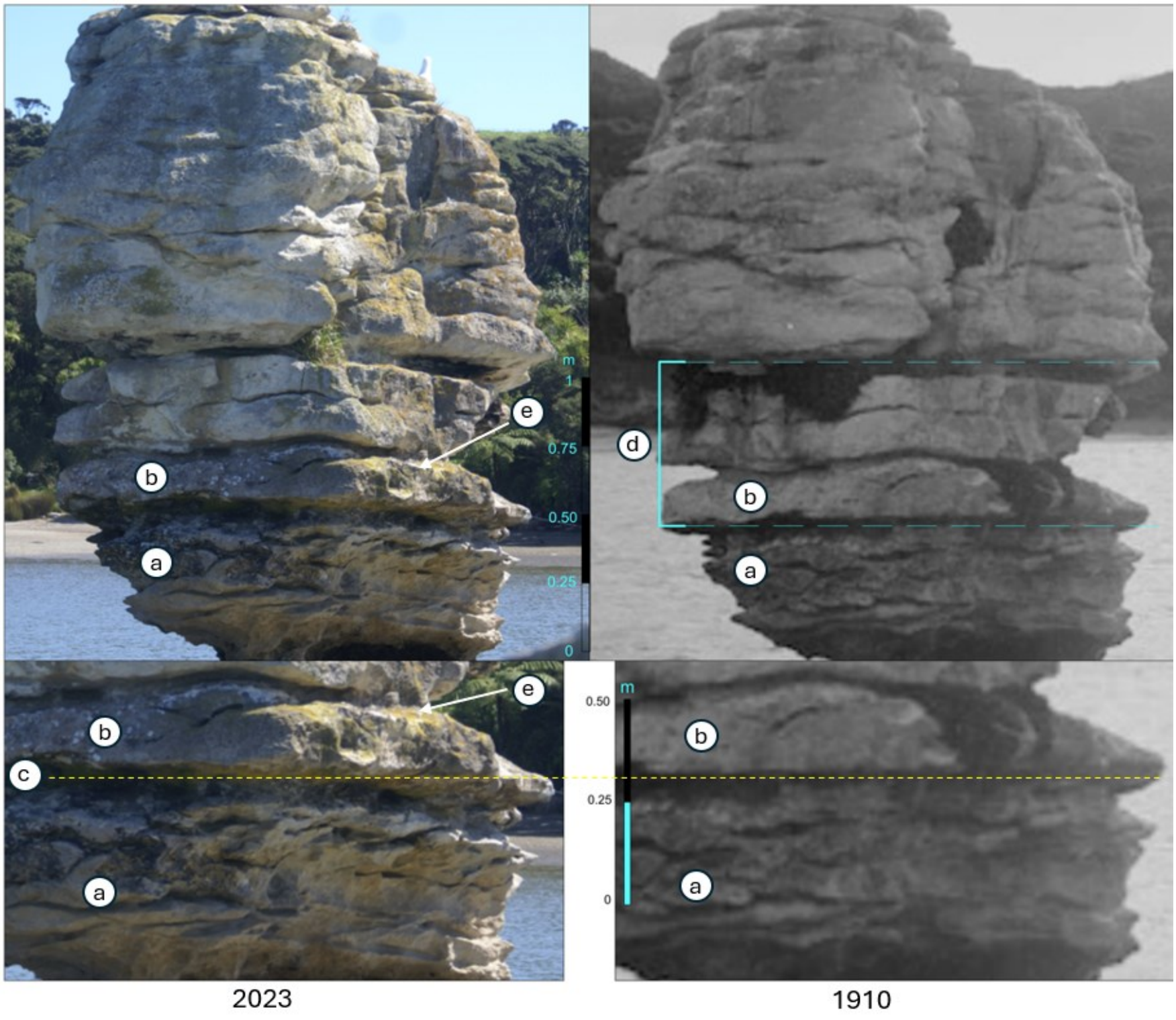

Appendix A.11: Figure 8.1.1. Geology of the Raglan Recreation Grounds

Appendix A..12: Figure 8.1.8. Cross-section of the Raglan Recreation Ground

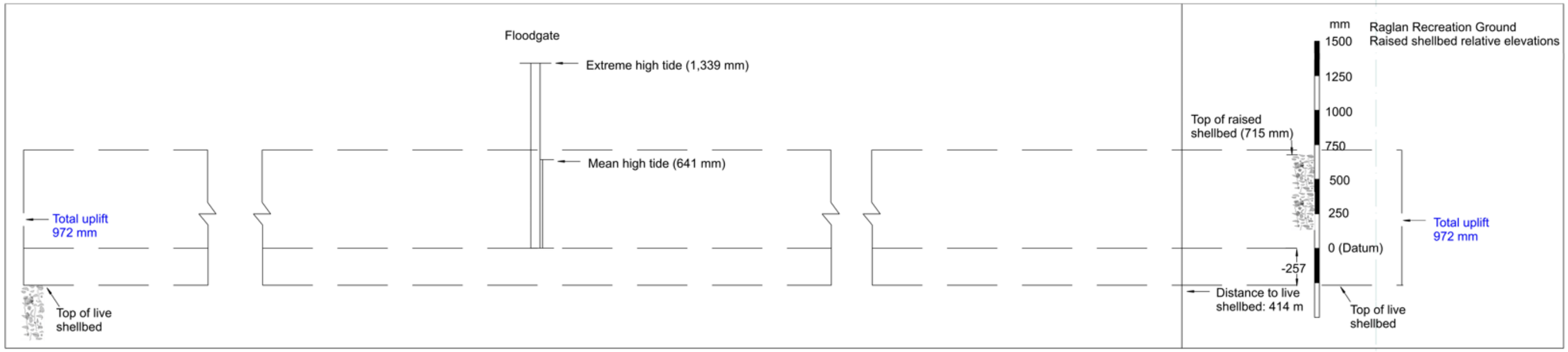

Appendix A.13: Figure 8.3.2. Geology of Patikirau Bay

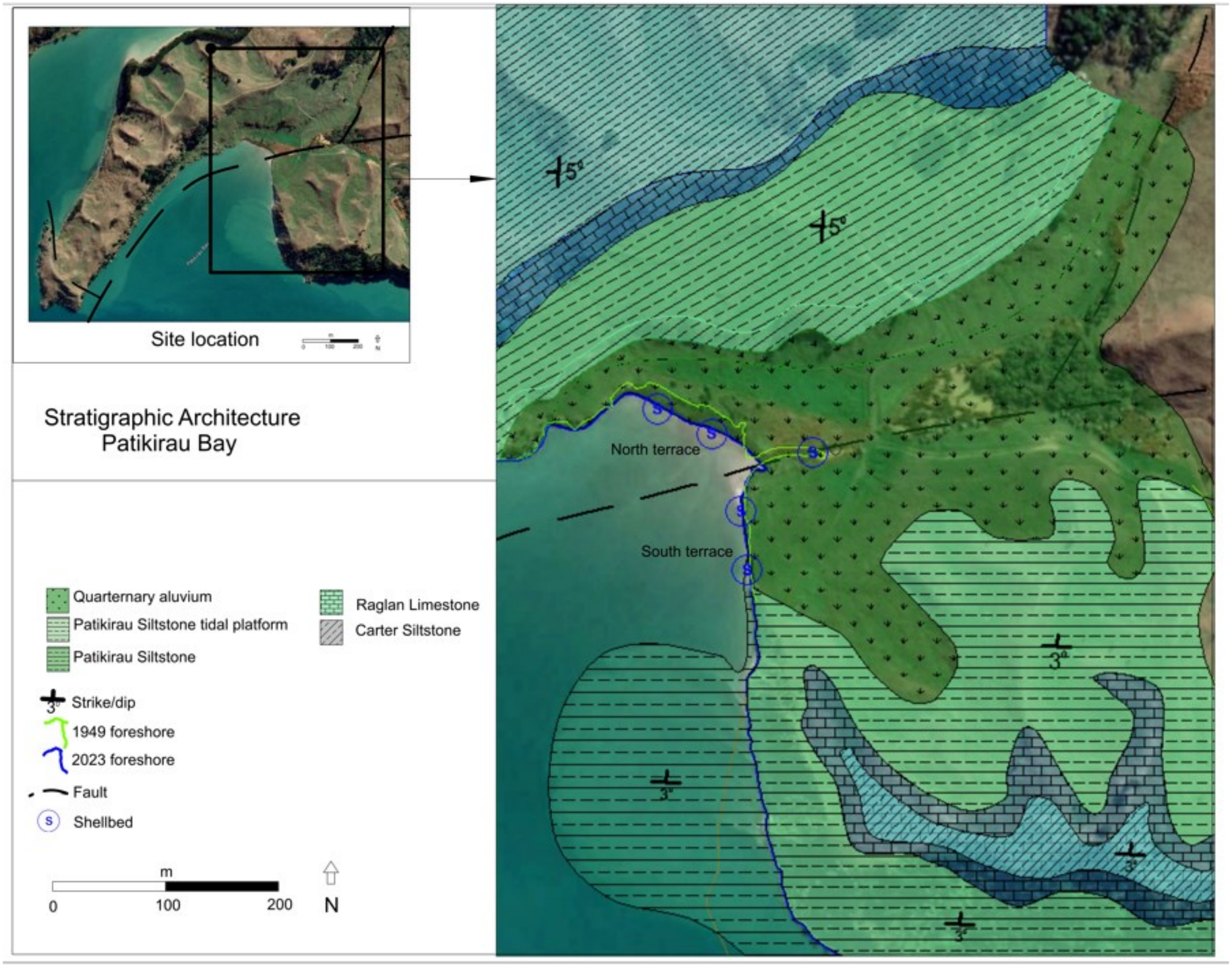

Appendix A.14: Figure 8.3.3. Patikirau Siltstone stress-release rupture

Appendix A.15: Figure 8.3.7. North Terrace Cross-section. Patikirau Bay

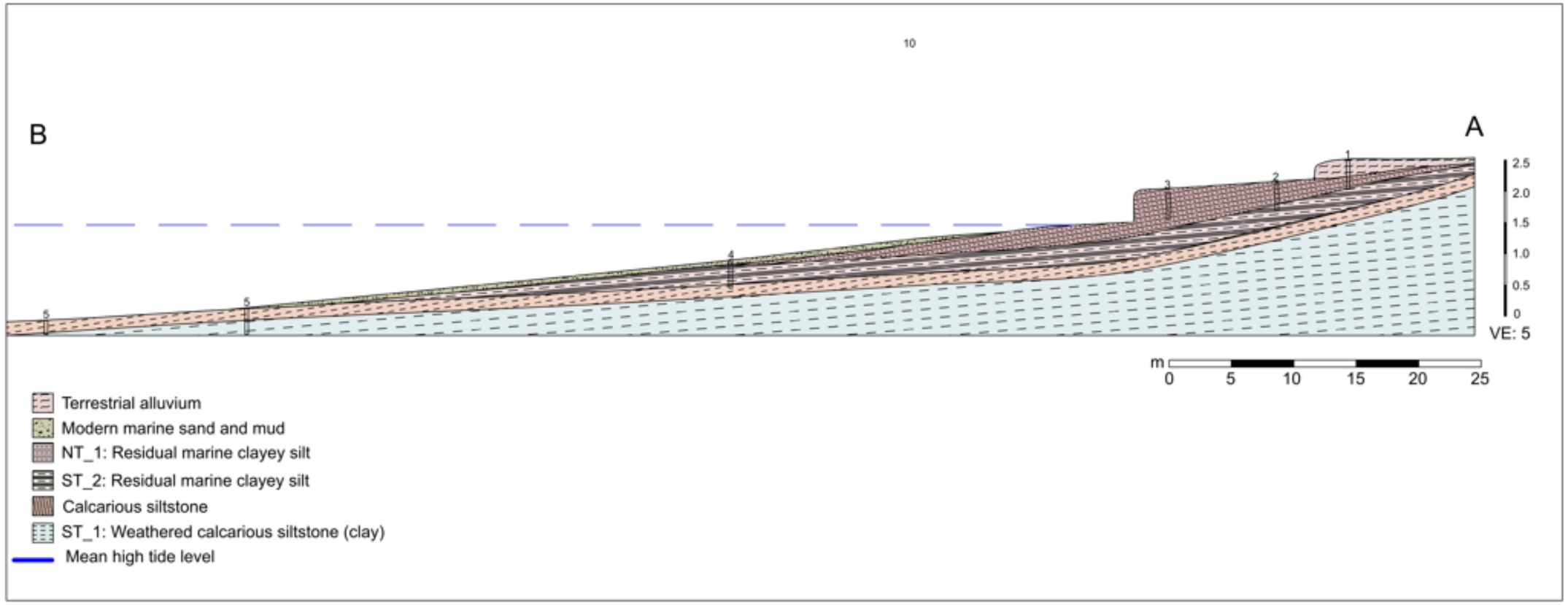

Appendix A.16: Figure 8.3.9. Comparison of the North Terrace erosion scarp profiles

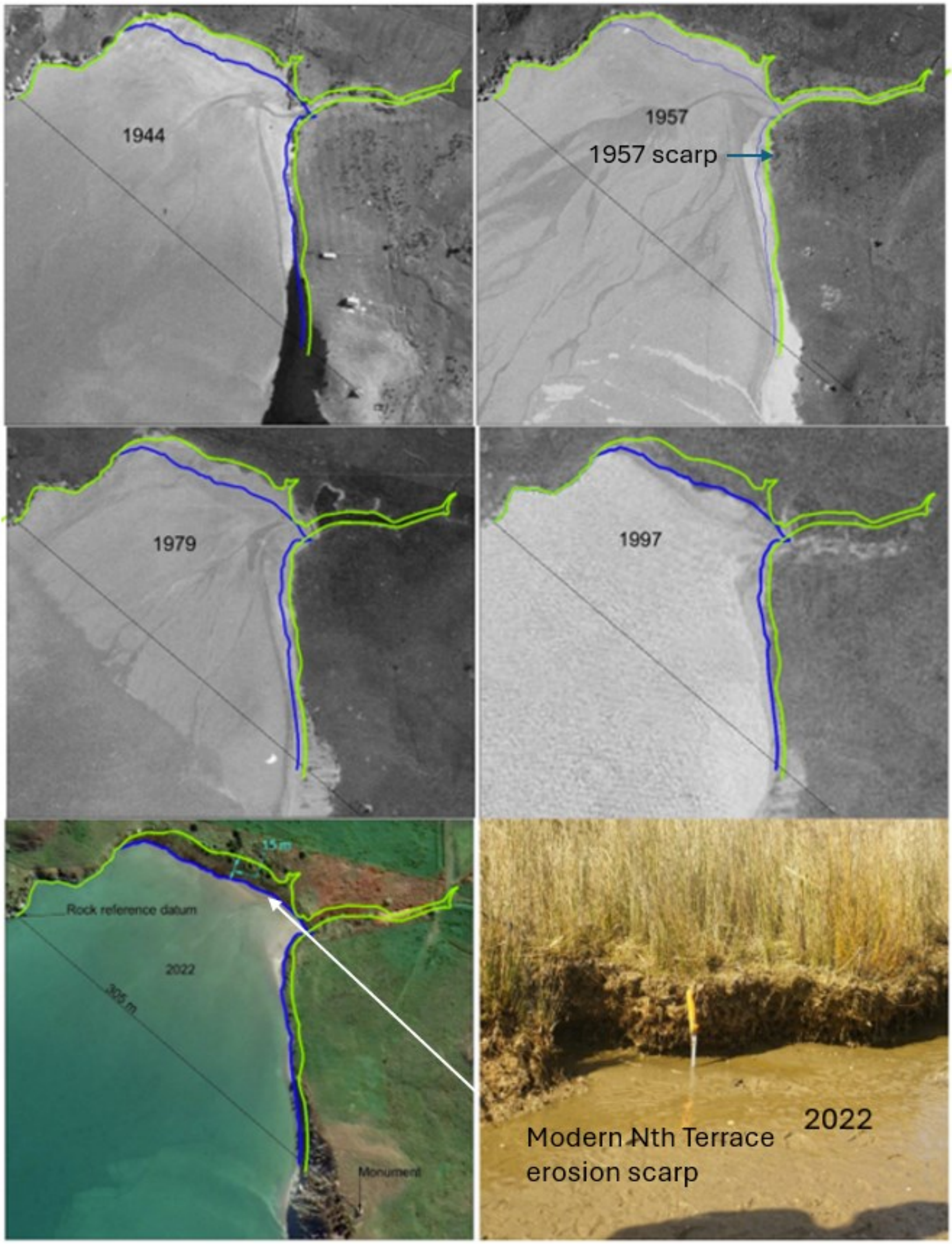

Appendix A.17: Figure 8.3.16. South Terrace cross-section

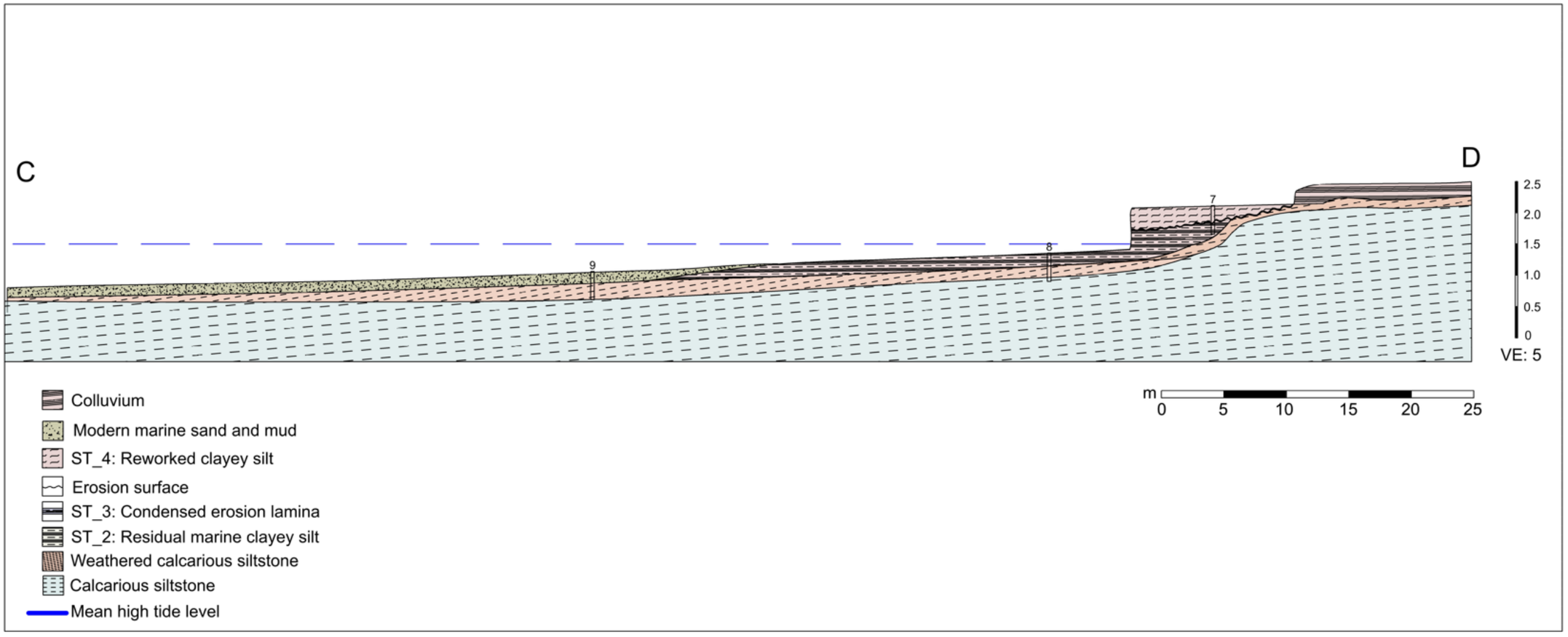

Appendix A.18: Figure 8.3.21. Long-section Patikirau Bay

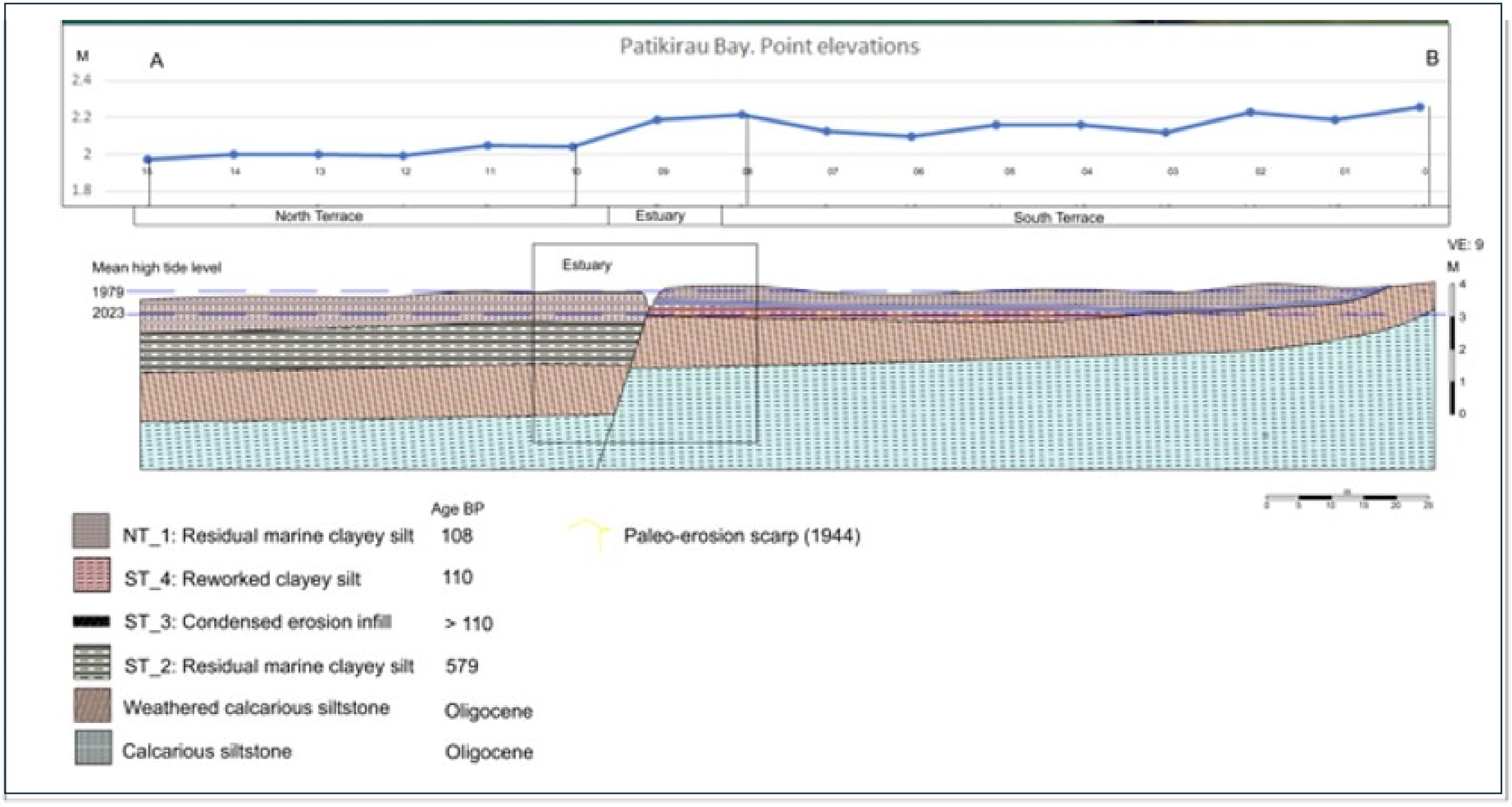

Appendix A.19: Figure 8.3.22. Model of Vertical land movement. Patikirau Bay

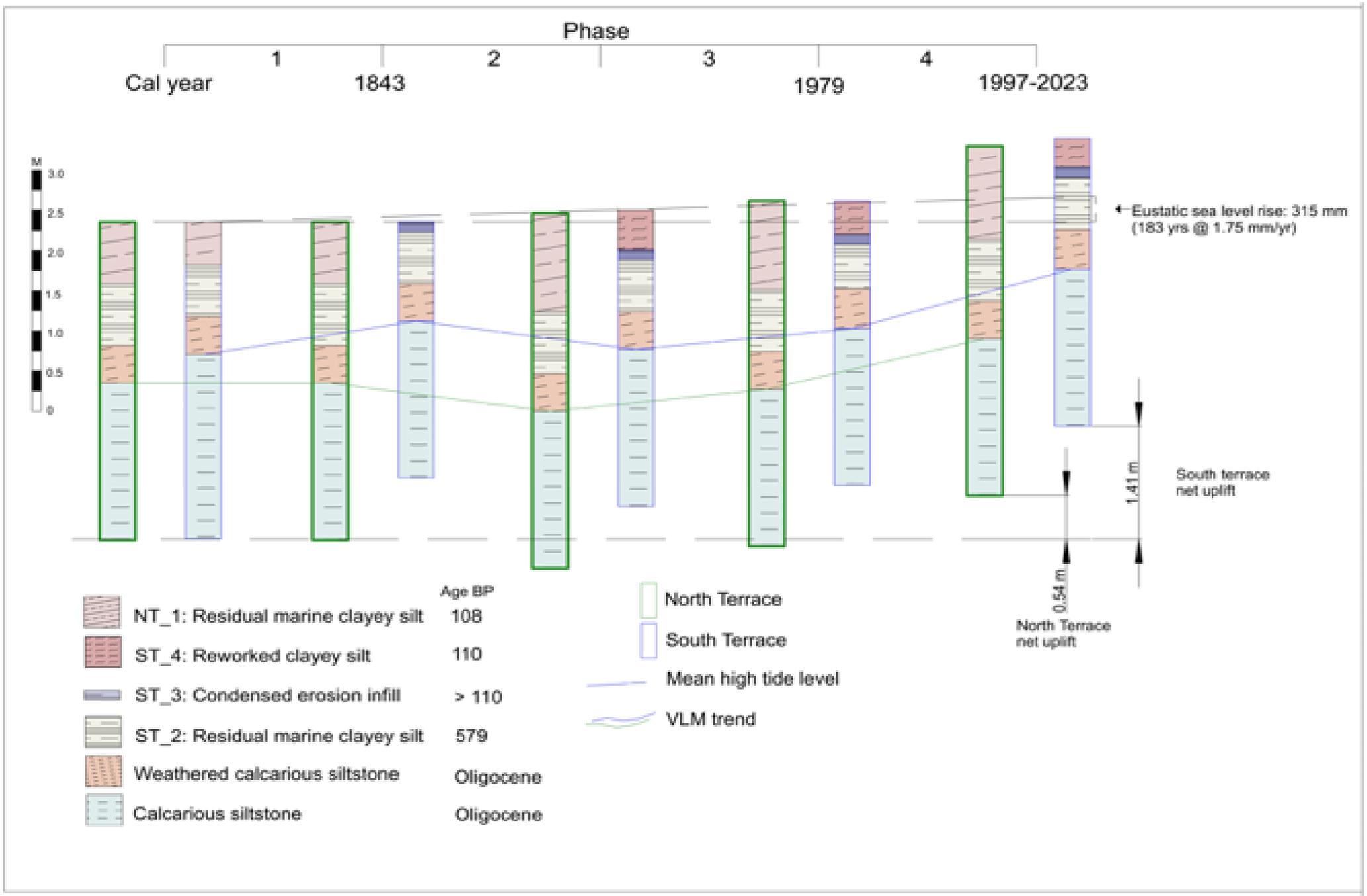

Appendix B: Dating Sample Data and Locations

Appendix B.1: Dating Sample Data

Location	Date Lab No (WK)	Thesis No	Age (pMC)*	Age (calibrated) 95% **	Lat	Long	Description*
Motukokako Peninsula	57038	BW_SB_1	104.4 +/- 0.4 %	2015 - 2017 Cal AD	37°47'11.19"S	174°53'59.39"E	Cockle valve
Motukokako Peninsula	57172	BW_1_B	102.9 +/- 0.3%	1964 Cal AD	"	"	Cockle valve
Rag. Rec. Ground SB 1	57039	RG_1_SB	637 +/- 27 BP	70 - 430 Cal BP	37°47'54.69"S	174°52'36.22"E	Cockle valve
Rag. Rec. Ground. SB 2	57324	RG_S2_1	6442 +/- 18 BP	6690 – 7090 Cal BP	"	"	Cockle valve
Rag. Rec. Ground. SB 2	57325	RG_S2_2	6423 +/- 18 BP	6670 – 7050 Cal BP	"	"	Cockle valve
Rag. Rec. Ground. SB 2	522702	RG_2_a	6465 +/- 20 BP	6560 – 6900 Cal BP	"	"	Cockle frag
Rag. Rec. Ground. SB 2	522703	RG_2_b	6460 +/- 20 BP	6560 – 6890 Cal BP	"	"	Cockle frag
Rag. Rec. Ground. SB 2	522704	RG_2_c	6430 +/- 20 BP	6520 – 6860 Cal BP	"	"	Cockle frag
Patikirau Bay	56887	SP_1a	6332 +/- 26 BP	6410 - 674 Cal BP	37°46'58.47"S	174°53'13.38"E	Cockle valve
Patikirau Bay	56888	SP_2a	103.5 +/- 0.3 %	1964 Cal AD	"	"	Cockle valve
Patikirau Bay	56886	SP_3a	109.5 +/- 0.3 %	1996 - 2001 Cal AD	37°47'0.47"S	174°53'10.77"E	Cockle valve
Patikirau Bay IT	57173	Pat_1_B	110.1 +/- 0.3%	1994 - 2001 Cal AD	37°46'58.47"S	174°53'13.38"E	Cockle valve
Patikirau Bay	57174	Pat_2_C	104.5 +/- 0.3%	2025 - 2017 Cal AD	"	"	Cockle valve
Patikirau Bay ST	57264	PST_1_1	579 +/- 21 BP	10 - 330 Cal BP	37°47'0.77"S	174°53'10.86"E	Cockle frag
Patikirau Bay NT	57322	PNT_1	109 +/- 0.3 %	1999 - 2003 Cal BP	37°46'57.50"S	174°53'8.76"E	Cockle valve
Patikirau Bay NT	57323	PHT_2	107 +/- 0.3 %	2003 - 2005 Cal BP	"	"	Cockle valve
Patikirau Bay	56889	BP_4a	86 +/- 13 BP	110 - 130 Cal AD	37°47'1.57"S	174°53'10.96"E	Equine Bone

* All cockle material is *Austrovenus stutchburyi*

Appendix B.2: Figure 8.3.11. Dating Sample locations

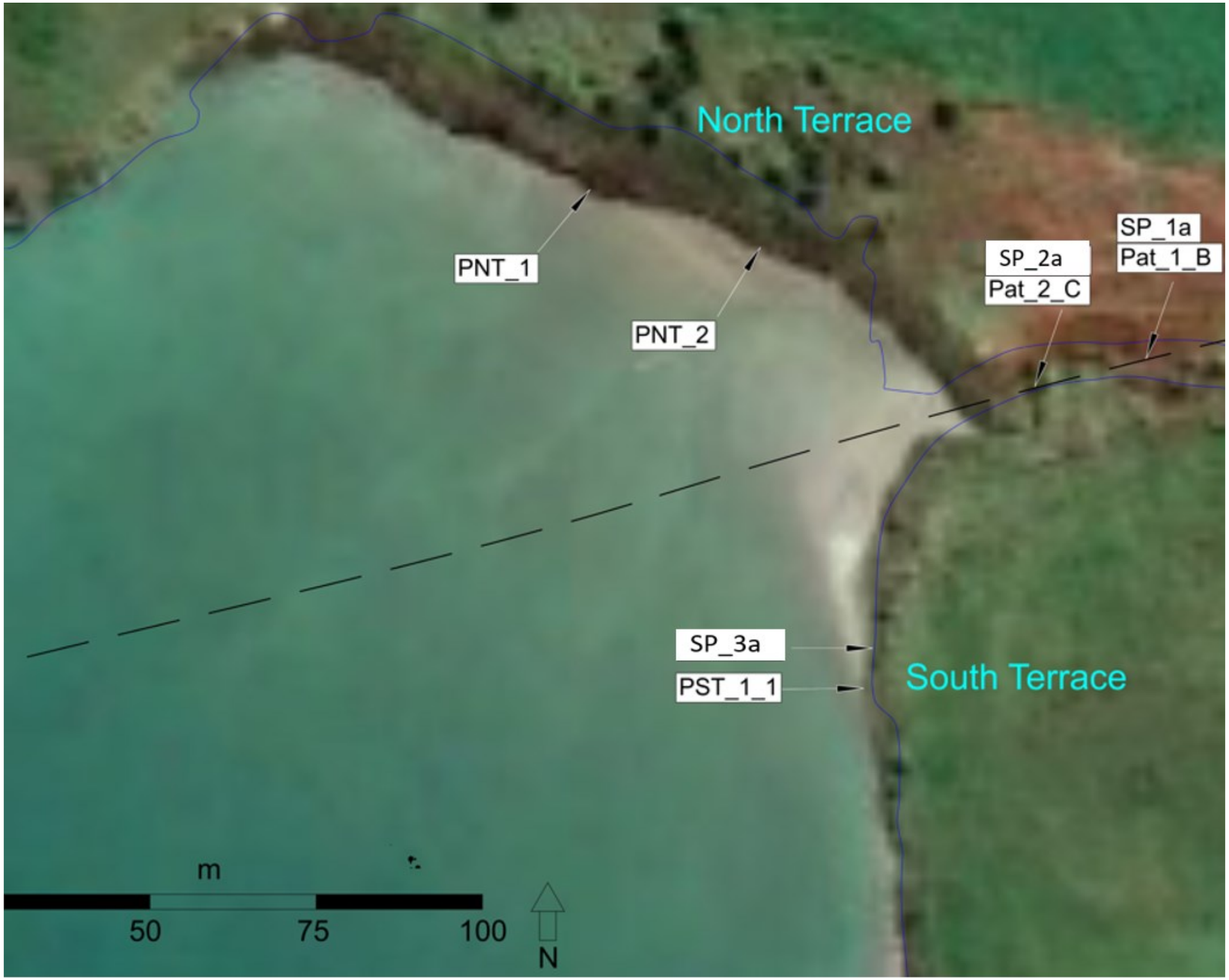

Appendix B.3: Dating Sample Laboratory Charts

^{14}C Lab Chart 1

THE UNIVERSITY OF WAIKATO
Te Whare Wānanga o Waikato

Radiocarbon Dating
Laboratory,
University of Waikato
Hamilton,
New Zealand.

Thursday, 14 March 2024

Radiocarbon Dating Laboratory

Report on Radiocarbon Age Determination for Wk- 57038

Submitter	M Carter
Submitter's Code	BW_SB_1
Site & Location	Raglan Birdwatchers, New Zealand
Sample Material	Marine shell Cockle
Physical Pretreatment	Surfaces cleaned. Washed in an ultrasonic bath. Tested for recrystallization: aragonite.
Chemical Pretreatment	Sample acid washed using 0.1N HCl, rinsed and dried.

$\delta^{13}C$	-1.2 ±	0.4 ‰	(CRDS)
$D^{14}C$	43.7 ±	3.4 ‰	
$F^{14}C\%$	104.4 ±	0.3 %	
Result	**104.4 ± 0.4 %**		

(AMS measurement)

Comments

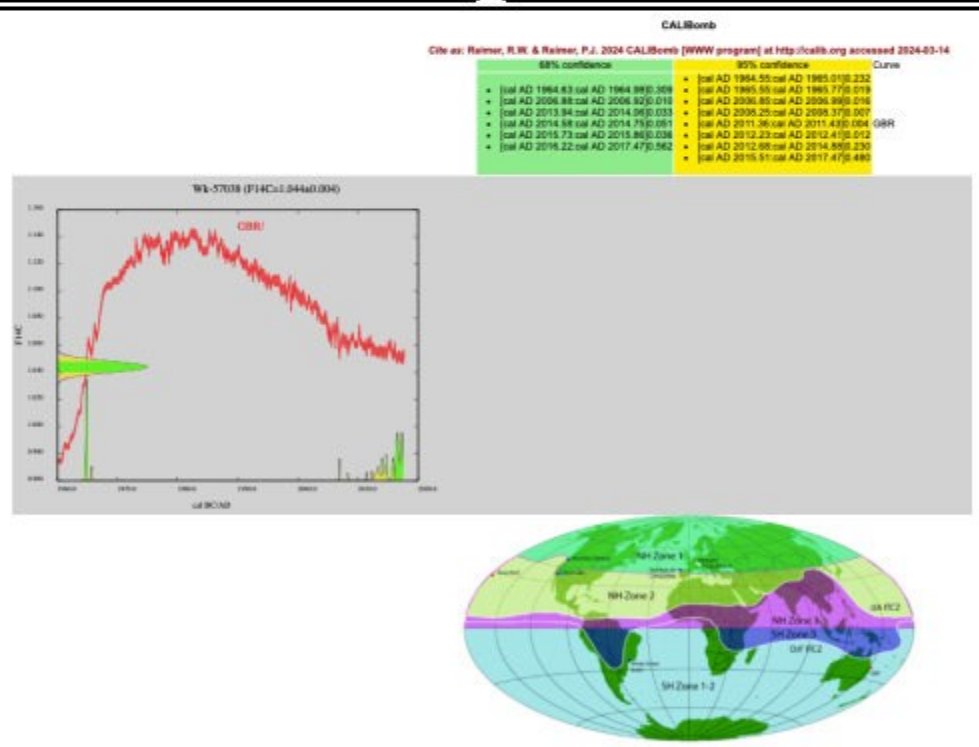

- Explanation of the calibrated Oxcal plots can be found at the Oxford Radiocarbon Accelerator Unit's calibration web pages (http://c14.arch.ox.ac.uk/embed.php?File=explanation.php)
- Result is *Conventional Age or Percent Modern Carbon (pMC)* following Stuiver and Polach, 1977, Radiocarbon 19, 355-363. This is based on the Libby half-life of 5568 yr with correction for isotopic fractionation applied. This age is normally quoted in publications and must include the appropriate error term and Wk number.
- Quoted errors are 1 standard deviation due to counting statistics multiplied by an experimentally determined Laboratory Error Multiplier.
- The isotopic fractionation, $\delta^{13}C$, is expressed as ‰ wrt PDB and is measured on sample CO_2.
- $P^{14}C\%$ is also known as *Percent Modern Carbon (pMC)*.

THE UNIVERSITY OF WAIKATO
Te Whare Wānanga o Waikato

Radiocarbon Dating Laboratory,
University of Waikato
Hamilton,
New Zealand.

Thursday, 14 March 2024

Radiocarbon Dating Laboratory

Report on Radiocarbon Age Determination for Wk- 57172

Submitter	M Carter
Submitter's Code	BW_1_B
Site & Location	Raglan, New Zealand
Sample Material	Marine shell Pipi
Physical Pretreatment	Surfaces cleaned. Washed in an ultrasonic bath. Tested for recrystallization: aragonite.
Chemical Pretreatment	Sample acid washed using 0.1N HCl, rinsed and dried.

$\delta^{13}C$	-0.2 ±	0.2 ‰	(CRDS)
$D^{14}C$	29.0 ±	2.6 ‰	
$F^{14}C\%$	102.9 ±	0.3 %	
Result	**102.9 ± 0.3 %**		

(AMS measurement)

Comments

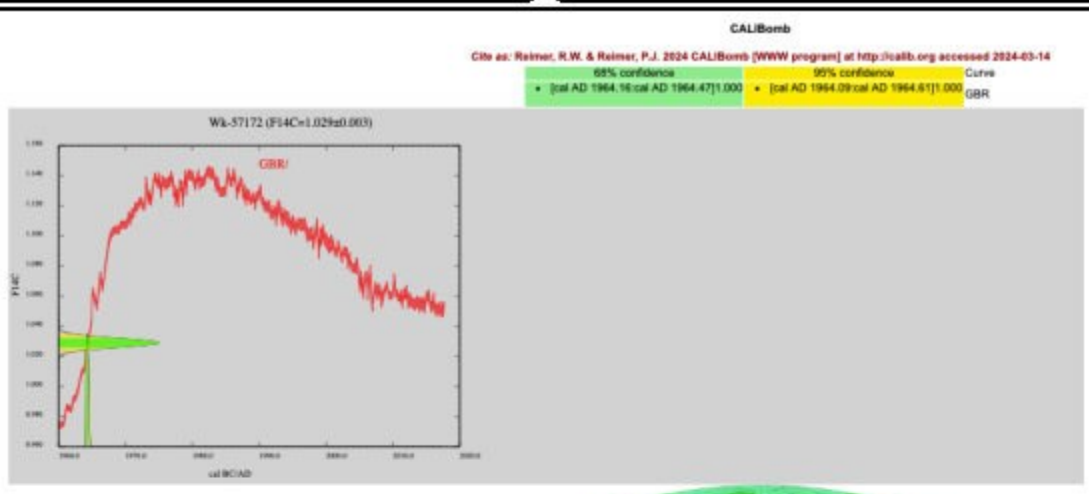

- Explanation of the calibrated Oxcal plots can be found at the Oxford Radiocarbon Accelerator Unit's calibration web pages (http://c14.arch.ox.ac.uk/embed.php?File=explanation.php)
- Result is *Conventional Age or Percent Modern Carbon (pMC)* following Stuiver and Polach, 1977, Radiocarbon 19, 355-363. This is based on the Libby half-life of 5568 yr with correction for isotopic fractionation applied. This age is normally quoted in publications and must include the appropriate error term and Wk number.
- Quoted errors are 1 standard deviation due to counting statistics multiplied by an experimentally determined Laboratory Error Multiplier.
- The isotopic fractionation, $\delta^{13}C$, is expressed as ‰ wrt PDB and is measured on sample CO_2.
- $P^{14}C\%$ is also known as *Percent Modern Carbon (pMC)*.

THE UNIVERSITY OF WAIKATO
Te Whare Wānanga o Waikato

Radiocarbon Dating Laboratory,
University of Waikato
Hamilton,
New Zealand.

Thursday, 14 March 2024

Radiocarbon Dating Laboratory

Report on Radiocarbon Age Determination for Wk- 57039

Submitter	M Carter
Submitter's Code	RG_1_SB
Site & Location	Raglan Birdwatchers, New Zealand
Sample Material	Marine shell Cockle
Physical Pretreatment	Surfaces cleaned. Washed in an ultrasonic bath. Tested for recrystallization: aragonite.
Chemical Pretreatment	Sample acid washed using 0.1N HCl, rinsed and dried.

$\delta^{13}C$	0.8 ±	0.4 ‰	(CRDS)
$D^{14}C$	-76.2 ±	3.1 ‰	
$F^{14}C\%$	92.4 ±	0.3 %	
Result	**637 ± 27 BP**		

(AMS measurement)

Comments

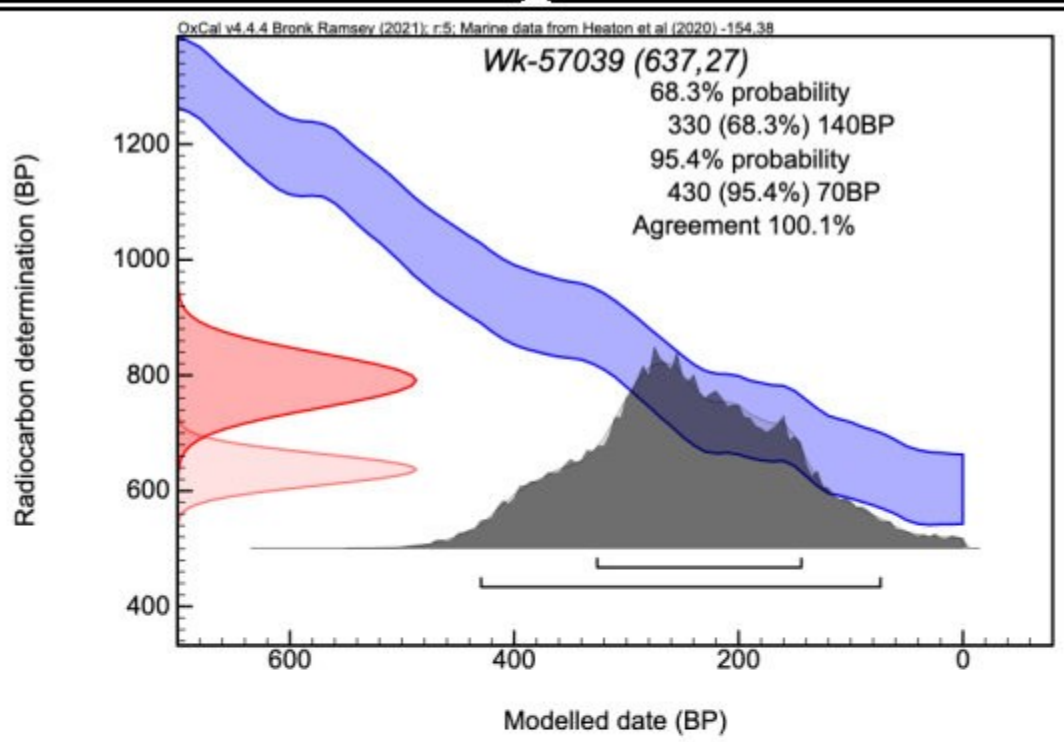

- Explanation of the calibrated Oxcal plots can be found at the Oxford Radiocarbon Accelerator Unit's calibration web pages (http://c14.arch.ox.ac.uk/embed.php?File=explanation.php)
- Result is *Conventional Age or Percent Modern Carbon (pMC)* following Stuiver and Polach, 1977, Radiocarbon 19, 355-363. This is based on the Libby half-life of 5568 yr with correction for isotopic fractionation applied. This age is normally quoted in publications and must include the appropriate error term and Wk number.
- Quoted errors are 1 standard deviation due to counting statistics multiplied by an experimentally determined Laboratory Error Multiplier.
- The isotopic fractionation, $\delta^{13}C$, is expressed as ‰ wrt PDB and is measured on sample CO_2.
- $P^{14}C\%$ is also known as *Percent Modern Carbon (pMC)*.

THE UNIVERSITY OF WAIKATO
Te Whare Wānanga o Waikato

Radiocarbon Dating
Laboratory,
University of Waikato
Hamilton,
New Zealand.

Thursday, 14 March 2024

Radiocarbon Dating Laboratory

Report on Radiocarbon Age Determination for Wk- 57324

Submitter	M Carter
Submitter's Code	RG_S2_1
Site & Location	Raglan Rec, New Zealand
Sample Material	Marine shell Cockle
Physical Pretreatment	Surfaces cleaned. Washed in an ultrasonic bath. Tested for recrystallization: aragonite.
Chemical Pretreatment	Sample acid washed using 0.1N HCl, rinsed and dried.

$\delta^{13}C$	0.0 ±	0.5 ‰	(CRDS)
$D^{14}C$	-551.6 ±	1.0 ‰	
$F^{14}C\%$	44.8 ±	0.1 %	
Result	**6442 ± 18 BP**		

(AMS measurement)

Comments

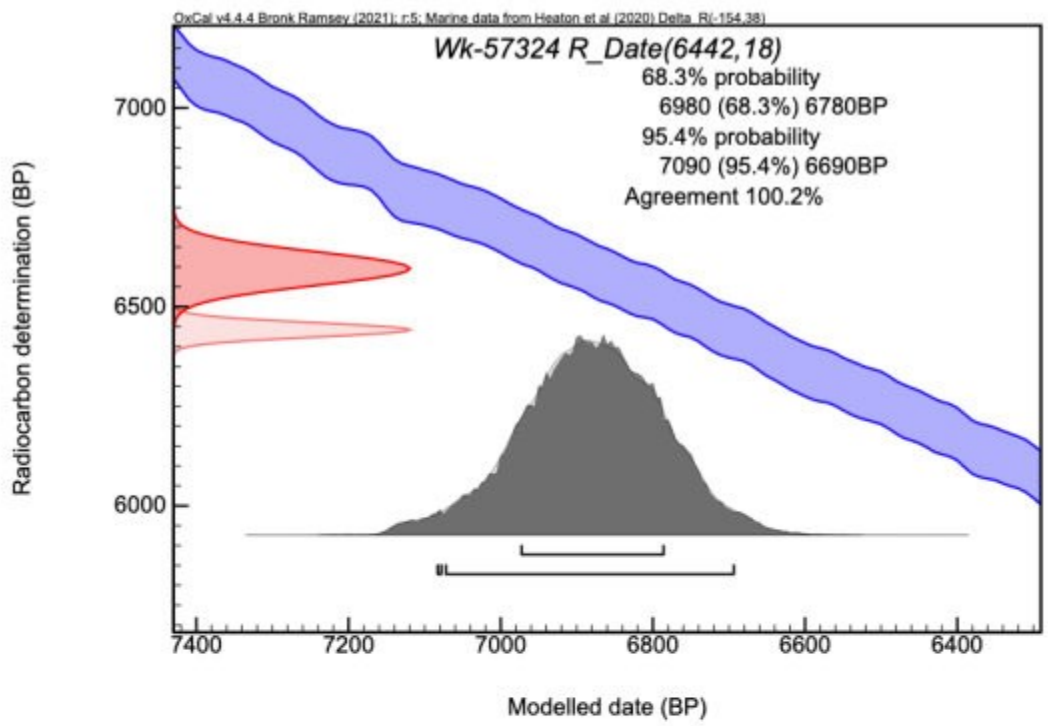

- Explanation of the calibrated Oxcal plots can be found at the Oxford Radiocarbon Accelerator Unit's calibration web pages (http://c14.arch.ox.ac.uk/embed.php?File=explanation.php)
- Result is *Conventional Age or Percent Modern Carbon (pMC)* following Stuiver and Polach, 1977, Radiocarbon 19, 355-363. This is based on the Libby half-life of 5568 yr with correction for isotopic fractionation applied. This age is normally quoted in publications and must include the appropriate error term and Wk number.
- Quoted errors are 1 standard deviation due to counting statistics multiplied by an experimentally determined Laboratory Error Multiplier.
- The isotopic fractionation, $\delta^{13}C$, is expressed as ‰ wrt PDB and is measured on sample CO_2.
- $P^{14}C\%$ is also known as *Percent Modern Carbon (pMC)*.

THE UNIVERSITY OF WAIKATO
Te Whare Wānanga o Waikato

Radiocarbon Dating Laboratory,
University of Waikato
Hamilton,
New Zealand.

Thursday, 14 March 2024

Radiocarbon Dating Laboratory

Report on Radiocarbon Age Determination for Wk- 57325

Submitter	M Carter
Submitter's Code	RG_S2_2
Site & Location	Raglan Rec, New Zealand
Sample Material	Marine shell Cockle
Physical Pretreatment	Surfaces cleaned. Washed in an ultrasonic bath. Tested for recrystallization: aragonite.
Chemical Pretreatment	Sample acid washed using 0.1N HCl, rinsed and dried.

$\delta^{13}C$	0.8 ±	0.5 ‰	(CRDS)
$D^{14}C$	-550.5 ±	1.0 ‰	
$F^{14}C\%$	44.9 ±	0.1 %	
Result	**6423 ± 18 BP**		

(AMS measurement)

Comments

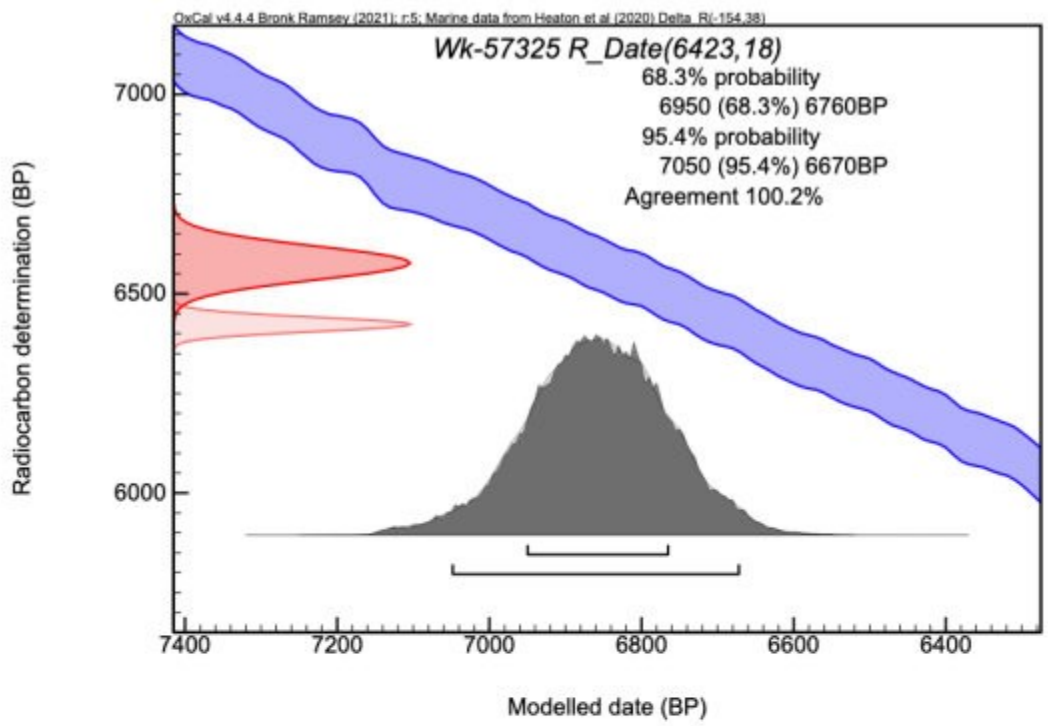

- Explanation of the calibrated Oxcal plots can be found at the Oxford Radiocarbon Accelerator Unit's calibration web pages (http://c14.arch.ox.ac.uk/embed.php?File=explanation.php)
- Result is *Conventional Age or Percent Modern Carbon (pMC)* following Stuiver and Polach, 1977, Radiocarbon 19, 355-363. This is based on the Libby half-life of 5568 yr with correction for isotopic fractionation applied. This age is normally quoted in publications and must include the appropriate error term and Wk number.
- Quoted errors are 1 standard deviation due to counting statistics multiplied by an experimentally determined Laboratory Error Multiplier.
- The isotopic fractionation, $\delta^{13}C$, is expressed as ‰ wrt PDB and is measured on sample CO_2.
- $P^{14}C\%$ is also known as *Percent Modern Carbon (pMC)*.

THE UNIVERSITY OF WAIKATO
Te Whare Wānanga o Waikato

Radiocarbon Dating Laboratory,
University of Waikato
Hamilton,
New Zealand.

Thursday, 14 March 2024

Radiocarbon Dating Laboratory

Report on Radiocarbon Age Determination for Wk- 57702

Submitter	M Carter
Submitter's Code	RG_2_a
Site & Location	Raglan, New Zealand
Sample Material	Estuarine Shell Cockle
Physical Pretreatment	Surfaces cleaned. Washed in an ultrasonic bath. Tested for recrystallization: aragonite.
Chemical Pretreatment	Sample acid washed using 0.1N HCl, rinsed and dried.

$D^{14}C$	-552.8 ±	1.1 ‰
$F^{14}C$%	44.7 ±	0.1 %
Result	**6465 ± 20 BP**	

(AMS measurement)

Comments

Please note: The Carbon-13 stable isotope value ($\delta^{13}C$) was measured on prepared graphite using the AMS spectrometer. The radiocarbon date has therefore been corrected for isotopic fractionation. However the AMS-measured $\delta^{13}C$ value can differ from the $\delta^{13}C$ of the original material and it is therefore not shown.

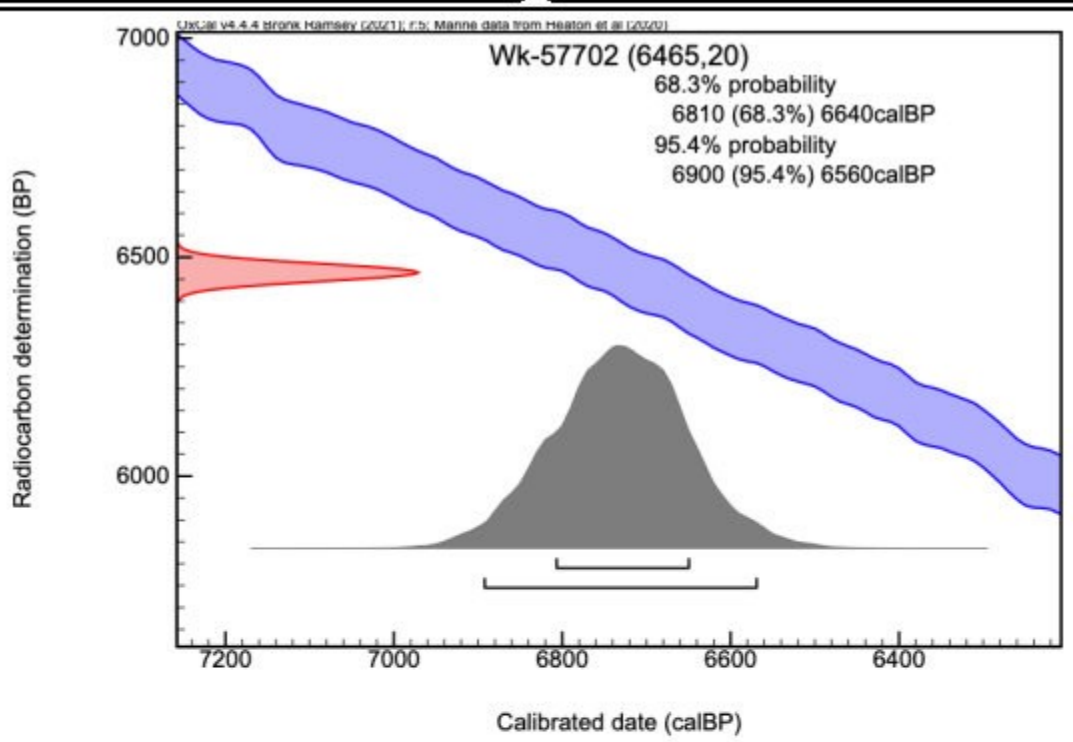

- Explanation of the calibrated Oxcal plots can be found at the Oxford Radiocarbon Accelerator Unit's calibration web pages (http://c14.arch.ox.ac.uk/embed.php?File=explanation.php)
- Result is *Conventional Age or Percent Modern Carbon (pMC)* following Stuiver and Polach, 1977, Radiocarbon 19, 355-363. This is based on the Libby half-life of 5568 yr with correction for isotopic fractionation applied. This age is normally quoted in publications and must include the appropriate error term and Wk number.
- Quoted errors are 1 standard deviation due to counting statistics multiplied by an experimentally determined Laboratory Error Multiplier.
- The isotopic fractionation, $\delta^{13}C$, is expressed as ‰ wrt PDB and is measured on sample CO_2.
- $P^{14}C$% is also known as *Percent Modern Carbon (pMC)*.

THE UNIVERSITY OF WAIKATO
Te Whare Wānanga o Waikato

Radiocarbon Dating Laboratory,
University of Waikato
Hamilton,
New Zealand.

Thursday, 14 March 2024

Radiocarbon Dating Laboratory

Report on Radiocarbon Age Determination for Wk- 57703

Submitter	M Carter
Submitter's Code	RG_2_b
Site & Location	Raglan, New Zealand
Sample Material	Estuarine Shell Cockle
Physical Pretreatment	Surfaces cleaned. Washed in an ultrasonic bath. Tested for recrystallization: aragonite.
Chemical Pretreatment	Sample acid washed using 0.1N HCl, rinsed and dried.

$D^{14}C$	-552.5 ±	1.1 ‰
$F^{14}C$%	44.7 ±	0.1 %
Result	**6460 ± 20 BP**	

(AMS measurement)

Comments

Please note: The Carbon-13 stable isotope value ($\delta^{13}C$) was measured on prepared graphite using the AMS spectrometer. The radiocarbon date has therefore been corrected for isotopic fractionation. However the AMS-measured $\delta^{13}C$ value can differ from the $\delta^{13}C$ of the original material and it is therefore not shown.

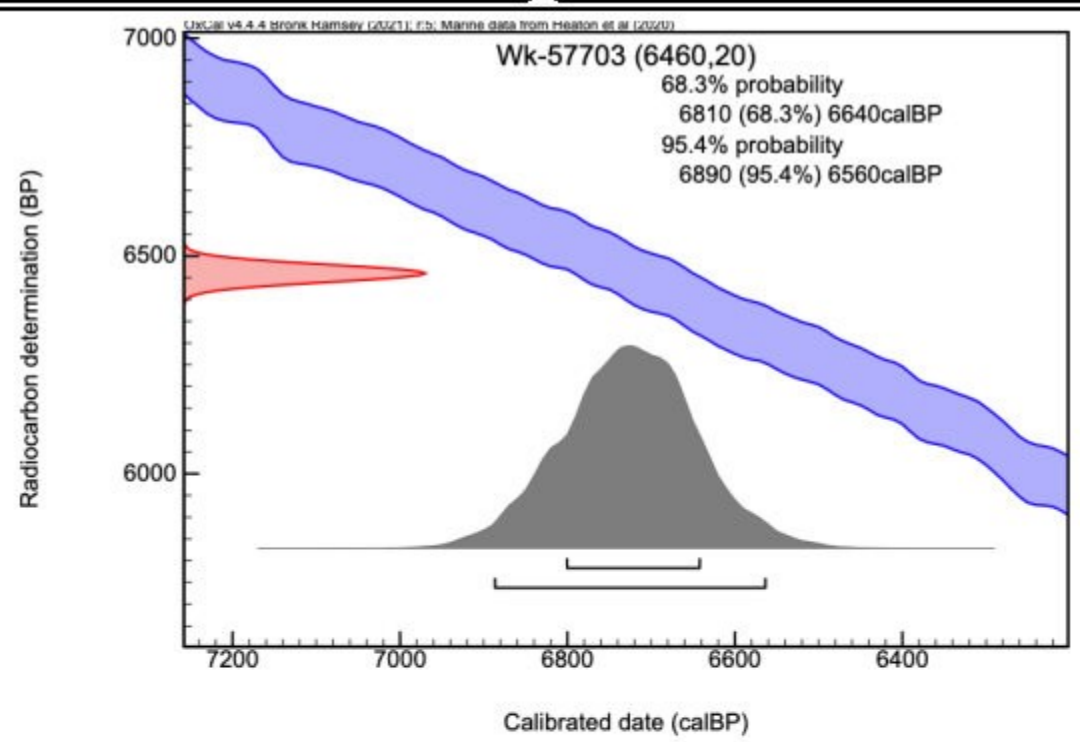

- Explanation of the calibrated Oxcal plots can be found at the Oxford Radiocarbon Accelerator Unit's calibration web pages (http://c14.arch.ox.ac.uk/embed.php?File=explanation.php)
- Result is *Conventional Age or Percent Modern Carbon (pMC)* following Stuiver and Polach, 1977, Radiocarbon 19, 355-363. This is based on the Libby half-life of 5568 yr with correction for isotopic fractionation applied. This age is normally quoted in publications and must include the appropriate error term and Wk number.
- Quoted errors are 1 standard deviation due to counting statistics multiplied by an experimentally determined Laboratory Error Multiplier.
- The isotopic fractionation, $\delta^{13}C$, is expressed as ‰ wrt PDB and is measured on sample CO_2.
- $P^{14}C$% is also known as *Percent Modern Carbon (pMC)*.

THE UNIVERSITY OF WAIKATO
Te Whare Wānanga o Waikato

Radiocarbon Dating Laboratory,
University of Waikato
Hamilton,
New Zealand.

Thursday, 14 March 2024

Radiocarbon Dating Laboratory

Report on Radiocarbon Age Determination for Wk- 57704

Submitter	M Carter
Submitter's Code	RG_2_c
Site & Location	Raglan, New Zealand
Sample Material	Estuarine Shell Cockle
Physical Pretreatment	Surfaces cleaned. Washed in an ultrasonic bath. Tested for recrystallization: aragonite.
Chemical Pretreatment	Sample acid washed using 0.1N HCl, rinsed and dried.

$D^{14}C$	-550.9 ±	1.1 ‰
$F^{14}C$%	44.9 ±	0.1 %
Result	**6430 ± 20 BP**	

(AMS measurement)

Comments

Please note: The Carbon-13 stable isotope value ($\delta^{13}C$) was measured on prepared graphite using the AMS spectrometer. The radiocarbon date has therefore been corrected for isotopic fractionation. However the AMS-measured $\delta^{13}C$ value can differ from the $\delta^{13}C$ of the original material and it is therefore not shown.

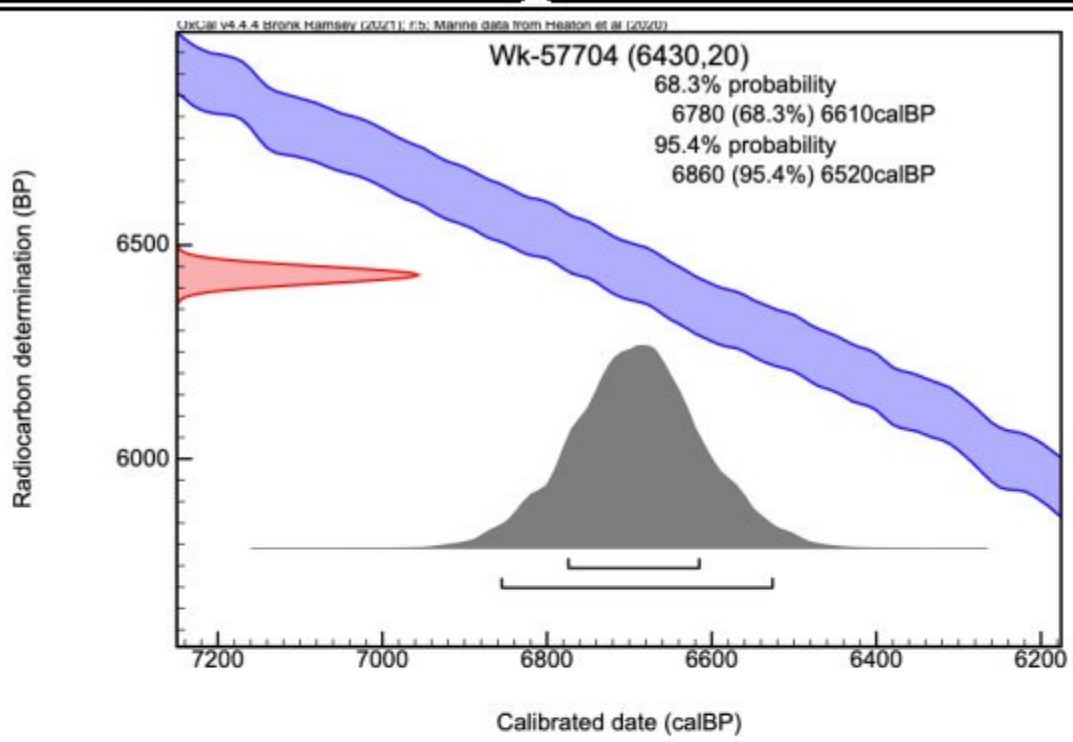

- Explanation of the calibrated Oxcal plots can be found at the Oxford Radiocarbon Accelerator Unit's calibration web pages (http://c14.arch.ox.ac.uk/embed.php?File=explanation.php)
- Result is *Conventional Age or Percent Modern Carbon (pMC)* following Stuiver and Polach, 1977, Radiocarbon 19, 355-363. This is based on the Libby half-life of 5568 yr with correction for isotopic fractionation applied. This age is normally quoted in publications and must include the appropriate error term and Wk number.
- Quoted errors are 1 standard deviation due to counting statistics multiplied by an experimentally determined Laboratory Error Multiplier.
- The isotopic fractionation, $\delta^{13}C$, is expressed as ‰ wrt PDB and is measured on sample CO_2.
- $P^{14}C$% is also known as *Percent Modern Carbon (pMC)*.

THE UNIVERSITY OF WAIKATO
Te Whare Wānanga o Waikato

Radiocarbon Dating Laboratory,
University of Waikato
Hamilton,
New Zealand.

Thursday, 14 March 2024

Radiocarbon Dating Laboratory

Report on Radiocarbon Age Determination for Wk- 56887

Submitter	M Carter
Submitter's Code	SP_1a
Site & Location	Patikirau Bay, Raglan, New Zealand
Sample Material	Marine shell Cockle
Physical Pretreatment	Surfaces cleaned. Washed in an ultrasonic bath. Tested for recrystallization: aragonite.
Chemical Pretreatment	Sample acid washed using 0.1N HCl, rinsed and dried.

$\delta^{13}C$	-1.5 ±	0.3 ‰	(CRDS)
$D^{14}C$	-545.4 ±	1.5 ‰	
$F^{14}C\%$	45.5 ±	0.1 %	
Result	**6332 ± 26 BP**		

(AMS measurement)

Comments

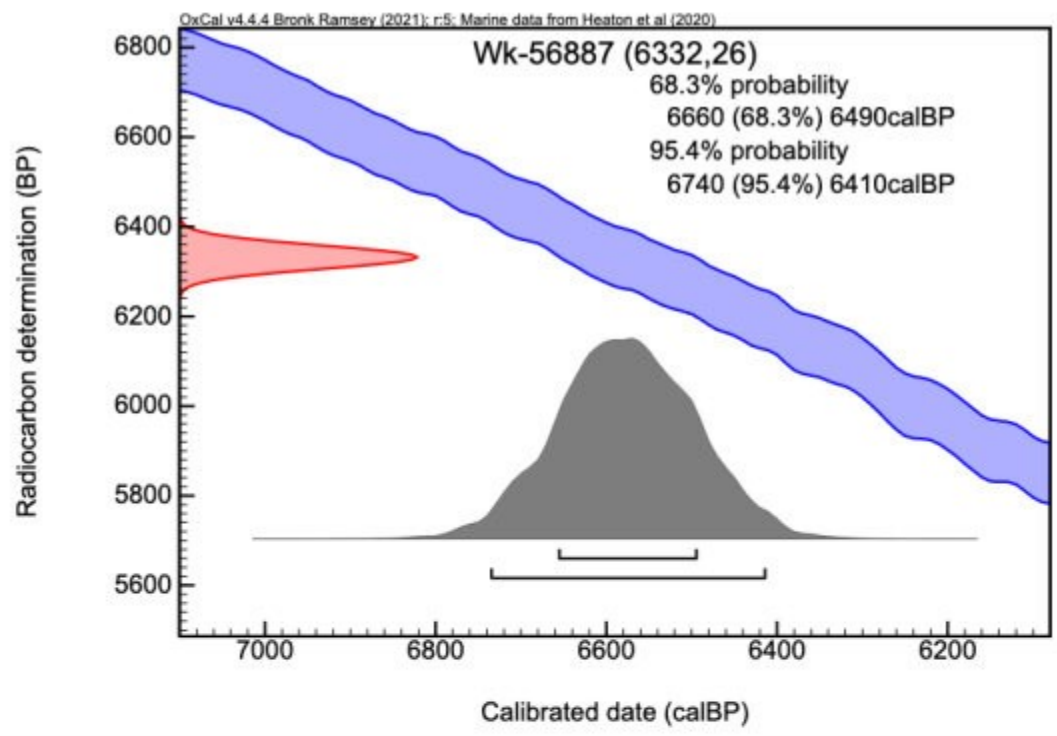

- Explanation of the calibrated Oxcal plots can be found at the Oxford Radiocarbon Accelerator Unit's calibration web pages (http://c14.arch.ox.ac.uk/embed.php?File=explanation.php)
- Result is *Conventional Age or Percent Modern Carbon (pMC)* following Stuiver and Polach, 1977, Radiocarbon 19, 355-363. This is based on the Libby half-life of 5568 yr with correction for isotopic fractionation applied. This age is normally quoted in publications and must include the appropriate error term and Wk number.
- Quoted errors are 1 standard deviation due to counting statistics multiplied by an experimentally determined Laboratory Error Multiplier.
- The isotopic fractionation, $\delta^{13}C$, is expressed as ‰ wrt PDB and is measured on sample CO_2.
- $P^{14}C\%$ is also known as *Percent Modern Carbon (pMC)*.

THE UNIVERSITY OF WAIKATO
Te Whare Wānanga o Waikato

Radiocarbon Dating
Laboratory,
University of Waikato
Hamilton,
New Zealand.

Thursday, 14 March 2024

Radiocarbon Dating Laboratory

Report on Radiocarbon Age Determination for Wk- 56888

Submitter	M Carter
Submitter's Code	SP_2a
Site & Location	Patikirau Bay, Raglan, New Zealand
Sample Material	Marine shell Cockle
Physical Pretreatment	Surfaces cleaned. Washed in an ultrasonic bath. Tested for recrystallization: aragonite.
Chemical Pretreatment	Sample acid washed using 0.1N HCl, rinsed and dried.

$\delta^{13}C$	-0.7 ±	0.3 ‰	(CRDS)
$D^{14}C$	34.7 ±	2.7 ‰	
$F^{14}C\%$	103.5 ±	0.3 %	
Result	**103.5 ± 0.3 %**		

(AMS measurement)

Comments

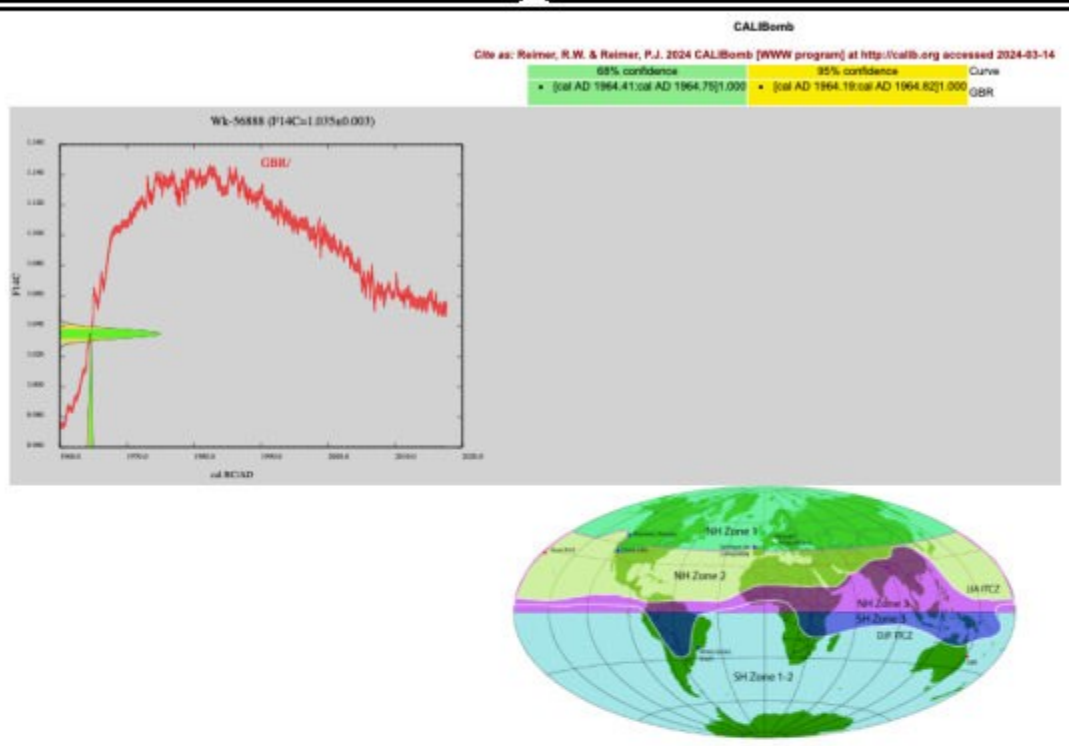

- Explanation of the calibrated Oxcal plots can be found at the Oxford Radiocarbon Accelerator Unit's calibration web pages (http://c14.arch.ox.ac.uk/embed.php?File=explanation.php)
- Result is *Conventional Age or Percent Modern Carbon (pMC)* following Stuiver and Polach, 1977, Radiocarbon 19, 355-363. This is based on the Libby half-life of 5568 yr with correction for isotopic fractionation applied. This age is normally quoted in publications and must include the appropriate error term and Wk number.
- Quoted errors are 1 standard deviation due to counting statistics multiplied by an experimentally determined Laboratory Error Multiplier.
- The isotopic fractionation, $\delta^{13}C$, is expressed as ‰ wrt PDB and is measured on sample CO_2.
- $P^{14}C\%$ is also known as *Percent Modern Carbon (pMC)*.

THE UNIVERSITY OF WAIKATO
Te Whare Wānanga o Waikato

Radiocarbon Dating
Laboratory,
University of Waikato
Hamilton,
New Zealand.

Thursday, 14 March 2024

Radiocarbon Dating Laboratory

Report on Radiocarbon Age Determination for Wk- 56886

Submitter	M Carter
Submitter's Code	SP_3a
Site & Location	Patikirau Bay, Raglan, New Zealand
Sample Material	Marine shell Cockle
Physical Pretreatment	Surfaces cleaned. Washed in an ultrasonic bath. Tested for recrystallization: aragonite.
Chemical Pretreatment	Sample acid washed using 0.1N HCl, rinsed and dried.

$\delta^{13}C$	0.3 ±	0.3 ‰	(CRDS)
$D^{14}C$	94.5 ±	2.8 ‰	
$F^{14}C\%$	109.5 ±	0.3 %	
Result	**109.5 ± 0.3 %**		

(AMS measurement)

Comments

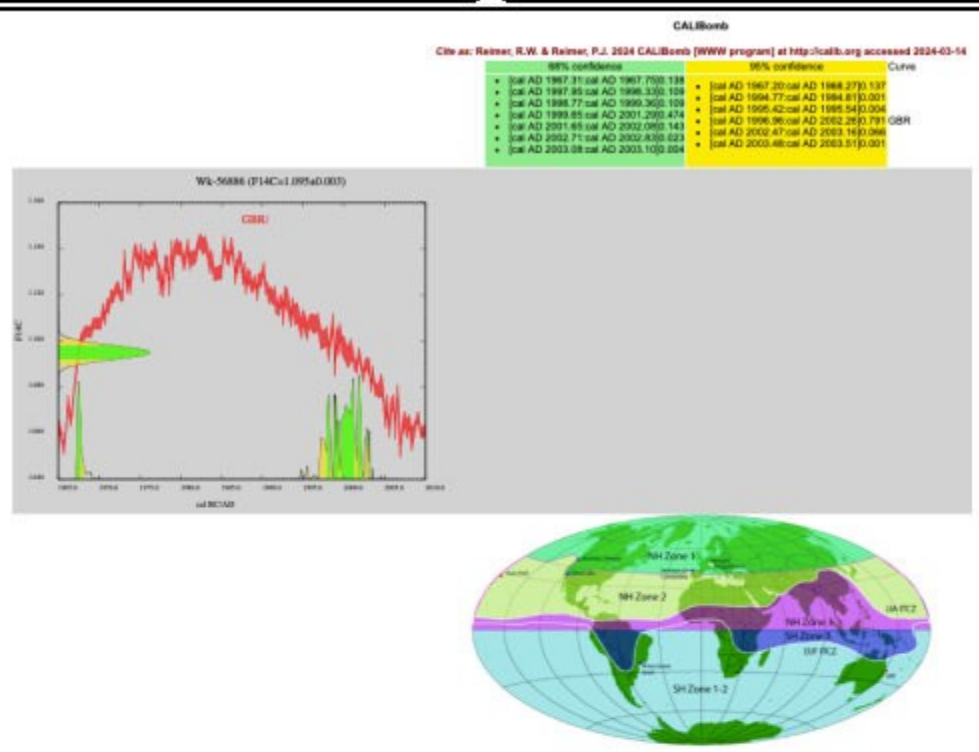

- Explanation of the calibrated Oxcal plots can be found at the Oxford Radiocarbon Accelerator Unit's calibration web pages (http://c14.arch.ox.ac.uk/embed.php?File=explanation.php)
- Result is *Conventional Age or Percent Modern Carbon (pMC)* following Stuiver and Polach, 1977, Radiocarbon 19, 355-363. This is based on the Libby half-life of 5568 yr with correction for isotopic fractionation applied. This age is normally quoted in publications and must include the appropriate error term and Wk number.
- Quoted errors are 1 standard deviation due to counting statistics multiplied by an experimentally determined Laboratory Error Multiplier.
- The isotopic fractionation, $\delta^{13}C$, is expressed as ‰ wrt PDB and is measured on sample CO_2.
- $P^{14}C\%$ is also known as *Percent Modern Carbon (pMC)*.

THE UNIVERSITY OF WAIKATO
Te Whare Wānanga o Waikato

Radiocarbon Dating Laboratory,
University of Waikato
Hamilton,
New Zealand.

Thursday, 14 March 2024

Radiocarbon Dating Laboratory

Report on Radiocarbon Age Determination for Wk- 57173

Submitter	M Carter
Submitter's Code	Pat_1B
Site & Location	Patikirau Bay, Raglan, New Zealand
Sample Material	Marine shell Pipi
Physical Pretreatment	Surfaces cleaned. Washed in an ultrasonic bath. Tested for recrystallization: aragonite.
Chemical Pretreatment	Sample acid washed using 0.1N HCl, rinsed and dried.

$\delta^{13}C$	-1.2 ±	0.2 ‰	(CRDS)
$D^{14}C$	101.1 ±	2.8 ‰	
$F^{14}C\%$	110.1 ±	0.3 %	
Result	**110.1 ± 0.3 %**		

(AMS measurement)

Comments

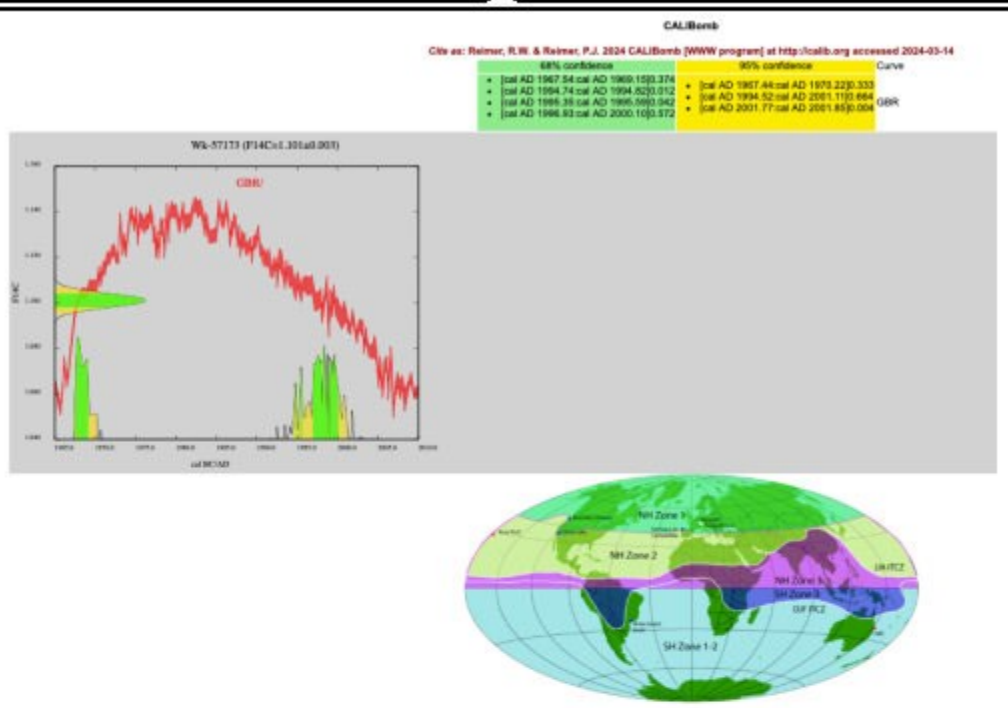

- Explanation of the calibrated Oxcal plots can be found at the Oxford Radiocarbon Accelerator Unit's calibration web pages (http://c14.arch.ox.ac.uk/embed.php?File=explanation.php)
- Result is *Conventional Age or Percent Modern Carbon (pMC)* following Stuiver and Polach, 1977, Radiocarbon 19, 355-363. This is based on the Libby half-life of 5568 yr with correction for isotopic fractionation applied. This age is normally quoted in publications and must include the appropriate error term and Wk number.
- Quoted errors are 1 standard deviation due to counting statistics multiplied by an experimentally determined Laboratory Error Multiplier.
- The isotopic fractionation, $\delta^{13}C$, is expressed as ‰ wrt PDB and is measured on sample CO_2.
- $P^{14}C\%$ is also known as *Percent Modern Carbon (pMC)*.

THE UNIVERSITY OF WAIKATO
Te Whare Wānanga o Waikato

Radiocarbon Dating Laboratory,
University of Waikato
Hamilton,
New Zealand.

Thursday, 14 March 2024

Radiocarbon Dating Laboratory

Report on Radiocarbon Age Determination for Wk- 57174

Submitter	M Carter
Submitter's Code	Pat_2_C
Site & Location	Patikirau Bay, Raglan, New Zealand
Sample Material	Marine shell Pipi
Physical Pretreatment	Surfaces cleaned. Washed in an ultrasonic bath. Tested for recrystallization: aragonite.
Chemical Pretreatment	Sample acid washed using 0.1N HCl, rinsed and dried.

$\delta^{13}C$	-1.0 ±	0.2 ‰	(CRDS)
$D^{14}C$	45.4 ±	2.5 ‰	
$F^{14}C\%$	104.5 ±	0.3 %	
Result	**104.5 ± 0.3 %**		

(AMS measurement)

Comments

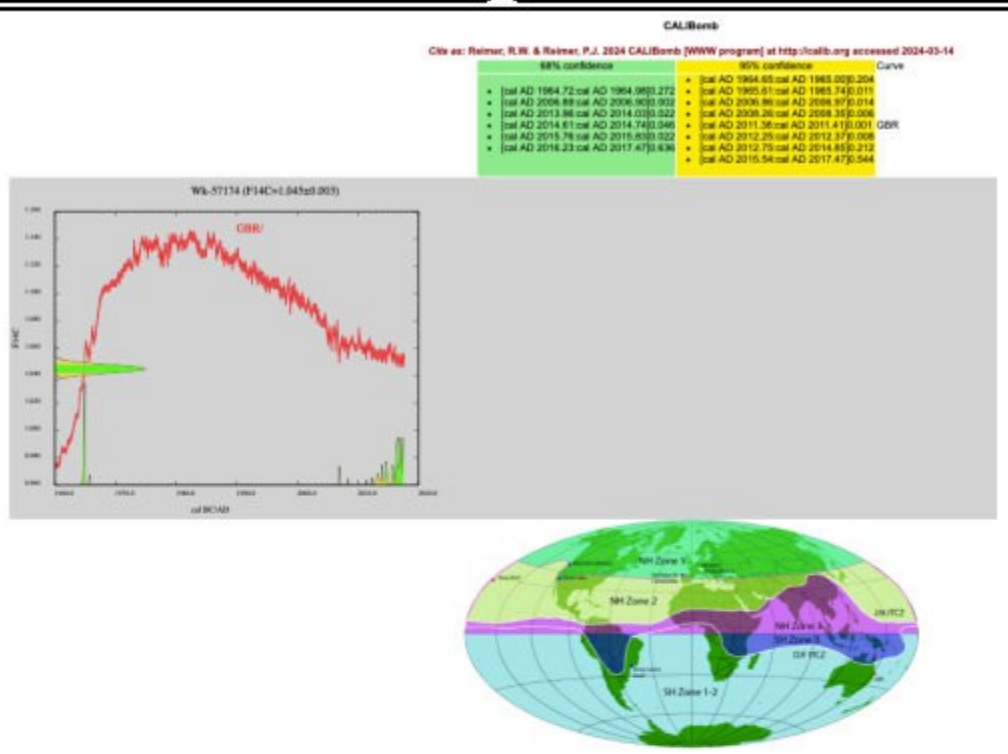

- Explanation of the calibrated Oxcal plots can be found at the Oxford Radiocarbon Accelerator Unit's calibration web pages (http://c14.arch.ox.ac.uk/embed.php?File=explanation.php)
- Result is *Conventional Age or Percent Modern Carbon (pMC)* following Stuiver and Polach, 1977, Radiocarbon 19, 355-363. This is based on the Libby half-life of 5568 yr with correction for isotopic fractionation applied. This age is normally quoted in publications and must include the appropriate error term and Wk number.
- Quoted errors are 1 standard deviation due to counting statistics multiplied by an experimentally determined Laboratory Error Multiplier.
- The isotopic fractionation, $\delta^{13}C$, is expressed as ‰ wrt PDB and is measured on sample CO_2.
- $P^{14}C\%$ is also known as *Percent Modern Carbon (pMC)*.

THE UNIVERSITY OF WAIKATO
Te Whare Wānanga o Waikato

Radiocarbon Dating Laboratory,
University of Waikato
Hamilton,
New Zealand.

Thursday, 14 March 2024

Radiocarbon Dating Laboratory

Report on Radiocarbon Age Determination for Wk- 57264

Submitter	M Carter
Submitter's Code	PST_1_1
Site & Location	Patikirau Bay, Raglan, New Zealand
Sample Material	Marine shell: Cockle
Physical Pretreatment	Surfaces cleaned. Washed in an ultrasonic bath. Tested for recrystallization: aragonite.
Chemical Pretreatment	Sample acid washed using 0.1N HCl, rinsed and dried.

$\delta^{13}C$	0.6 ±	0.2 ‰	(CRDS)
$D^{14}C$	-69.5 ±	2.5 ‰	
$F^{14}C\%$	93.0 ±	0.2 %	
Result	**579 ± 21 BP**		

(AMS measurement)

Comments

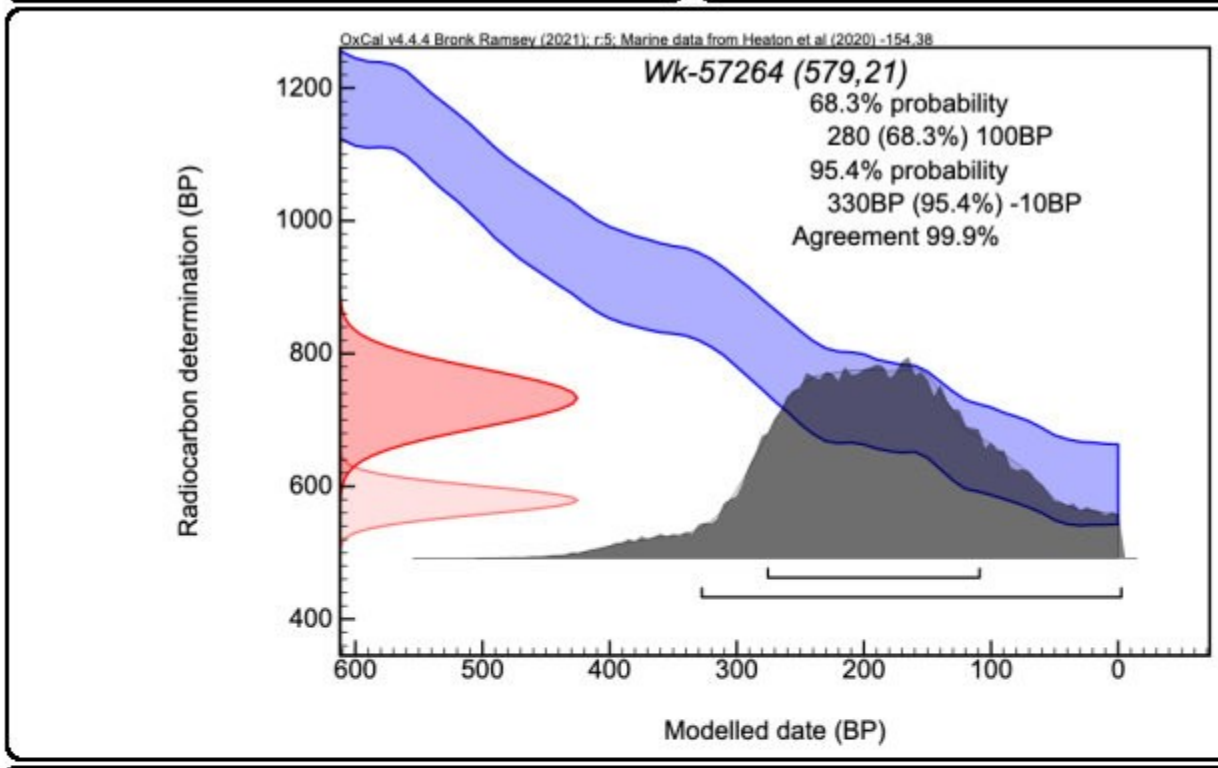

- Explanation of the calibrated Oxcal plots can be found at the Oxford Radiocarbon Accelerator Unit's calibration web pages (http://c14.arch.ox.ac.uk/embed.php?File=explanation.php)
- Result is *Conventional Age or Percent Modern Carbon (pMC)* following Stuiver and Polach, 1977, Radiocarbon 19, 355-363. This is based on the Libby half-life of 5568 yr with correction for isotopic fractionation applied. This age is normally quoted in publications and must include the appropriate error term and Wk number.
- Quoted errors are 1 standard deviation due to counting statistics multiplied by an experimentally determined Laboratory Error Multiplier.
- The isotopic fractionation, $\delta^{13}C$, is expressed as ‰ wrt PDB and is measured on sample CO_2.
- $P^{14}C\%$ is also known as *Percent Modern Carbon (pMC)*.

THE UNIVERSITY OF WAIKATO
Te Whare Wānanga o Waikato

Radiocarbon Dating
Laboratory,
University of Waikato
Hamilton,
New Zealand.

Thursday, 14 March 2024

Radiocarbon Dating Laboratory

Report on Radiocarbon Age Determination for Wk- 57322

Submitter	M Carter
Submitter's Code	FNT_1
Site & Location	Patikirau Bay, Raglan, New Zealand
Sample Material	Marine shell Cockle
Physical Pretreatment	Surfaces cleaned. Washed in an ultrasonic bath. Tested for recrystallization: aragonite.
Chemical Pretreatment	Sample acid washed using 0.1N HCl, rinsed and dried.

$\delta^{13}C$	-0.9 ±	0.5 ‰	(CRDS)
$D^{14}C$	89.8 ±	2.7 ‰	
$F^{14}C\%$	109.0 ±	0.3 %	
Result	**109.0 ± 0.3 %**		

(AMS measurement)

Comments

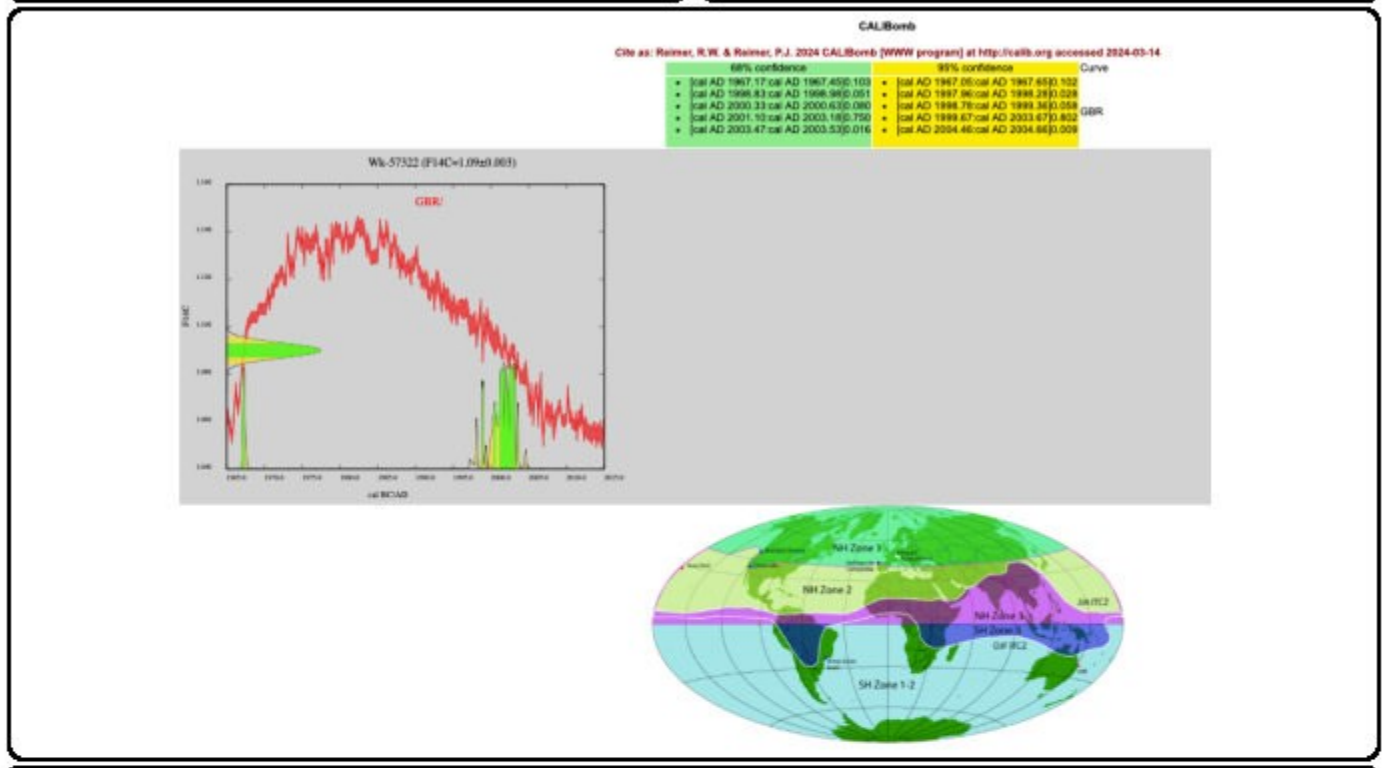

- Explanation of the calibrated Oxcal plots can be found at the Oxford Radiocarbon Accelerator Unit's calibration web pages (http://c14.arch.ox.ac.uk/embed.php?File=explanation.php)
- Result is *Conventional Age or Percent Modern Carbon (pMC)* following Stuiver and Polach, 1977, Radiocarbon 19, 355-363. This is based on the Libby half-life of 5568 yr with correction for isotopic fractionation applied. This age is normally quoted in publications and must include the appropriate error term and Wk number.
- Quoted errors are 1 standard deviation due to counting statistics multiplied by an experimentally determined Laboratory Error Multiplier.
- The isotopic fractionation, $\delta^{13}C$, is expressed as ‰ wrt PDB and is measured on sample CO_2.
- $P^{14}C\%$ is also known as *Percent Modern Carbon (pMC)*.

THE UNIVERSITY OF WAIKATO
Te Whare Wānanga o Waikato

Radiocarbon Dating Laboratory,
University of Waikato
Hamilton,
New Zealand.

Thursday, 14 March 2024

Radiocarbon Dating Laboratory

Report on Radiocarbon Age Determination for Wk- 57323

Submitter	M Carter
Submitter's Code	FNT_2
Site & Location	Patikirau Bay, Raglan, New Zealand
Sample Material	Marine shell Cockle
Physical Pretreatment	Surfaces cleaned. Washed in an ultrasonic bath. Tested for recrystallization: aragonite.
Chemical Pretreatment	Sample acid washed using 0.1N HCl, rinsed and dried.

$\delta^{13}C$	0.1 ±	0.5 ‰	(CRDS)
$D^{14}C$	77.1 ±	2.1 ‰	
$F^{14}C\%$	107.7 ±	0.2 %	
Result	**107.7 ± 0.3 %**		

(AMS measurement)

Comments

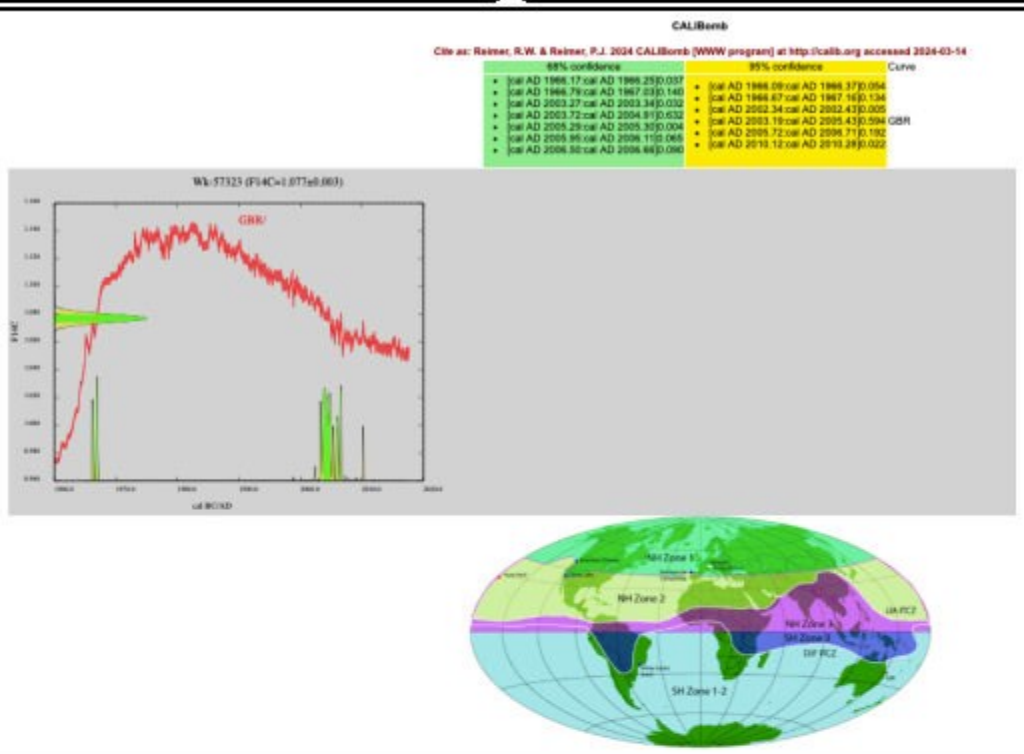

- Explanation of the calibrated Oxcal plots can be found at the Oxford Radiocarbon Accelerator Unit's calibration web pages (http://c14.arch.ox.ac.uk/embed.php?File=explanation.php)
- Result is *Conventional Age or Percent Modern Carbon (pMC)* following Stuiver and Polach, 1977, Radiocarbon 19, 355-363. This is based on the Libby half-life of 5568 yr with correction for isotopic fractionation applied. This age is normally quoted in publications and must include the appropriate error term and Wk number.
- Quoted errors are 1 standard deviation due to counting statistics multiplied by an experimentally determined Laboratory Error Multiplier.
- The isotopic fractionation, $\delta^{13}C$, is expressed as ‰ wrt PDB and is measured on sample CO_2.
- $P^{14}C\%$ is also known as *Percent Modern Carbon (pMC)*.

THE UNIVERSITY OF WAIKATO
Te Whare Wānanga o Waikato

Radiocarbon Dating Laboratory,
University of Waikato
Hamilton,
New Zealand.

Thursday, 14 March 2024

Radiocarbon Dating Laboratory

Report on Radiocarbon Age Determination for Wk- 56889

Submitter	M Carter
Submitter's Code	BP_1a
Site & Location	Patikirau Bay, Raglan, New Zealand
Sample Material	Bone Equine pastern
Physical Pretreatment	Sample cleaned and ground.
Chemical Pretreatment	Sample was decalcified in 2% HCl, rinsed and dried. Then gelatinised at pH=3 with HCl at 90 degrees for 4 hours. Ultrafiltered and freezedried.

$D^{14}C$	-10.7 ±	1.5 ‰
$F^{14}C$%	98.9 ±	0.2 %
Result	**86 ± 13 BP**	

(AMS measurement)

Comments

Please note: The Carbon-13 stable isotope value ($\delta^{13}C$) was measured on prepared graphite using the AMS spectrometer. The radiocarbon date has therefore been corrected for isotopic fractionation. However the AMS-measured $\delta^{13}C$ value can differ from the $\delta^{13}C$ of the original material and it is therefore not shown.

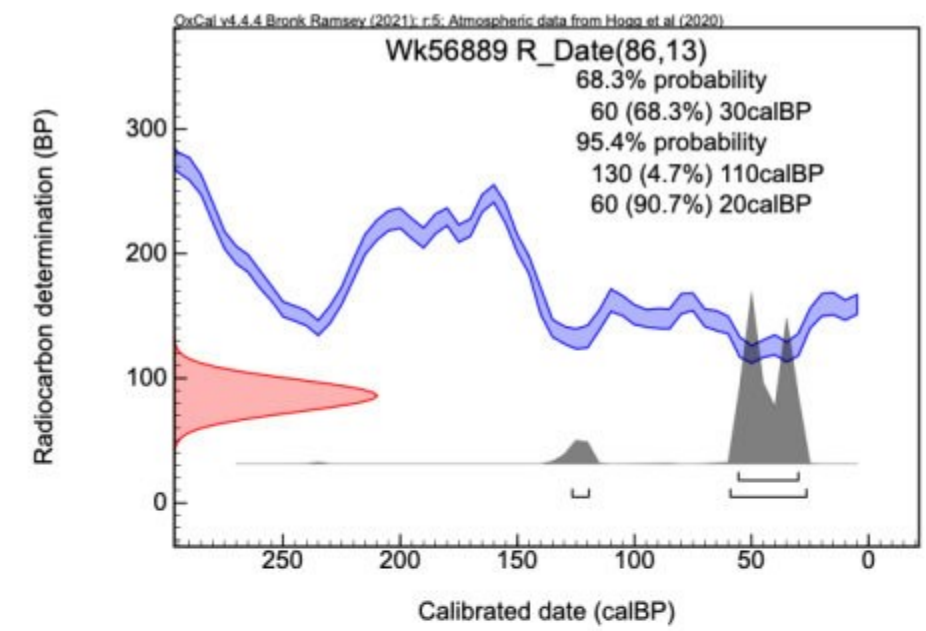

- Explanation of the calibrated Oxcal plots can be found at the Oxford Radiocarbon Accelerator Unit's calibration web pages (http://c14.arch.ox.ac.uk/embed.php?File=explanation.php)
- Result is *Conventional Age or Percent Modern Carbon (pMC)* following Stuiver and Polach, 1977, Radiocarbon 19, 355-363. This is based on the Libby half-life of 5568 yr with correction for isotopic fractionation applied. This age is normally quoted in publications and must include the appropriate error term and Wk number.
- Quoted errors are 1 standard deviation due to counting statistics multiplied by an experimentally determined Laboratory Error Multiplier.
- The isotopic fractionation, $\delta^{13}C$, is expressed as ‰ wrt PDB and is measured on sample CO_2.
- $P^{14}C$% is also known as *Percent Modern Carbon (pMC)*.

Appendix B.4: U-Th speleothem dating results

Sample ID	Lab number	Mass/g	238 ng/g	2SE	238/V	Depth/mm	95%err	230/238A	95% ext.	234/238A	95% ext.	Age/Ka	95%err	232/238A	2SE	230/232i	2sd	230/232A	Age cr Ka	2se	[4/8]i Corr	2se	AgeCr/Age			Seq	Comments	Age Ka 1950	± 95%
P10-1	UMF240130-341	0.0730	131	26	2.2216			0.2233	0.0017	1.0653	0.0028	25.588	0.236	0.013573	0.000279	1.50	1.50	16.5	23.484	2.148	1.0698	0.0030	92%			252	10 341 P10-1	23.4	2.1
P10-2	UMF240130-343	0.0630	272	54	4.0138			0.2150	0.0013	1.0685	0.0031	24.440	0.185	0.005781	0.000133	1.50	1.50	37.2	23.551	0.891	1.0732	0.0033	96%			252	11 343 P10-2	23.49	0.90

Appendix C: Foraminifera Concentrations

Appendix C.1: Foraminifera concentrations data*

Location	Site No	Lab No	Thesis No	**Concentration (%)***	Age BP (pMC)	Description	Elevation (cm) **	Lat	Long
Motukokako Point	SB_2	57038	BW_SB_1	**2**	104	Bivalve infill	85	37°47'11.19"S	174°53'59.39"E
"	"	57172	BW_1_B	**3**	103	Bivalve infill	85	"	"
	SB_2_1			**0.8**		Host bed seds	85	"	"
	SB_2-2			**0.01**		Bivalve infill	50	37°47'14.80"S	174°54'1.99"E
	SB_2_2			**9**		Host bed seds	50	"	"
	SB_2_3			**3**		Host bed seds	60	37°47'19.29"S	174°54'5.28"E
	SB_2_4			**10**		Host bed seds	60	37°47'27.55"S	174°53'53.70"E
Rag. Rec. Ground A	SB_1	57039	RG_1_SB		637	Cockle frag	97	37°47'54.69"S	174°52'36.22"E
	"		RG_1	**0.5**		Host bed seds	40	"	"
	"		RG_2	**7**		Host bed seds	85	"	"
Rag. Rec. Ground B	SB_1_2	57324	RG_S2_1	**17**	6442	Bivalve infill	30	37°47'54.84"S	174°52'35.99"E
	"		RG_3	**0**		Host bed seds	100	"	
Patikirau Creek A	SB_3_1	57173	Pat_1_B	**3**	110	Bivalve infill	30	37°46'58.47"S	174°53'13.38"E
				4		Host bed seds	30	"	"
Patikirau Bay Sth Terrace	SB_3_2	56886	SP_3a	**2**	110	Bivalve infill	50	37°47'0.47"S	174°53'10.77"E
			ST_4	**5**		Host bed seds	80	"	"
			ST_3	**2**		"	45	"	"
			ST_2	**15**		"	30	"	"
			ST_1	**0**		"	20	"	"
Patikirau Bay Nth Terrace	SB_3_3	57322	PNT_1	**5**	109	Bivalve infill	30	37°46'57.50"S	174°53'8.76"E
				10	109	Host bed seds	30	"	"

* Proportion (%) of benthic forams by number of total grains of diameter 212 to 355 µm (sieve size) ** Above their tide-zone equivalents

Appendix C.2: Foraminifera Concentration Sample Locations